THE UNIVERSITY
of EDINBURGH

This thesis has been submitted in fulfilment of the requirements for a postgraduate degree (e.g. PhD, MPhil, DClinPsychol) at the University of Edinburgh. Please note the following terms and conditions of use:

This work is protected by copyright and other intellectual property rights, which are retained by the thesis author, unless otherwise stated.
A copy can be downloaded for personal non-commercial research or study, without prior permission or charge.
This thesis cannot be reproduced or quoted extensively from without first obtaining permission in writing from the author.
The content must not be changed in any way or sold commercially in any format or medium without the formal permission of the author.
When referring to this work, full bibliographic details including the author, title, awarding institution and date of the thesis must be given.

Investigating the Renal and Vascular Mechanisms of Salt-Induced Hypertension in C57BL6/J Mice

Ailsa Florence Ralph

Doctor of Philosophy

The University of Edinburgh

2020

Declaration

I declare that this thesis has been composed solely by myself and that it has not been submitted, in whole or in part, in any previous application for a degree. The work contained herein is my own except where explicitly stated otherwise in the text or by reference or acknowledgement.

Ailsa Ralph

Abstract

Dietary salt intake has a detrimental relationship with blood pressure (BP); the more salt consumed per day, the higher the incidence of hypertension and its cardiorenal consequences within a population. However, the underlying mechanisms responsible remain controversial. Research supports roles for both the kidneys and the vasculature in salt-induced hypertension. Here, I investigated the effect of a high salt diet (HSD) on BP, renal function and the vascular responses to vasoconstrictors and vasodilators in adult male C57BL6/JCrl mice. In my experiments, mice were fed either a HSD (3% sodium) or a standard salt (0.25% sodium) diet (SSD). BP was measured in conscious, freely moving animals by radiotelemetry. After measurements on the SSD, mice were fed the HSD and BP increased by ~5mmHg after 3-4 days and remained elevated for up to 3 weeks. Plasma aldosterone concentration was suppressed after 1 week HSD. Assessment of the acute pressure natriuresis (PN) response under anaesthesia illustrated increased urinary sodium excretion at any given BP and messenger RNA (mRNA) levels of some key renal sodium transporters were appropriately decreased by the HSD. Isolated renal arteries displayed increased sensitivity to the vasoconstrictor phenylephrine after 1 week of high salt. In mesenteric arteries, no functional changes were observed to the HSD, supported by no changes in endothelial NO synthase mRNA levels compared to the SSD. Urinary catecholamine concentration was used as an index of sympathetic nerve system (SNS) activity. Adrenaline excretion increased significantly on the HSD, indicating SNS involvement. To test this, the ganglionic blocker hexamethonium was administered via intraperitoneal injection and the resulting transient dip in BP was modestly increased and persisted after 3 weeks of the HSD. In conclusion, I observed a sustained salt-induced increase in BP in C57BL6/JCrl mice. Appropriate adaptation of aldosterone production and the acute PN response to salt challenge was seen. Increased excretion of adrenaline, elevated contractility of renal arteries and a greater effect on SBP with hexamethonium suggests over-activity of the SNS is an important factor in salt-induced hypertension in C57BL6/JCrl mice.

Lay Summary

We consume ~10g of salt per day within our diet, which is almost twice that of the daily-recommended allowance worldwide. This has a serious impact upon health, as it increases the risk of cardiovascular disease and death. Around a quarter of the population are more susceptible to these salt-induced changes and are known as ‘salt-sensitive’. In research, this trait is identified by testing whether increasing the amount of salt within an individual’s diet also increases their blood pressure.

The processes leading to this harmful increase and cardiovascular risk are currently unknown, but a few theories are being investigated. Some suggest that the kidneys are enabling this rise as they can retrieve the excess salt and pass it back into the bloodstream, instead of expelling it in urine with other waste products. Others prefer the network of blood vessels, known as the vasculature, as the culprit. If the walls of arteries do not relax in response to excess salt, resistance to blood flow cannot be reduced and so pressure remains high.

My aim was to further investigate the contribution of these mechanisms to high blood pressure caused by salt. To do this, research mice were given access to either a high salt diet or a standard diet for up to 3 weeks. Blood pressure, measured in these animals whilst they were conscious and freely-moving, rose after just 3-4 days of excess salt and remained high for 3 weeks, confirming that they are salt-sensitive. Next, I measured the ability of their kidneys to filter salt. The proteins responsible for passing salt back into the bloodstream, known as sodium transporters, were less abundant in the kidneys of those receiving high salt compared to those receiving the standard diet. This, along with increased salt in the urine, confirmed that the kidneys were appropriately expelling the excess salt.

Since kidney function adapted, I investigated the role of the vasculature by using two types of arteries: mesenteric, which are resistance arteries from the gut, and renal arteries. By applying drugs to induce either artery wall

contraction or relaxation, I noticed that the renal arteries were more sensitive to contraction after 1 week of a high salt diet, whereas their ability to relax was similar to those on the standard diet. An increased concentration of adrenaline in the bloodstream was also found after 1 week of high salt intake. Adrenaline, widely known as the ‘fight-or-flight’ hormone, is produced and released from the adrenal gland upon the command of the sympathetic nervous system, and can cause arteries to contract. Therefore, I hypothesised that the sympathetic nervous system is stimulated by dietary salt and potentially drives the harmful increase in blood pressure.

To test this, the drug known as hexamethonium, which blocks the activity of the sympathetic nervous system, was administered at different times during the high salt diet. After 3 weeks of excess salt, hexamethonium caused a significant decline in systolic blood pressure, which mice took longer to recover from. To conclude, high salt consumption in these salt-sensitive mice caused increased amounts of adrenaline in the bloodstream, renal arteries to contract to lower concentrations of vasoconstrictor and increased blood pressure. After prolonged exposure to high salt, blood pressure was transiently reduced by halting the activity of the sympathetic nervous system.

Presentations of the work in this thesis

Published abstracts

Ralph AFR, Grenier C, Costello H, Stewart K, Czopek A, Dhaun N, Bailey MA. “Does dietary salt induce vascular dysfunction in C57BL6/J mice?” *The Physiology Society Europhysiology Meeting, London, 2018* (poster presentation).

Ralph AFR, Costello H, Grenier C, Stewart K, Dhaun N, Bailey MA. “Adaptation of C57BL6/JCrl mice to high dietary salt intake” *Experimental Biology Main Meeting, Orlando, 2019* (poster presentation).

Acknowledgements

I would like to acknowledge and whole-heartedly thank my primary supervisor, Professor Matthew Bailey, for his unwavering support and for being a boundless source of knowledge, advice, positivity and inspiration. I would also like to thank my secondary supervisor, Dr Neeraj Dhaun (Bean), for the help and encouragement during my PhD.

Honourable mentions must go to Dr Celine Grenier for the excellent assistance with my vascular work, particularly your proficiency at wire myography, and Mr Kevin Stewart for performing the surgeries for radiotelemetry and pressure natriuresis, and for passing on your vast and superior animal handling expertise. I am extremely grateful to Mr Dave Binnie as well for all your excellent work with my mice, even though you prefer rats!

Special thanks go to Hannah, my close friend and partner-in-crime, for the pilot radiotelemetry data and for all the help and the sharing of the burden that was steroid analysis, animal checks and procedures at stupid o'clock, qPCR work, and for the emotional support in general. A big thank you to the E3.24 office for the midday chats and coffee breaks, with particular mention to AB's ladies Olivia, Natalie, Kathleen, Bonnie and Marie-Louise for being so lovely and genuinely hilarious. Thanks also to the Bailey lab group, and to the BDD lab group for the sharing of knowledge, resources and entertaining Christmas parties.

I am also grateful to all the BRR/LF2 staff, with a shout-out to Sandra for going above and beyond with the care of my mice, and to Will for the metabolic cage training and carrying out my IP injections. Thanks to Dr Alicja Czopek for the myography training and assistance, to Dr Laura Denby for the artery RNA extraction help, and to Dr Jessica Ivy for the qPCR protocol.

I would also like to acknowledge and thank my wonderful family for all your encouragement and support throughout the highs and lows, and for listening whenever I've needed. A big thanks to my friends outside the lab, with a

shout-out to Alex, Nikki and Ross for the advice, science chats and for making my time in China enjoyable. Thank you to my partner Harry for your support and patience, and for the coffees and road trips whenever I needed a thesis-free day and a breath of fresh air.

Table of Contents

List of Figures

List of Tables

List of Abbreviations

	11βHSD2	11β-hydroxysteroid dehydrogenase type 2
	12-h	12-hour
	24-h	24-hour
A	ACh	Acetylcholine
	ATP	Adenosine triphosphate
	ANGII	Angiotensin II
	ANOVA	Analysis of variance
	AR	Adrenergic receptor
	AU	Arbitrary unit
	AUC	Area under the curve
B	BP	Blood pressure
C	CASH	Consensus Action on Salt and Health
	CCA	Calcium channel antagonist
	cDNA	Complementary DNA
	CKD	Chronic kidney disease
	CO	Cardiac output
	Cp	Crossing point
	CRC	Concentration-response curve
	CVD	Cardiovascular disease
D	DASH	Dietary Approaches to Stop Hypertension
	DBP	Diastolic blood pressure
	DMT	Danish Myo Technology
	DOCA	Deoxycorticosterone acetate
	DSI	Data Science International
E	ECFV	Extracellular fluid volume
	EDTA	Ethylenediaminetetraacetic acid
	ELISA	Enzyme linked immunosorbent assay
	ENaC	Epithelial sodium channel
	eNOS	Endothelial nitric oxide synthase
F	FITC	Fluorescein isothiocyanate
	FMD	Flow-mediated dilation

G	Gbw	Grams per body weight
	g/day	Grams per day
	GFR	Glomerular filtration rate
	GMP	Guanosine monophosphate
	GPX	Glutathione peroxidase
H	HPRT	Hypoxanthine-guanine phosphor-ribosyltransferase
	HSD	High salt diet
I	I_1-receptors	Imidazoline receptors
	IC	Internal circumference
	INTERMAP	International Study of Macronutrients and Blood Pressure
	IP	Intraperitoneal injection
	IQR	Interquartile range
	ITGAM	Integrin αM
K	KPSS	Potassium-rich physiological saline solution
	KW	Kidney weight
M	MABP	Mean arterial blood pressure
	MBP	Mean blood pressure
	MESOR	Midline-estimating statistic of rhythm
	mmHg	Millimetres of mercury
	mmol/d	Millimoles per day
	mRNA	Messenger RNA
N	Na^+-K^+ ATPase	Sodium-potassium adenosine triphosphatase
	NADPH	Nicotinamide adenine dinucleotide phosphate
	NCC	Sodium-chloride cotransporter
	NHE3	Sodium-proton exchanger 3
	NKCC	Sodium-potassium-chloride cotransporter
	NO	Nitric oxide
O	OD	Optical density

P	PhE	Phenylephrine
	PN	Pressure natriuresis
	PSS	Physiological saline solution
	PVAT	Perivascular adipose tissue
Q	qPCR	Quantitative polymerase chain reaction
R	RAAS	Renin-angiotensin-aldosterone system
	RBF	Renal blood flow
	RDN	Renal denervation
	ROS	Reactive oxygen species
	rRNA	Ribosomal RNA
	RT	Reverse transcription
	RVR	Renal vascular resistance
S	SBP	Systolic blood pressure
	SD	Standard deviation
	SIK1	Salt-inducible kinase-1
	SNP	Sodium nitroprusside
	SNS	Sympathetic nervous system
	SSD	Standard salt diet
	SVR	Systemic vascular resistance
T	TBE	Tris/Borate/EDTA
	TBP	TATA-binding protein
	TGF	Tubuloglomerular feedback
	TPR	Total peripheral resistance
U	UK	United Kingdom
	US	United States
V	VSM	Vascular smooth muscle
W	WHO	World Health Organisation
Z	ZT	Zeitgeber Time

1 Introduction

1.1 Salt Intake

Salt has been considered an important mineral for thousands of years. During the first century AD, salt was perceived by the Romans as a symbol of wealth, status and vigour (1). However, such regard for salt has since been overturned, particularly upon entering the 21st century. Globally, dietary salt intake far exceeds physiological need which, in direct contrast to ancient Rome, has been associated with significant disease burden (2).

Salt intake refers to the consumption of the compound sodium chloride (NaCl) within food and drink. For every 1 g of NaCl consumed, 0.4 g comprises of the cation sodium. Intake is reported as either millimoles per day (mmol/d) or grams per day (g/day), with a conversion rate of 1 mmol = 23 milligrams (mg) sodium.

1.1.1 Global estimates of dietary salt intake

The excessive consumption of dietary salt is a global issue. The World Health Organisation (WHO) has circulated a guideline of no more than 5 grams per day (g/day) of dietary salt for the adult population, aiming to reduce global intake by 30% in the next decade (3, 4). Nevertheless, the world mean g/day of dietary salt still exceeds this guideline to this day. With physiological need estimated at 10-20 mmol/d of sodium, which is equivalent to 0.46 g/d, intake is well beyond that which is required (5). Powles *et al*. (6) examined daily intakes across the globe in 2010 and reported the world mean dietary salt intake at 10 g/day, which is more than double that recommended by the WHO. Over 100 countries included in the analysis were consuming >2.5 g/day above the recommended 5 g/day, with Central Asia consuming the most at 12.2 g/day, Western Europe at 9.7 g/day and Central Latin America among the lowest at 8.0 g/day (6). Such excessive intake has

persisted over time, as these values were similar when compared to those in 1990 (6) and again in 2018 (7).

1.1.2 Sources of dietary salt

Sodium is involved in many vital processes within human physiology, ranging from neuronal and muscular activity to fluid homeostasis. Dietary NaCl represents the primary supply of this essential electrolyte. In developed countries, manufactured foods are the main culprits behind the high salt content of our diet. A survey of the population of the United Kingdom (UK) collected information on the various, day-to-day sources of dietary salt. Within the average UK household, 5% of overall salt intake is from that which is naturally present within foods, 15% is added during the preparation and consumption of food (i.e seasoning at the dinner table), and the significant remainder (80%) is added during the manufacturing process (8, 9).

Dietary practices, and therefore sources of dietary salt, differ with culture. Some countries in Asia have the highest salt intakes recorded (6), yet processed foods are not the main source of their dietary salt. Further analysis of the International Study of Macronutrients and Blood Pressure (INTERMAP) findings revealed most of the dietary salt arises from that added to home-cooked meals in China. In Japan, seasoning with soy sauce and the consumption of salt-preserved vegetables and seafood accounts for much of the measured intake (10).

Since salt intake is in excess across the globe, it is important to pinpoint and subsequently address the major sources and accompanying practices. A leading example is Finland's success story. For 30 years, the country has been campaigning to reduce salt intake via raising public awareness and encouraging the food industry to adhere to strict guidelines regarding the labelling and addition of salt to pre-prepared foods. As a result, habitual salt intake has declined by 25%: from 12 g to 9 g/day by 2002 (11). Label transparency, i.e providing clear warnings on high salt products, and the regular monitoring of population salt intake have been key in accomplishing

this feat (12, 13). In the UK, following the implementation of the salt reduction strategy Consensus Action on Salt and Health (CASH) in 2003, the last 7 years have seen a significant reduction in the salt content of foods with an improvement in UK salt intake: from 9.6 to 8.1 g/day by 2011 (14, 15). A pivotal event in this case has also been the labelling of foods, for example the employment of the traffic-light labelling system to visually inform consumers on the salt content of a product, with red denoting high salt and green, low (16). Hence, investigating and raising awareness of the potential adverse health effects of high salt has also become a priority in order to reduce salt intake worldwide.

1.2 Salt and Disease

In 2017, high dietary salt intake was accredited as the most significant dietetic risk factor for all-cause mortality (2). In the United States (US) alone, reducing salt intake was estimated to prompt a 44,000-92,000 decrease in the number of deaths per year (17). This demonstrates that high intake of salt has a negative impact upon health. Whilst attempting to elucidate the underlying causes, high salt intake has been found to associate with many of the major morbidities that contribute to the modern-day global burden of disease.

1.2.1 Salt intake and cardiovascular disease

Epidemiological studies have uncovered a worldwide association between dietary salt content and cardiovascular disease (CVD) and its related pathologies. A systemic review performed by Strazzullo *et al*. (18) analysing >11,000 cardiovascular events observed that the higher the salt content of the diet, the greater the risk of stroke and overall CVD. Similar relations have been found for stroke (19), as well as left ventricular remodelling (20) and coronary heart disease (21).

Lowering salt intake offsets this, with studies reporting reduced risk and occurrence of these cardiovascular events and disease with restricted salt intake (21, 22). An example can be derived from Finland's efforts as, in the

wake of their salt reduction initiative, a 60% decline in the deaths related to coronary heart disease and stroke was achieved (23). However, analysis of the PURE cohort identified that salt intake was only associated with an increased risk of adverse cardiovascular outcomes, such as stroke, in communities consuming the lowest (<4.43 g/day) and the highest (>5.08 g/day) amounts of salt per day. No association between risk and intake was seen in those consuming a moderate amount of salt (between 4.43 and 5.08 g/day) (24). This recent evidence suggests that this relationship may follow a U-shaped curve, rather than conforming to a linear relationship.

1.2.2 Salt intake and renal disease

High dietary salt intake is also a risk factor for chronic kidney disease (CKD), defined as a glomerular filtration rate (GFR) of <60 mL/min^{-1} persisting for over 3 months and the presence of the protein albumin in the urine. Urinary albumin itself has been reported as a risk factor for CKD advancement and the accompanying development of CVD (25). Excretion positively correlates with salt intake (26), thus high amounts of both may have adverse cardiorenal consequences. Upon reducing salt intake, a decline in urinary albumin was also observed (27) along with improved antiproteinuric responses to therapeutic intervention (28), suggesting that initiatives to reduce salt intake may also benefit those with CKD.

1.2.3 Salt intake and other morbidities

Dietary salt intake is further associated with other morbidities, such as those comprising the metabolic syndrome. The high salt content of soft drinks, such as cream soda, has secondary links with obesity via fluid intake. Moderate reductions in salt intake appear to have a snowball effect: decreasing intake by 1 g/day induced a significant decrease in soft drink and overall fluid intake (29, 30). This result, coupled with the strong relationship between the indigestion of soft drinks and obesity (31), suggests a potential role for salt intake in obesity and the likely benefit of salt restriction to help combat obesity. In addition to this, salt intake has been associated with numerous

other conditions, such as the risk of gastric cancer (32) as well as the inflammatory disorders rheumatoid arthritis and multiple sclerosis (33-35).

Nonetheless, studies in diabetic humans have demonstrated further evidence for the complexity of the relationship of salt intake and disease. For example, a lower mortality rate was noted with higher urinary sodium levels, used as a surrogate measure for intake, in type 1 (36) and type 2 (37) diabetics. The patients involved in these studies possessed pre-existing renal and cardiovascular comorbidities at the time. Many conditions at once appear to complicate the effects of dietary salt intake, demonstrating that different systems may have a range of different responses.

The mechanisms underlying the detrimental influence dietary salt has upon health are as of yet unclear, however its effect upon blood pressure (BP) may play a crucial role.

1.3 Salt and Blood Pressure

1.3.1 Evidencing the relationship between dietary salt and blood pressure

High BP, clinically defined as hypertension at a BP >140/90 mmHg, potentially links excessive salt intake with its adverse health effects. The relationship between dietary salt intake and BP has been gaged within numerous population studies and clinical trials.

1.3.1.1 Population studies

The relationship between dietary salt and BP was evaluated in the work of Louis Dahl. During his research, he investigated the significant variability in mean daily salt intake and the prevalence of hypertension between populations. As a result, he demonstrated a positive correlation between the two variables across five distinct populations: as daily salt intake increased, so did the prevalence of hypertension (38, 39). Dahl's observation sparked the interest of the research field, and a flurry of further studies and analyses followed. Froment *et al.* scrutinized the mean sodium intakes of 28

populations against systolic BP (SBP) and diastolic BP (DBP) and reported a strong association (40), concordant with Dahl's findings.

Dietary salt and BP examinations within, rather than across, individual populations have also been carried out. For example, data obtained from an isolated, 'salt-less' society of Yanomamo Indians illustrated an exceedingly low mean daily salt intake accompanied by little to no changes in long-term BP (41), demonstrating the absence of high salt coincides with the absence of high BP. A further example was observed from a north-south divide in Japan, in which a high incidence of hypertension-related disease was reported within areas consuming high amounts of salt, and vice versa (5, 38). The international study of electrolyte excretion and BP, known as INTERSALT, delved further into these observations (42). This large, observational study used a standardised approach in which daily urinary sodium excretion was treated as a surrogate measure for salt intake in 10,079 participants from 52 populations. Sodium excretion was observed to weakly but positively correlate with rising BP, but only upon the inclusion of populations with extreme salt intakes, such as the aforementioned Yanomamo Indians (42). Within individual participants in each population, BP rose by 3.0-6.3 mmHg with each 100 mmol rise in sodium excretion. Similar interpopulation rates were also observed across the globe (43), further evidencing that the link between BP and salt is a potentially global phenomenon. However, these analyses have been criticised and so these findings and analyses remain somewhat controversial (44).

1.3.1.2 Clinical Trials

Whilst population-based, noninterventional studies provide important observational data, interventional clinical trials allow researchers to assess a treatment in comparable groups in a controlled environment. Most have approached this by restricting dietary salt intake and measuring the BP response, with the hope of clarifying the link between salt intake and BP. The results have often been summarised within meta-analyses.

Reductions in BP with dietary salt restriction have been reported. Midgley *et al*. (45) reviewed 56 randomised trials and noted that a restriction of dietary sodium intake, which reduced urinary sodium excretion to 95 mmol/d, elicited a decrease in BP within hypertensive subjects, but not in subjects with a normal BP. Moreover, He & MacGregor (46) limited the inclusion criteria to trials lasting more than 4 weeks. They also reported that BP dropped significantly (-4.96 mmHg SBP; -2.73 mmHg DBP) in hypertensive subjects upon reducing dietary salt intake to the daily WHO recommendation of ~5 g/day. However, this time a small but significant reduction in the BP of normotensive subjects, referring to those with a BP at around 120/80 mmHg, was also seen (-2.03 mmHg SBP; -0.97 mmHg DBP). Both effects were dose-dependent; incremental decreases in salt intake also provoked similar decreases in BP, however greater responses were observed in those with hypertension (46).

In contrast, studies exist which do not support the association of dietary salt and BP. For example, Graudal *et al*.'s (47) analysis noted no significant effect of reducing sodium intake on either SBP or DBP. In addition, Hooper *et al*. (48) concluded any reductions observed in BP with restricting salt intake were minimal and unrelated.

1.4 Salt Sensitivity

The existence of both supportive and contradictory evidence for the relationship between salt and BP demonstrates the heterogeneous nature of the physiological response to salt. An example comes from further analysis of the Dietary Approaches to Stop Hypertension (DASH) trial. Whilst an association between SBP and salt was observed, the response within the individual participants varied significantly (49). Furthermore, as touched upon in the previous section, mixed findings regarding the responsiveness of BP to a reduction in salt intake in normotensive individuals also exist. Miller *et al.,* (50) reported that restricting salt intake by 83 mmol/d elicited a highly variable, but overall significant, decrease in BP in healthy subjects with normal BPs. Together, these studies demonstrate BP responses to salt are

not uniform, but individualised, in both normotensive and hypertensive humans.

1.4.1 Defining salt-sensitivity

Dahl *et al.* were the first to gain awareness of the heterogenous nature of the BP response to dietary salt intake. Throughout their work in the 1950s, Dahl and colleagues consistently observed that a number of study subjects, including humans and experimental models of hypertension, exhibited no BP response at all to substantial increases in dietary salt intake, whereas others responded significantly (51, 52). This was despite the rigorous control of environmental influences in the animal studies and appeared independent of dietary duration, as the BP of some remained within the normal range even after months of excessive consumption. They began to question this phenomenon and thus, this marked the beginning of the two distinct categories; animals were divided into those with the greatest BP responses, referred to as ‘susceptible’, and those lacking any BP response, referred as ‘resistant’ (53). As a result, in 1962, the popular Dahl salt-sensitive and salt-resistant rat strains were generated (53, 54), refined (55) and have been characterised in an attempt to gain mechanistic insights into these varying BP responses ever since (reviewed by Lerman *et al*. (56)).

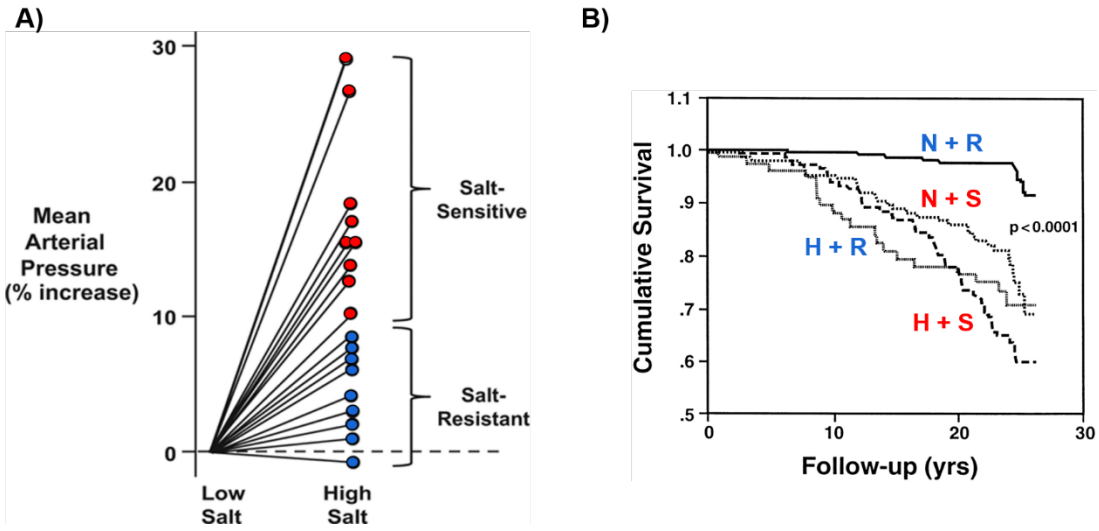

Figure 1.1: The salt intake-blood pressure response and implications for mortality.
A: graph depicting the BP responses to salt, adapted from Hall (57) with data from Kawasaki *et al*. (58). B: Kaplan-Meier survival curves depicting 4 different cohorts: normotensive and salt-resistant (N+R), normotensive and salt-sensitive (N+S), hypertensive and resistant (H+R), and hypertensive and salt-sensitive (H+S) subjects adapted from Weinberger *et al*. (59).

Kawasaki *et al*.'s report contained one of the first critical observations of the salt-sensitivity of BP in humans, leading to a definition (58). Hypertensive subjects were recruited, and BP was measured following a diet containing 9 mmol/d sodium for one week, which was then increased to 249 mmol/d. They noted that BP increased significantly in some of the subjects, but not all (58) (Figure 1.1 A). Those displaying such an increase were categorised as 'salt-sensitive', and those who did not as 'nonsalt-sensitive', which also became known as salt-resistant.

Thus, salt-sensitivity is defined as a BP which directly correlates with salt intake; as salt intake rises, so does BP. Salt-resistant individuals exhibit a lack of responsivity of BP to changes in salt intake. Generally, it is predicted that 30-50% of the hypertensive population are salt-sensitive, whereas a smaller but significant 25% of the normotensive population are salt-sensitive (60). Therefore, these differing responses could contribute to the significant heterogeneity observed in previous research.

1.4.2 Characteristics of salt-sensitivity

1.4.2.1 Demographic factors

Salt-sensitivity of BP is a dynamic trait; it changes throughout life. It has long been established that, particularly within industrialised countries, BP changes over time. A longitudinal study of both hypertensive and normotensive subjects demonstrated an age-related increase in BP, which was much more pronounced when accompanied by salt-sensitivity rather than salt-resistance (61). Importantly, the degree of the salt-sensitivity of BP also increases with age (61). Thus, age is a formative factor.

Race appears to be another demographic influence on the prevalence of salt-sensitivity. Studies have consistently found that the incidence of salt-sensitivity is higher within black hypertensive subjects, reported at 73% compared to 56% of white hypertensive subjects (62). Similar proportions have been noted in the normotensive population as well (62).

1.4.2.2 Genetic components and heritability

Since salt-sensitivity has been noted more frequently within certain races, a genetic component may potentially exist. Research has given credence to this, as significant similarities have been observed in the BP responses to reduced salt intake within families (63, 64), thus illustrating that this trait may be somewhat heritable. This has led to screening studies in an attempt to confirm and characterise the potential genetic basis to salt-sensitivity. For example, a candidate gene association study found a link between two variants of the sodium-bicarbonate co-transporter gene (*SLC4A5*) and salt-sensitivity (65). However, these are only two of many studies that have been assessed and some show promise however, with such complexity involved in BP homeostasis, no conclusive findings have arisen yet.

Since the focus of this thesis is on the physiological mechanisms underlying the BP response to salt intake, the genetic input has only been briefly outlined here. It has been reviewed in-depth elsewhere by Beeks *et al*., (66) and Felder *et al*., (67).

1.4.3 Salt sensitivity and disease

Weinberger *et al*. (59) made some fundamental observations regarding the salt-sensitivity of BP. Although salt-sensitivity has important implications for BP, it was also found to have a crucial impact on mortality, irrespective of BP. A long-term follow-up study was performed in which 430 normotensive and 278 hypertensive humans were initially screened for salt-sensitivity and then were re-evaluated 27 years later. Mortality was significantly, and unsurprisingly, linked to age and BP at the start of the study, however it was also linked to salt-sensitive status. Upon expressing cumulative mortality against years of follow-up (Figure 1.1 B), it was evident that survival dramatically reduced in the presence of salt-sensitivity in both hypertensive and normotensive humans (59), showing that salt-sensitivity is a potential predictor of mortality, regardless of BP status.

Following on from this, salt-sensitivity has also been identified as a risk factor for a number of diseases. In hypertensive humans, the presence of left ventricular hypertrophy (68) and microalbuminuria (69) was more often associated with the salt-sensitive trait over salt-resistance. Furthermore, salt-sensitivity was linked to nocturnal hypertension, in which the regular, healthy dip in BP that occurs overnight is absent (70), but returns upon decreasing dietary salt consumption (71). Together, these increase the risk of suffering cardiovascular events (68), thus suggesting that salt-sensitivity could be the underlying feature contributing to an individual's susceptibility for disease development and death.

1.4.4 Limitations of the measurement of salt-sensitivity in humans

There are many challenges facing the measurement of salt-sensitivity in humans. First, the use of two distinct categories, salt-sensitive and salt-resistant, can be misleading. This simplified approach assumes a biphasic response in which an individual's BP either changes with salt intake or it does not. This is not the case, however, as demonstrated by Luft *et al*. (72). Rather than an all-or-nothing reaction, BP elevations ranged from 1.5% to 34% that of baseline with increasing salt intake (60, 72), illustrating the continuous

nature of the trait. Due to this, there is significant variability between the definitions used by researchers to classify salt-sensitivity. In Kawasaki *et al*.'s study, individuals were deemed salt-sensitive following a 10% change in BP upon altering the salt content of the diet (58). However, others have classified salt-sensitivity in their study participants as an increase of 5 mmHg (73), whereas in other studies an increase in BP any less than 10 mmHg conferred resistance or was undefinable (62).

Along with discrepancies in the definition of salt-sensitivity, there are also differences in the methods used to evaluate it. As recognised by Weinberger and Fineberg, there is a volume element in BP responsivity, which is also influenced by the demographic factors (61) outlined in section 1.4.2 above. Protocols have thus been developed which integrate the expansion and contraction of volume into the steps towards the classification of salt-sensitivity. This involves the rapid infusion of saline, followed by volume and sodium depletion using a combination of a low salt diet and a diuretic prior to measurements (61). Acute manipulation of sodium and body fluid volumes may be beneficial for elucidating the mechanisms underlying the salt-sensitivity of BP, however the processes uncovered by this approach may differ from those underlying the long-term changes associated with habitual salt intake.

In addition to this are the methods used to determine salt intake, which range from self-reporting via questionnaires to the measurement of 24-hour urinary sodium excretion. The accuracy of both have been questioned. Challenges arise with self-reporting due to the difficulty to measure or keep track of salt added as seasoning at the table or in processed or takeaway foods. Further, the use of 24-hour urinary sodium excretion has also been criticised for underestimating an individual's intake, as studies usually acquire a single 24-hour sample before and after salt treatment and thus do not consider other means of loss, such as by sweat, or the day-to-day variability of salt intake. Regardless of this, 24-hour urinary sodium excretion remains superior to self-

report, as it is informative, reliable and practical to measure when determining salt intake for research purposes.

1.4.4.1 Clinical biomarkers of salt-sensitivity

The above methodologies suit the determination of salt-sensitivity within a research setting; however, overall they can be laborious and expensive and so are unlikely to be applicable to clinical practice. Researchers have attempted to rectify this by searching for biomarkers that are easy to measure non-invasively in the clinic. The ability to screen and identify the salt-sensitivity of BP could lead to the personalisation of treatment and improved outcomes for patients, as well as address the burden it places upon healthcare providers. Examples of potential biomarkers are plasma renin activity and atrial natriuretic peptide, as levels have been associated with salt-induced BP changes (74). Furthermore, urinary exosomes have been assessed as potential indicators of salt-sensitivity, as their contents can provide a snapshot of the processes occurring within the nephron. For example, it was hypothesised that excretion of protein mediators of tubular sodium reabsorption in urinary exosomes could reflect adverse changes in sodium handling and BP (75). However, these measures have proven inconsistent in the differentiation of salt-sensitivity from resistance (74). Therefore, a reliable biomarker has yet to be uncovered.

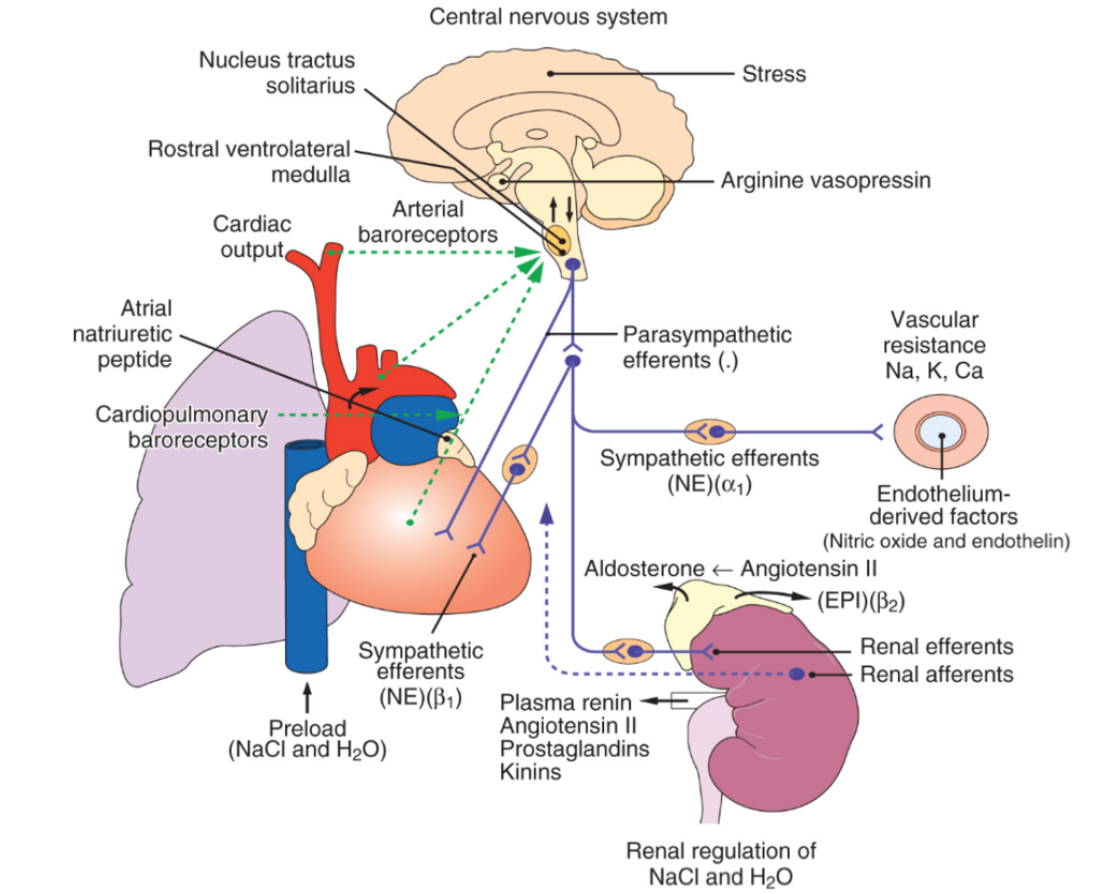

Figure 1.2: Multisystem involvement of blood pressure regulation.

Multiple systems and processes provide input into the regulation of blood pressure, as illustrated by this diagram adapted from Coffman (76). Cardiac output and total peripheral resistance determine blood pressure, which are determined themselves by the heart, the kidneys, the vasculature, the central and peripheral nervous systems, body fluid volumes and hormones, all of which contribute via complex feedback mechanisms.

1.4.5 Mechanisms underlying salt-sensitivity of blood pressure

The salt-sensitive trait has an adverse impact upon cardiovascular risk, potentially mediated by its effect on BP. However, the underlying mechanisms remain contentious and unclear. This is partially due to the shear complexity of the regulation of BP. Multiple systems contribute to its control, as demonstrated in Figure 1.2 and reviewed by Coffman (76), each of which is under the influence of a plethora of factors. Continued investigation into the processes by which salt influences BP can provide a better understanding of salt-sensitivity and thus shed some light on how it contributes to the risk of disease and mortality.

To achieve this, two overarching questions must first be addressed. How is salt-sensitive hypertension initiated, and how is it sustained? This thesis focuses on the two main contenders in the current field to answer these questions. Is dysfunction of the kidney or the vasculature responsible for initiating and maintaining salt-induced increases in BP? The hypotheses and proposed mechanisms are explored in the rest of this chapter.

1.5 Renal Dysfunction

1.5.1 Guyton's hypothesis: role of the kidney in long-term blood pressure control

Guyton and Coleman's computational model of the circulation introduced a new perspective to the views on the long-term regulation of BP in the late 20th century. It centres around the principle that variations in effective blood volume, rather than total peripheral resistance (TPR), initiate changes in BP (77, 78) (Figure 1.3). A major determinant of effective blood volume is extracellular fluid volume (ECFV), which itself is strictly regulated by salt and water balance. An imbalance between salt intake and output, for example during high dietary salt consumption, causes ECFV expansion, increased cardiac output (CO) and consequential rises in BP unless neutralised.

The kidneys are crucial in the maintenance of this balance over time. If increased salt intake is not counterbalanced through increased renal excretion, the excess salt and water can be retained and ultimately lead to circulatory failure. The kidney carefully regulates the balance of salt and water in the body through the pressure natriuresis (PN) response, in which increased pressure triggers the excretion of excess salt and water in urine. In healthy, normotensive humans, this increased output will offset high salt intake and normalise ECFV and thus BP. Equally, when BP declines below a certain level, kidney function shifts to favour the detainment of salt and water. Excretion decreases, and as a result, effective blood volume and CO increase once more, restoring BP.

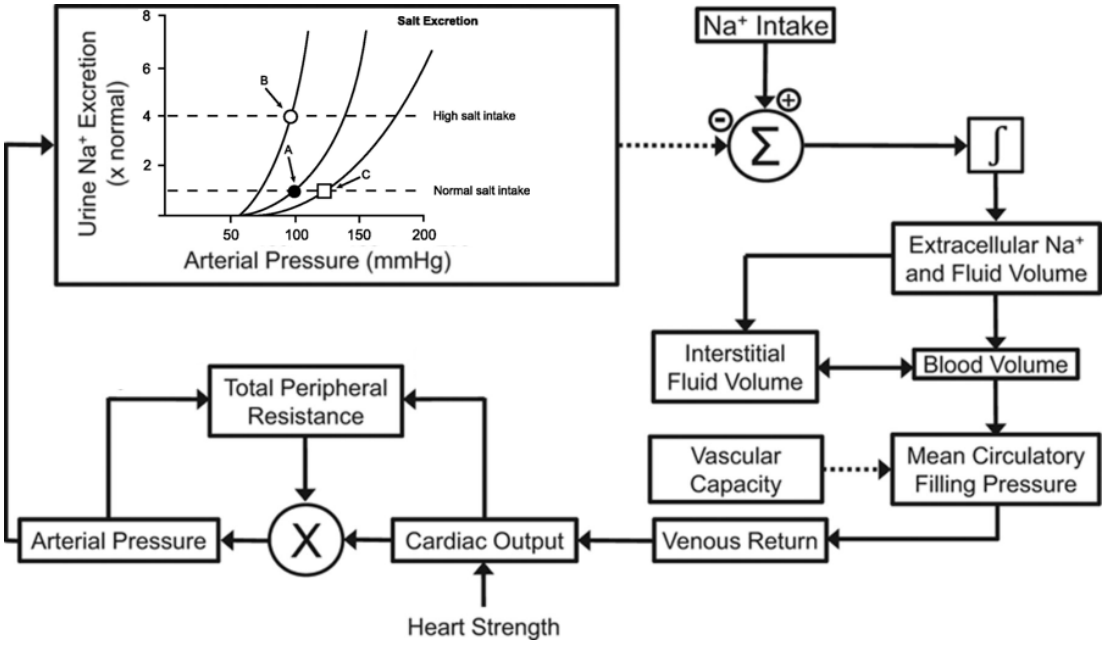

Figure 1.3: Schematic overview of the renal-body fluid feedback mechanism.
Diagram, merged and adapted from Hall (57) and Mullins *et al*., (79), illustrates the principles of the renal-body fluid feedback mechanism. Guyton's hypothesis proposes that an increase in salt intake disrupts the salt/water equilibrium of the body, leading to temporary rises in arterial pressure, which is corrected through a pressure-mediated increase in urinary sodium (Na^+) excretion. Initially, the salt/water imbalance induces extracellular fluid volume expansion, which influences blood volume and causes an increase in cardiac output. Transient rises in arterial pressure above a set point are detected by the kidney, which acts to increase urinary Na^+ excretion and normalise pressure as demonstrated by the renal function curve A. Curve B depicts a leftward shift during high salt intake to ensure more Na^+ is excreted at any given arterial pressure. Curve C depicts an impaired pressure response as it is shifted to the right, demonstrating that a higher arterial pressure is required to offset the changes to the salt/water equilibrium.

In the long-term, intake equals output and BP remains constant. Guyton described this fundamental feedback mechanism as possessing an 'infinite gain property' – the ability to recover the pressure-fluid equilibrium is boundless, and therefore, theoretically, alterations in BP would not be sustained without renal involvement (78).

1.1.1.1 Hall's approach to renal dysfunction in salt-induced hypertension

Hall's approach (57) adopts many of the concepts of Guyton's model. He argues that renal dysfunction, specifically blunting of the PN relationship, initiates salt-induced hypertension as it supports the retention of sodium.

1.5.2 The kidney in salt-sensitive hypertension

The contribution of the kidney to the genesis of salt-sensitive hypertension is evident within renal disorders. Damage during moderate to late-stage renal disease has been associated with increasing salt-sensitivity (80). For example, pre-hypertensive subjects with IgA nephropathy exhibited higher markers of glomerular and tubulointerstitial injury, which directly correlated with BP salt-sensitivity. Upon dietary salt restriction, BP decreased, as did their injury scores (81). This demonstrates that the degree of salt-sensitivity was related to the degree of renal damage prior to the occurrence of pathological increases in BP, which reversed when the environmental stimulus, dietary salt, was removed. Furthermore, salt-sensitivity is often enhanced with progressive renal decline seen in ageing (60) and in other diseases such as diabetes (82).

Cross-transplantation studies provide compelling evidence for the kidney as the main driver of sustained salt-induced increases in BP. Hypertensive patients with renal failure underwent kidney transplantation procedures with organs donated from normotensive volunteers, which lowered their BP to within the normal range 4.5 years on (83). Additionally, the post-transplantation BP responses of the previously hypertensive patients to salt intake were similar to those from the healthy controls (83). This shows that introducing a ‘normal’ kidney reversed the salt-sensitive hypertensive phenotype.

The evidence outlined above demonstrates that salt-induced increases in BP may originate and persist due to intrinsic disturbances within renal function. The potential mechanisms of this are evaluated next.

1.5.3 Pressure natriuresis relationship

The PN relationship defines the renal response of adjusting urinary sodium and water excretion to changes in arterial pressure, thus maintaining BP at an equilibrium point. Experiments performed by Hall and colleagues provide evidence for such a link between pressure and renal sodium excretion. Renal

arterial pressure was servo-controlled, which disabled the kidney's ability to detect pressure elevations, and a split-bladder preparation was utilised to collect urine and measure sodium excretion. Due to this, the PN response was lost and BP rose as if unimpeded (84), illustrating its important regulatory role.

1.5.3.1 Impairment of the pressure natriuresis relationship in salt-induced hypertension

According to Guyton's theory, any increase in pressure will be normalised by salt/fluid loss, unless intake or the PN curve is altered, or both (78). In salt-sensitivity, the excess salt due to high intake is said to be retained, causing ECFV expansion, increases in CO and a steady rise in BP. Kawasaki *et al*. (58) reported that salt-sensitive hypertensive subjects retained more sodium than those who were classified as salt-resistant whilst on a high salt diet. Additionally, sodium excretion similar to that of normotensive humans has also been observed, despite a higher BP that should, theoretically, induce an increase in excretion to equalise such a change (82). Thus, salt-sensitive humans are unable to excrete surplus salt as well as salt-resistant humans. This abnormal excretion of sodium is a potential indicator of a defect in the PN relationship, specifically a shift of the equilibrium point to a higher pressure, a characteristic of many human hypertensive phenotypes (57), as reviewed in (85). This means the PN curves, when measured, resemble curve C in Figure 1.3.

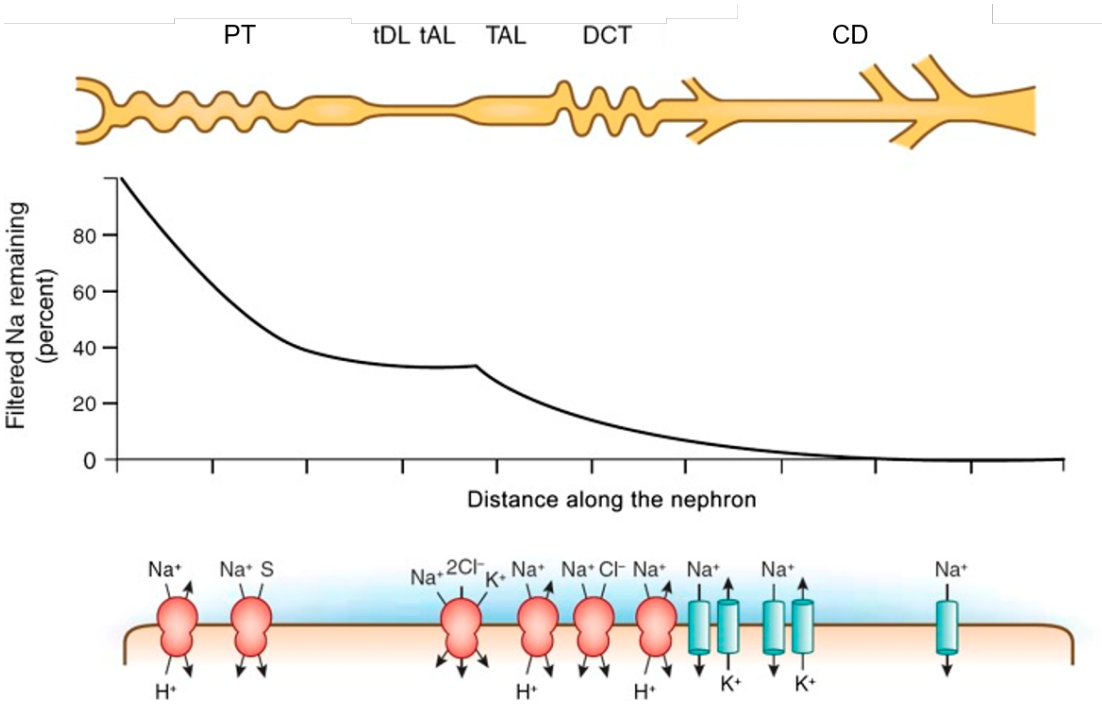

Figure 1.4: Percentage filtered sodium and renal sodium transporter distribution in the nephron. Schematic representation of renal sodium reabsorption across the nephron during a typical standard salt diet (100 mmol/d), adapted from Palmer & Schnermann (86). The graph depicts the sodium (Na) remaining in the glomerular filtrate expressed against the distance of the nephron as it travels along it. The red shapes denote transporters or exchangers, and the blue shapes ion channels, involved in the reabsorption process. The yellow tubule denotes the nephron divided into the different labelled segments. The proximal tubule (PT) accounts for 70% of sodium reabsorption, thin descending limb (tDL), thin ascending limb (tAL) and thick ascending limb (TAL) of the loop of Henle for 20-30%, the distal convoluted tubule (DCT) for 5-7% and lastly the collecting duct (CD), which accounts for tiny, final adjustments prior to excretion.

1.5.4 Renal salt handling

The kidneys are responsible for the filtration and excretion of electrolytes such as sodium, a process that is essential for fluid and BP homeostasis. Around 99.5% of sodium in the glomerular filtrate is transferred back into the bloodstream via reabsorption, thus usually <1% is expelled in the urine via excretion. These values reflect basal conditions and vary with dietary salt intake. Reabsorption is an active process fuelled by the sodium-potassium ATPase (Na^+-K^+ ATPase) located on the basolateral membrane. It is mediated by transporters situated along the nephron, which retrieve sodium from the tubule lumen via the apical membrane, pass it across to the basolateral membrane of the absorptive cells, and into the interstitial space.

Due to the presence of these transporters, the segments of the nephron have differing sensitivities to sodium (Figure 1.4); ranging from 70% reabsorption by the proximal tubule via the sodium/proton exchanger 3 (NHE3) to 0-5% by the distal convoluted tubule via epithelial sodium channels (ENaC). The expression and activity of these transporters, thus the overall reabsorption process, adjusts inversely with salt intake; when excess salt is present, transporter activity decreases, and vice versa when salt is scarce.

1.5.4.1 Abnormal renal tubular sodium reabsorption in salt-induced hypertension

Abnormal renal salt handling could play a key part in sodium retention and thus salt-sensitive hypertension. Using a Guytonian approach (78), an impairment in renal excretion capacity following high dietary salt intake could furnish the blunted PN response and therefore instigate and/or maintain salt-induced increases in BP.

This is evidenced by monogenic human diseases characterised by salt-induced hypertension originating from mutations in genes involved in tubular sodium reabsorption either directly, or as a secondary effect. A particular example is ENaC. ENaC, comprised of the three subunits α, β and γ, is responsible for mediating the fine control of sodium reabsorption in the terminal segment of the nephron, the distal tubule. Gain-of-function mutations in the β and γ subunits materialise as salt-sensitive hypertension known as Liddle's syndrome, which is associated with unregulated channel activity and, consequentially, aberrantly increased reabsorption of sodium. It has recently been documented that common variants of the genes encoding the ENaC subunits exist within populations and have been hypothesised to underlie the variations in the BP response to salt. The GenSalt study found an association between these variants, the salt-sensitivity of BP and the BP-lowering effects of dietary salt restriction (87). Additionally, single nucleotide polymorphisms identified in the genes of known regulators of the sodium-potassium-chloride cotransporter 2 (NKCC2), the transporter responsible for reabsorption in the thick ascending limb of the loop of Henle, has also been linked to renal

damage and salt-sensitivity potentially via increased NKCC2 activity (88). These results confer an important role for renal sodium reabsorption in salt-sensitive hypertension, specifically dysregulated transporter function.

1.5.5 Humoral mediators: the renin-angiotensin-aldosterone system

The renin-angiotensin-aldosterone system (RAAS) is an important modulator of BP via its control of fluid balance and sodium excretion. Upon activation, renin is secreted into the bloodstream from the kidneys and acts upon angiotensinogen, cleaving it to produce angiotensin I and subsequently angiotensin II (ANGII) via angiotensin converting enzyme. ANGII triggers the release of the steroid hormone aldosterone from the adrenal cortex and collectively, these final components act to increase tubular sodium reabsorption.

During increased salt intake, RAAS activity is inhibited and results in decreased levels of ANGII and aldosterone, which has been shown to augment the PN relationship and thus sodium excretion (89). However, the absence of the suppression of RAAS activity has been associated with salt-sensitivity. According to the prevailing theory, persistently high levels of ANGII and aldosterone upon salt loading blunt the PN relationship, which supports a higher BP (57, 78). Further to this, primary aldosteronism is a human disorder that is characterised by pathologically increased aldosterone production, resulting in excessive water and sodium retention and hypertension. This phenotype is exaggerated when combined with high salt intake (90), which has also been reflected in animal studies as the infusion of aldosterone with renal impairment induces increased BP that is dependent upon salt intake (91).

1.6 Vascular Dysfunction

1.6.1 The vasodysfunction theory

Vasodysfunction, referring to an impaired vascular response to increases in dietary salt intake, as a cause of sustained salt-sensitive hypertension is advocated by Morris *et al*. (92). The focus is upon investigating the

mechanisms underlying the abnormal vascular response to high salt intake and its role in the genesis of hypertension in salt-sensitive humans. According to this theory, high dietary salt intake causes haemodynamic changes within those who are salt-resistant and normotensive, such as increased CO and stroke volume. This also stimulates sodium retention and changes to body fluid volumes in these individuals. A resulting decrease in systemic vascular resistance (SVR), rather than solely an elevation in renal sodium excretion, normalises these events and thus prevents any adverse salt-induced alterations to BP. However, SVR fails to decrease in salt-sensitivity and so remains irregularly high, leading to salt-induced BP elevation.

By shedding light on the salt-induced vascular effects here, it could provide an insight into those mediating the high SVR, also synonymously referred to as TPR, previously observed within many forms of hypertension (92).

1.6.1.1 Contrasting views to the conventional theory

Hall's standpoint supports the Guytonian hypothesis that chronic changes in BP following high salt are dependent on increased sodium retention through impaired renal excretion capacity (57, 78) (Figure 1.5 A). Whereas, the premise of Morris *et al*.'s (92) theory is that pathologically high SVR in response to high salt intake, due to underlying vascular abnormalities, triggers salt-induced hypertension (Figure 1.5 B & C). Thus, the focus shifts from renal to vascular defects, such as impaired vasodilation, as the salt-induced initiating event.

Morris *et al*. (92) describe the haemodynamic changes that occur following increased dietary salt intake as typical. For example, the increase in sodium retention and CO that are stated as changes leading to high BP in salt-sensitivity in the conventional theory, are actually standard responses to high salt intake and are present in both salt-sensitive and salt-resistant subjects with a normal BP (Figure 1.5).

Hall's theory allows for increases in SVR; however, he states that such increases occur as consequences of a high BP rather than as an initiating event. Upon running Guyton's computational model, a change in TPR could not support any long-term changes in BP as it does not modify the PN relationship (78). However, not all humans display evidence of impaired renal sodium handling, and there is clinical data for vascular dysfunction present before and after salt-induced increases in BP.

Figure 1.5: Conventional volume-loading vs. vasodysfunction theory of salt-sensitive hypertension.

Schematic overviews of the sequence of events in salt-sensitive humans leading to increases in blood pressure as per A) the volume-loading theory (57, 77) and C) vasodysfunction theory (92). The red boxes indicate the proposed pathologic events initiating salt-induced hypertension. The volume-loading theory (A) characterises salt-sensitive humans as experiencing pathological sodium retention, which causes a sustained increase in blood pressure. B) Data from normotensive humans obtained by Schmidlin *et al*. (73) illustrates a blunted decrease in systemic vascular resistance (SVR) in the salt-sensitive group, whereas both groups had a positive cumulative sodium (Na^+) balance. The red arrows depict the changes in salt-sensitive humans, and the blue the changes in salt-resistant humans. Thus, the vasodysfunction theory (C) characterises salt-sensitive humans as having abnormally high SVR, which causes sustained increases in blood pressure. Adapted from Morris *et al*. (92). RVR; renal vascular resistance.

A) **Volume-loading theory**

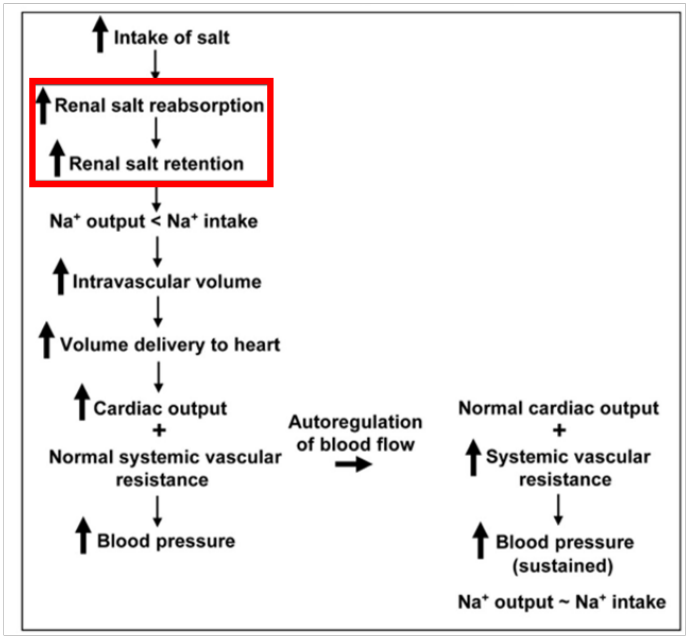

B)

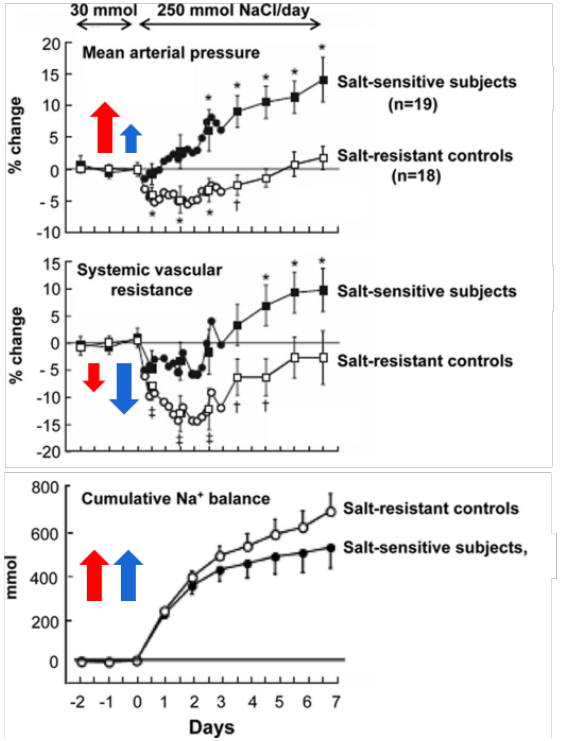

C) **Vasodysfunction theory**

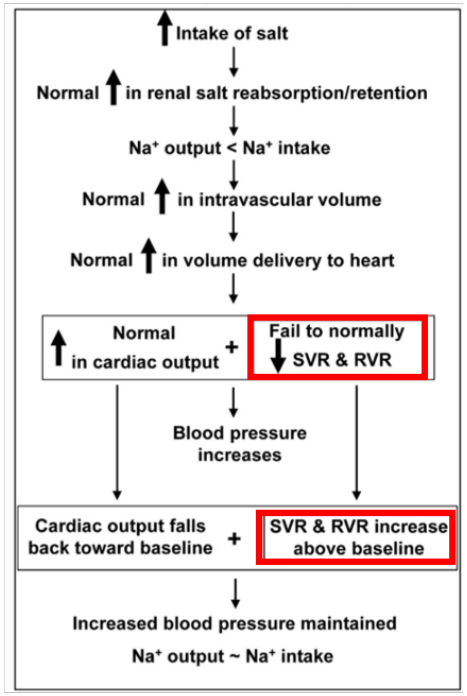

1.6.2 Vascular resistance response to high salt intake

The effects of salt on vascular resistance have been studied for decades. In normotensive subjects, peripheral vascular resistance decreased during a high salt intake (72) whereas the reverse was noted within pre-hypertensive subjects (93). This illustrates an abnormal vascular response to salt preceding hypertension.

Further to this, Schmidlin *et al*. (73) have aptly demonstrated the role of the systemic vasculature in the genesis of salt-sensitive hypertension. In 11 salt-sensitive and 12 salt-resistant humans with normal BPs, dietary salt intake was increased from 30 to 250 mmol/d whilst mean arterial BP (MABP), SVR and sodium balance were measured simultaneously over a 1-week period. Salt-sensitive humans displayed a progressive increase in MABP; however, SVR did not decrease to the same extent as in salt-resistant humans with high salt. No differences were noted in cumulative sodium balance – in fact, balance became positive in both the groups, suggesting an increased but equal retention of sodium (73) (Figure 1.5 B). These findings reveal that inappropriately high SVR, rather than sodium retention, accompanied the salt-induced increase in MABP observed, thus supporting vascular dysfunction as the initiating event.

1.6.3 Vascular physiology and function

Vessel diameter is an important determinant of vascular resistance. The diameter of small arteries, arterioles and capillaries regulates tissue blood supply rapidly in response to haemodynamic changes. They consist of three distinct layers suited to this role: the endothelium, a single layer of cells that directly interfaces the circulating blood; the vascular smooth muscle (VSM) layer which physically carries out the changes in vessel diameter; and the adventitia, a layer of fibrous connective tissue surrounding and supporting the artery.

1.6.3.1 Vascular smooth muscle-mediated function

Vasoconstriction involves the active narrowing of the vessel diameter via VSM contraction. This process is mediated by calcium-dependent actin-myosin interactions. Contraction can be triggered by changes in pressure via the myogenic response. A constant, basal level of contraction, referred to as tone, is required in order to adjust blood flow. However, in hypertension, the chronic increase in pressure can overstimulate VSM cells and lead to hypersensitivity and remodelling, as reviewed by (94).

1.6.3.2 Endothelium-mediated function

Vasodilation is instigated primarily by the endothelial layer. Positioned with exclusive access to the vasoactive components carried in the bloodstream, the endothelium mediates vascular tone, inflammation, and cell-cell adhesion. This monolayer generates and secretes its own range of vasoactive stimuli to adjust vessel diameter, the most widely researched being nitric oxide (NO). NO, converted from the amino acid L-arginine by endothelial NO synthase (eNOS), stimulates vasodilation by diffusing through to the VSM layer and inhibiting contraction in a cyclic GMP-dependent manner. Other vasoactive stimuli inducing vasodilation consist of prostacyclin and acetylcholine (ACh) (95), and those influencing vasoconstriction consist of endothelin and ANGII (96).

Moreover, the vasodilatory response can transpire through mechanical stimulation. Shear stress, generated by the force of blood flow, can itself activate NO signalling and vessel relaxation through deformation of endothelial cells (97).

1.6.4 Impaired vasodilation in salt-sensitivity

Since an inability to decrease SVR in response to high salt is observed, this suggests impaired vasodilation may have a role in salt-sensitivity and its impact on BP. Investigations have involved the administration of ACh, as it induces endothelial-dependent vasodilation, and sodium nitroprusside (SNP), as it induces endothelial-independent vasodilation through NO donation.

Miyoshi *et al*. (98) explored this in hypertensive salt-sensitive and salt-resistance humans and, by comparing these two groups, observed that the salt-sensitive humans displayed significantly decreased ACh-induced, but not SNP-induced, vasodilation during increases in salt intake. Tzemos *et al*., (99) also examined this in healthy normotensive humans, noting that increasing salt intake to 200 mmol/d increased SBP whilst also suppressing ACh-evoked vasodilation alone. Jablonski *et al*., (100) reported that restriction of dietary salt intake to ~70 mmol/d reduced BP and enhanced flow-mediated and ACh-induced vasodilation in older adults with borderline high BP. However, these effects were deemed unrelated to the BP changes observed, thus illustrating that the benefits of salt restriction go beyond the reduction in BP.

This vasodilatory impairment has also been seen with salt-resistance, and independently to BP. DuPont *et al*. (101) recruited subjects with normal BPs and measured flow-mediated dilation (FMD) in response to significantly increased salt intake at 300-350 mmol/d or decreased intake at 20 mmol/d. Compared with decreased salt intake, FMD was attenuated after 7 days high salt. Similar findings were reported by Barić *et al*. (102), in which the salt-induced blunting of vasodilation was also unrelated to fluid volume and retention, suggesting salt itself triggers this impaired response autonomously.

The effect of dietary salt on vascular function is evident in both hypertensive and normotensive, salt-resistant and salt-sensitive subjects. Thus, these results show that salt has an impact upon overall vascular health, irrespective of BP. Since dysregulated endothelial function is predictive of later cardiovascular events (103), perhaps this underlies the link between high salt intake and increased CVD and death. Many potential mechanisms have been suggested, including reduced NO bioavailability and/or VSM sensitivity to NO (104-106), redox imbalance and oxidative stress contributing to NO uncoupling (107, 108), and inflammation (109, 110).

1.7 Hypothesis and Aims

1.7.1 Summary and aims

Two main theories propose contrasting mechanisms behind how an increase in dietary salt intake leads to the initiation and maintenance of hypertension. The conventional approach identifies a disturbance in renal excretion as the culprit, inducing sodium retention and allowing salt-induced increases in ECFV, CO and thus BP (57). On the other hand, the vascular approach attributes it to an inappropriately high SVR, in the absence of pathologic changes to sodium balance and fluid volumes (92).

Therefore, the aims of my PhD are to further investigate the salt-induced changes to renal and vascular function, and thus their role in generating salt-sensitive hypertension.

1.7.2 Selection of diet

Human physiology requires <1 g/d of salt, whereas average global intake exceeds this by ten-fold, recorded at 10 g/d (6). High salt diets have been used in cardiovascular research to interrogate its adverse impact upon health, ranging from 1.3% Na to 8% NaCl (111, 112). For my PhD, I selected a high salt diet consisting of 3% Na and a standard salt diet consisting of 0.25% Na. This created around a ten-fold difference in dietary salt, which is reflective of current, excessive human consumption across the globe.

1.7.3 Selection of mouse model

There are numerous studies of experimental salt-sensitivity (113, 114). Approaches used in the past involve the pharmacological induction of salt-sensitive hypertension, for example by ANGII or deoxycorticosterone acetate (DOCA)-salt infusion, as well as genetic manipulation of components ranging from 11β-hydroxysteroid dehydrogenase type 2 (11βHSD2) involved in mineralocorticoid signalling (111, 115) to salt-inducible kinase-1 (SIK1) in the regulation of Na^+-K^+ ATPase function (114, 116). In my thesis, I take a reciprocal approach and examine the responses of C57BL6/J mice to salt.

C57BL6/J mice have been widely used in cardiovascular research; however, the current literature fails to unite regarding their BP responsiveness to salt. Many cite this strain as salt-resistant and so use it as a control or a background for transgenic models (117-121), although reports have demonstrated its salt-sensitivity (122, 123). In a pilot radiotelemetry study performed by a member of our lab, BP was seen to increase in C57BL6/JCrl mice during 1 week of high salt feeding (Figure 1.6 A), with MABP significantly increasing by ~9 mmHg in the first 3 days (Figure 1.6 B). These observations were part of a larger experiment, and so the effects of salt alone were only observed for 1 week. This illustrates that C57BL6/JCrl mice may potentially have a salt-sensitive BP. Consequently, to delve into my above aim, I aspire to determine their BP response to salt and hence characterise the mechanisms underlying this response.

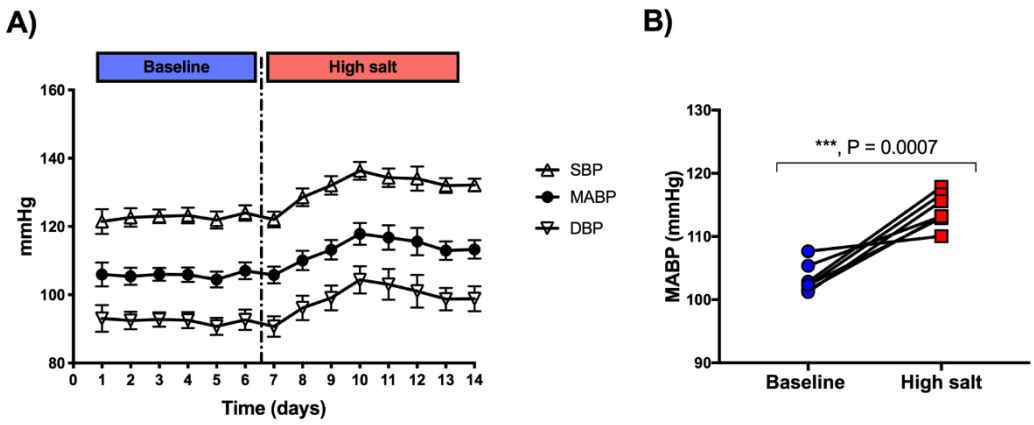

Figure 1.6: Pilot data on the blood pressure response to salt in C57BL6/JCrl mice.
A radiotelemetry experiment performed in C57BL6/JCrl mice (n=7) by Miss Hannah Costello identified an increase in systolic (SBP), diastolic (DBP) and mean arterial blood pressure (MABP). Telemeter devices were implanted under isoflurane anaesthesia, mice recovered over 1 week and then baseline measurements were obtained on a standard salt diet (0.25% Na) for a further week. Mice were then transferred to a high salt diet (3% Na) for another week. Data are mean ± SD. A) mean day-to-day SBP, DBP and MABP increased with high salt intake. B) 24-hour mean MABP. Analysis via a paired *t* test was carried out.

1.1.2 Hypothesis

The hypothesis of my thesis is:

C57BL6/JCrl mice display salt-induced hypertension attributed to renal dysfunction, specifically an impaired PN relationship in response to high salt.

2 Materials and Methods

2.1 Animals

2.1.1 Sources of animals and husbandry

All experiments involving animals were performed within the UK Home Office regulations under a Home Office Project Licence and in accordance with the Animals (Scientific Procedures) Act 1986. The proposed design and protocols were reviewed and accepted by the University's Animal Welfare and Ethics Review Board prior to an experimental start date. Adult male C57BL6J/Crl mice aged 8-10 weeks old were obtained from Charles River Laboratories (Tranent, UK) and housed at the Bioresearch & Veterinary Services small animal facilities (University of Edinburgh, UK). Here, they underwent an acclimatisation period of at least one week prior to an experimental start date and were maintained under controlled conditions, which included 12-hour light-dark cycling (7AM-7PM) and a temperature of 22-5 ºC.

2.1.2 Diet and water intake

Throughout all experiments, mice had access to water *ad libitum*. A standard salt diet (Rat and mouse maintenance diet 1; RM1; Special Diet Services, UK) containing 0.25% Na was provided to all mice during acclimatisation and as the control diet. The high salt diet consisted of a pellet diet containing 3% Na (829504: Special Diet Services, UK). For the remainder of my thesis, I abbreviate these diets as follows: the 0.25% Na diet as the standard salt diet (SSD) and the 3% Na diet as the high salt diet (HSD).

2.2 Measuring Blood Pressure using Radiotelemetry

Radiotelemetry is the gold standard for assessing cardiovascular parameters such as BP, heart rate and locomotor activity in rodents. It allows round-the-clock measurements within conscious, unrestrained animals and so

significantly minimises the impact of human-related stress upon these recordings (56).

2.2.1 Device set-up

PA-C10 telemeter devices were purchased from Data Science International (DSI). Since devices are transported in the “off” mode, they were switched “on” via a magnet and activated via coupling them with receivers and obtaining an offset BP recording of ± 3 mmHg. The devices were set-up using their individual calibration values with the data acquisition software provided by DSI, Ponemah v6.12.

2.2.2 Surgical procedure for device implantation

The implantation of telemeter devices was completed by the manager of the Centre’s *in vivo* Physiology Laboratory, Mr Kevin Stewart. Inhalation anaesthetic consisting of 4% isoflurane in oxygen was delivered within an induction chamber. Following this, mice were transferred to a heat mat in the supine position and isoflurane was reduced to 2-3% via a nose cone to maintain appropriate anaesthetic depth. A small dab of Lacri-lube® eye ointment was used to prevent ocular dryness whilst unconscious. Buprenopine (0.1 mg/kg, Vetergesic®) was administered by subcutaneous injection, followed by a bolus of 0.9% sterile physiological saline solution.

The exposed neck of the animal was shaved to allow greater access and wiped with an iodine scrub, before a 3 cm skin incision was made along the midline. The skin was gently prised from the muscle using tissue-separating scissors, creating a subcutaneous pouch in which the transmitter would sit. Following this, the carotid artery was located and carefully teased away from the vagus nerve in order to apply a ligature and occlude the vessel in preparation for an incision. Using a bent 23-gauge needle (BD Microlance, FST), the incision was made between the ligatures and the gel-containing catheter of the device was cautiously threaded into the artery and held in place by further ligatures. Tissue glue (3M Vetbond) was applied as an extra precaution. Once this had set, the area was irrigated with sterile saline and the transmitter inserted into the previously made pouch under the skin.

Having checked and confirmed the functionality of the device in its new position with a radio, the wound edges were drawn together and secured using 4-0 absorbable suture silk (Vicryl).

Isoflurane delivery ceased and animals received oxygen whilst they gradually came around from the anaesthesia, before being transferred to an incubator heated to 34 ºC for recovery. Analgesic was administered orally within strawberry-flavoured jelly cubes (Hartley's, UK) made up with 0.02mg/ml buprenoprine (Vetergesic®). Mice had previously been familiarised with the jelly, without the analgesic, before the study and so consumption was not a concern. During the first week of recovery, mice had *ad libitum* access to the jelly and soft RM1 (0.25% Na) pellets that had been soaked in drinking water, referred to as mash, until body weight normalised.

2.2.3 Data acquisition and analysis

During the 6-week experimental period, the telemeter devices recorded BP, heart rate and activity over one minute every half an hour at a frequency of 1 Hz. Daily (24-hour) averages were calculated to visualise and compare the day-to-day impact of dietary salt modification. To assess any changes to the day-night pattern, 5-day data bins were used and a 5-hour moving average was applied to smooth the data. 'Daytime' data consists of 12-hour averages between 7:00AM and 6:30PM (Zeitgeber; ZT 0-12) and 'night-time' data between 7:00PM and 6:30AM (ZT 12-24).

2.3 *In vivo* Assessment of the Acute Pressure Natriuretic Response and Renal Blood Flow

The renal response to increases in sodium intake and BP can be assessed experimentally *in vivo* via the following protocol. All surgical techniques were performed by the Centre's manager of the *in vivo* Physiological Laboratory Mr Kevin Stewart, and all sampling and analysis was carried out by myself.

2.3.1 Surgical protocol

Following either the SSD or HSD, mice were anaesthetised with an intraperitoneal injection (IP) of 120 mg/kg thiobarbiturate (Inactin®, Sigma).

Anaesthetic depth was determined via blink or toe pinch reflexes and maintained accordingly with small bolus doses of 10-50 mg/kg when necessary. Each animal was placed on a heat mat in the supine position allowing access to the abdomen and thorax, and body temperature was monitored through the TCAT-2LV animal temperature controller using a RET-4 rectal probe (Physitemp, New Jersey).

Local anaesthesia consisting of 1.5% lidocaine was subcutaneously administered to the neck. Following this, the left jugular vein was cannulated to aid the administration of infusate, pharmacological substances and further anaesthetic when required. This was done by gently separating the perivascular fat to expose the vein, ligating it and applying a small incision for the insertion of P10 tubing (Smiths medical) held in place by a 5.0 suture silk ligature (Fine Science Tools, Germany). This cannula was used to infuse the animal with an infusate solution (100 mM NaCl, 15 mM $NaHCO_3$, 5 mM KCl) containing 0.25% fluorescein isothiocyanate (FITC) inulin (pH 7.4, Sigma UK) at a rate of 0.25 mL/hr/10gbw via an infusion pump (AL2000, World Precision Instruments) throughout the surgical and experimental protocol. A tracheostomy was performed to keep the airway clear.

Carotid artery cannulation allowed for the monitoring of BP via PowerLab data acquisition software connected to a ML224 Bridge Amp (AD Instruments) and for blood sample collection. The artery was carefully detached from the vagus nerve and two ligatures were applied a few millimetres apart. This temporarily occluded blood flow in order to make an incision and insert and secure P10 tubing containing 20 units/mL heparin saline (Sigma Aldrich, UK) without excessive blood loss. A bladder catheter, consisting of P50 tubing attached to a segment of P10 tubing, was prepared for urine sampling. Following the final step in the surgical procedure, the infusion rate was increased to 0.3 mL/hr/10gbw to help replenish any lost fluids. At the end of the protocol, animals were humanely euthanised with an overdose of anaesthetic and circulatory cessation was confirmed via cervical dislocation.

2.3.2 Inducing the acute pressure natriuresis response

During the surgical protocol, a laparotomy was carried out in order to expose the mesenteric and coeliac arteries, along with the distal aorta. Loosely tied ligatures were prepared and placed around these major arteries. Animals underwent an equilibration period of 30 minutes before the sampling periods were started. These consisted of a 30-minute baseline period, followed by two 20-minute ligation periods in which BP was increased. Within the first ligation period, the coeliac and mesenteric arteries were tied off to raise BP, followed by the distal aorta in the second ligation period to amplify this. Urine was collected via the bladder catheter into 500 µL Eppendorf tubes throughout each of these periods, weighed and stored at -20 ºC in mineral oil to avoid sample loss by evaporation. Arterial blood samples (50 µL) were acquired via the carotid artery cannula at the start and end of each period. At the end of the experimental protocol, a terminal blood sample was collected into ethylenediaminetetraacetic acid (EDTA)-coated tubes (Sarstedt, Germany). Haematocrit was recorded and plasma was then obtained via centrifuging the blood samples at 2,000 xg for 5 minutes and stored at -20 ºC.

2.3.3 Measuring renal blood flow

Renal blood flow (RBF) was assessed *in vivo* using a mouse PSL series nano-flow probe (Transonic Systems, Netherlands). The left renal artery was isolated by carefully separating the adherent perivascular fat and the probe was placed and held around the artery, as depicted in Figure 2.1. Flow was recorded via PowerLab data acquisition software connected through a perivascular flowmeter (Transonic Systems, Netherlands).

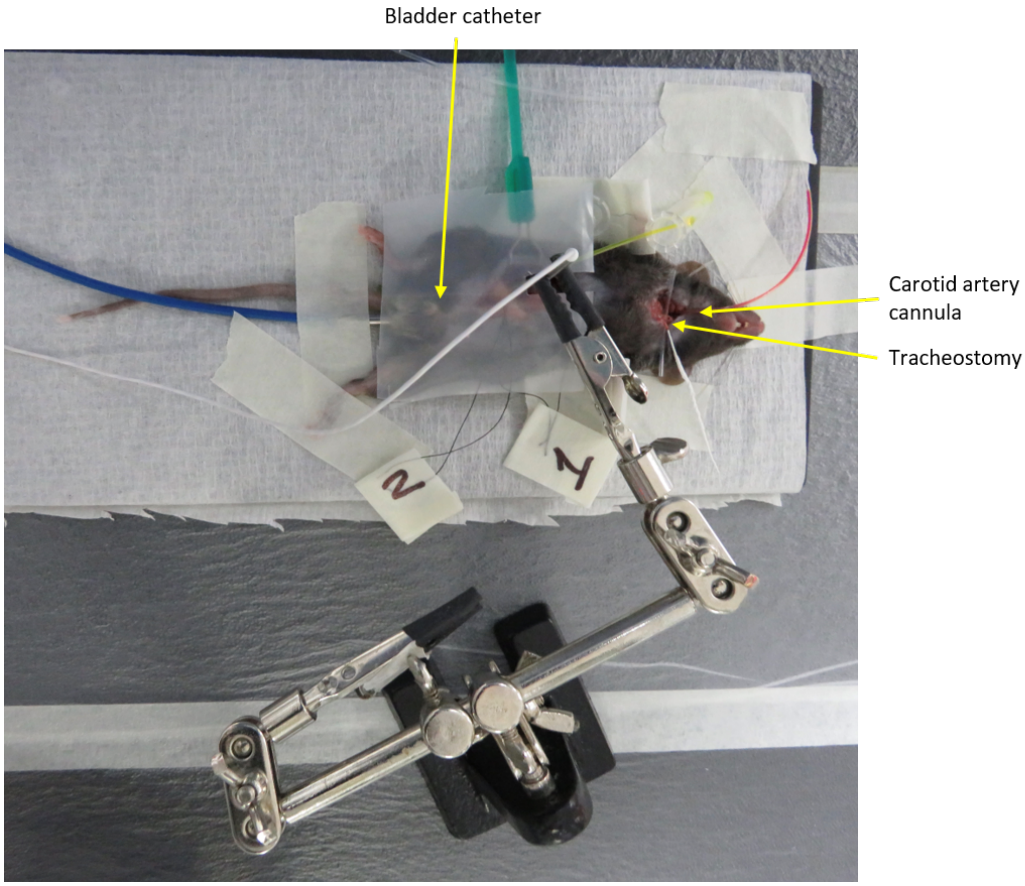

Figure 2.1: Photograph depicting the experimental setup for inducing the acute pressure natriuresis response.

The ties labelled '1' illustrate those around the mesenteric and coeliac arteries to be tightened during the first ligation period, and the ties labelled '2' illustrate those around a section of the distal aorta to be tightened during the second ligation period.

2.3.4 Sample analysis

2.3.4.1 FITC-inulin assay

The gold standard for determining glomerular filtration rate (GFR) involves measuring the urinary excretion rate of FITC-inulin, a biologically inactive substance which is freely filtered and non-toxic. Since it is not metabolised, secreted or reabsorbed along the nephron, its clearance at specific timepoints can be used to estimate GFR (124). HEPES buffer (pH 7.4) was used to dilute urine 1:10,000 and plasma 1:100 as FITC-inulin fluorescence is pH-dependent. A FITC-inulin stock solution at 1 mg/ml was made in order to generate a standard curve and each sample was applied to a Microfluor black 96-well plate (Thermoscientific, UK) in duplicate. Plates were read at a

wavelength of 538 nm following excitation at 428 nm by a microplate reader (Infinite M1000, Tecan). Firstly, urinary flow rate was calculated by multiplying the volume of urine produced (mL) by the specific density of urine at 0.016, and further divided by the duration of the collection period (mins). GFR (mL/min) was then calculated using the equation below:

$$GFR = \frac{(Urinary[inulin]\ x\ urinary\ flow\ rate)}{Plasma\ [inulin]}$$

2.3.4.2 Electrolyte analysis

Electrolyte analysis was carried out using the Spotchem EL electrolyte analyser (Woodley Veterinary Diagnostics, UK). Whole blood samples were measured undiluted, and urine and plasma samples were measured via the method described in detail later in section 2.7.2 Electrolyte Analysis.

2.4 Estimating Messenger RNA Transcript Levels using qPCR

Quantitative PCR (qPCR) was used to quantify messenger RNA (mRNA) expression. This sensitive, high-throughput method allowed the fast and precise interrogation of the biological processes involved within the renal and vascular responses to high salt. As two tissue types were investigated, a general overview applicable to the processing and analysis of both will be provided here. The specific protocol for kidneys can be found in Results chapter 4 section 4.2.2, and for arteries in chapter 5 section 5.2.3.

2.4.1 Preparation of samples

The tissues of interest were rapidly excised and placed in RNA*later* RNA stabilisation reagent (QIAGEN, UK) for 24 hours at 4 ºC, before being transferred to -80 ºC in sterile 2 mL Eppendorf tubes and stored until the time of the analysis. The culling of animals and tissue harvest were not performed at any specific time of day. Prior to sample handling, workspaces and equipment were sterilised via autoclaving and the use of RNaseZap™ RNase decontamination solution (InvitrogenTM). Reagents such as RNase-free water (QIAGEN, UK) and disposable equipment such as RNase-free filter

tips and tubes were also utilised where possible, as the introduction of contaminating RNases can compromise the experimental output. With these precautions in place, frozen samples were submerged into room temperature lysis buffer, Buffer RLT (QIAGEN, UK), along with a stainless-steel bead and homogenised until liquefied at top speed using a TissueLyser II (QIAGEN, UK). RNA was then extracted using spin columns via the instructions of tissue-specific RNeasy Isolation kits (QIAGEN, UK). The resulting RNA was either stored at -80 ºC or kept on wet ice for subsequent quality control assessments outlined below.

2.4.2 RNA concentration and integrity

The Nanodrop 1000 spectrophotometer (Thermoscientific, UK) was used to quantify the RNA obtained by reading its absorbance at 260nm and providing a concentration in ng/µL. A measure of RNA purity can also be generated by using sample absorbance ratios. RNA with an absorbance ratio at 260 and 280 nm (A260/280) ranging 1.7 - 2.2 was taken forward, as an A260/280 ratio <1.7 suggests contaminating agents such as phenol may be present.

Another indicator of RNA integrity is the absorbance ratio at 260 and 230 nm (A260/230), as co-purified contaminants can produce an A260/230 ratio of <1.8. However, there is some uncertainty as to whether a low A260/230 ratio significantly affects downstream investigations such as qPCR. Since no universal limit has been agreed upon and other studies have proceeded without considering the A260/230 ratio with successful qPCR results (125), RNA samples were not excluded based on A260/230 ratios alone here.

RNA integrity was also confirmed by gel electrophoresis using 1% agarose with 0.5% Tris-borate-EDTA (TBE) and 0.05% ethidium bromide. RNA samples (0.5-1 µg per lane) were loaded onto the gel mixed with the tracking dye Orange G and separated at 80 V for 1 hour. The appearance of two distinct bands, with the top band double the intensity of the bottom, represent 28S ribosomal RNA (rRNA) and 18S rRNA and thus, intact RNA (Figure 2.2). The smudging or merging of bands was indicative of damaged RNA, and so samples were not carried forward.

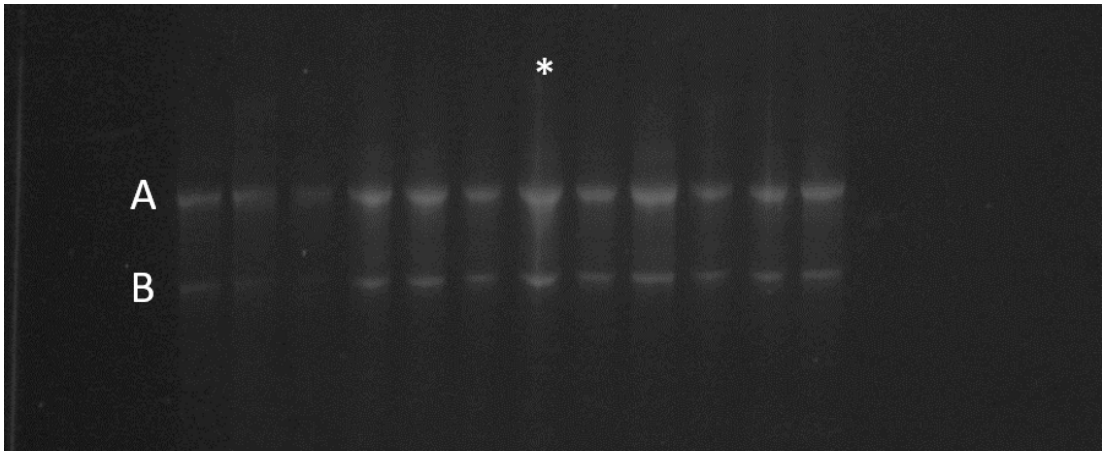

Figure 2.2: Photograph representing RNA samples resolved by gel electrophoresis.
Each lane was loaded with 0.5-1 µg RNA, run at 80 V for 1 hour. As a result, two separate ribosomal bands stained with ethidium bromide were observed, confirming the RNA sample was intact. (A) 28S ribosomal RNA; (B) 18S ribosomal RNA; (*) degraded RNA sample.

2.4.3 Reverse transcription

The Applied Biosystems high capacity cDNA reverse transcription (RT) kit (Life Technologies) was used to synthesise complementary DNA (cDNA) from RNA. Samples and kit reagents were defrosted on wet ice, before the RNA samples were diluted with RNase-free water to the same concentration. With a total volume of 20 µL per reaction, a mastermix was made up with the following components: 10 µL 2x RT buffer, 1 µL 20x enzyme mix, and 9 µL diluted RNA sample. Alongside this, controls were set up with RNase-free water replacing either the enzyme mix or the RNA sample. Once complete, samples and controls were run under the following conditions: 37 ºC for 60 minutes, 95 ºC for 5 minutes and 4 ºC for an optional length of time, in the Veriti 96-well thermocycler (Applied Biosystems, UK). The resulting cDNA was stored at -20 ºC.

2.4.4 Gene expression by qPCR

2.4.4.1 Designing assays

The Universal ProbeLibrary assay design center (URL: https://lifescience.roche.com/en_gb/brands/universal-probe-library.html#assay-design-center) was a useful tool for generating assays against specific genes-of-interest. Assays, consisting of primer sets and a suitable hydrolysis probe, were chosen based on whether the amplicon

traversed the boundary between two exons or, ideally, an exon and an intron. This did not include those situated within the first or the final intron, as these regions often contain single nucleotide polymorphisms (126). Further criteria included similar melting points for both forward and reverse primers, %GC content >50 and nucleotide repetition <4 in a row, as these increase the probability of complications such as mispriming.

Once generated, primer sets were checked via nucleotide BLAST using the NCBI database (URL: https://blast.ncbi.nlm.nih.gov/Blast.cgi?PAGE_TYPE=BlastSearch). All assays used are shown in Table 2.1. Primer sets were purchased from either Eurofins Scientific or Integrated DNA Technologies, which arrived lyophilised and thus were reconstituted in RNase-free water to 100 µM, aliquoted and stored at -20 ºC.

Table 2.1: Table of quantitative PCR assays.

Assays against specific genes-of-interest were designed using the Universal ProbeLibrary assay design center. Each of the primer sets depicted met the following criteria: did not span the first or last intron, possessed similar melting points (Tm) and had a %GC content between 40-60%.

Gene	Protein	Accession #	Forward Primer	Reverse Primer	UPL Probe #	Amplicon Length (nt)
Tbp	TBP	NM_013684	gggagaatcatggaccagaa	gatgggaattccaggagtca	97	90
Hprt	HPRT	NM_145991	tggcatgacactgaaatctgta	ggcttgagacactggtctaggta	26	91
Actb	β-actin	NM_007393.5	ctaaggccaaccgtgaaaag	accagaggcatacaggaca	64	104
Rn18s	18S rRNA	NM_003278.1	ctcaacacgggaaacctcac	cgctccaccaactaagaacg	77	110
Nos3	eNOS	NM_008713	atccagtgccctgcttca	gcagggcaagttaggatcag	12	68
Adra1a	α1A-AR	NM_013461	ctgaaggtccgcttctcct	gccctggagcttcgtttat	81	68
Adra1d	α1D-AR	NM_013460.4	gtcttcgtcctgtgctggtt	ggtttcagctgagggaacag	34	71
Adra1b	α1B-AR	NM_007416	tcttcatcgctctcccactt	gggttgaggcagctgttg	20	106
Agtr1a	AT_{1A}-R	NM_177322.3	actcacagcaaccctccaag	ttggtctcagacactgttcaaaa	9	67
Nox2	NOX2	NM_007807.5	tgccaacttcctcagctaca	gtgcacagcaaagtgattgg	20	73
Nox4	NOX4	NM_001285833.1	gctgttgcatgtttcaggtg	ctgggatgatgtctggttaaga	79	94
Gpx1	GPX-1	NM_008160	gtttcccgtgcaatcagttc	caggtcggacgtacttgagg	2	81
Itgam	CD11b	NM_001082960	agccccacactagcatcaa	tccatgtccacagagcaaag	71	73
Scnn1a	ENaC-α	NM_011324.2	ccaagggtgtagagttctgtga	agaaggcagcctgcagttta	45	78
Slc12a1	NKCC2	NM_183354	tgctggtgccaacatctct	atggtccctctggggatg	85	63
Slc12a3	NCC	NM_019415	cctccatcaccaactcacct	ccgcccacttgctgtagta	12	60
Slc9a3	NHE3	NM_001081060	tccatgagctgaatttgaagg	tacttggggagcgaatgaag	5	87

2.4.4.2 qPCR

The aforementioned assays were performed using qPCR to detect and quantify any changes in mRNA expression in response to increasing dietary salt. In preparation, forward and reverse primer sets were combined in a separate aliquot to the 100 µM stocks and diluted 1:50 with RNase-free water (QIAGEN, UK).

A standard curve was generated using all cDNA samples, creating a top standard of 50 ng via a 1:8 dilution into RNase-free water. A 1:2 serial dilution was then carried out, producing an 8-point standard curve in which the least concentrated was diluted 1:512 to 0.78 ng cDNA, and the final point on the curve contained only RNase-free water.

cDNA samples were thawed on wet ice and diluted 1:30. MicroAmp 384-well PCR plates were set-up on ice and the following reagents were added to each well: 5 µL mastermix (PerfeCTa q-PCR FastMix® II, Quanta Biosciences), 0.1 µL primer pairs, 0.1 µL hydrolysis probe (Universal ProbeLibrary, Roche), 2.8 µL RNase-free water and 2 µL diluted cDNA sample. This created a total reaction volume of 10 µL per well. Standards and samples were loaded in triplicate using repeat and multichannel pipetters to increase the accuracy and speed of plating up.

Once assembled, plates were sealed and centrifuged to ensure the mixing of components. Assays were run in the Roche Lightcycler® 480 using a run-template consisting of 60 cycles of these reaction conditions: preincubation at 95 ºC for 10 minutes, amplification at 95 ºC for 10 seconds followed by 60 ºC for 30 seconds, before cooling at 40 ºC for 30 seconds. In the ‘Analysis’ section of the Lightcycler® 480 software, standard curves and the resulting crossing point (Cp) values were generated through absolute quantification (Figure 2.3). The quality of the standard curves and thus the experimental results was defined by an error <0.5 and an efficiency ranging 1.7 – 2.3.

Each of the triplicate values was reviewed and any with a standard deviation above 0.5 was removed from the analysis.

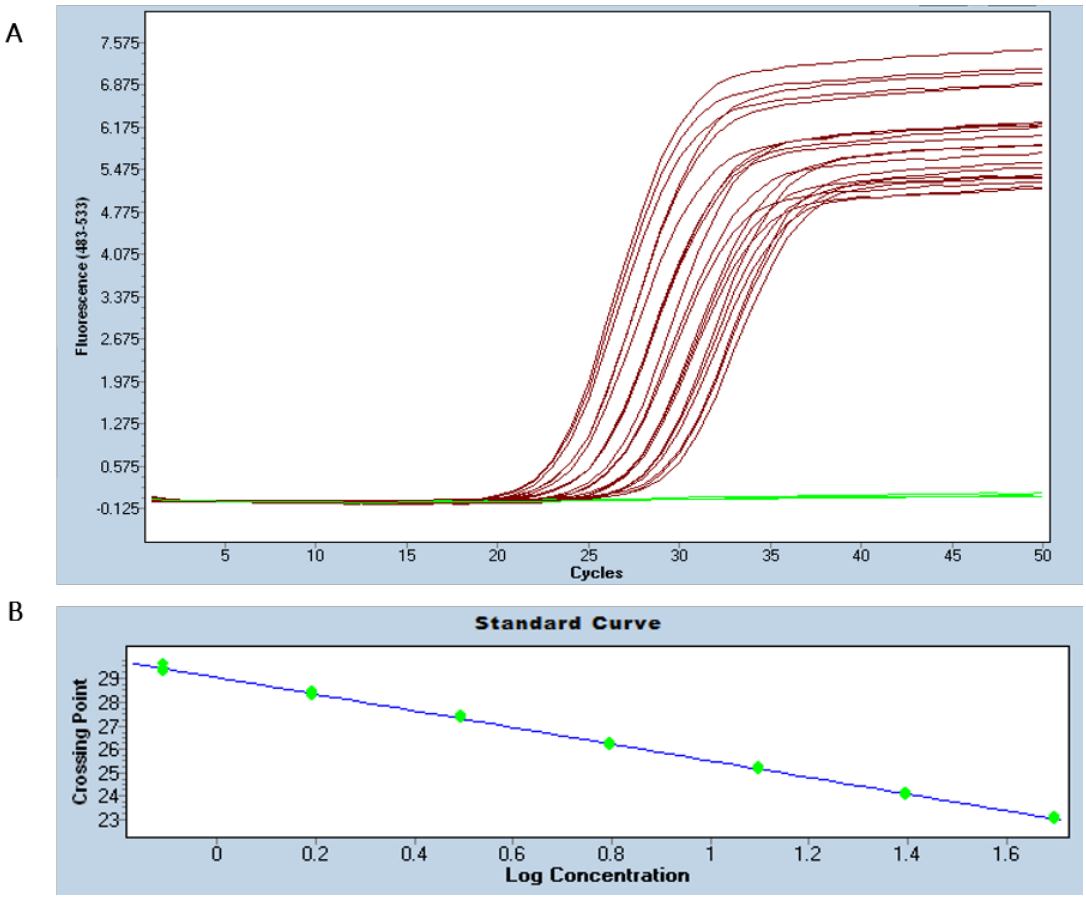

Figure 2.3: Representative example of suitable curves generated by quantitative PCR.
Screenshot depicting the curves produced by Roche Lightcycler® 480 software in renal cortex samples. A: Amplification curve depicting the triplicate fluorescence values of the 8-point standard curve against the number of cycles. The brown represents the standards containing serial diluted cDNA (1-7) and the green represents the last standard (8) and the controls. B: Standard curve with crossing point values against concentration resulting from A. This is then used to determine sample concentration.

2.4.4.3 Reference genes

Reference genes, commonly referred to as housekeepers, are expressed at a certain level regardless of the experimental setting and therefore are essential in quantifying the effect an experimental change has, if any, upon the abundance of mRNA produced by a gene-of-interest. The first step involves identifying suitable reference genes by screening a selection in the tissue to be tested.

Here, the reference genes hypoxanthine-guanine phosphor-ribosyltransferase (*Hprt*), TATA-binding protein (*Tbp*), β-actin (*Actb)* and eukaryotic 18S rRNA (*Rn18s*) were chosen as their mRNA transcript levels did not change with varying dietary sodium content (for kidneys, see Figure 4.3; for arteries, see Figure 5.3). Each reference gene was normalised so that the mean concentration of the control group (SSD) was equal to one. This balances out any variation that occurs across the reference genes, for example all Cp values ranged 22 – 35 apart from 18S rRNA, which generated Cp values ranging 8 – 17. The mRNA abundance of experimental samples was normalised to the mean of at least three of these reference genes, as the use of multiple reference genes has been strongly advocated within the literature (127).

2.5 Measuring Vascular Function with Wire Myography

Wire myography is an *ex vivo* technique allowing the investigation of arterial function under experimental conditions. Here, the multi wire myograph 610 M system from Danish Myo Technology (DMT) was used to determine whether varying dietary salt content had an impact, if any, upon the vascular reactivity of isolated murine artery segments.

2.5.1 Vessel Isolation

Mice were culled via cervical dislocation between 7 and 10AM. Vessel types were isolated under a dissecting microscope and stored within cold physiological saline solution (PSS; 119.0 mM NaCl, 3.7 mM KCl, 2.5 mM $CaCl_2$, 1.2 mM $MgSO_4$, 25.0 mM $NaHCO_3$, 1.2 mM KH_2PO_4, 27.0 μM EDTA, 5.5mM D-glucose) on wet ice to be used within 1-2 hours. The mesentery was removed and pinned out in a petri dish of cold PSS, allowing the isolation and gentle removal of second-order mesenteric arteries. Kidneys with intact vasculature and abdominal aortic attachments were removed, placed in a petri dish of cold PSS as well and the renal arteries were dissected.

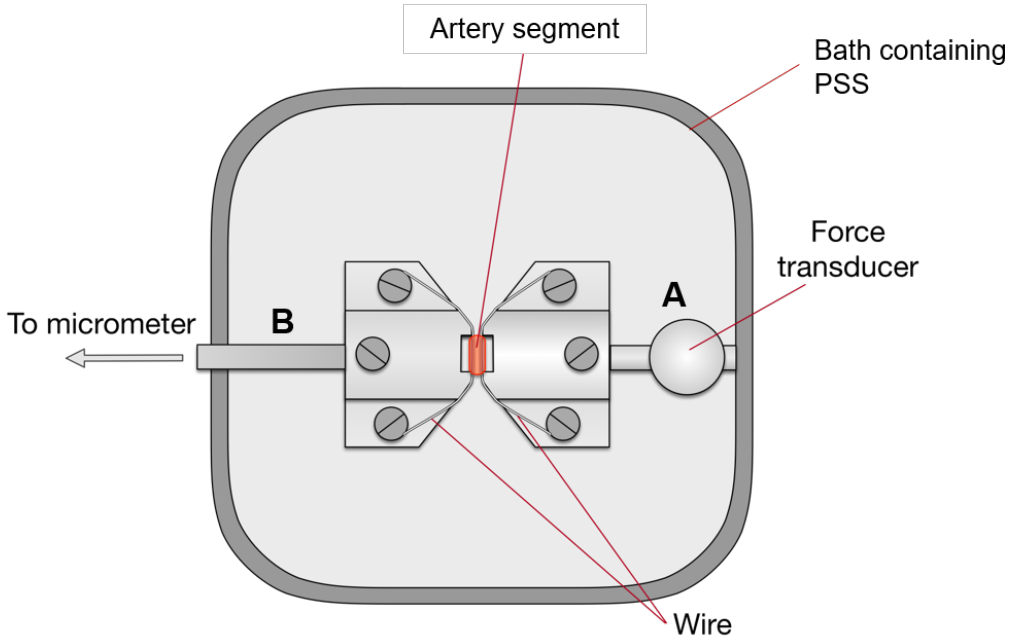

Figure 2.4: Diagram of the wire myograph bath, from Prince (128).
The artery segment was held between two jaws, the right (A) connected to a force transducer recording any alterations to vessel tension and the left (B) connected to a micrometer for manually adjusting the wire position to change vessel tension. This diagram was adapted for this thesis from the original copy created by Dr Richard Prince at the University of Manchester (128) (licence URL: https://creativecommons.org/licenses/by-nc/2.0/uk/; last accessed 21/10/2019).

2.5.2 Vessel mounting

The myograph possesses four individual units containing baths which were supplied with a gas feed and vacuum connections for the removal of solutions. Each unit was washed out with cold PSS before being heated to 37 ºC, filled with 6 mL PSS warmed in a water bath and bubbled with a combination of 95% oxygen and 5% carbon dioxide known as ‘carbogen’ to mimic physiological conditions. Dissected arteries were transferred into the units, a segment per bath. Under a microscope, two ~2 cm lengths of stainless steel 40 µm wire were delicately threaded, one-by-one, into the vessel lumen. The vessel was then positioned between the jaws and the ends of the wires attached to the screws (Figure 2.4). If the vessel was slightly too long, it was either swapped for a fresh segment or, if this was not possible, a small slit was made in the overhanging edge to exclude it from the normalisation procedure. Having checked the wires were rigid, straight and level within the vessel lumen, units were returned to the myograph,

connected to the gas and fresh, warm PSS was introduced into the baths. Mounted artery segments were then left to equilibrate.

2.5.3 Normalisation for resting tension

Before beginning the experimental protocol, it was necessary to establish and place the vessels under resting tension. This introduced a basal stretch and so attempted to recreate the transmural pressure the vessel was normally under *in vivo*. To achieve this, the DMT normalisation module utilises the isometric method, which requires the vessel length and tension, referred to as force here, in order to calculate the internal circumference (IC; mm) and thus the pressure required to generate resting tension. The length of the artery segment was measured using the scale on the eyepiece of the dissecting microscope. The vessel tension was adjusted by turning the micrometer (Figure 2.4) to separate the wires and the distance between them was measured (μm). By adjusting the micrometer to distend the vessel in a stepwise manner to create a maximum force of 13.3 kPa, which is equivalent to a transmural pressure of 100 mHg, a length-tension graph was produced with IC against vessel tension. This allowed for the calculation of the vessel diameter at 100 mmHg, referred to as IC100, which in turn was used to generate IC1 and thus, the distance the wires needed to be moved apart in order to stretch the vessel and place it under its individual resting tension. Vessels then underwent a 45-minute equilibration period.

2.5.4 Experimental protocol

Artery segment viability was first examined with the addition of 6 mL PSS containing a high concentration of potassium (KPSS; 124.6 mM KCl, 2.5 mM $CaCl_2$, 1.2 mM $MgSO_4$, 25.0 mM $NaHCO_3$, 1.2 mM KH_2PO_4, 27.0 μM EDTA, 5.5 mM D-glucose) to elicit a strong contractile response by depolarisation. Once the contraction had reached a peak and levelled off, as visualised within the data acquisition software LabChart, the bathes were emptied and washed three times with warm PSS. This process was repeated a further two times before the vessels were left to rest for 20 – 30 minutes.

The vasodilatory response, and thus the integrity of the endothelium, was assessed with the addition of the vasoconstrictor phenylephrine (PhE; 10^{-4} M) and the subsequent addition of the endothelial-dependent vasodilator acetylcholine (ACh; 10^{-4} M). Once again, baths were washed out with warm PSS and vessels were left.

To evaluate vascular reactivity, concentration-response curves (final concentrations in the bath: 10^{-9} to 10^{-3} M) were generated in 6 mL PSS from PhE, ACh and endothelial-independent vasodilator sodium nitroprusside (SNP). Appropriate time intervals were left between doses as to allow the vessel response to stabilise without the overall contraction or relaxation dropping off, and 20-30-minute washout periods occurred between drugs. At the end of the experimental protocol, three additional rounds of KPSS were added and depolarisation measured in order to ensure the vessel had not been damaged and viability reduced over the course of the experiment.

2.5.5 Data analysis

The data were acquired using the software Labchart 7 pro v7.3.2. For vasoconstriction, data consists of the maximum force output (mN) per dose of PhE. This is then presented as a percentage of the mean force generated by the three additions of KPSS at the start. Arteries were excluded from the analysis if the final KPSS response was >50% lower than that at the start of the protocol. For vasodilatory concentration-response curves, arteries were pre-incubated with PhE to sufficiently pre-constrict the vessels. Data regarding vasodilatory responses consists of the minimum value per dose of ACh or SNP. This is then expressed as a percentage of the residual PhE-induced tension leftover.

Concentration-response curves were produced in GraphPad Prism v8.2.0. The data were fitted with the equation log(dose) vs. response during nonlinear regression analysis, in which the following parameters were compared. For vasoconstriction, this allowed for the calculation of $\log EC_{50}$, defined as the concentration required to reach 50% of the maximum PhE-induced contraction, and the %efficacy (%Emax), defined as the maximum

effect PhE can have under these circumstances. For vasodilation evoked by ACh or SNP, these parameters consist of $logIC_{50}$, representing the concentration required to achieve 50% inhibition of pre-constriction, and %Relax, defined as the maximum inhibitory, thus vasodilatory effect.

2.6 Metabolic Cage Experiments

2.6.1 Experimental set-up

Mice were individually housed within metabolic cages for the collection of urine and faeces, and the measurement of water and dietary intake. Separate cohorts of mice spent either 24 hours at different dietary time-points in these cages or were housed continuously during dietary manipulation. If mice were to spend longer than 24 hours in the metabolic cages, a 5-day acclimatisation period was performed prior to any sampling (129). For 12-hour collection periods, mice were transferred to the cages at the beginning of the light cycle (7AM). Daytime samples were taken at 7PM, thus represent the time period 7AM-7PM, and night-time samples were taken at 7AM, representing the period 7PM-7AM. Urine samples were centrifuged to remove any diet particulates and stored at -20 ºC unless otherwise stated. These were then further analysed to determine electrolyte and catecholamine excretion.

2.6.2 Electrolyte analysis

2.6.2.1 Urinary electrolytes

Urinary electrolyte levels of sodium (Na^+), potassium (K^+) and chloride (Cl^-) were analysed using the Spotchem EL electrolyte analyser (Woodley Veterinary Diagnostics, UK). Urine samples from metabolic cage studies were diluted 1:1 with deionised water and applied to the EL electrode-plates alongside a reference solution. Values were given as mmol/L, which were converted to µmol/h by multiplying readings by the urinary flow rate.

2.6.2.2 Sodium and water balance

Sodium balance was calculated before and after the administration of the HSD. Units of urinary sodium concentration, as measured previously, were

converted from mmol/L to µmol/L. Water balance was calculated using daily urine volume and water intake. The volume of fluid excreted was subtracted from the fluid consumed by each mouse. The units were converted from mL to µL and then normalised to grams of body weight (gbw).

2.6.3 Urinary catecholamine concentration

Urinary concentrations of adrenaline and noradrenaline were determined via IBL CatCombi ELISA (TECAN). Day (7AM-7PM) and night (7PM-7AM) urine samples were collected from mice housed in metabolic cages for 24-hours at a time at different dietary time-points, centrifuged, and supplemented with 0.01 mol/L hydrochloric acid for storage purposes. All samples and kit reagents were allowed to come to room temperature prior to use. Standard, control and experimental urine samples (20 µL per sample) were pipetted onto extraction plates and diluted 1:25 with bidistilled water. Catecholamines were subsequently extracted through 5-30-minute incubations with the provided extraction and release buffers on an orbital shaker (400-600 rpm). The extracted samples were divided (100 µL for adrenaline, 25 µL for noradrenaline) and plated out in duplicate for the measurement of each catecholamine. The manual ELISA protocol was carried out following the manufacturer's instructions, with washes consisting of 290 µL wash buffer (diluted 1:10 with bidistilled water) per well, repeated four times.

The OD was measured at 405 nm with a microplate reader (Infinite M1000, Tecan) and plotted against log(concentration). A four-parameter logistic curve was fitted and the unknown urinary concentrations of adrenaline and noradrenaline (R^2 = 0.998 for each) were interpolated. Urinary flow rate was utilised to calculate excretion for each urine sample.

2.7 Measuring Plasma Aldosterone

2.7.1 Plasma sampling

Daytime terminal plasma samples were obtained via decapitation completed by either the manager of the Centre's Physiological Laboratory Mr Kevin Stewart, or post-doctoral researcher Dr Celine Grenier. This allowed for the

collection of a sufficiently large volume of blood to measure the concentration of aldosterone. Samples were collected throughout the daytime. Plasma was acquired via centrifugation at 2,000 xg for 5 minutes at 4 ºC and stored at -80 ºC.

2.7.2 Plasma aldosterone ELISA

An aldosterone ELISA kit (Enzo Life Sciences, UK) was used to determine plasma aldosterone concentration. All samples and kit components were allowed to reach room temperature, before plasma was diluted 1:4 with assay buffer to be assayed in duplicate via the manufacturer's protocol. The measurement of absorbance occurred at 405 nm, corrected with 550 nm, using a microplate reader (Infinite M1000, Tecan).

Average net OD was calculated and expressed as a percentage of the net maximum binding (B0) OD, known as percent bound. A standard curve was then generated with percent bound vs. log(concentration) and unknown values were interpolated to determine the concentration of plasma aldosterone.

2.8 Statistical Analyses

All data included in this work were analysed using the software GraphPad Prism v8.2.0. With the exception of the balance results, data are expressed as mean ± standard deviation (SD). The number of biological and/or technical replicates (n) is included within the figure legends and the specific Methods section for each experiment in the Results chapters. Throughout this work, significance is reported at $P < 0.05$ alongside the statistical tests used. Many of the statistical tests in this thesis make the assumption that the data follow a Normal, or Gaussian, distribution. Prior to performing any of these analyses, the normality of the data set was first assessed using the Shapiro-Wilk test. With the cut-off at 0.05, data sets generating *P* values above this were then compared using the following parametric tests.

t test: *t* testing was utilised to determine the presence of a significant difference between the means of two groups. The choice between an

unpaired and a paired *t* test was made based on the experimental design. For example, an unpaired *t* test was selected to compare two separate groups, whereas paired was selected to compare a variable in a single group measured before and after a treatment, such as the HSD here. Two-tailed *t* tests were used to test the hypothesis that the HSD caused a significant difference, whether it be a decrease or an increase in a variable such as kidney weight.

One-way ANOVA: This was performed to compare one variable, such as BP, between three groups or more. The resulting *P* value was corrected for multiple comparisons, in which the mean of each group was compared with the mean of every other group included in the analysis. For this reason, Tukey post-testing was carried out. An ordinary one-way ANOVA was used when groups were unrelated, however when the groups were matched a repeated measures ANOVA was performed. In this work, the need for this occurred when one variable, such as BP, was measured in an animal receiving the SSD followed by the HSD. It controls for factors influencing experimental variability, and thus was used as statistical power is increased when matching is effective, as determined by significance. This also confirms the suitability of the test.

Two-way ANOVA: A two-way ANOVA was carried out to determine the effect of two factors upon a response. In this thesis, factors consist of dietary salt intake and time or drug concentration. The resulting ANOVA table has been presented with the data, and depicts *P* values for testing three null hypotheses:

1. The mean of each column is the same, for example no differences are observed in artery contraction between the SSD and the HSD
2. The mean of each row is the same, for example no differences are observed in artery contraction between each concentration of PhE
3. No interaction occurs between the above factors, for example the concentration of PhE has the same effect upon artery contraction within both dietary groups.

Sidak multiple comparisons test was implemented following two-way ANOVA. This method of post-hoc testing discourages the reporting of false negatives, thus has increased power compared to other methods. It also follows the assumption that each comparison is independent from one another, which is beneficial when comparing separate, unrelated cohorts.

3 Effect of High Dietary Salt Intake on Blood Pressure in C57BL6/JCrl Mice

3.1 Introduction

The mouse strain C57BL6/J is widely used as a control or as the background upon which to generate a transgenic mouse model in cardiovascular research. It is commonly cited as a salt-resistant strain and several studies have reported little to no effect of salt upon BP (117-121); however, others have noted pronounced BP changes in response to increasing dietary salt intake in these mice (112, 122, 123). In this chapter, the standard salt diet (SSD; 0.25% Na) was fed to C57BL6/JCrl mice, a substrain from Charles River, UK. Dietary sodium content was then increased ten-fold (HSD; 3% Na) and the impact upon BP and other related parameters was characterised.

3.1.1 Aims

1. To determine the impact high dietary salt intake has on BP, heart rate and locomotor activity.
2. To assess whether changes in dietary salt intake influence the day-night pattern of BP, heart rate and locomotor activity.
3. To decipher whether any salt-induced changes in the above parameters can be reversed by reducing dietary salt intake.

3.1.2 Approach to achieve the chapter aims

- BP, heart rate and locomotor activity were measured in a single cohort of freely moving, conscious C57BL6/JCrl mice using radiotelemetry.
- To determine the impact of dietary salt, mice received the HSD for 3 weeks before being returned to the SSD administered during baseline recordings.

3.2 Methods

The methods used within this chapter are described in detail in the main Methods section. The specific timeline and experimental design used to address the above aims is recounted in this chapter.

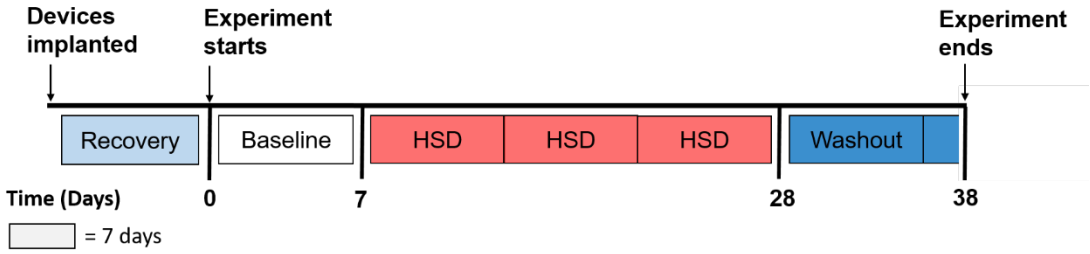

Figure 3.1: Timeline for the radiotelemetry experiment.
Radiotelemeter devices were surgically implanted into a single cohort of male 9-12-week-old C57BL6/JCrl mice (n=7) on a standard salt (0.25% Na) diet using the anaesthetic isoflurane. Mice recovered for 7 days before baseline measurements began. After these next 7 days, mice received a high salt diet (HSD; 3% Na) and measurements were taken for a further 3 weeks (day 8 to day 28). On experimental day 28, mice were transferred back to the standard salt diet received during the baseline measurements for a further 10 days. The rectangular boxes represent 7-day periods, and washout refers to the removal of the HSD.

3.2.1 Experimental design for radiotelemetry

BP, heart rate and locomotor activity were recorded by radiotelemetry in an experiment involving a single cohort of 7 male C57BL6/JCrl mice, aged 9-12 weeks with a mean body weight of 28 ± 2 g. A repeated measures design was used in which each animal was exposed to all treatment conditions and the response monitored over time. This longitudinal approach is an experimental refinement in the laboratory and by increasing statistical power, it reduces the number of animals required to identify a biologically important difference, for example an effect of high salt. Figure 3.1 depicts the experimental timeline and the sequence of treatment conditions applied.

Mice were given access to the SSD (0.25% Na) and singly housed under quiet conditions with the usual 12-hour light-dark cycle. This was done prior to the implantation of the telemeter devices, as described in Methods section 2.2.2. The surgical procedure to insert the devices was performed by the

manager of the Centre's *in vivo* Physiology Laboratory Mr Kevin Stewart. Following this, mice recovered for 7 days as determined by the restoration of pre-operative body weight. Mice were checked daily to monitor their condition according to the Home Office requirements for actual severity reporting. Once body weight had normalised, baseline BP, heart rate and activity were acquired over the next 7 days. Of these, only 5 days were used in the analysis: data from day 4 and day 6 were rejected because of technical failures in the recording equipment resulting in significant periods (6-9 hours) of data loss.

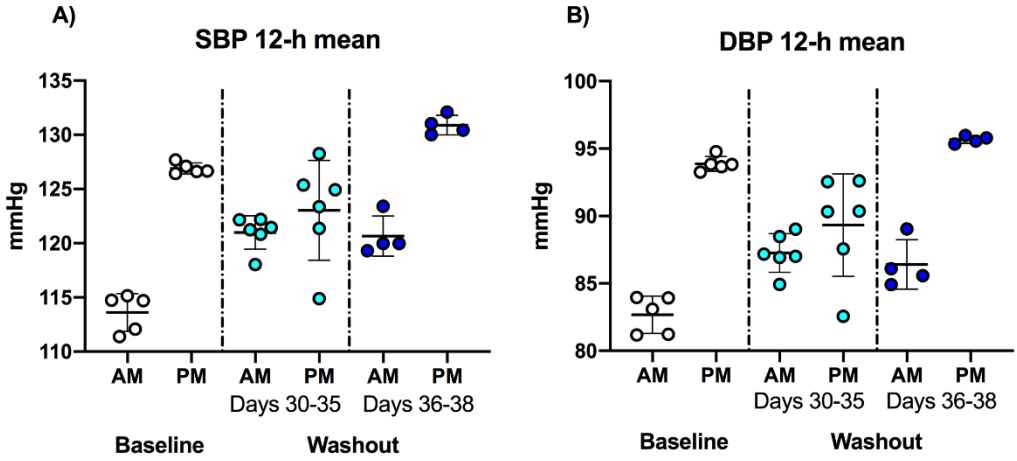

Figure 3.2: Blood pressure during interruption of the 12-hour light-dark cycle.
Blood pressure was measured by radiotelemetry whilst mice (n=7) received a standard salt (0.25% Na) diet at the beginning of the experiment for baseline recordings and at the end for a washout period. The data were collected over 12-hour (12-h) periods for each mouse, then averaged and presented as one 12-h period per data point. During this final period, the light-dark cycle was interrupted. As a result, the day-night circadian variability of BP flattened, as seen in the 12-h means of A) systolic (SBP) and B) diastolic blood pressure (DBP) between experimental days 29 and 35. The cycle returned after day 35, as did the normal day-night pattern in A) SBP and B) DBP. Daytime refers to 7AM-7PM, and night-time refers to 7PM-7AM.

Next, dietary salt intake was increased by replacing the SSD with the HSD (containing 3% Na) for 3 weeks. Data was obtained throughout the high salt phase. After 3 weeks, once BP was observed to be stable, a 'washout' period was introduced (Figure 3.1) in which the HSD was replaced with the SSD once again, aided by transferring mice into different cages. Data collection was extended for a further 10 days following this modification. Data from experimental days 29-35 were removed from the post-acquisition analysis.

As depicted in Figure 3.2, BP 'dipping' disappeared during the inactive phase (7AM-7PM; daytime) within these days due to unplanned disruption of the light-dark cycle. This was restored after day 35 and so data collected on days 36 to 38 were included in the analysis (Figure 3.2).

3.2.2 Data analysis

Data on BP, locomotor activity and heart rate were transmitted by implantable DSI telemeter devices and acquired over one minute every half an hour by the software Ponemah v6.12 over the 6-week experimental period. Data were grouped and handled in either 24- or 12-hour periods during the analysis. Pulse pressure was calculated by subtracting DBP from SBP, and activity was normalised to counts per minute (counts/min). Averages (24-hour) were taken for SBP, DBP, MBP, pulse pressure, heart rate, and locomotor activity, which were then compared to determine the daily impact of increasing dietary salt intake. A 5-hour moving average was used to smooth the data and 5-day data bins, as shown in Figure 3.3, were taken forward to display and investigate any changes to day-night rhythmicity.

Daytime data is defined in this chapter as data collected between 7:00AM and 6:35PM (ZT 0-12) and night-time as between 7:00PM and 6:35AM (ZT 12-24). During these time-points, 12-hour averages were calculated and compared. The percentage night-time dip occurring during the day-night transition was calculated using the equation below:

$$\frac{(Night\ BP - Day\ BP)}{Night\ BP}\ x\ 100$$

The washout period could not be included in this as only 4 days of measurements were obtained, for reasons noted above. Statistical analysis was performed using GraphPad Prism v.8.0 and significance denoted as $P<0.05$, corrected for multiple comparisons. Daytime and night-time 12-hour averages were analysed using a repeated measures one-way ANOVA with multiple comparisons carried out by Tukey post-hoc testing. However, due to

the differing number of days within the baseline and washout periods, the Graphpad Prism software assumes the data sets are missing values and so this model could not be applied to the 24-hour averages. Instead, a mixed effects model was used to assess the variation between groups, as the reasons for the missing values are random and unrelated to the experimental conditions applied or measured (i.e technological difficulties causing loss of data).

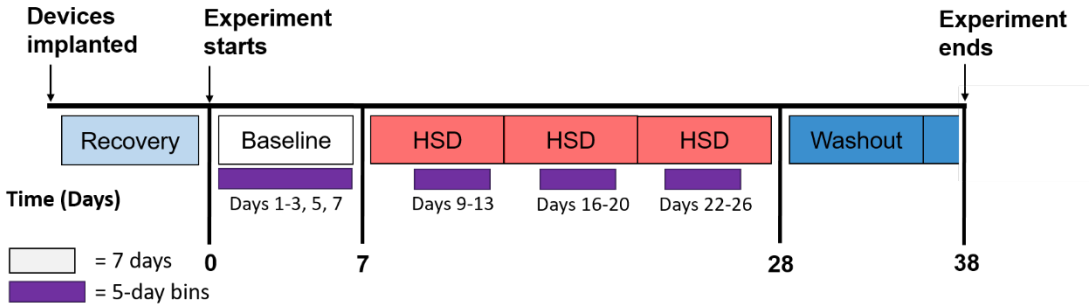

Figure 3.3: Timeline for the radiotelemetry experiment with 5-day data bins.
Cardiovascular parameters were measured via radiotelemetry in C57BL6/JCrl mice (n=7) in which recordings were taken on a standard salt (0.25% Na) diet to establish a baseline, on a high salt diet (HSD; 3% Na) for 3 weeks and back on the standard diet for a washout period. During the data analysis, 5-day data bins were extracted. These are representative of when the parameters reached a stable state, i.e when changes due to diet manipulation had levelled out. Due to an interruption in data acquisition during the baseline period, 5 consecutive days could not be obtained and so days 1-3, 5 and 7 were taken forward. The rectangular boxes in grey depict 7-day periods, and those in purple depict the 5-day periods subject to data binning. Washout refers to the removal of the HSD.

Figure 3.4: Blood pressure and other cardiovascular variables (24-hour) during high salt feeding.

Systolic (SBP), diastolic (DBP), mean blood pressure (MBP), heart rate and locomotor activity were measured via radiotelemetry in a single cohort of C57BL6/JCrl mice (n=7). Pulse pressure (PP) was calculated by subtracting DBP from SBP. Data are presented as 24-hour (24-h) means ± SD. A) SBP, DBP and MBP traces during 7 days of baseline measurements, followed by 3 weeks of a high salt diet (HSD; 3% Na). High salt feeding was separated into 1-week periods and B) MBP, C) SBP, D) DBP, E) heart rate, F) pulse pressure (PP) and G) activity effects were compared amongst each other, and with baseline measurements. These comparisons were made using repeated measures one-way ANOVA with Tukey post-hoc testing. ***$p<0.001$, **$p<0.01$ and *$p<0.05$.

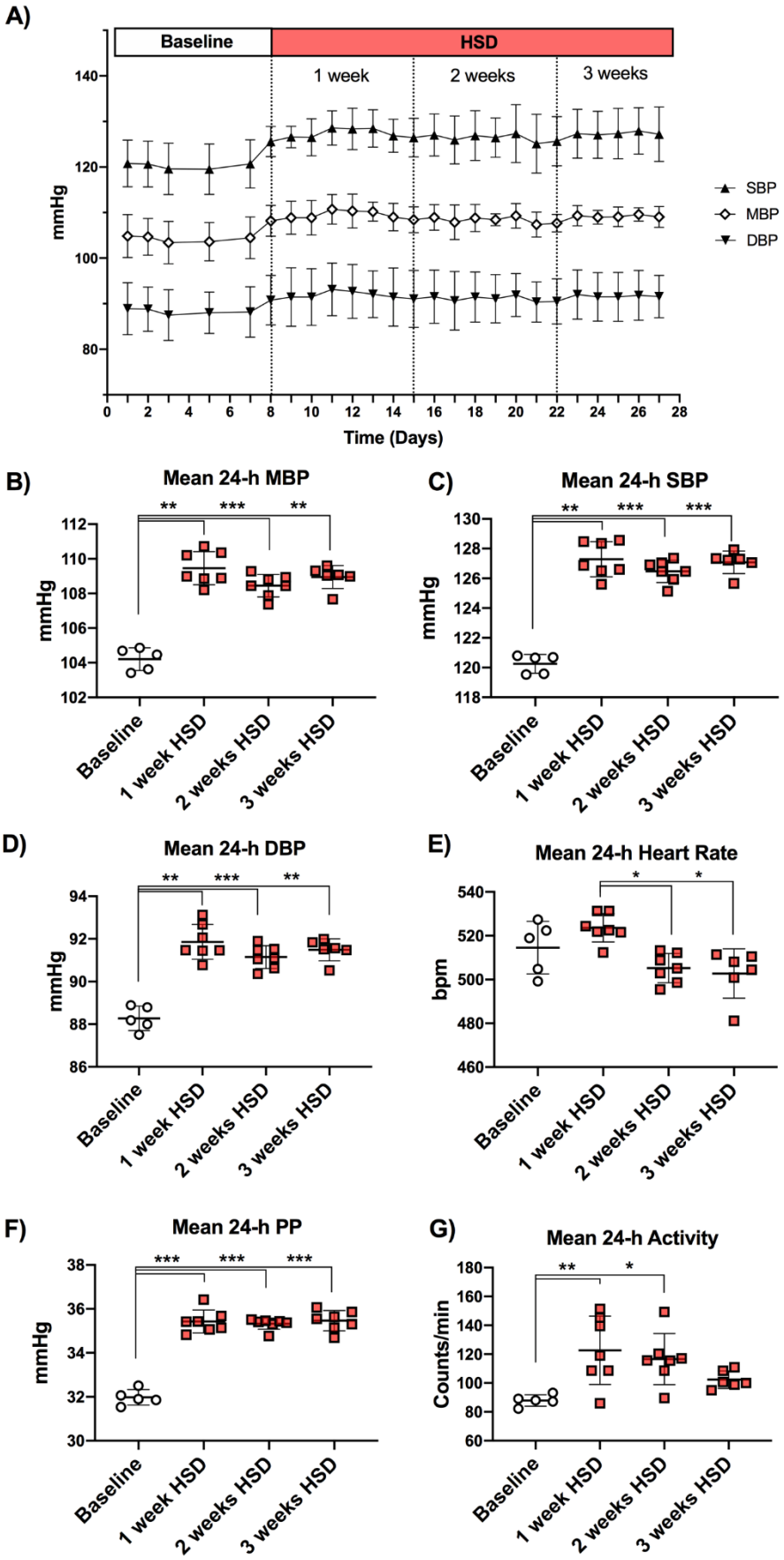
A)
Baseline
HSD
1 week
2 weeks
3 weeks
mmHg
Time (Days)
SBP
MBP
DBP
B)
Mean 24-h MBP
C)
Mean 24-h SBP
D)
Mean 24-h DBP
E)
Mean 24-h Heart Rate
bpm
F)
Mean 24-h PP
G)
Mean 24-h Activity
Counts/min
Baseline
1 week HSD
2 weeks HSD
3 weeks HSD

3.3 Results

3.3.1 High dietary salt intake elevates blood pressure

SBP, DBP and MBP were measured in conscious unrestrained mice on the SSD followed by the HSD. Baseline measurements were taken from the mice with access to the SSD. During this time, 24-hour averaged SBP was at 120.2 ± 0.6 mmHg and DBP at 88.3 ± 0.6 mmHg, and as a result, MBP was at 104.2 ± 0.7 mmHg. After day 7 of the experimental timeline, the SSD was replaced with the HSD. SBP rose by 7.0 mmHg within the first 4 days, reaching 127.2 ± 1.2 mmHg, and DBP by 3.8 mmHg to 92.1 ± 0.8 mmHg. Thus, MBP increased to 109.4 ± 1.0 mmHg (Figure 3.4 A & B). All three measures were significantly higher compared to baseline (SBP P=0.002; DBP P=0.010; MBP P=0.003). This increase was sustained at 2 weeks (SBP 126.5 ± 0.8 mmHg P=0.0001; and DBP 91.2 ± 0.5 mmHg P =0.0005; MBP 108.5 ± 0.7 mmHg P=0.0003 all compared to baseline) and 3 weeks of high salt feeding (SBP 127.1 ± 0.8 mmHg P=0.0006; DBP 91.5 ± 0.5 mmHg P=0.004; MBP 108.9 ± 0.7 mmHg P=0.002 compared to baseline) (Figure 3.4 A-D).

Heart rate remained largely unaltered by increasing dietary salt intake, as compared to baseline measurements. During baseline recordings, 24-hour mean heart rate was 515 ± 12 bpm, which rose very slightly but insignificantly to 524 ± 7 bpm (P=0.561) after 1 week of high dietary salt intake. A minor decline was noted between 1 and 2 weeks (505 ± 7 bpm, P=0.013 compared to 1 week of high salt) which then persisted throughout the final week (503 ± 11 bpm, P=0.050) (Figure 3.4 E).

Pulse pressure was generated by subtracting DBP from SBP. At baseline, pulse pressure was 32.0 ± 0.4 mmHg, which rose significantly upon increasing dietary salt intake. Within the first week, pulse pressure increased by 3.4 mmHg, which was sustained throughout the experimental period (35.4 ± 0.5 mmHg after 1 week, 35.3 ± 0.3 mmHg after 2 weeks and 35.5 ± 0.5 mmHg after 3 weeks HSD; all P=0.0002 compared to baseline) (Figure 3.4 F).

The implanted telemeter devices also measured locomotor activity as the mice moved around their cages, which was then normalised to counts/min. Activity, averaged over 24-hours, during baseline was 88 ± 4 counts/min. This increased significantly to 123 ± 24 counts/min after the HSD was introduced (P=0.007) and after 2 weeks, remained elevated at 117 ± 18 counts/min (P=0.030). Within the third week of increased dietary salt intake, the level of activity dropped slightly to 102 ± 6 counts/min, which was not different to baseline (P=0.471) (Figure 3.4 G). This suggests that the mice were more active during the HSD, which normalised after 3 weeks.

3.3.2 Effect of high dietary salt intake on the circadian rhythm of blood pressure, heart rate and locomotor activity

On the SSD, SBP exhibited a clear day-night pattern. During the day (7AM-7PM), SBP was 115.4 ± 1.9 mmHg when mice are typically at rest and rose to 125.5 ± 0.7 mmHg at night (7PM-7AM), which repeated every 24 hours (Figure 3.5 A-D). When the SSD was replaced with the HSD, the rhythm persisted throughout the duration of the experiment despite the increased salt intake (Figure 3.5 A). This is also depicted within Table 3.1, as the dip in SBP between night and day was 8.0% during baseline and increased to 12.0-14.5% during the HSD period, illustrating that elevated dietary salt intake did not impact the circadian regulation of SBP. Daytime SBP increased moderately to 119.5 ± 0.9 mmHg (P=0.024 compared to baseline) after 1 week, which reversed after 2 weeks to 116.6 ± 1.4 mmHg (P=0.800 compared to baseline), before returning to 118.7 ± 0.5 mmHg after 3 weeks of high salt (P=0.036 compared to 2 weeks HSD) (Figure 3.5 B). SBP at

night, however, rose considerably to 135.7 ± 1.1 mmHg during the first week, which persisted throughout the duration of the HSD (all $P<0.0001$ compared to baseline) (Figure 3.5 C). Although the typical day-night pattern of SBP was conserved with high salt intake, a potential phase shift was observed (Figure 3.5 E). The rapid increase that occurs during awakening, referred to as the 'morning surge' in humans, occurred later in the subsequent weeks than in the first week as the traces shifted to the right.

Table 3.1: Blood pressure 'dip' between sleeping and awake states in C57BL6/JCrl mice during high dietary salt intake.

	Active (night); mmHg	**Inactive (day); mmHg**	**Active-Inactive; mmHg**	**%dip**
SBP				
Baseline	125.5 ± 0.7	115.4 ± 1.9	10.1 ± 2.2	8.0 ± 1.7
1 week HSD	135.7 ± 1.1	119.5 ± 0.9	16.2 ± 1.4	11.9 ± 0.9
2 weeks HSD	136.4 ± 0.5	116.6 ± 1.4	19.8 ± 1.4	14.5 ± 1.0
3 weeks HSD	136.0 ± 0.6	118.7 ± 0.5	17.3 ± 0.7	12.7 ± 0.5
DBP				
Baseline	91.9 ± 0.6	84.4 ± 1.3	7.5 ± 1.6	8.1 ± 1.7
1 week HSD	97.5 ± 0.7	86.3 ± 0.6	11.2 ± 0.6	11.4 ± 0.5
2 weeks HSD	97.8 ± 1.0	83.6 ± 1.2	14.1 ± 1.8	14.4 ± 1.7
3 weeks HSD	98.1 ± 0.5	83.6 ± 0.9	14.5 ± 1.0	14.8 ± 0.9

Systolic (SBP) and diastolic blood pressure (DBP) were measured via radiotelemetry in a single cohort of C57BL6/JCrl mice (n=7) fed a standard diet for baseline recordings followed by a high salt diet (HSD) for 3 weeks. Data are presented as 12-hour averages ± SD generated for daytime (7AM-7PM) during inactivity and night-time (7PM-7AM) when mice were active. The decline of blood pressure between sleep and awake states, referred to as the blood pressure 'dip' occurring at night-time in humans, was quantified and expressed as a percentage (%) of blood pressure during the awake state.

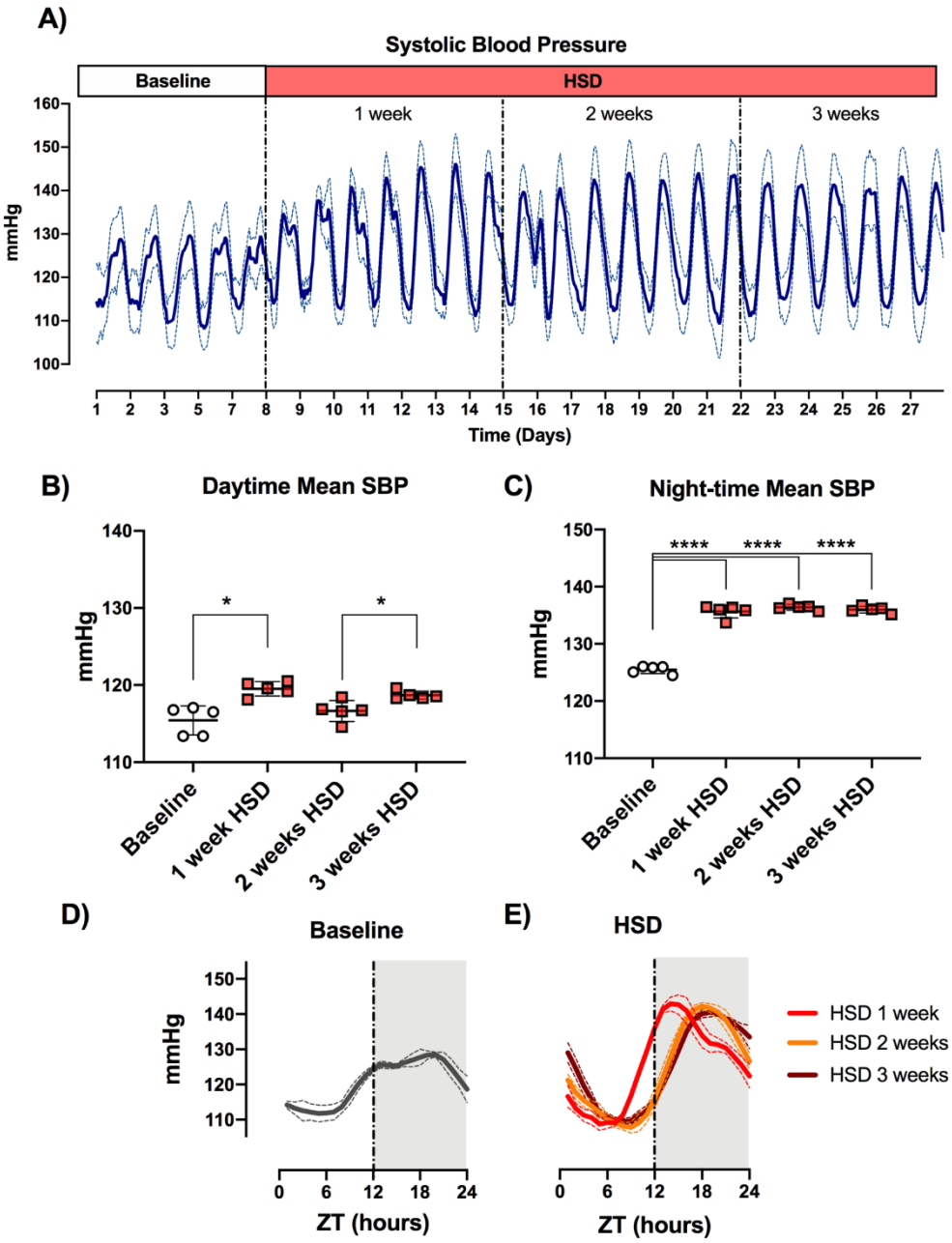

Figure 3.5: Systolic blood pressure in C57BL6/JCrl mice with high dietary salt intake.

Systolic blood pressure (SBP) was measured via radiotelemetry in C57BL6/JCrl mice (n=7). Mice were fed a standard salt (0.25% Na) diet for baseline recordings followed by a high salt diet (HSD; 3% Na) for 3 weeks. Data are presented as 5-hour moving averages ± SD. A) SBP trace throughout the experiment. From this, 5-day data bins were extracted and 12-hour averages of SBP were taken for B) daytime (7AM-7PM) and C) night-time (7PM-7AM) for baseline and each of the 1-week periods of the HSD. Thus, data are presented as one 12-h period per data point. Averages were also calculated for every hour of the 24-hour light-dark cycle for SBP during D) baseline and E) high dietary salt intake. The grey background represents night-time, i.e the dark cycle ZT 12-24. Analysis of the 12-hour means was done using repeated measures one-way ANOVA with Tukey post-hoc testing for multiple comparisons. ****p<0.0001, *p<0.05.

DBP also demonstrated a robust rhythm during the collection of baseline data, with daytime DBP at 84.4 ± 1.3 mmHg and night-time DBP increasing to 91.9 ± 0.6 mmHg (Figure 3.6 A-D). Once the mice were given access to the HSD, similar events as seen with SBP transpired. At baseline, DBP dropped by 8.1% between night and day, whereas DBP dropped by 11.4-14.8% during increased dietary salt intake (Table 3.1). This demonstrates that an adequate BP dip still occurred despite the dietary alteration in these mice. During the day, DBP was modestly but insignificantly higher at 86.3 ± 0.6 mmHg (P=0.202 compared to baseline) after 1 week of the HSD, which declined back to baseline over the course of the following weeks (83.6 ± 1.2 mmHg, P=0.038 at 2 weeks; 83.6 ± 0.9 mmHg, P=0.012 at 3 weeks compared to 1 week HSD) (Figure 3.6 B). DBP at night elevated substantially to 97.5 ± 0.7 mmHg after 1 week (P<0.0001), 97.8 ± 1.0 mmHg after 2 weeks (P=0.0002) and 98.1 ± 0.5 mmHg after 3 weeks of high salt intake (P=0.0004) compared to baseline (Figure 3.5 C). The 'morning surge' of DBP, illustrated in Figure 3.6 E, shifted to the right in the last weeks of the HSD in a possible phase shift similar to that displayed by SBP.

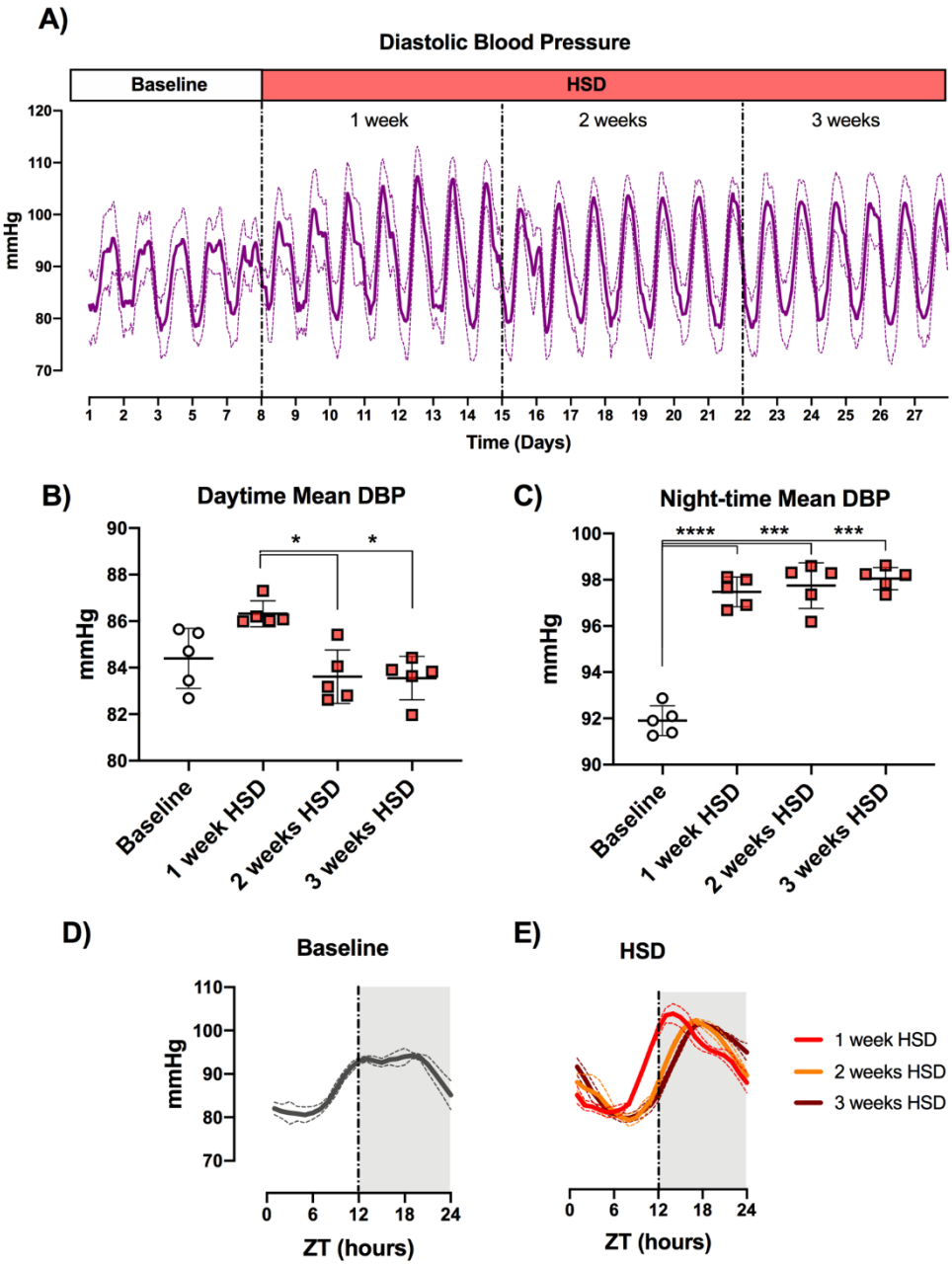

Figure 3.6: Diastolic blood pressure in C57BL6/JCrl mice during high dietary salt intake.

Diastolic blood pressure (DBP) was measured via radiotelemetry in C57BL6/JCrl mice (n=7). Mice were fed a standard salt (0.25% Na) diet during baseline measurements before they were transferred to a high salt diet (HSD; 3% Na) for 3 weeks. Data are presented as 5-hour moving averages ± SD. A) DBP trace throughout the experiment. From this, 5-day data bins were obtained and 12-hour means were generated for B) daytime (7AM-7PM) and C) night-time (7PM-7AM) for DBP baseline and after 1-3 weeks HSD. Thus, data are displayed as one 12-hour period per data point. Means were also calculated for every hour of the 24-hour light-dark cycle for DBP during D) baseline and E) high dietary salt intake. Analysis consisted of repeated measures one-way ANOVA with Tukey post-hoc testing. ****p<0.0001, ***p<0.001, *p<0.05.

As shown in Figure 3.7, 24-hour averaged pulse pressure increased during the HSD period. With daytime pulse pressure at 31.1 ± 0.6 mmHg and night-time at 33.0 ± 0.4 mmHg during the baseline period, a small but clear shift between day and night was exhibited, confirming the presence of circadian regulation (Figure 3.7 A-C). Following administration of the HSD, daytime pulse pressure increased to 33.9 ± 0.4 mmHg (P=0.0006), as did night-time pulse pressure to 37.2 ± 0.7 mmHg (P=0.0002) during the first week. This significant elevation was sustained throughout the duration of the HSD, with both day and night pulse pressure remaining higher than baseline (daytime P=0.007; night-time P=0.0002 after 3 weeks of the HSD) (Figure 3.7 B & C).

Heart rate displayed day-night fluctuations throughout the course of the experiment, i.e during the data collection from both the baseline and high salt periods (Figure 3.7 D). At baseline, mice had a 12-hour mean heart rate of 500 ± 22 bpm during the day and 530 ± 6 bpm during the night, illustrating a typical increase overnight and thus an appropriate daily rhythm. After 1 week of high salt intake, daytime heart rate was unchanged at 505 ± 8 bpm (P=0.985 compared to baseline). Following two further weeks of high dietary salt intake, heart rate declined to 471 ± 14 bpm (P=0.007 compared to 1 week HSD) (Figure 3.7 E). Night-time heart rate, however, increased slightly to 543 ± 6 bpm, bordering upon statistical significance (P=0.051 compared to baseline), which was sustained but also not significant during 2 weeks (541 ± 8 bpm, P=0.144) and 3 weeks of high dietary salt intake (536 ± 14 bpm P=0.837) compared to heart rate at baseline (Figure 3.7 F).

Figure 3.7: Pulse pressure and heart rate in C57BL6/JCrl mice during high dietary salt intake.
Pulse pressure (PP) was calculated from systolic and diastolic blood pressure measured via radiotelemetry in C57BL6/JCrl mice (n=7). Mice were fed a standard salt (0.25% Na) diet during baseline recordings, after which they were transferred to a high salt diet (HSD; 3% Na) for 3 weeks. Data are presented as 5-hour moving averages ± SD. A) PP and D) heart rate traces throughout the experiment. Twelve-hour means were extracted from 5-day data bins during daytime (7AM-7PM) for B) PP and E) heart rate, and night-time (7PM-7AM) for C) PP and F) heart rate for baseline and 1-3 weeks HSD. Thus, data are presented as a 12-hour mean of all mice per data point. These means were analysed with repeated measures one-way ANOVA with Tukey post hoc testing. ***p<0.001, **p<0.01.

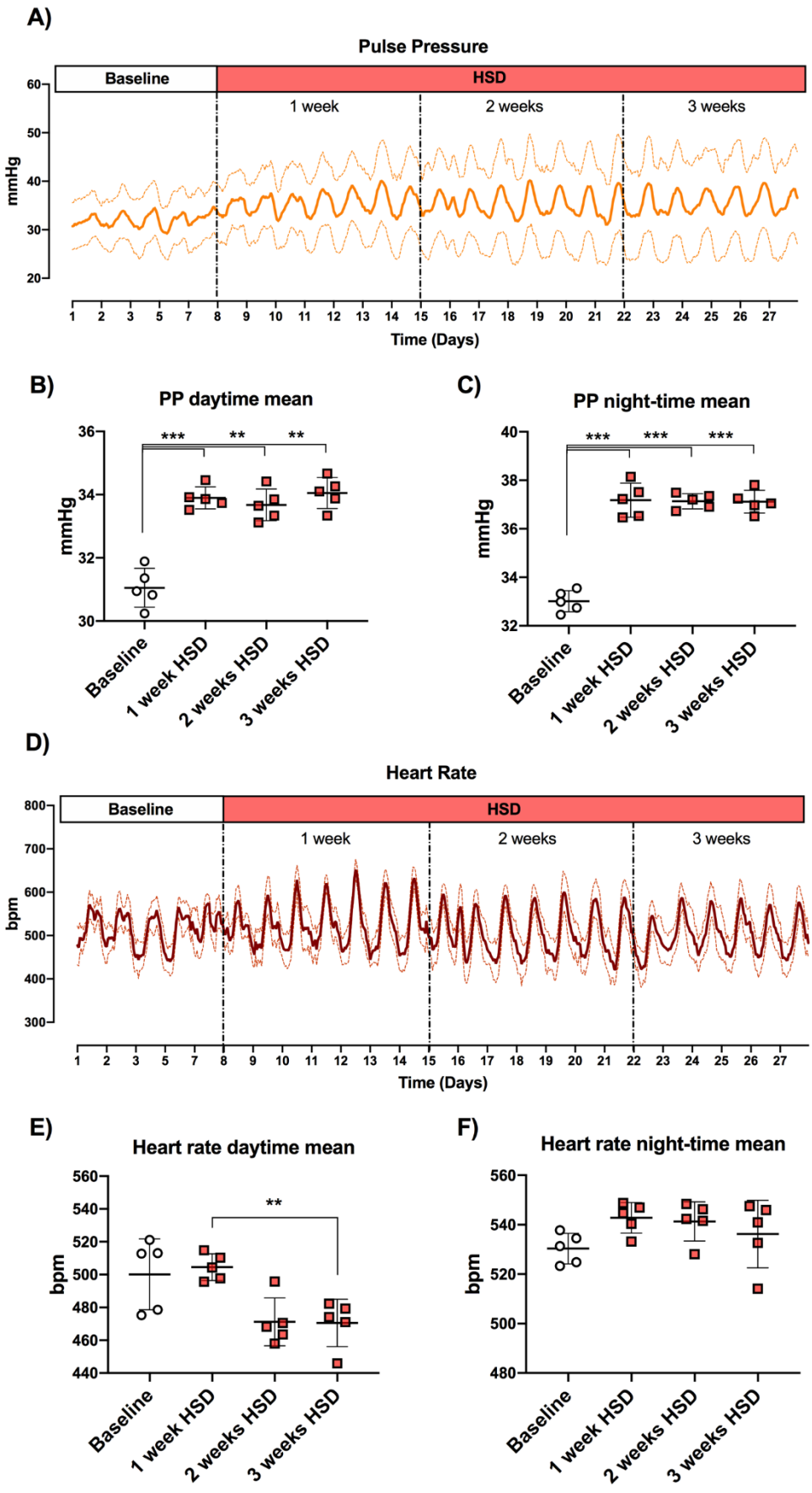
A)
Pulse Pressure
Baseline
HSD
1 week
2 weeks
3 weeks
mmHg
Time (Days)
B)
PP daytime mean
mmHg
***
**
**
Baseline
1 week HSD
2 weeks HSD
3 weeks HSD
C)
PP night-time mean
mmHg
***
***
***
Baseline
1 week HSD
2 weeks HSD
3 weeks HSD
D)
Heart Rate
Baseline
HSD
1 week
2 weeks
3 weeks
bpm
Time (Days)
E)
Heart rate daytime mean
bpm
**
Baseline
1 week HSD
2 weeks HSD
3 weeks HSD
F)
Heart rate night-time mean
bpm
Baseline
1 week HSD
2 weeks HSD
3 weeks HSD

Locomotor activity is expressed as counts per minute. Movement varied with day and night, with 56 ± 5 counts/min of daytime activity and 127 ± 8 counts/min of night-time activity collected over the baseline period. This illustrates the mice were largely at rest during the day and mobile during the night at baseline (Figure 3.8 A-C). Daytime activity was mostly unaltered by high dietary salt intake, with 66 ± 11 counts/min at week 1 and 64 ± 42 counts/min at week 2 of the HSD period. By the third week, activity was moderately reduced to 43 ± 5 counts/min, which was notably lower than that of 1 week of high salt intake (P=0.013) but not baseline (Figure 3.8 B). On the other hand, movement at night increased as dietary salt content increased. Activity following 1 week of high salt was not different to that at baseline, however by the second week, activity increased to 184 ± 24 counts/min (P=0.013). This declined slightly to 167 ± 11 counts/min by the third week but remained significantly higher than activity at baseline (P=0.023) (Figure 3.8 C). As seen in both SBP and DBP, the rise in locomotor activity as the dark period (night-time) began also appeared to be delayed after 2 and 3 weeks of high dietary salt intake. Once more, a phase shift could potentially be occurring, which suggests mice are less active until later in the dark period (Figure 3.8 D & E).

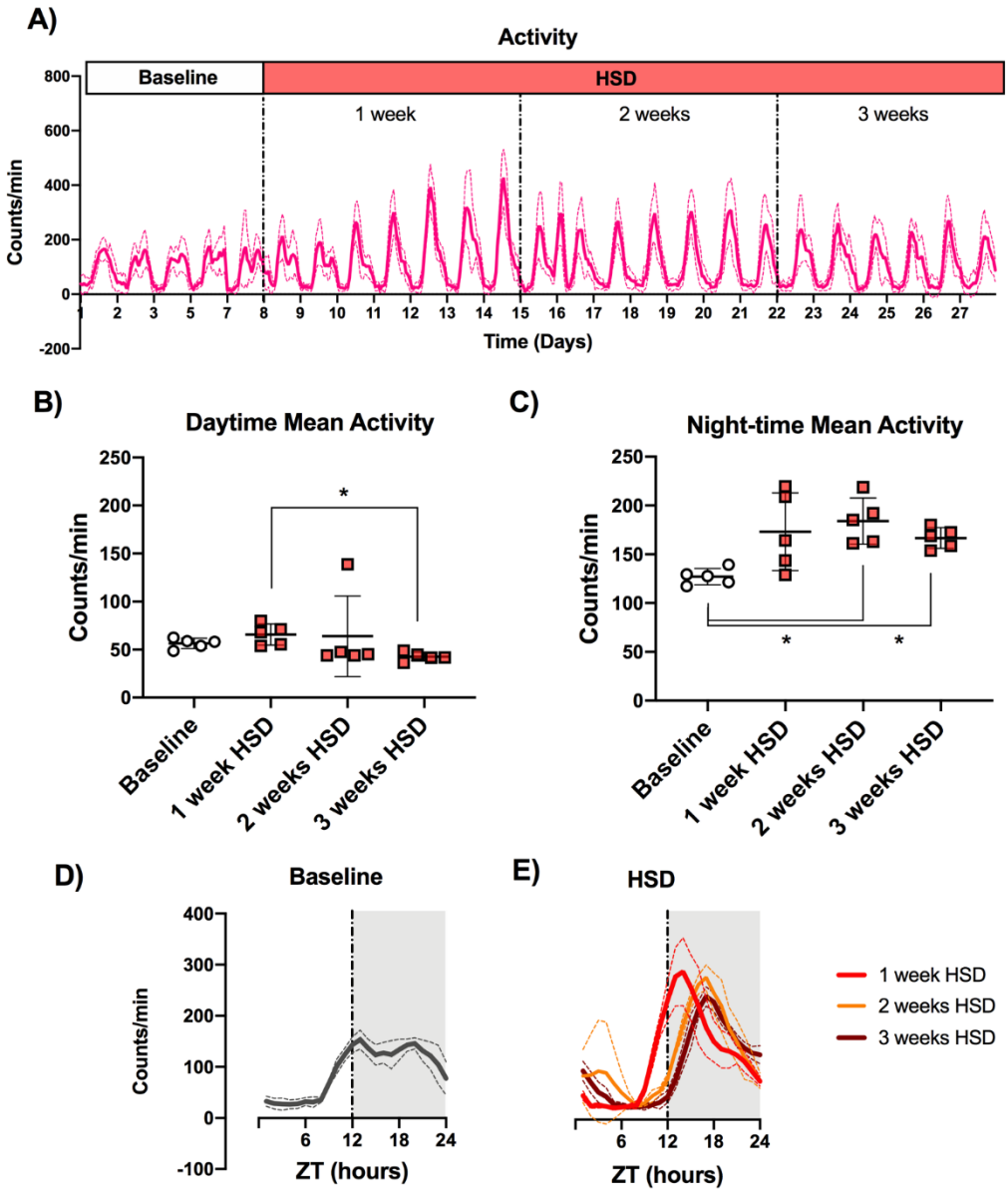

Figure 3.8: Locomotor activity in C57BL6/JCrl mice during high dietary salt intake.

Locomotor activity was measured via radiotelemetry in C57BL6/JCrl mice (n=7). It is representative of the amount mice moved during the experimental period. Mice were fed a standard salt (0.25% Na) diet for baseline recordings, which was then replaced with a high salt diet (HSD; 3% Na) for 3 weeks. Data are presented as 5-hour moving averages ± SD. A) Locomotor activity throughout the experiment. From these, 5-day data bins were obtained, and 12-hour means were taken at B) day-time (7AM-7PM) and at C) night-time (7PM-7AM), each data point displaying one 12-hour mean from all mice. Means were also calculated for every hour of the 24-hour light-dark cycle for activity during D) baseline and E) the HSD. Data were analysed and compared with repeated measures one-way ANOVA with Tukey post-hoc tests. *p<0.05.

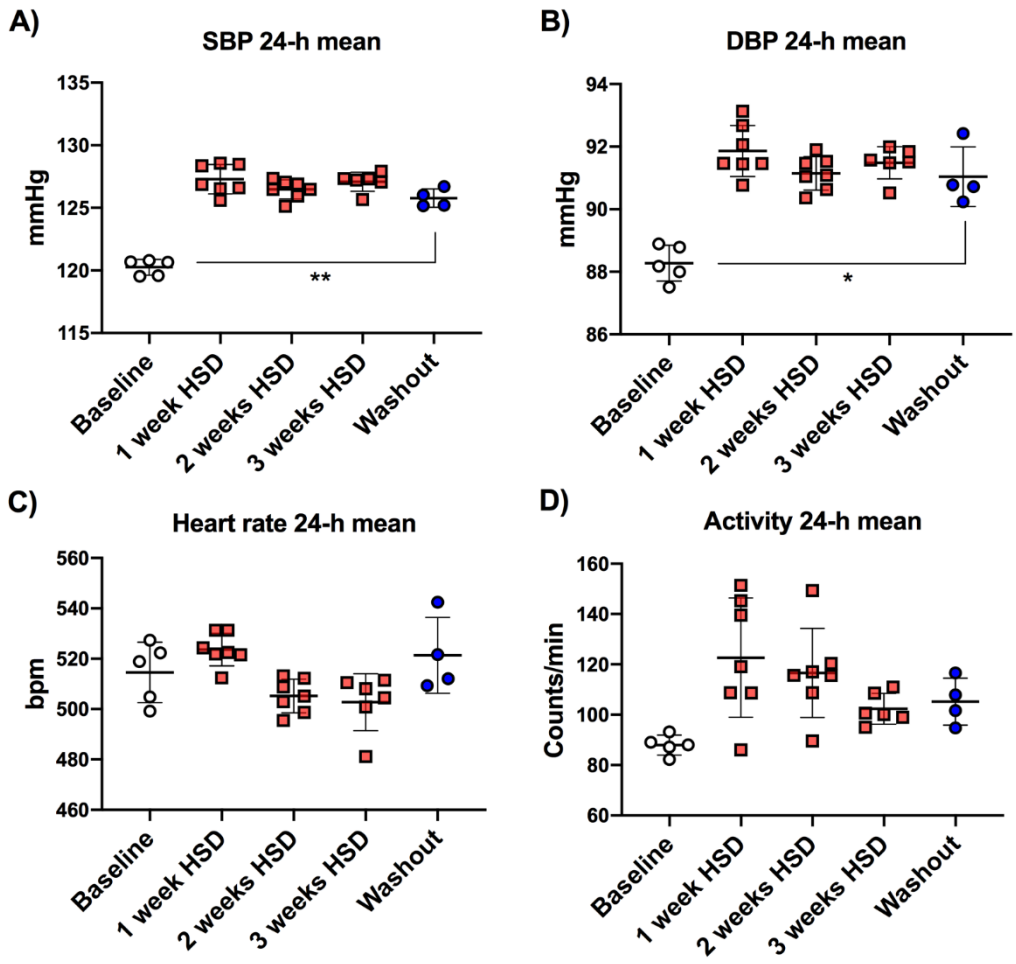

Figure 3.9: Blood pressure, heart rate and activity in C57BL6/JCrl mice after removal of the high salt diet.

Systolic (SBP) and diastolic blood pressure (DBP), heart rate and activity were measured via radiotelemetry in C57BL6/JCrl mice (n=7). Mice were given access to a standard salt (0.25% Na) diet for baseline recordings, then transferred to a high salt diet (HSD; 3% Na) for 3 weeks and finally returned to the standard diet for a 'washout' period. From the recordings, 24-hour (24-h) means containing data from all mice were obtained for A) SBP, B) DBP, C) heart rate and D) activity during baseline, each 1-week period of the HSD, and during washout. Data are mean ± SD analysed using a repeated measures mixed-effects model with multiple comparisons carried out by Tukey post-hoc testing. $^{**}p<0.01$, $^{*}p<0.05$.

3.3.3 Impact of reducing dietary salt on blood pressure, heart rate and locomotor activity

After 3 weeks of high dietary salt intake, mice were transferred back to the SSD upon which the baseline measurements were taken, referred to as a washout period. As outlined in section 3.2.1, the HSD was replaced on experimental day 29 and data was only acquired for experimental days 35 to 38, thus the mice had been receiving the SSD for 6 days prior to this. Little to

no differences were seen in 24-hour averaged BP following the removal of the HSD, as SBP was 125.8 ± 0.7 mmHg (*P*=0.470) and DBP was 91.0 ± 1.0 mmHg (*P*=0.957) compared to the third week of high dietary salt intake. SBP and DBP remained significantly higher than baseline (SBP *P*=0.003; DBP *P*=0.019; Figure 3.9 A & B). Heart rate was also unchanged at 521 ± 15 bpm compared to 3 weeks of the HSD (*P*=0.662) and compared to baseline (*P*=0.521; Figure 3.9 C). Additionally, no differences were seen in activity during washout and 3 weeks of HSD (105 ± 9 counts/min; *P*=0.984) nor during baseline (*P*=0.198; Figure 3.9 D).

3.4 Discussion

The overarching purpose of this chapter was to determine the impact dietary salt intake has on BP. Understanding this relationship is of considerable importance due to the alarmingly high daily consumption of dietary salt across the globe. Salt intake is recommended at <5 g/day, however the most recently calculated population means consistently exceed this, some by almost double that of the daily recommendation (7). A BP sensitive to salt is not universal; it occurs within ~25-33% of the global population as determined by age, ethnicity and comorbidities such as CKD (130). Ambiguity within the field originates from the use of the deceptively distinct categories ‘salt-sensitivity’ and ‘salt-resistance’ to determine the BP response to dietary salt. The physiological response is in fact continuous and dependent upon many interindividual variables, including those listed above. For example, previous studies have reported BP to rise anywhere between 1.5% and 34% following increased dietary salt intake (60).

Despite this variability, one observation remains constant: habitually high salt intake and increasing BP are associated with elevated risks of cardiovascular disease and mortality, which is reduced following restriction of dietary salt intake (68, 131, 132). Consequently, risk increases regardless of how minor the BP effect is (133). By investigating the mechanisms underlying salt-sensitivity of BP, we can begin to understand and unpick the link with cardiovascular risk.

Thus, the work in this chapter aimed to determine and define the extent of the BP response to increasing dietary salt intake in the C57BL6/JCrl mouse substrain.

3.4.1 High dietary salt intake and blood pressure in C57BL6/JCrl mice

The relationship between dietary salt intake and BP has been studied for near 60 years (38), and has led to the development of a plethora of genetically modified animal models in order to improve our knowledge on it. Examples include the Dahl salt-sensitive rat and mice with altered genes involved in the regulation of the RAAS or sodium reabsorption (111, 119, 134), providing invaluable insights into the processes involved. A substantial proportion of these murine transgenic models utilise the background strain C57BL6/J, of which there appears to be a divide or a lack of information in the literature regarding its salt-BP status.

Table 3.2: Comparison of baseline C57BL6/J mouse parameters with previous literature (Table 1; Van Vliet et al., (135).

24-h cardiovascular parameters	**C57BL6/J mice** (Van Vliet *et al*.)	**C57BL6/JCrl mice** (this work)
SBP (mmHg)	119 ± 2	120 ± 1
DBP (mmHg)	87 ± 2	88 ± 1
MBP (mmHg)	104 ± 2	104 ± 1
PP (mmHg)	31.6 ± 1.5	32.0 ± 0.4
Heart rate (bpm)	591 ± 6	515 ± 12

Systolic (SBP), diastolic (DBP), mean blood pressure (MBP) and heart rate were measured by radiotelemetry in C57BL6J/Crl mice (n=7). Pulse pressure (PP) was calculated by subtracting DBP from SBP. This table depicts 24-hour (24-h) averages of these cardiovascular parameters over the baseline period in which mice received a standard salt (0.25% Na) diet in this chapter and in work by Van Vliet *et al*., (135).

The work within this chapter characterises the effect of dietary salt intake on BP in C57BL6/JCrl mice by radiotelemetry. Baseline measurements collected in this experiment correlate extremely well with those collected by other radiotelemetry studies in C57BL6/J mice (135, 136). Table 3.2 shows my BP data are near identical compared with the reported values of Van Vliet *et al*. (135). These measurements were performed under similar circumstances as

the experiment in this chapter, for example mice were aged 9-12 weeks and fed chow consisting of 0.26% Na (135). The data taken during the 12-hour light and dark cycles also correlate well. Therefore, this gives us confidence within the data obtained by radiotelemetry in this chapter.

After 7 days of acquiring baseline data, the SSD (0.25% Na) was replaced with the HSD (3% Na). High dietary salt intake raised SBP by 7.0 mmHg and DBP by 3.8 mmHg within the first 4 days of the diet switch, and all BP measurements remained significantly higher compared to baseline for the full 3-week experimental period. Previous research with similar dietary sodium contents and dietary durations has reported comparable results. For example, Helkamaa *et al*. noted a 7.4 mmHg elevation in SBP and 2.0 mmHg in DBP after 3 weeks high salt in C57BL6/J mice utilised as wild-type controls (123), and Combe *et al*. demonstrated increased SBP at night after 2 weeks in these mice as a comparison to the substrain C57BL6/N (122). These studies occurred within male mice; however, female C57BL6/J mice also demonstrate a remarkable rise in BP in response to high salt (112).

On the other hand, conflicting data exists. No significant changes in MBP in male C57BL6/J mice were observed after 4 days (118) or 2 weeks of high dietary salt intake (120). There are a number of possible explanations for these discrepancies. Many studies compare a transgenic model designed to enhance a cardiovascular phenotype with the C57BL6/J background strain it was generated on and therefore may potentially miss or underestimate any effect in this strain. The second of note is the technique utilised to obtain BP data. The data revealing significant salt-induced changes within this mouse strain, including that presented within this chapter, have been measured using radiotelemetry. In contrast to this, BP measurements were obtained by the tail-cuff method or via a catheter under anaesthesia in studies reporting little to no changes with salt. This is discussed in further detail below (section 3.4.2).

Despite the contrasting results reported on the relationship between salt and BP in C57BL6/J mice in the literature, we report that increasing dietary salt

intake by ten-fold induced and sustained significant elevations in BP in C57BL6/JCrl mice.

3.4.2 Current methods of blood pressure measurement in rodents

Much of the BP data available has been obtained using the following methods: tail-cuff, catheterisation and radiotelemetry. These techniques allow for the monitoring of BP in rodents under an assortment of experimental settings, such as unconscious or conscious, restrained or freely moving and invasively or noninvasively. Each approach has its strengths and its drawbacks, which were taken into consideration whilst designing the experiments of in this chapter.

3.4.2.1 Tail-cuff method

The tail-cuff technique uses volume-pressure recording, in which blood flow in the tail artery is partially occluded and BP is extrapolated from the resulting pulsatile flow. This is beneficial as it is non-invasive, inexpensive, supports repeated measurements in conscious animals and numerous studies have reported that the BP data generated correlate well with other techniques performed simultaneously (137, 138). However, the accuracy of these measurements is heavily dependent upon immobilisation of the animal, which is achieved using restraint tubes. This introduces an additional source of stress alongside noise, human interaction and an unfamiliar environment. Rodents fail to adapt to this, and such a stressor has been shown to significantly impact both BP and heart rate data, even after attempts were made to familiarise animals with the technique (139, 140). Further to this, vasoconstriction induced by some commonly used cardiovascular interventions, such ANGII, can also lead to inaccurate BP readings (56).

3.4.2.2 Catheterisation

Generally, this approach involves the insertion of a catheter connected to a transducer into either the carotid or femoral artery to obtain BP measurements (141). This can be carried out in anaesthetised animals following non-recovery surgery, or in conscious, freely moving animals with exteriorised catheters. The former enables researchers to examine the

effects of potentially harmful drug doses on BP as well as carry out blood sampling without introducing stress-related artefacts into the data. On the other hand, BP measurements performed this way are limited to a single time-point due to the terminal nature of the work and are also subjected to the effects anaesthetic itself has upon haemodynamics (141). For this reason, it may be difficult to accurately measure physiological responses.

On the contrary, the use of exteriorised catheters addresses most of these shortcomings. Indwelling catheters are surgically inserted and externally secured at the back of the neck of the experimental animal. These are connected to pressure transducers via a longer lead referred to as a jacket and tether system, thus permitting the conscious animals to move about within range of the lead. Exteriorised catheters facilitate the direct monitoring of daily BP over a longer time frame and over multiple interventions, such as before and after a treatment, with the capability for repeated drug infusions or blood sampling as well (142). Despite this, complications frequently occur. Use can be problematic not only due to the risk of infection, but also due to the loss of catheter patency. Based on previous research, an experimental timeline of 1-2 weeks is recommended as catheter performance decreases by 50% a month after initial insertion (141).

3.4.2.3 Radiotelemetry

Radiotelemetry is the gold-standard technique and has been validated by several studies (56, 143, 144). It enables direct monitoring of multiple cardiovascular parameters, such as heart rate and locomotor activity in addition to BP. The transmitter devices are coupled with a receiver positioned beneath the animal's cage, and thus when implanted, devices facilitate the accurate, 24-hour measurement of BP in conscious, unrestrained animals. Importantly, this approach minimises stress induced by human contact (56). Drawbacks include expense and invasiveness of the surgical procedure to implant the devices. As with exteriorised catheters, single housing of experimental animals is usually required which, in itself, is a stressor. However, companies such as TSE Systems have begun to offer

Stellar Telemetry technology capable of measuring BP in animals housed in groups. The inclusion of a distinctive identification code per transmitter here allows the acquisition of data from multiple devices per receiver, which is extremely beneficial in terms of animal welfare.

3.4.2.4 The method of blood pressure measurement in this chapter

For the work within this chapter, radiotelemetry was used to measure BP. When selecting this approach, directness and accuracy of measurements were prioritised. Previously reported salt-induced effects on BP can occur within <10 mmHg and can influence its circadian regulation. Since the effect size is likely to be small, techniques such as tail-cuff or catheterisation may not be sensitive enough. These methods have been used in the literature reporting little to no impact of dietary salt intake on BP, as discussed within section 3.4.1. For this reason, a technique with the ability to acquire 24-hour measurements and the sensitivity to detect small but biologically important changes was required.

Radiotelemetry also supported the chosen experimental design. Complete with time spent recovering from surgery; the experiment was due to last 6 weeks in total with measurements taken before and after the HSD. DSI telemetry devices possess a battery life of up to 8 weeks, which far exceeds that offered by exteriorised catheters. Further to this, previous studies have reported other cardiovascular parameters, such as heart rate and locomotor activity, to have a significant influence upon BP (135, 145, 146). Radiotelemetry supported the collection of these, as well as the experimental design in which their response to high dietary salt intake could be investigated.

Overall, this experiment required the measurement of potentially small salt-induced changes upon multiple cardiovascular parameters over the 24-hour light-dark cycle in conscious, freely moving mice for the full experimental period. Out the approaches detailed above, radiotelemetry was best suited for this. A refinement of this approach would be the addition of a control group receiving the SSD throughout the experiment. This would allow the

simultaneous characterisation of the long-term, baseline cardiovascular parameters of C57BL6/JCrl mice by radiotelemetry. However, due to the equipment and space available, this group could not be accommodated.

3.4.3 Does high salt intake influence the day-night variability of cardiovascular physiology in C57BL6/JCrl mice?

BP is adapted to the light-dark cycle and so normally exhibits a day-night pattern that resets after 24 hours. In humans, BP typically dips by 10-20% during the night, rises rapidly during a 'morning surge' and reaches a peak ~6 hours before nightfall (147). This pattern is clinically important as adverse cardiovascular events appear to adhere to it and occur more frequently within the first 6 hours of the day, for example an increased frequency of all stroke types was noted between early morning and midday (148). Furthermore, the absence of a night-time dip in BP confers an increased risk of cardiovascular disease and death, which is particularly pronounced when accompanied by salt-sensitivity (149, 150).

Human beings are diurnal, whereas mice are nocturnal and so their sleep-wake cycle is inverted in comparison, meaning that their morning surge occurs at dusk instead as they awaken and so forth (151). In this experiment, C57BL6/JCrl mice exhibited a BP with typical 24-hour pattern. Table 3.1 displays the sleep-wake cycle of BP and the amount BP dipped between night (awake) and day (sleep). This dip increased with salt intake, which is likely due to elevated BP during the awake (night-time) period. However, it was still in keeping with the anticipated 10-20% dip during sleep and so illustrates that C57BL6/JCrl mice possess the appropriate day-night variation in BP regardless of dietary salt content. In fact, salt appeared to enhance it.

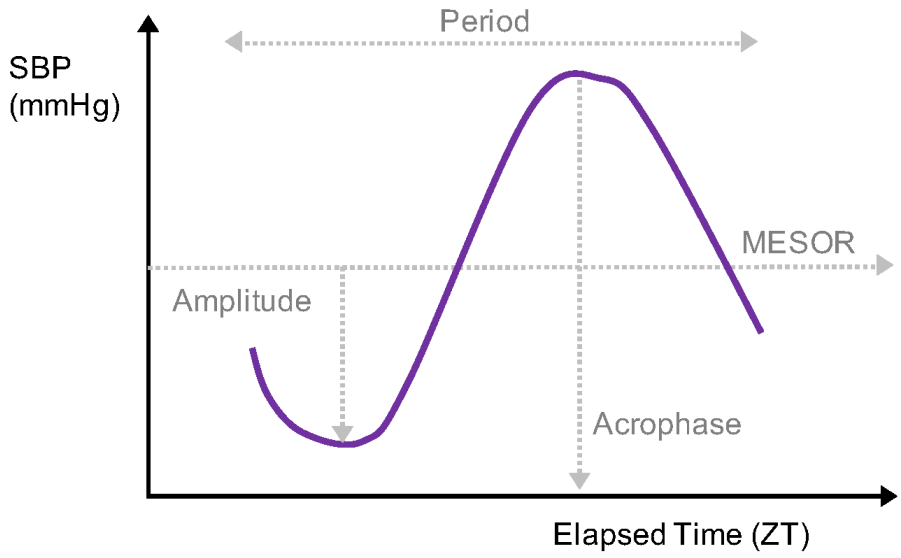

Figure 3.10: Cosinor curve fitting.
A graph depicting a cosinor curve fit to obtain the amplitude, acrophase, midline estimating statistic of rhythm (MESOR) and period. SBP; systolic blood pressure, ZT; Zeitgeber time.

During the first 3-4 days of high salt intake, small increases in both daytime SBP and DBP were noted which reversed with continued salt loading. Averaged 24-hour traces revealed a steep increase in BP between ZT 6-12, equivalent to the morning surge in humans, after 1 week of high salt intake. However, this steep increase shifted to the right after further high salt intake, occurring between ZT 12-18 instead after 2-3 weeks, and thus illustrating a phase shift indicative of a delayed surge. Further analysis is required to confirm this. Cosinor analysis can be performed, in which the data are fitted to sine curves for the purpose of analysing a circadian rhythm (Figure 3.10). In this case, the midline estimating statistic of rhythm (MESOR), a rhythm-adjusted mean, is used. As a potential phase shift has been indicated by my previous analysis, cosinor analysis would facilitate the calculation of acrophase (Figure 3.10). This is the time period at which the peak of the wave occurs, referred to as the morning surge in humans. Therefore, cosinor analysis could allow me to accurately determine whether in fact this peak has moved with increased salt intake.

This shift was also observed in locomotor activity. Previous research has demonstrated that the activity cycle of mice can influence BP rhythmicity

(135, 145, 146). The link was established when mean arterial BP (MABP) was observed to fluctuate within, as well as in-between, the 12-hour periods of light and dark, which was attributed to changes in activity (135). Circadian regulation of BP has also been reported to depend upon activity to a certain extent. Mice with a disrupted circadian clock displayed a clear diurnal rhythm in BP with cycles in locomotor activity until BP was analysed solely during periods of inactivity, or rest, in which rhythm disappeared (146). This suggests activity was partially driving BP rhythm in these mice, and so is an important influence upon BP. In this chapter, C57BL6/JCrl mice had higher activity counts per minute at night throughout the protocol, confirming their nocturnal status. When observing activity levels in response to high salt intake, night-time activity was elevated after 2-3 weeks compared to baseline, and so could be potentially contributing to the maintenance of high night-time BP with high salt at these time-points. A delayed day-night transition in SBP and DBP was observed after 2 and 3 weeks of high dietary salt intake. A similar pattern was observed in locomotor activity. In addition, daytime activity levels decreased following 3 weeks, suggesting that the mice were less active after a prolonged period of high dietary salt intake. It is possible these are linked, and locomotor activity has a potential role in this salt-induced BP effect.

However, further research would be required to delve into this and determine cause-and-effect, for example whether the BP transition is delayed due to altered episodes of locomotor activity, or vice versa. Cosinor analysis, as described above and depicted in Figure 3.10, could elucidate the impact of high salt intake on the day-night patterns of both BP and locomotor activity. Additionally, reversing the light-dark cycle or analysing BP solely within specific periods of activity and inactivity rather than between the general light and dark periods, as performed in a previous study (146), may shed more light on this relationship. Further to this, little to no differences in activity level were observed in both night and day after 3-4 days of high dietary salt intake despite rapidly increasing BP. Activity is also a measure of whether the

mouse is still (inactive) or in motion (active) at the time of data collection and so is a relative measure, which should be taken into consideration.

Heart rate also expresses a day-night rhythm. In C57BL6/JCrl mice, we observed a decrease in heart rate after 3 weeks of high salt intake, which is supported by the literature in which similar reductions were noted in this strain in response to dietary salt (145). Following increased salt intake, cardiac output (CO) is reduced in an attempt to offset any BP changes. CO is a product of heart rate and stroke volume, and thus decreases in heart rate can contribute to the physiological adaptation to high salt intake. In this case, the decline in heart rate in C57BL6/JCrl mice can be attributed to daytime heart rate whilst mice were at rest rather than at night during their most active phase. Contrary to this, heart rate remained similar to baseline after the first week of high salt intake, suggesting that perhaps C57BL6/JCrl mice initially struggle to adapt to the increased salt intake. Despite this apparent adaptation in the later weeks of high salt intake, BP still remains substantially higher than baseline, thus another component of the homeostatic mechanism may be preventing the desired normalisation of BP. This is currently unclear and warrants further investigation.

CO can be estimated through thermal dilution. This has been carried out within anaesthetised dogs and pigs; the animals are injected with room temperature saline solution via the venous system, such as the superior vena cava. With a sensor-containing catheter placed in the arterial system, such as the main pulmonary artery, thermodilution curves can be created and CO estimated using the Stewart-Hamilton equation (152). This has proven much more challenging in rodents due to their small size and the placement of the injection and sensor (153), however ADI instruments supply equipment for repeatable CO estimation specific to rodents, making this possible. In this case, CO could be estimated before and after high salt intake in C57BL6/JCrl mice.

Pulse pressure increases by ~2.5 mmHg during the day and by ~4 mmHg at night with high dietary salt intake in this experiment. Pulse pressure can be

indicative of a number of other cardiovascular parameters, such as heart rate and vascular compliance. From the above results, we can predict that such increases in pulse pressure with salt do not originate from changes to heart rate, as heart rate declines after 2-3 weeks of high salt intake. That leaves a potential role for vascular dysfunction to be investigated.

3.4.4 Are C57BL6/JCrl mice salt-sensitive?

The determination of salt-sensitivity in humans is a complex process dependent upon many factors, such as socio-demographic background, age, and genetics (59). Over the years, there has been much debate over the generation and use of a standardised definition, for example some researchers label an individual as salt-sensitive if BP elevates >10 mmHg with high salt feeding whereas others argue this response is far too variable between individuals to measure on just one occasion (49, 60). The major challenge, however, of investigating the salt-sensitivity of BP in human subjects is the inability to control variables, such as adherence to a diet with a strict sodium content. Therefore, the use of animal models is advantageous. An animal is classified as salt-resistant if no response to high dietary salt is observed, and salt-sensitive if an increase in blood pressure is induced and sustained. The results of this experiment conclude that C57BL6/JCrl mice are salt-sensitive, as they demonstrate significant sustained salt-induced increases in BP.

The next steps consist of examining the potential underlying mechanisms, with a particular focus upon the first week of high dietary salt intake due to the initiation of salt-induced hypertension and so the failure of homeostatic mechanisms to adapt to increased salt within this period.

3.4.5 Summary of results

1. High dietary salt intake substantially increased BP in C57BL6/JCrl mice after 1-3 weeks.
2. The day-night variability of BP, heart rate and activity remained intact after salt loading, dipping appropriately during the sleep phase.

3. Night-time BP and activity displayed similar patterns in response to high dietary salt intake after 2-3 weeks, but not during the first week.
4. No effect was observed on BP, heart rate or activity after reducing the dietary sodium content. However, this may be inconclusive due to confounding environmental factors.

4 Adaptation of Renal Function to High Dietary Salt in C57BL6/JCrl Mice

4.1 Introduction

The kidneys play a critical role within BP regulation, as detailed by Guyton's model (77, 78). If an imbalance arises between salt intake and excretion, BP is altered, thus triggering compensatory changes to renal sodium output referred to as the renal-body fluid feedback mechanism. This inherent autoregulation is governed by the acute PN relationship, which links BP regulation to salt/water balance. Evidence for this linkage arises from research into single gene mutations that generate an abnormal BP, revealing that the causative genes are frequently associated with renal sodium reabsorption (79).

Hall proposed that salt-induced elevations in BP cannot be sustained in the absence of renal impairment, predominantly dysregulation of the acute PN relationship (57). In salt-sensitivity, the acute PN relationship is said to be reset toward supporting a higher BP, potentially due to underlying intra-renal processes influencing GFR or sodium reabsorption (57). As a result, excess salt cannot be expelled and so is retained, contributing to further BP changes and other injurious effects.

The previous chapter demonstrated that increasing dietary salt intake initiated and sustained significant increases in the BP of C57BL6/JCrl mice, confirming their salt-sensitive status. Based on the above models and the important influence the kidney has on salt handling and BP control, it was hypothesised that renal dysfunction, specifically an impaired PN relationship, drives the salt-induced hypertension of these mice.

4.1.1 Aims

1. To compare the acute PN relationship between a group receiving high dietary salt intake and a group receiving standard salt intake.
2. To examine the effects of high salt intake on *in vivo* renal haemodynamics, such as GFR and RBF.
3. To investigate the influence of high salt on the transcriptional profile of renal sodium transporters, compared to standard salt

4.1.2 Approach to achieve the chapter aims

- The acute PN relationship was assessed *in vivo* by experimentally inducing stepwise pressure ramps under anaesthesia to increase BP and measuring subsequent urinary sodium excretion. This approach makes the assumption that, since BP rises, renal perfusion pressure also rises. Two experiments were performed, each with a group receiving the HSD and a contemporaneous control group on the SSD.
- *In vivo* measurements of renal haemodynamics were obtained in the same groups as above under anaesthesia with the infusion of FITC-inulin and its detection in urine to determine GFR. A Doppler ultrasound flow-probe was positioned around the renal artery to measure RBF during these manufactured BP elevations.
- The transcriptional status of renal sodium transporters was determined in a separate experiment by measuring mRNA abundance via qPCR.
- The effect of dietary salt was assessed by measuring the above parameters after the SSD (0.25% Na) or after 3 days or 1 week of the HSD (3% Na). The effect on mRNA abundance was investigated after 3 days, 1 week or 2 weeks of the HSD in separate experiments. These time-points were selected based on the salt-induced BP changes observed in the previous chapter.

4.2 Methods

The procedures performed to obtain the results in this chapter are described in detail in the main Materials and Methods chapter. Specific experimental details and timelines are presented here for clarity.

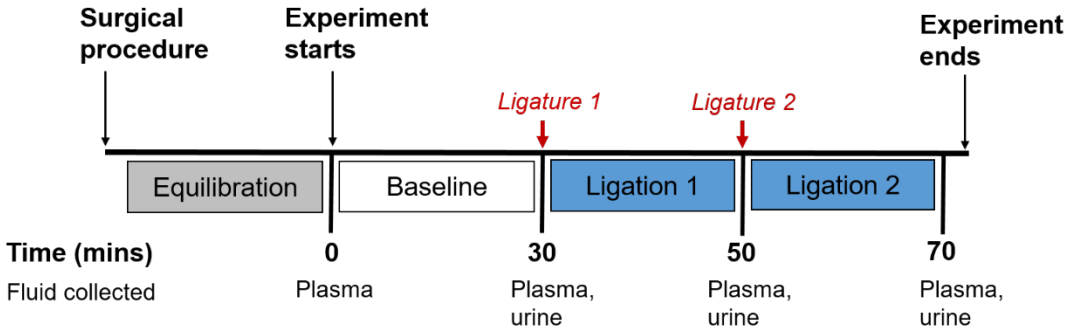

Figure 4.1: Experimental protocol and timeline for the assessment of the acute pressure natriuresis response.
C57BL6/JCrl mice (n=6-9 per dietary group) aged 11-12 weeks old were fed either a standard salt (0.25% Na) or high salt diet (3% Na) before pressure natriuresis surgery was performed under anaesthesia via thiobarbiturate injection. Following the procedure, mice were left for a 30-minute equilibration period. Once a stable blood pressure had been established, baseline measurements of blood pressure and renal blood flow were collected over a further 30 minutes before the first ligature around the mesenteric and celiac arteries was applied (Ligature 1). After 20 minutes, the second ligature was tightened (Ligature 2), occluding the abdominal aorta, and measurements were taken for another 20 minutes. Plasma was sampled via carotid artery cannula and urine via bladder catheter. At the end of the experimental protocol, terminal plasma samples were collected, and mice were humanely euthanised via an overdose of anaesthetic.

4.2.1 Surgical assessment of the acute pressure natriuresis response

Two experiments were performed in which adult male C57BL6/JCrl mice aged 11-12 weeks received the HSD for either 3 days or 1 week prior to the *in vivo* measurement of the acute PN response, with contemporaneous controls receiving the SSD. This study design was used due to the invasive, terminal nature of the surgery. Furthermore, due to this, the experiments were performed at different times. By including mice on the SSD as controls in each experiment, this accounts for the potential variability in the equipment used, techniques applied, and substances administered at the time the experiment was performed which could negatively impact the relationships observed. For example, the use of historical controls may introduce an unnecessary level of variability and lead to the underestimation of any effects seen. Thus, each experiment was performed and analysed independently with contemporaneous controls to avoid this.

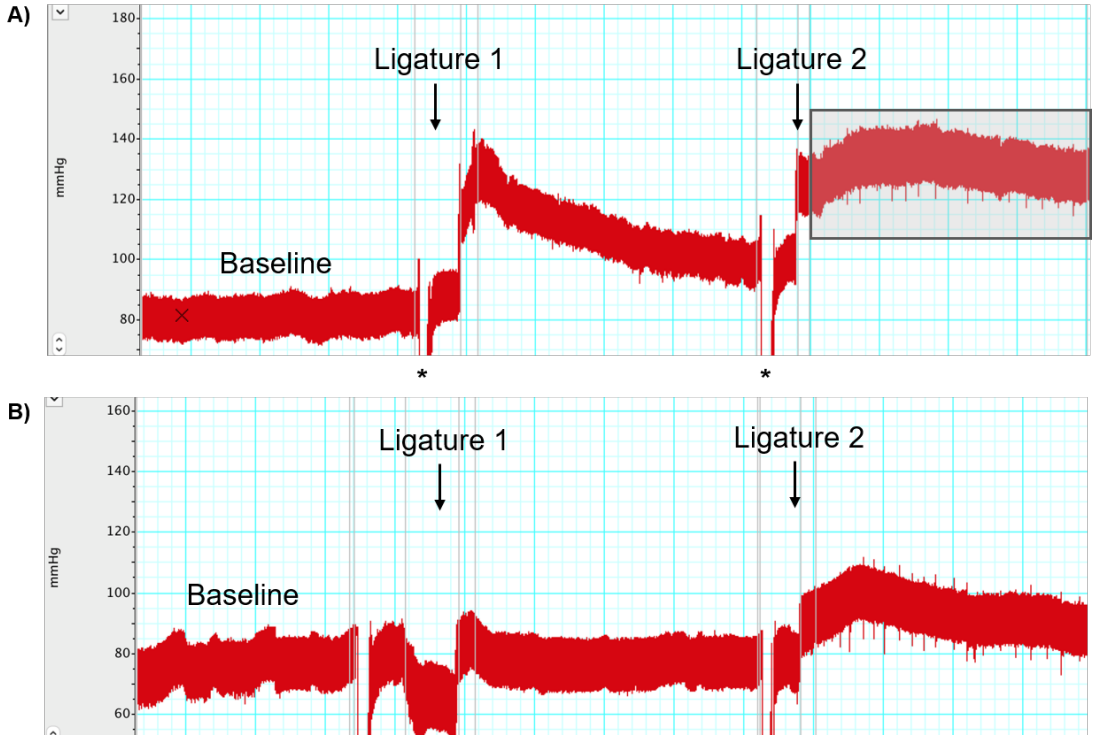

Figure 4.2: Representative BP traces and the acquisition of data in Labchart.
BP was measured by cannulation of the carotid artery in C57BL6/JCrl mice following either a standard or high salt diet. Data (mmHg on y-axis vs mins on x-axis) were acquired using the software Labchart 7 pro version 7.3.2, which presented as a trace like that shown. A: BP increases following each of the two ligatures. Data were obtained by isolating sections of the trace corresponding to the different experimental periods by drawing boxes, as represented by the grey box here selecting data following the second ligature. The asterisks depict areas of the trace that were avoided, as this was when blood sampling occurred. B: Example of when an inadequate pressure ramp transpired, thus resulting in exclusion from the analysis further down the line.

Mice were surgically prepared as described in Methods 2.3.1 by Mr Kevin Stewart, the manager of the Centre's *in vivo* Physiology Laboratory. The procedure was carried out under anaesthesia, which was maintained throughout the experimental protocol via the left jugular vein cannula. Due to the challenging and time-consuming nature of the surgeries, they were carried out throughout the day and thus sampling did not occur at any specific, predetermined times.

Figure 4.1 is a schematic representation of the protocol and timeline over which the acute PN response was examined. Following the surgery, mice underwent a 30-minute equilibration period prior to the start of the experiment, as monitored by the stabilisation of BP. Arterial occlusion was

utilised to induce consecutive pressure ramps, the first occurring upon ligation of the mesenteric and celiac arteries and the second upon ligation of the abdominal aorta. The effect upon BP, here as a representative of renal perfusion pressure, is shown in Figure 4.2 A. If the ligations failed to produce appropriate ramps in BP, the data were excluded from the post-acquisition analysis (Figure 4.2 B).

4.2.1.1 Data acquisition and analysis

BP and heart rate: BP was measured via carotid artery cannulation and the data was acquired from the three experimental periods baseline, ligature 1 and ligature 2 (30, 50 and 70 mins, respectively) as illustrated in Figure 4.2. Data from each period were isolated and average cyclic measurements were taken in Labchart (maximum for SBP, minimum for DBP, 1/3 Max + 2/3 Min for MABP, and rate for heart rate).

GFR and urinary flow rate: Throughout the experimental protocol, FITC-inulin was delivered as a component of the infusate via the left jugular vein. Blood samples were obtained via the carotid artery cannula and centrifuged for plasma. Urine was collected via bladder catheter. The clearance of FITC-inulin at the time-points 30, 50 and 70 mins was utilised to estimate GFR.

RBF and RVR: Doppler ultrasound via a nano-flow probe (Transonic Systems, Netherlands) was utilised to measure RBF through the left renal artery in the same cohorts. This was also acquired by Labchart and mean flow (mL/min) was obtained for each experimental time-point. Renal vascular resistance (RVR) was then calculated as below:

$$RVR = \frac{MABP}{RBF}$$

4.2.1.2 Data normalisation and analysis

Following the completion of the experimental protocol, mice were humanely euthanised with an overdose of anaesthetic before the kidneys were excised and weighed. Data for GFR and urinary flow rate were normalised to kidney weight per gram (KW), which itself was unaffected by dietary salt intake (SSD

0.31 ± 0.04 vs. 3 days HSD 0.33 ± 0.03, *P*=0.219; SSD 0.31 ± 0.03 vs. 1 week HSD 0.32 ± 0.03, *P*=0.749).

Repeated measures two-way ANOVA was performed to determine the effect of dietary sodium content, time and whether any interaction was occurring between the two factors. The resulting *P* values were corrected for multiple comparisons made by Sidak testing and have been presented within tables alongside the data, with significance denoted as $P<0.05$.

Figure 4.3: Reference genes for renal cortex and medulla qPCR.

C57BL6/JCrl mice received either a standard salt diet (SSD; 0.25% Na) or a high salt diet (HSD; 3% Na) for 3 days, 1 week or 2 weeks (n=6-8 per group) before kidneys were excised, divided into cortex and medulla and quantitative PCR (qPCR) was carried out. The mRNA abundance of the reference genes *Hprt*, *Tbp*, *Actb* and *Rn18S* was assessed and those unaltered by increasing dietary salt content for the renal cortex after 3 days (A-D) and 1 or 2 weeks (E-H) HSD and for the renal medulla after 3 days (I-L) and 1 or 2 weeks (M-P) HSD were taken forward. Mean abundance of three reference genes were utilised for each sample (D, H, L, P), which was then used to normalise the mRNA abundance of the experimental genes-of-interest. Data are presented as mean ± SD. The mRNA abundance following 3 days of HSD was analysed via unpaired *t* test, and mRNA abundance following 1 or 2 weeks of HSD via ordinary one-way ANOVA with multiple comparisons made by Tukey testing. Significance was denoted as $P<0.05$.

Cortex

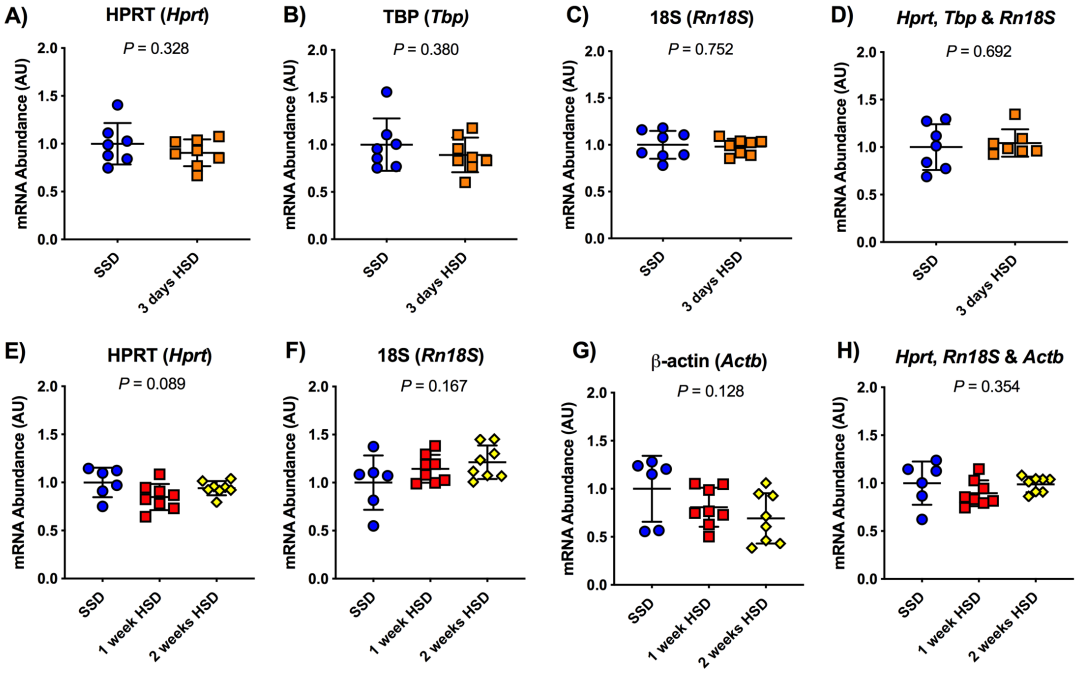

Medulla

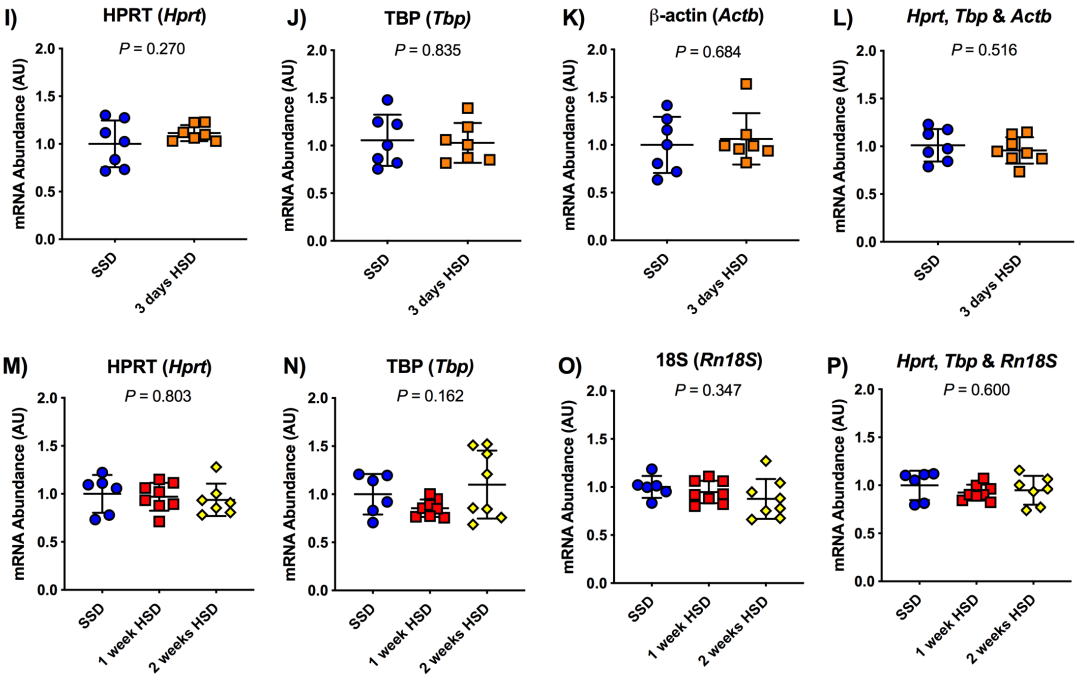

4.2.2 Determination of renal mRNA abundance

Renal mRNA abundance was quantified via qPCR in a separate experiment, in which three dietary groups were utilised: one received the SSD, another 1 week of the HSD, and the last 2 weeks of the HSD. Materials and Methods chapter section 2.4 covers the general protocol of RNA isolation and mRNA detection in tissue, whereas the methodological details specific to renal tissue in these experiments are outlined below.

4.2.2.1 Sample preparation and RNA isolation

The kidneys were quickly excised during the daytime through a midline incision after clamping the renal blood supply. Following dissection, they were decapsulated and divided by region using a scalpel. The resulting cortical and medullary samples were flash-frozen and stored at -80 ºC until the time of analysis. Frozen tissue was transferred to room temperature RLT buffer, disrupted using stainless steel beads in the Tissue Lyser II and taken through the RNeasy Mini Isolation kit as per the manufacturer's instructions (all QIAGEN, UK). The integrity of the extracted RNA from both cortical and medullary samples was confirmed as described in Methods 2.4.2, with A260/280 ratios ranging 2.0 - 2.1. Reverse transcription was performed, in which RNA samples were diluted appropriately to generate 500 ng cDNA, and qPCR analysis was carried out as described (Methods section 2.4.4). Samples were diluted 1:40 for the detection of the experimental genes.

4.2.2.2 Reference genes

Reference genes were screened separately for renal cortex and medulla samples to determine at least three in which expression did not change after increased dietary salt intake. Genes *Hprt*, *Rns18* (18S rRNA) and *Actb* (β-actin) were selected for the renal cortex, and *Hprt*, *Rns18* and *Tbp* for the renal medulla after 3 days (Figure 4.3 D & L) and after 1 and 2 weeks (Figure 4.3 H & P) of dietary intervention.

4.2.2.3 Data normalisation and analysis

Within these experiments, the animals receiving the SSD made up the control group. For each of the reference genes, the mean concentration of the SSD group was adjusted to equal 1 and applied to the rest of the samples. All three were then averaged. The mRNA abundance of the experimental genes-of-interest were normalised to this, and thus each gene-of-interest is presented relative to the mean mRNA abundance of the three reference genes ± SD.

With one comparison to make, statistical analysis consisted of unpaired *t* testing. With more than two groups to compare, ordinary one-way ANOVA was carried out and the resulting *P* value corrected for multiple comparisons by Sidak testing.

Figure 4.4: Cardiovascular variables during assessment of the acute pressure natriuresis relationship after 3 days of high salt intake.

Measurements of blood pressure (BP) and heart rate (HR) were taken during pressure natriuresis (PN) surgery in C57BL6/JCrl mice on a standard salt diet (SSD 0.25% Na; n=9) and after 3 days of a high salt diet (HSD 3% Na; n=9) under thiobarbiturate anaesthesia. Mice underwent 30-minute baseline (B) measurements of A: systolic BP (SBP), B: diastolic BP (DBP), C: mean arterial BP (MABP), and D: HR. Increased pressure was simulated by ligating the mesenteric and celiac arteries and measurements were collected for 20 minutes (50-min time-point, L1). This was exacerbated by performing the second ligation (70-min time-point, L2) which involved tying off the abdominal aorta and taking further measurements. A: SBP presented as mean/min ± SD. B-D: BP and HR presented as mean ± SD. E: *P* values following a repeated measures two-way ANOVA, corrected for multiple comparisons made by Sidak post-testing. Data are mean ± SD. ****$p<0.0001$, *$p<0.05$.

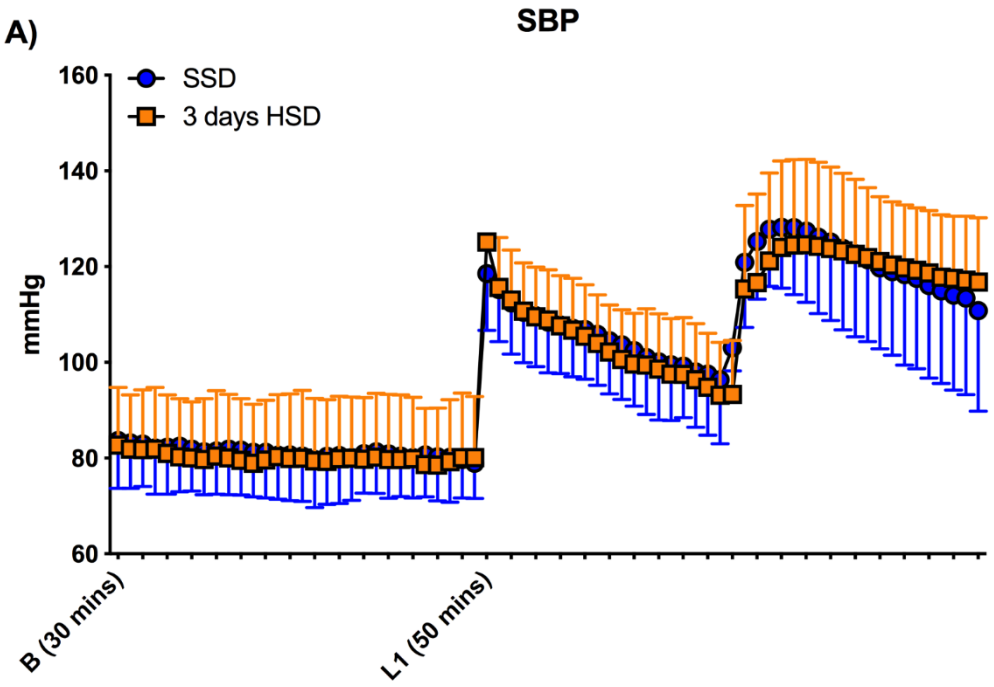

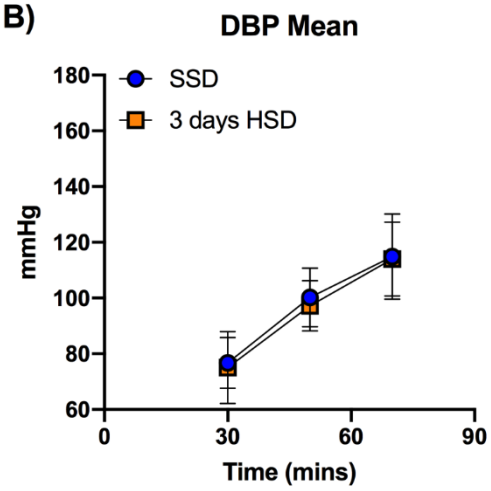

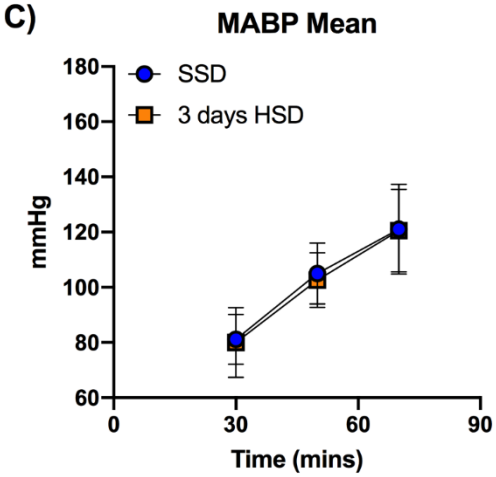

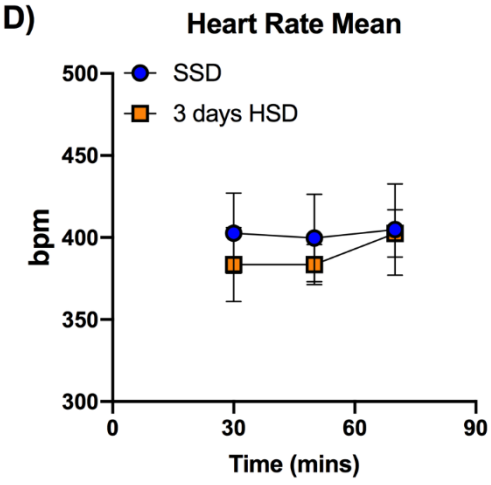

E)

Two-way ANOVA P values	*DBP*	*MABP*	*HR*
Time (mins)	**<0.0001, ******	**<0.0001, ******	0.221
Diet	0.567	0.690	**0.044, ***
Interaction	0.963	0.974	0.489

4.3 Results

4.3.1 Blood pressure and heart rate upon induction of serial pressure ramps after 3 days of high dietary salt intake

Figure 4.4 demonstrates the cardiovascular status of the mice during the execution of pressure ramps following 3 days of high dietary salt intake. BP increased significantly with each major artery ligation, as can be observed minute-by-minute in SBP in Figure 4.4 A. During the baseline period, BP was comparable between the dietary groups. For example, MABP after the SSD was 81.1 ± 8.5 mmHg and 80.0 ± 11.9 mmHg after 3 days HSD (P=0.997). With the first ligation, MABP rose to 105.0 ± 10.4 mmHg after the SSD and similarly to 102.6 ± 9.4 mmHg after the HSD (P=0.968). After the second ligation, MABP was further increased to 121.1 ± 15.3 mmHg and 120.6 ± 14.1 mmHg respectively (P=0.999; Figure 4.4 C). MABP was elevated equally at each time-point, illustrating that 3 days of high dietary salt intake did not affect MABP at the time of the surgery, nor did it alter the MABP response to pressure ramps. This effect was also seen within DBP (Figure 4.4 B & E).

No significant changes in heart rate accompanied the stepwise ligations (Figure 4.4 D & E). Following the SSD, mean heart rate was 403 ± 23 bpm at baseline, 400 ± 25 bpm during the first ligation and 405 ± 26 bpm during the second. Mean heart rate of mice after the HSD was very slightly lower at 384 ± 21 bpm at baseline (P=0.210), which did not change following the first pressure ramp but elevated to 402 ± 14 bpm during the second (P=0.995 compared to baseline). Overall, a modest effect of the HSD after 3 days is reported (Figure 4.4 E).

A)

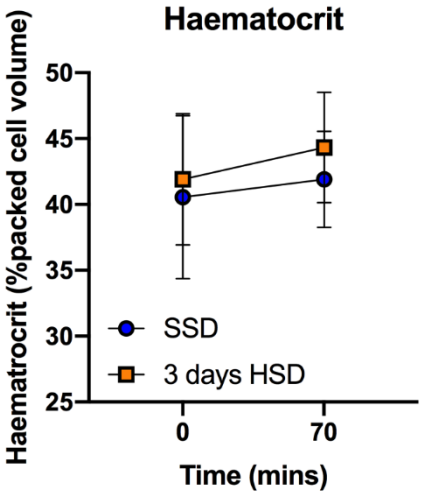

B)

Two-way ANOVA P values	*Haematocrit*
Time (mins)	0.190
Diet	0.315
Interaction	0.708

Figure 4.5: Haematocrit (%) during the assessment of the acute pressure natriuresis relationship after 3 days of high salt.

C57BL6/JCrl mice underwent pressure natriuresis surgery following either a standard salt diet (SSD 0.25% Na; n=9) or 3 days of a high salt diet (HSD 3% Na; n=9) under anaesthesia. Blood samples were taken via carotid artery cannula at the start of the experiment after a 30-minute equilibration period and at the end after the ligation of the abdominal aorta. Following centrifugation, haematocrit was determined using a micro haematocrit reader. A: mean haematocrit ± SD, B: *P* values from a repeated measures two-way ANOVA with Sidak post-testing. Significance was denoted as $P<0.05$.

Haematocrit was not significantly altered between the start of the experiment and the end, nor between the dietary groups (Figure 4.5). At the beginning of the baseline period, haematocrit was 41 ± 6 % in mice on SSD and 42 ± 5 % in mice after HSD ($P=0.974$). After the final ligation, haematocrit was 42 ± 3% and 44 ± 4% respectively ($P=0.823$). This was slightly higher than pre-baseline levels, however no overall significant effect was observed (Figure 4.5 B).

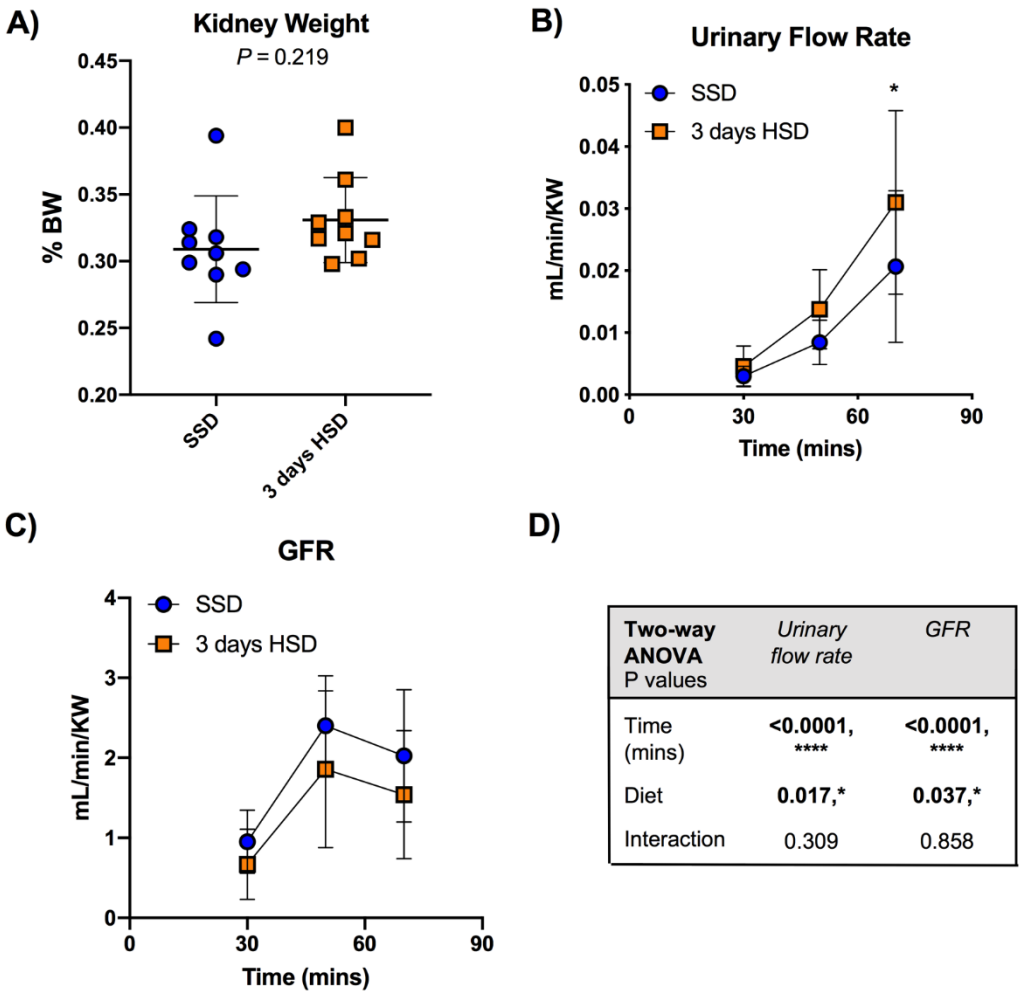

Two-way ANOVA P values	*Urinary flow rate*	*GFR*
Time (mins)	**<0.0001, ******	**<0.0001, ******
Diet	**0.017,***	**0.037,***
Interaction	0.309	0.858

Figure 4.6: Urinary flow rate and glomerular filtration rate following 3 days of high dietary salt intake.

Urinary flow rate and glomerular filtration rate (GFR) were evaluated during pressure natriuresis surgery in anaesthetised C57BL6/JCrl mice after the standard salt diet (SSD 0.25% Na; n=9) or after 3 days of high salt diet (HSD 3% Na; n=9). Urinary flow rate was determined by recording the volume of urine collected over the time it was collected for. GFR was estimated through FITC-inulin clearance, and both were expressed relative to kidney weight (KW). Both were measured during baseline, ligation 1 involving occlusion of the celiac and mesenteric arteries, and ligation 2 involving occlusion of the abdominal aorta. After mice were humanely euthanised by anaesthetic overdose, kidneys were excised and weighed. Data are mean ± SD, presented as A: KW normalised to body weight (BW) and analysed via unpaired *t* test, B: urinary flow rate, C: GFR and D: table depicting repeated measures two-way ANOVA results with Sidak post-hoc analysis. *****p*<0.0001, **p*<0.05.

4.3.2 Effect of high dietary salt intake for 3 days on renal haemodynamics

Kidney weight (KW) did not differ between mice fed SSD or 3 days HSD (*P*=0.219; Figure 4.6 A). Urinary flow rate was comparable between the dietary groups at baseline (SSD 0.0030 ± 0.0015 vs. HSD 0.0046 ± 0.0030 mL/min/KW; *P*=0.973). The serial pressure ramps resulted in stepwise increases in urinary flow rate, with a modest effect of diet (Figure 4.6 B & D). Urinary flow rate increased substantially from baseline to 0.0084 ± 0.0033 in the SSD group and 0.0138 ± 0.0060 mL/min/KW in the HSD group when the first ligation was carried out (*P*=0.469). When the second ligation was performed, urinary flow rate was significantly greater in mice fed 3 days of the HSD than in mice fed the SSD (0.0310 ± 0.0140 vs 0.0206 ± 0.0115 mL/min/KW, respectively; *P*=0.039). Thus, an overall significant effect of diet was seen (Figure 4.6 D).

Baseline GFR was largely unaffected by dietary sodium content, measured at 0.95 ± 0.37 mL/min/KW in the SSD group and 0.67 ± 0.41 mL/min/KW in the group after 3 days high salt intake (*P*=0.809). This increased to 2.40 ± 0.59 and 1.86 ± 0.92 mL/min/KW, respectively, with the first ligation but GFR was not different between the dietary groups (*P*=0.364). With the second ligation, GFR in both groups fed the SSD and HSD declined, measured at 2.03 ± 0.77 mL/min/KW in mice fed the SSD and 1.98 ± 0.75 mL/min/KW in mice fed 3 days of the HSD (*P*=0.425; Figure 4.6 C). Overall, a small dietary effect was found (Figure 4.6 D), however this was not reflected in the post-hoc analysis.

4.3.2.1 Renal blood flow after 3 days high salt

Both dietary salt and the induced pressure ramps produced a significant effect on RBF, as can be seen minute-by-minute in Figure 4.7 A. Each ligation step generated an increase in RBF; yet, this elevation was significantly less in the group fed 3 days of high dietary salt intake (Figure 4.7 B & D). During baseline, RBF between the two dietary groups was similar (SSD 1.06 ± 0.15 vs. HSD 0.90 ± 0.18 mL/min; *P*=0.306) however following

the first ligation, RBF in the SSD group increased to 1.20 ± 0.13 mL/min whereas RBF in the HSD remained similar to baseline flow at 0.93 ± 0.21 mL/min (*P*=0.028). RBF in the SSD group increased again with the final ligation of the abdominal aorta, reaching 1.48 ± 0.25 mL/min. RBF in the HSD group also rose during this step, which was measured at 1.15 ± 0.25 mL/min, although it was evidently lower than flow in the SSD group (*P*=0.008). Therefore, RBF increased with each ligation, however this was significantly blunted in the HSD group.

Minor alterations to RVR were noted during the ligation steps; nevertheless, these did not pass the threshold for statistical significance (Figure 4.7 C & D). Baseline RVR was calculated at 77.1 ± 9.6 AU in the SSD group and 91.3 ± 16.9 AU in the HSD group, thus there was no effect of diet prior to the pressure ramps (*P*=0.542). During the first ligation, RVR was higher in mice in the HSD group compared to mice in the SSD group (SSD 87.9 ± 9.1 vs. HSD 118.4 ± 38.2 AU; *P*=0.035). During the second, RVR dipped very slightly but remained higher in the HSD group (SSD 84.1 ± 15.3 vs. HSD 110.7 ± 33.5 AU; *P*=0.079) which bordered on statistical significance. Due to assessment via two-way ANOVA, high salt intake influenced RVR and resulted in significant changes compared to that of the SSD group.

Figure 4.7: Renal blood flow after 3 days of high dietary salt intake measured during pressure natriuresis surgery.

Renal blood flow (RBF) was measured in anaesthetised C57BL6/JCrl mice after either a standard salt diet (SSD 0.25% Na; n=9) or a high salt diet (HSD 3% Na; n=9) via Doppler ultrasound. Mice underwent baseline measurements, followed by serial pressure ramps induced by ligating the mesenteric and celiac arteries and the abdominal aorta. Renal vascular resistance (RVR) was mean arterial blood pressure (MABP) over RBF. Data are mean ± SD shown as A: RBF per minute, B: RBF, C: RVR and D: *P* values from a repeated measures two-way ANOVA, corrected for multiple comparisons with Sidak post-testing. Significance denoted as $P<0.05$. ****$p<0.0001$, ***$p<0.001$.

A)

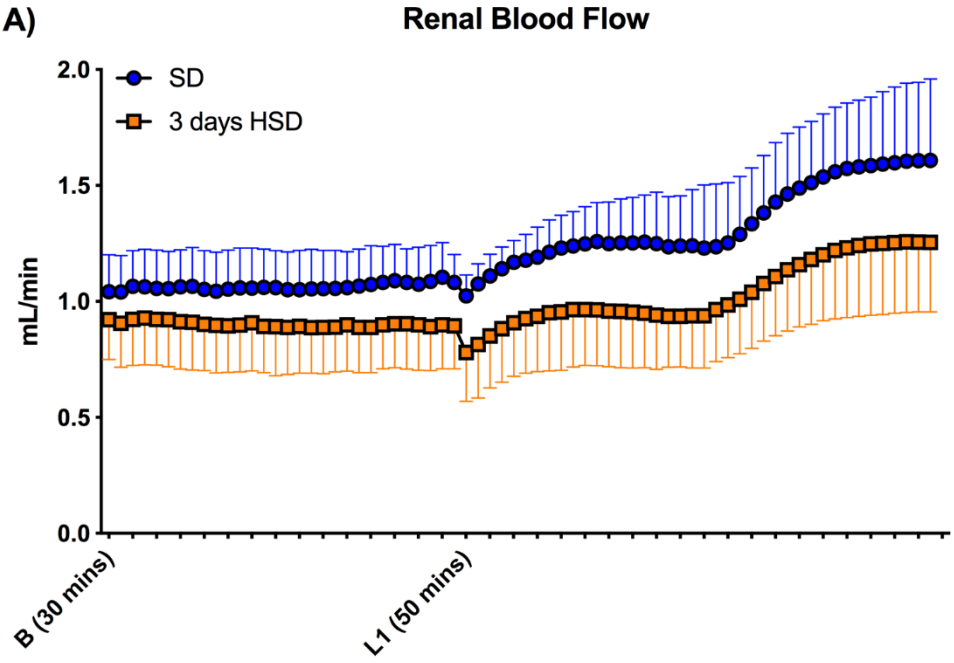

B)

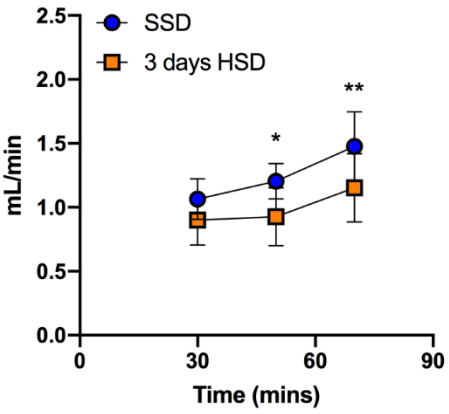

C)

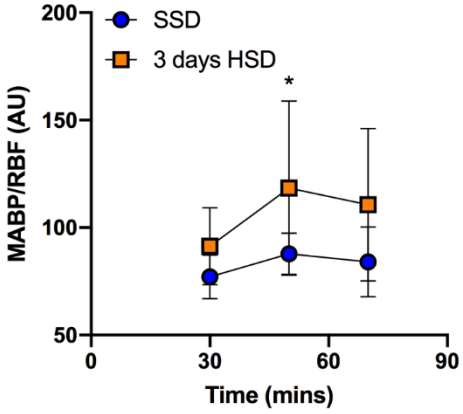

D)

Two-way ANOVA P values	*RBF*	*RVR*
Time (mins)	**<0.0001, ******	0.074
Diet	**<0.0001, ******	**0.0009,*****
Interaction	0.526	0.590

4.3.3 High dietary salt intake for 3 days causes a leftward shift in the acute pressure natriuresis curve

SBP, measured through cannulation of the carotid artery, rose significantly with the serial pressure ramps. The extent of these elevations was comparable between the dietary groups, as SBP in the SSD group rose from 89.9 ± 10.0 mmHg at baseline to 114.5 ± 13.1 mmHg and finally to 133.6 ± 19.2 mmHg after the final ligation. Similarly, SBP in the group fed 3 days of the HSD rose from 90.0 ± 13.0, to 113.2 ± 12.6 and then to 133.5 ± 18.7 mmHg (Figure 4.8 A & C).

Urine samples were collected from a bladder catheter and sodium excretion was quantified (Figure 4.8 B). During the 30-minute baseline period, urinary sodium excretion was not different between the SSD group and the group after 3 days of the HSD (0.37 ± 0.15 vs. 0.82 ± 0.54 µmol/min, respectively; P=0.893). However, following the first ligation, urinary sodium excretion increased in the HSD group to 1.87 ± 1.61 µmol/min, whereas excretion remained stable at 0.46 ± 0.42 µmol/min in the SSD group (P=0.189). This difference became even greater and crossed the significance threshold during the second ligation period, in which urinary sodium excretion increased to 4.89 ± 3.59 µmol/min in the HSD group and 1.62 ± 1.17 µmol/min in the SSD group (P=0.0003). Hence, the final pressure ramp raised urinary sodium excretion, with mice in the 3 days HSD group excreting more compared to mice in the SSD group (Figure 4.8 B & C). A modest interaction between the dietary groups was noted (Figure 4.8 C), possibly due to an increase occurring after the HSD but not after the SSD during the first ligation.

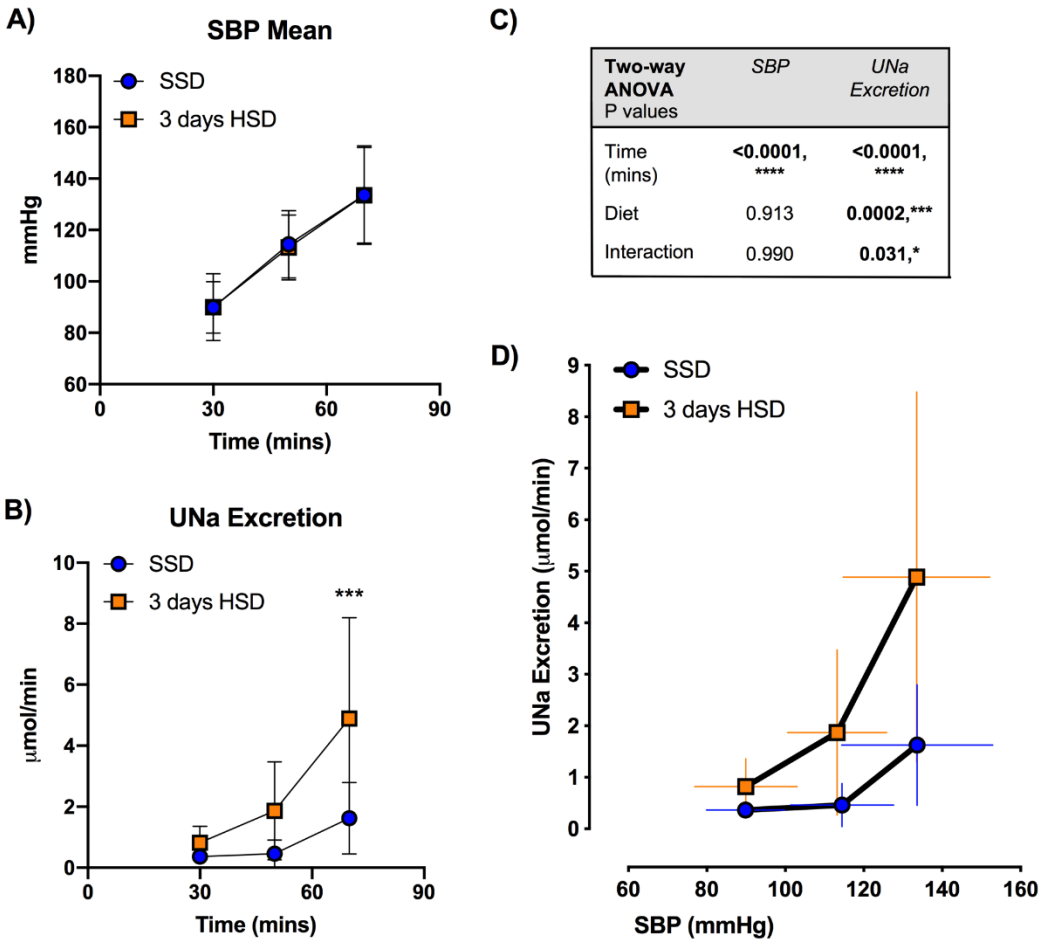

Figure 4.8: Acute pressure natriuresis relationship after 3 days of high salt feeding.
The acute pressure natriuresis relationship was experimentally assessed in C57BL6/JCrl mice after a standard salt diet (SSD 0.25% Na; n=9) or 3 days of a high salt diet (HSD 3% Na; n=9). Under thiobarbiturate anaesthesia, systolic blood pressure (SBP) was measured via carotid artery cannula and urinary sodium (UNa) excretion was quantified from samples taken via bladder catheterisation. Ligation of the mesenteric and celiac arteries, followed by ligation of the abdominal aorta, induced pressure ramps during which SBP and UNa were measured. Data presented are mean ± SD. A: SBP, B: UNa excretion, C: *P* values generated from a repeated measures two-way ANOVA, corrected for multiple comparisons via Sidak post-testing, and D: pressure natriuresis curve depicting the relationship between SBP (x-axis) and UNa excretion (y-axis)., ****p <0.0001, ***p <0.001, *p <0.05.

The generation of a PN curve estimates the relationship between BP, here SBP, and urinary sodium excretion (Figure 4.8 D). The first ligation increased SBP in both dietary groups by ~23 mmHg, and the second by ~19 mmHg. In mice in the SSD group, urinary sodium excretion remained similar to baseline and during this first rise in SBP and only began to increase after this. In mice in the 3 days HSD group, an increase in urinary sodium excretion was stimulated after the first ligation and elevated with SBP. It was significantly

greater than that of the SSD after the second ligation, despite near-identical rises in SBP. Thus, in the HSD group, an increase in urinary sodium excretion was stimulated at a lower SBP than in the SSD group, causing a leftward shift of the PN relationship (Figure 4.8 D).

4.3.4 Renal sodium transporter expression after 3 days high dietary salt intake

Figure 4.9 displays the expression of key transporters responsible for renal sodium handling in C57BL6/JCrl mice after either the SSD or 3 days of high dietary salt intake. When mice were fed the HSD, the mRNA abundance of cortical transporters NHE3 and NCC were comparable to that of mice fed the SSD (Figure 4.9 A, P=0.475; Figure 4.9 B, P=0.717), illustrating that expression was not influenced by high salt intake at this time-point. Nonetheless, the mRNA abundance of the α-subunit of ENaC (ENaCα) was significantly lower in the HSD group than in the SSD group (Figure 4.9 C, P=0.004). This shows that the expression of ENaC, responsible for the fine-tuning of sodium reabsorption, was downregulated with the HSD. The mRNA abundance of the medullary cotransporter NKCC2 was similar between the dietary groups (Figure 4.9 D), suggesting its expression was not affected by high salt intake.

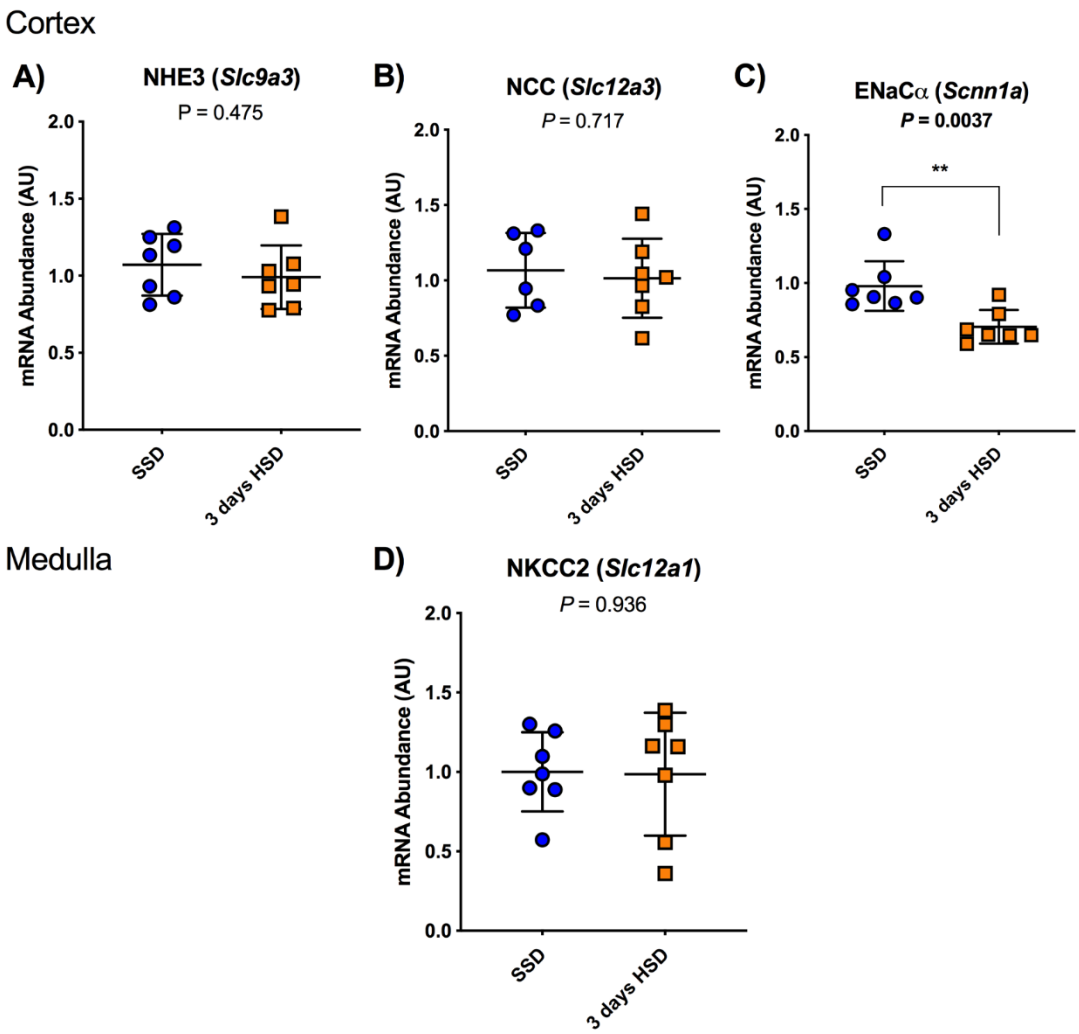

Figure 4.9: Renal sodium transporter mRNA transcript abundance following 3 days high salt.
Kidneys from a separate cohort of C57BL6/JCrl mice on either a standard salt diet (SSD 0.25% Na; n=7) or 3 days of a high salt diet (HSD 3% Na; n=7) were removed during the daytime and separated into cortical and medullary regions. The mRNA abundance of key renal sodium transporters A: sodium-proton exchanger isoform 3 (NHE3), B: sodium-chloride (Cl^-) cotransporter (NCC), C: epithelial sodium channel subunit-α (ENaCα) and D: sodium-potassium (K^+)-Cl^- cotransporter (NKCC2) was assessed by qPCR. Data are expressed as ± SD relative to the averaged mRNA abundance of three reference genes. Gene names are presented in brackets, with the names of the proteins they encode in front. Analysis consisted of unpaired *t* tests. $^{**}p<0.01$.

4.3.5 Blood pressure and heart rate upon induction of serial pressure ramps after 1 week of high dietary salt intake

The cardiovascular variables BP and heart rate were measured in the SSD group or after 1 week of the HSD during the experimental protocol outlined in Figure 4.1. The results are displayed in Figure 4.10. The ligation steps caused significant elevations in BP within both dietary groups (Figure 4.10 A & E). However, BP remained similar between the groups. At baseline, MABP was 72.6 ± 5.2 mmHg in the SSD group and 75.0 ± 6.8 mmHg in the HSD group (*P*=0.996). MABP rose with each ligation to 101.5 ± 12.9 mmHg in the SSD group and 97.3 ± 11.9 mmHg in the HSD group (*P*=0.860), and finally 109.1 ± 13.4 mmHg and 106.1 ± 9.8 mmHg respectively (*P*=0.830; Figure 4.11 C). Similar effects were observed in DBP (Figure 4.10 B & E), demonstrating that BP and the responses to artery occlusion were similar between the dietary groups and so unchanged by high dietary salt for a week.

Mean heart rate was attained during each 20-30-minute period as well (Figure 4.6 D). The serial pressure ramps did not alter heart rate in either dietary group (Figure 4.10 E). No statistically significant differences were found, however opposing trends were observed between the dietary groups. In the SSD group, mice displayed a mean heart rate of 407 ± 32 bpm at baseline, which decreased to 392 ± 33 bpm during the initial ligation and remained stable at 391 ± 46 bpm during the final ligation. In the 1 week HSD group, mean heart rate was 384 ± 32 bpm during baseline, which rose to 386 ± 41 bpm after ligature 1 then to 398 ± 61 bpm after ligature 2.

Figure 4.10: Blood pressure and heart rate measured during pressure natriuresis surgery after 1 week of high salt intake.

Blood pressure (BP) and heart rate (HR) were measured in C57BL6/JCrl mice on a standard salt diet (SSD 0.25% Na; n=7) or after 1 week of the high salt diet (HSD 3% Na; n=6) throughout the surgical protocol in which pressure ramps were provoked. Measurements were obtained under anaesthesia from thiobarbiturate injection. After a 30-minute baseline (B) period, the mesenteric and celiac arteries were occluded to evoke the first pressure ramp (50-min time-point, L1) and responses recorded for 20 minutes, before the abdominal aorta was then ligated (70-min time-point, L2) to evoke the second pressure ramp. A: systolic BP (SBP) is presented per minute, and mean B: diastolic BP (DBP), C: arterial BP (MABP) and D: HR are presented per 20-30-min experimental period. Data are mean ± SD. Significance denoted as $P<0.05$. Repeated measures two-way ANOVA was performed, with P values corrected for multiple comparisons by Sidak testing reported in table E. ****$p<0.0001$.

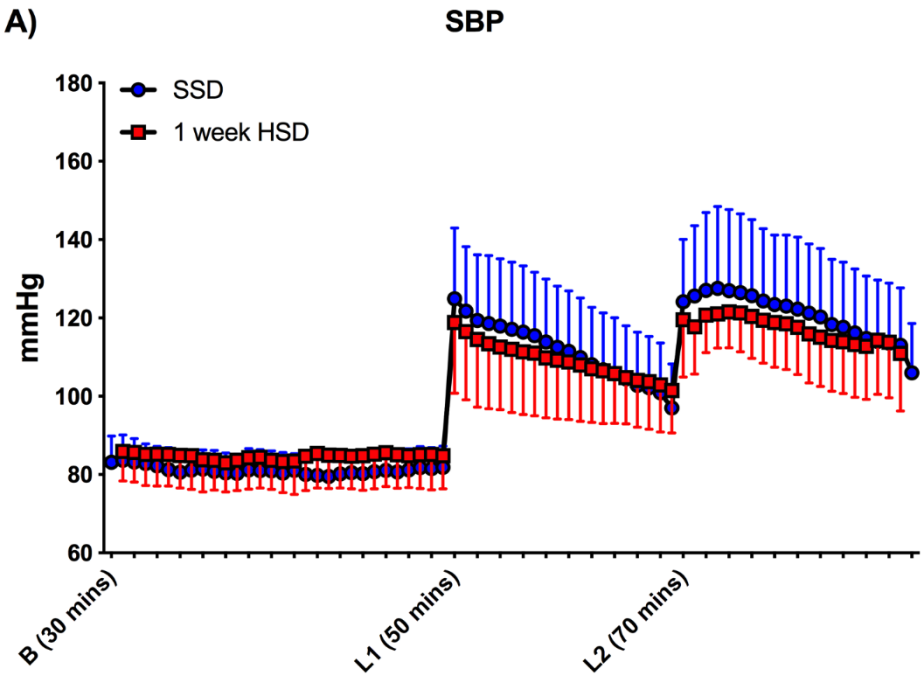

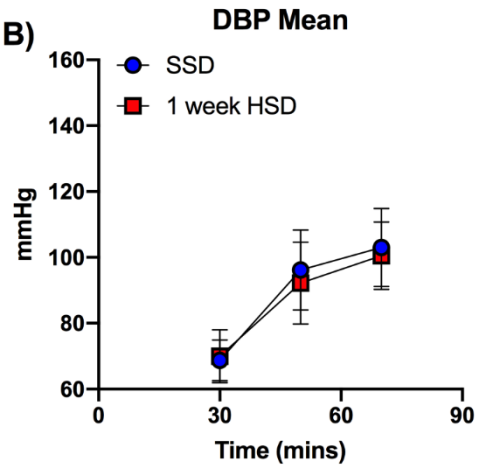

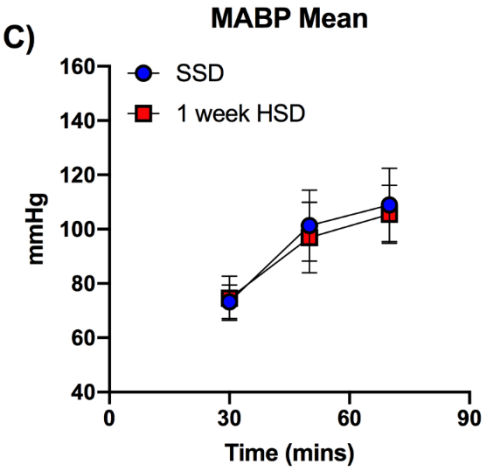

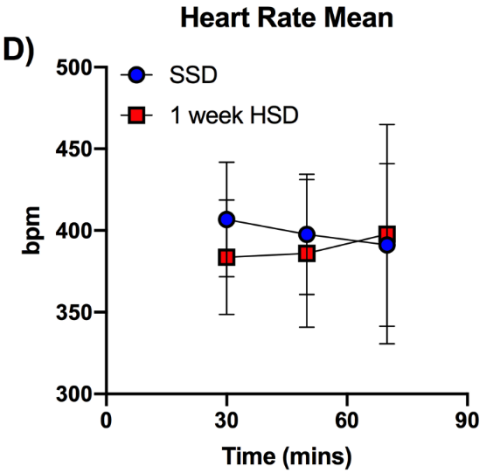

E)

Two-way ANOVA P values	*DBP*	*MABP*	*HR*
Time (mins)	**<0.0001, ******	**<0.0001, ******	0.981
Diet	0.609	0.378	0.531
Interaction	0.810	0.788	0.711

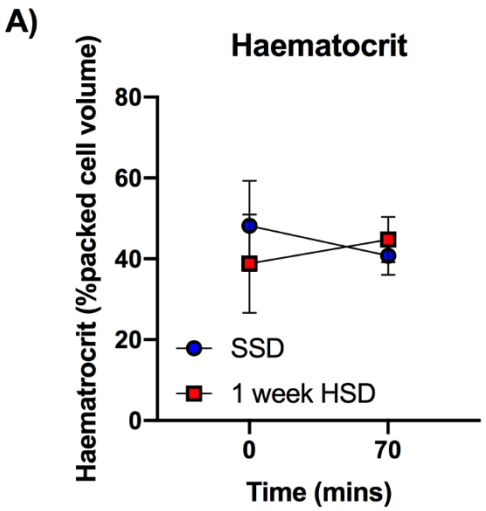

B)

Two-way ANOVA P values	*Haematocrit*
Time (mins)	0.852
Diet	0.485
Interaction	0.089

Figure 4.11: Haematocrit (%) during interrogation of the acute pressure natriuresis relationship following 1 week of high salt intake.

Haematocrit was measured in anaesthetised C57BL6/JCrl mice during pressure natriuresis surgery after a standard salt diet (SSD 0.25% Na; n=7) or 1 week of a high salt diet (HSD 3% Na; n=6). Measurements were taken from blood sampled through carotid artery cannulation prior to the baseline period and after the final ligation. Samples were then centrifuged, and readings were obtained with a micro haematocrit reader. A: mean haematocrit ± SD, B: *P* values from a repeated measures two-way ANOVA corrected for multiple comparisons via Sidak testing, with significance denoted as $P<0.05$.

There was quite a bit of variation in the haematocrit measurements taken at the beginning of the experiment (Figure 4.11), with 48 ± 10 % in the SSD group and 41 ± 7 % in the HSD group. However, at the end of the experiment, this variability had mostly levelled out to 42 ± 3 % in the SSD group and 45 ± 5 % in the HSD group. Two-way ANOVA reported no effect of diet or the ligation steps (Figure 4.11 B).

4.3.6 Effect of 1 week of high dietary salt intake on renal haemodynamics

KW was not different between the two dietary groups ($P=0.749$; Figure 4.12 A). Urinary flow rate increased significantly following each ligation step (Figure 4.12 B & D). No differences in urinary flow rate were noted between mice in the SSD group and the HSD group. At baseline, flow rates were similar between the groups, measured at 0.0017 ± 0.0014 mL/min/KW in the SSD group and 0.0019 ± 0.0009 mL/min/KW in the HSD group ($P>0.999$). The first ligation elevated urinary flow rate to 0.0117 ± 0.0078 in the SSD

mice and 0.0106 ± 0.0051 mL/min/KW in the HSD mice (*P*=0.990), and the second ligation to 0.0183 ± 0.0085 and 0.0216 ± 0.0112 mL/min/KW respectively (*P*=0.816). Thus, urinary flow rate increased with each ligation and was unaffected by diet (Figure 4.12 B & D).

Over the course of the surgery, only modest changes were observed in GFR, none of which were diet-related (Figure 4.12 C). A small but statistically significant effect of the pressure ramps was noted (Figure 4.12 D). During the baseline period, GFR was near-identical within the dietary groups, measured at 0.35 ± 0.24 mL/min/KW in the SSD group and 0.33 ± 0.21 mL/min/KW in the HSD group (*P*=0.999). GFR subsequently rose to 0.50 ± 0.23 and 0.75 ± 0.22 mL/min/KW respectively following the initial ligation, however this not different between the dietary groups (*P*=0.245). The final ligation was accompanied by a reduction in GFR close to that at baseline, measured at 0.38 ± 0.22 mL/min/KW in the SSD group and 0.54 ± 0.20 mL/min/KW in the HSD group (*P*=0.486), which remained slightly higher than its baseline value. Overall, GFR was unaltered in C57BL6/JCrl mice after 1 week of the HSD compared to mice on the SSD under these circumstances.

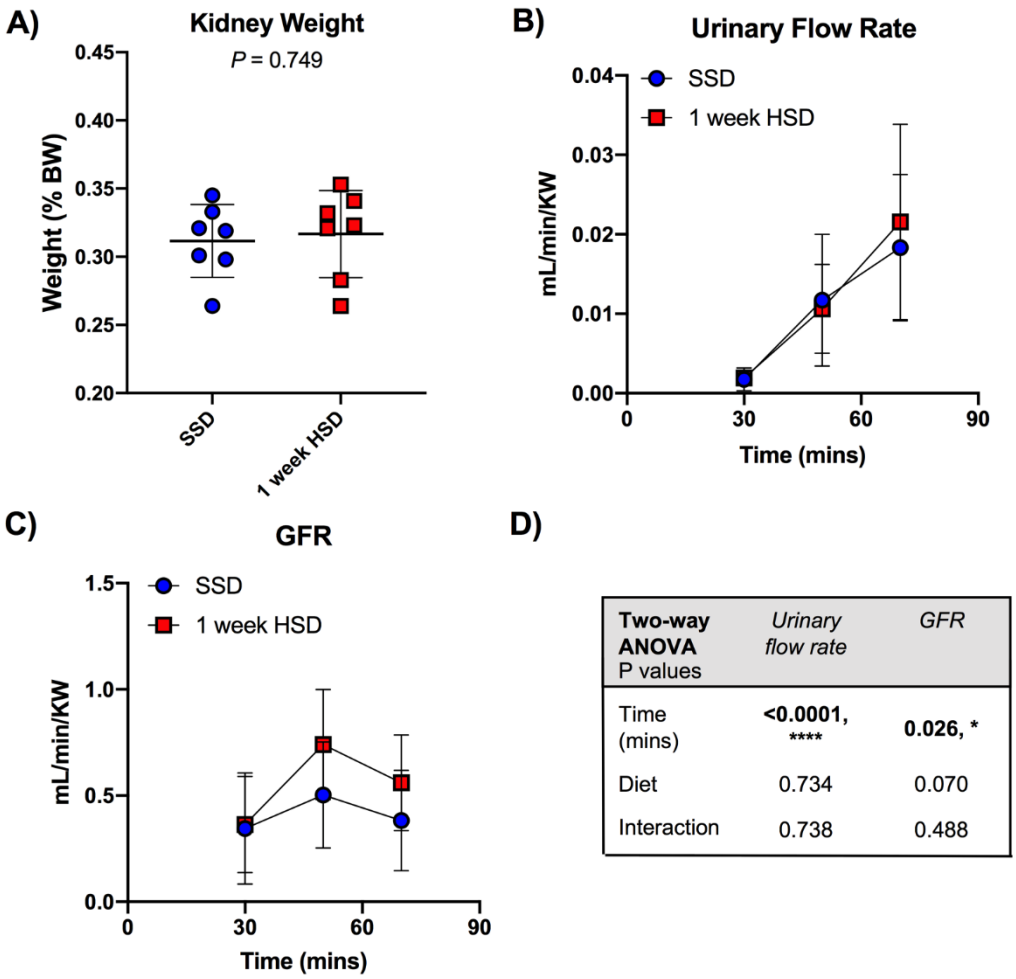

Two-way ANOVA P values	*Urinary flow rate*	*GFR*
Time (mins)	**<0.0001, ******	**0.026, ***
Diet	0.734	0.070
Interaction	0.738	0.488

Figure 4.12: Urinary flow and glomerular filtration rate following 1 week of high salt feeding.
C57BL6/JCrl mice underwent pressure natriuresis surgery in which urinary flow and glomerular filtration rate (GFR) were assessed after a standard salt diet (SSD 0.25% Na; n=7) or a high salt diet (HSD 3% Na; n=6) under thiobarbiturate anaesthesia. Measurements were obtained during baseline, the ligation of mesenteric and celiac arteries and the ligation of the abdominal aorta. Urine volume was recorded, divided by the collection time and expressed relative to kidney weight (KW) as urinary flow rate. This was then used, along with FITC-inulin clearance, to calculate GFR. At the end of the experiment, mice were humanely culled via an overdose of anaesthetic and kidneys were dissected for weighing. Data are mean ± SD displayed as A: KW (% body weight; BW) analysed via unpaired *t* test, B: urinary flow rate, C: GFR and D: *P* values resulting from a repeated measures two-way ANOVA, corrected for multiple comparisons by Sidak testing. *****p*<0.0001, **p*<0.05.

Figure 4.13: Renal blood flow following 1 week high salt intake during the assessment of acute pressure natriuresis relationship.

Renal blood flow (RBF) was measured by Doppler ultrasound in anaesthetised C57BL6/JCrl mice after a standard salt diet (SSD 0.25% Na; n=7) or a high salt diet (HSD 3% Na; n=6) during pressure natriuresis surgery. Measurements were obtained during a 30-minute baseline period, after the first ligation of the mesenteric and celiac arteries, and finally after the second ligation of the abdominal aorta. Mean arterial blood pressure (MABP) over RBF generated renal vascular resistance (RVR). Data are mean ± SD shown as A: RBF per minute, B: RBF, C: RVR and D: *P* values from repeated measures two-way ANOVA, corrected for multiple comparisons with Sidak post-testing. **p*<0.05.

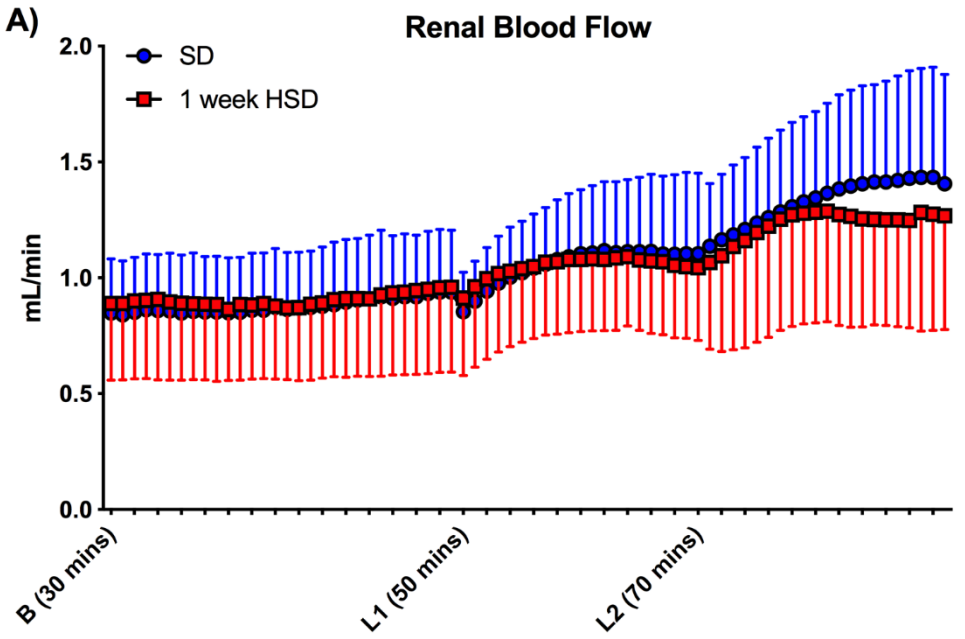

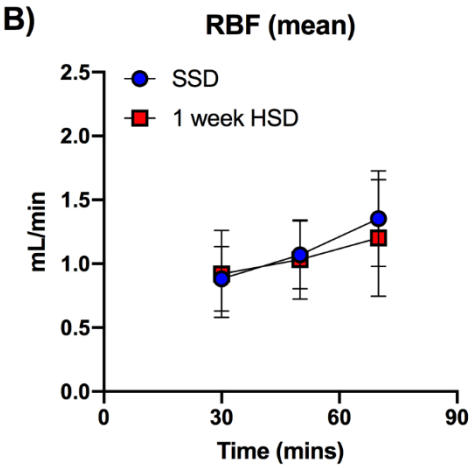

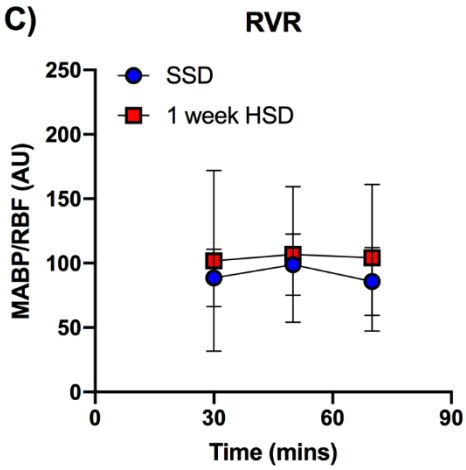

D)

Two-way ANOVA P values	*RBF*	*RVR*
Time (mins)	**0.026, ***	0.878
Diet	0.655	0.361
Interaction	0.775	0.956

4.3.6.1 Renal blood flow after 1 week high salt

Figure 4.13 A depicts RBF per minute following either the SSD or 1 week of the HSD. During the baseline period, RBF was measured at 0.88 ± 0.23 mL/min in the SSD group and 0.92 ± 0.31 mL/min in the HSD group, illustrating that flow was comparable between the dietary groups at this time (*P*=0.995). The induction of the pressure ramps by artery ligation caused a mild increase in RBF, but diet had no overall effect upon this (Figure 4.13 B & D). The first ligation step induced small increases in RBF in both dietary groups (SSD 1.07 ± 0.25 vs. HSD 1.03 ± 0.28 mL/min; *P*=0.996). RBF was further increased after the second ligation step, with no differences noted between groups (SSD 1.35 ± 0.35 vs. HSD 1.20 ± 0.42 mL/min; *P*=0.816).

Neither diet had any impact on RVR in these mice. At baseline, RVR was 88.5 ± 19.4 AU in the SSD group and 101.8 ± 64.0 AU in the 1 week HSD group (*P*=0.934), displaying some variability but no dietary effects. RVR was not altered by the pressure ramps, as it was calculated at 98.8 ± 20.6 AU and 106.8 ± 48.0 AU (*P*=0.984) during the first ligation and 85.8 ± 22.9 AU and 104.2 ± 51.9 AU (*P*=0.843) during the second ligation respectively (Figure 4.13 C & D).

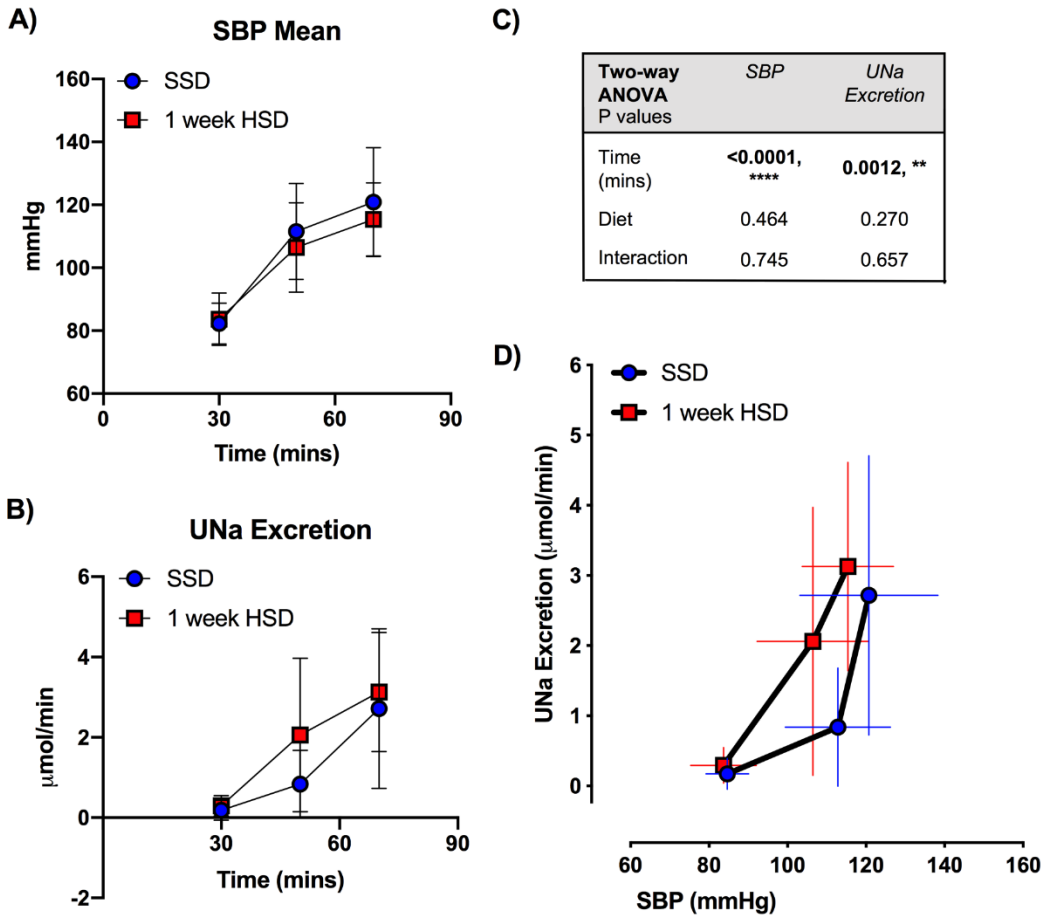

Figure 4.14: Acute pressure natriuresis relationship after 1 week of high dietary salt.
C57BL6/JCrl mice received the standard salt diet (SSD 0.25% Na; n=7) or 1 week of the high salt diet (HSD 3% Na; n=6). Surgical assessment of the acute pressure natriuresis relationship was carried out under anaesthesia via thiobarbiturate injection. Blood pressure (BP) was measured via cannulation of the carotid artery, and urinary samples were taken via bladder catheter. Serial pressure ramps were provoked by occluding major arteries mesenteric and celiac, followed by the abdominal aorta. During baseline and each ligation step, A: systolic BP (SBP) and B: urinary sodium (UNa) excretion were measured. Data are mean ± SD presented as a C: table reporting *P* values from repeated measures two-way ANOVA with post-hoc Sidak analysis, and D: pressure natriuresis graph depicting the relationship between SBP (x-axis) and UNa excretion (y-axis). ****$p<0.0001$, **$p<0.01$.

4.3.7 High dietary salt intake for 1 week causes a leftward shift in the acute pressure natriuresis relationship

At baseline, no differences were observed in SBP between mice fed the SSD or 1 week of the HSD (84.7 ± 5.4 mmHg SSD vs. 83.7 ± 8.3 mmHg HSD; *P*=0.996). SBP increased with each ligation, to 112.8 ± 13.4 mmHg in the SSD group and 106.4 ± 14.2 mmHg in the HSD group (*P*=0.860) and finally to 120.7 ± 17.6 and 115.4 ± 11.6 mmHg, respectively (*P*=0.830; Figure 4.14

A). High dietary salt intake did not affect SBP or changes in SBP in response to pressure ramps (Figure 4.14 C).

High dietary salt also did not influence the amount of sodium excreted during the 30-minute baseline period, as excretion was 0.17 ± 0.22 μmol/min in the SSD group and 0.29 ± 0.25 μmol/min in the HSD group (*P*=0.999). This increased with each pressure ramp in both dietary groups to 0.84 ± 0.84 μmol/min in the SSD group and 2.06 ± 1.91 μmol/min in the HSD group (*P*=0.386) and lastly to 2.72 ± 1.99 μmol/min and 3.13 ± 1.49 μmol/min, respectively (*P*=0.947; Figure 4.14 B). Thus, higher urinary sodium excretion was found following the pressure ramps similarly in both groups (Figure 4.14 C).

Figure 4.14 D is a graphical representation of the acute PN relationship in anaesthetised C57BL6/JCrl mice after the SSD or 1 week of the HSD. The ligation of major arteries induced significant, stepwise elevations in SBP in both dietary groups. Urinary sodium excretion increased with SBP. Mice fed 1 week of HSD excreted a slightly greater sodium load than mice fed SSD at a similar SBP, however this was not statistically significant. Therefore, a small but evident leftward shift in the acute PN relationship was displayed after 1 week in the HSD group (Figure 4.14 D).

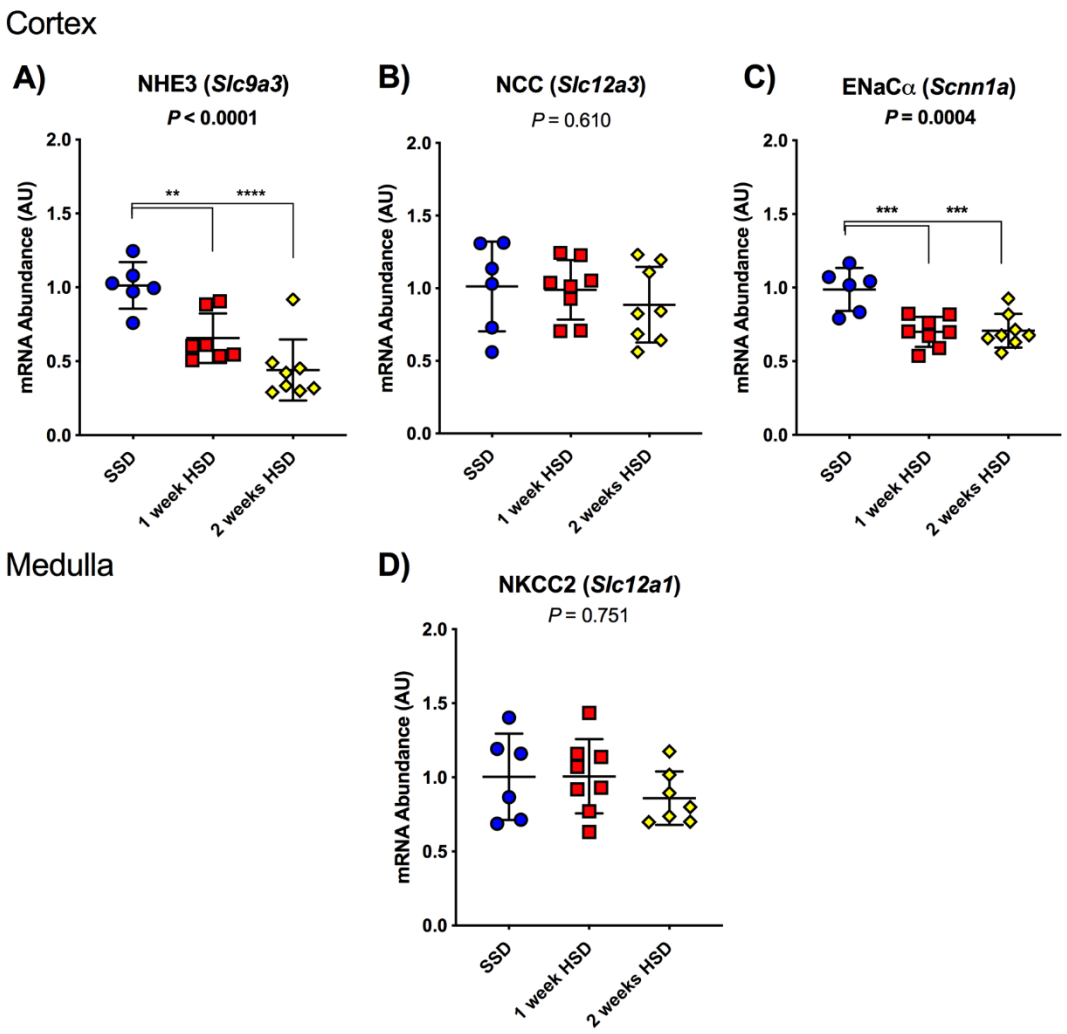

Figure 4.15: Renal mRNA abundance of sodium transporters after 1 week and 2 weeks of high salt feeding.
C57BL6/JCrl mice were fed either a standard salt diet (SSD 0.25% Na; n=6) or a high salt diet (HSD 3% Na) for 1 week (n=7-8) or 2 weeks (n=8). Kidneys were removed and divided into cortex and medulla, before qPCR analysis was performed. Renal cortical expression of A: sodium (Na)-proton exchanger isoform 3 (NHE3), B: Na-chloride (Cl-) cotransporter (NCC), C: epithelial Na channel subunit-α (ENaCα) and medullary expression of D: Na-potassium (K+)-Cl cotransporter (NKCC) was determined. Data are mean ± SD, normalised to mean mRNA abundance of three reference genes shown previously. Analysis was carried out by ordinary one-way ANOVA corrected for Tukey post-testing. ****p<0.0001, ***p<0.001, **p<0.01.

4.3.8 Renal sodium transporter mRNA profile after 1 and 2 weeks high dietary salt intake

C57BL6/JCrl mice received the SSD or the HSD for 1 and 2 weeks before the expression of key mediators of sodium transport along the nephron was assessed. In the renal cortex, mRNA abundance of the exchanger NHE3 was

significantly lower after 1 week (P=0.005) and 2 weeks of the HSD group (P<0.0001) compared to the SSD group (Figure 4.15 A), indicating that NHE3 expression was downregulated with high salt intake. A difference between dietary durations was also noted (P=0.034) as a larger decrease in NHE3 expression was seen after 2 weeks of high salt intake. On the other hand, cortical abundance of NCC remained similar within all groups (Figure 4.15 B, P=0.610). High dietary salt intake significantly downregulated the expression of ENaCα in the cortex after 1 and 2 weeks compared to the SSD group (both P=0.0008; Figure 4.15 C). The mRNA abundance of the medullary co-transporter NKCC2 was similar between the groups (P=0.751; Figure 4.15 D), suggesting that high salt does not impact its expression in this case.

4.4 Discussion

4.4.1 Blood pressure and sodium excretion: defining the link

Long-term BP control is fundamentally reliant upon sodium balance, a concept modelled by Guyton and colleagues which challenged the cardiovascular-centric views of BP regulation at the time (77). Prior to the 1950s, the prevailing theories involved the heart as a regulator of BP via CO, and the vasculature via SVR. The publication of Guyton *et al*.'s model in 1972 brought additional factors, such as volume, pressure, compliance and flow within the system, into the equation (154). Rather than regarding BP as solely a product of SVR and CO, it was proposed that it is also determined by vascular capacitance and ECFV, known as effective blood volume. A mismatch between sodium intake and excretion alters ECFV, affecting BP and thus renal perfusion pressure, which in-turn stimulates the kidneys to counteract the change in pressure by modifying sodium excretion – this defines the acute PN relationship. Therefore, steady-state BP results from the equilibrium between ECFV, ascertained by sodium balance, and PN.

In this chapter, the effect of high dietary salt intake on the acute PN relationship in C57BL6/JCrl mice was experimentally assessed after either

the SSD or HSD to test the hypothesis of my thesis that impaired PN underlies their salt-sensitive BP.

4.4.2 Experimental induction of the acute pressure natriuresis response

In earlier research by groups in the Centre, the acute PN relationship in experimental hypertension has been investigated. The approach used involved mechanically increasing BP through arterial ligation, which in-turn increases renal perfusion pressure. The resulting effect upon urinary sodium excretion is then measured. The overall aim is, therefore, to interrogate the ability of the kidneys to respond to this rise in pressure. This protocol was initially developed within dogs (155), before it was adapted and performed in rats (156). The resulting curves express BP as a surrogate for renal perfusion pressure against urinary sodium excretion. Theoretically, any alteration in perfusion pressure is met by compensatory changes in urinary sodium excretion via the acute PN response. Evidence from BP studies, however, illustrates that this response is abnormal in hypertension. For example, the gradient of this curve is significantly reduced and shifted to the right, demonstrating that sodium excretion is only increased to offset haemodynamic changes at a higher BP (79).

During my PhD at the Centre, Roman & Cowley's protocol to induce the PN response (156) was adjusted and optimised for mice. With each arterial ligation, we observed successful increases in BP and RBF, and autoregulation of GFR in all mice included. Potential problems arising from this protocol relate to the length and invasiveness of the surgical preparation, as this leaves the mice vulnerable to detrimental changes in body temperature and the extravasation of fluid.

The protocol used in this chapter involved the ligation of major conduit arteries to provoke the acute PN response mechanically, although alternative approaches exist within the field. For example, other researchers have opted for the pharmacological approach. Kunau *et al.* examined the effect of

adrenaline administration, which resulted in increases in BP and consequently renal perfusion pressure (157). Furthermore, the use of aldosterone (158) and vasopressin (159) have been evaluated as well. This is advantageous in that it is far less invasive than occluding arteries, which are only accessed via performing a laparotomy. For this reason, recovery surgery could be carried out, allowing the collection of multiple post-operative samples and measurements from conscious animals (159). Nevertheless, these approaches induce the acute PN response through hormonal mechanisms, for example the infusion of aldosterone and adrenaline influence renal function partially through stimulation of the RAAS. Therefore, my aim for this chapter was simply to investigate whether high salt feeding affects the intrinsic ability of the kidneys to respond to increases in renal perfusion pressure, without the added complexity of systemic hormonal manipulation. Thus, mechanically inducing these pressure rises was more suited to achieve this aim.

4.4.2.1 Limitations: blood pressure measurement under general anaesthesia

In these experiments, prior to the induction of pressure ramps, BP measurements were obtained from C57BL6/JCrl mice during a 30-minute baseline period after 3 days or 1 week of the HSD and compared to mice on the SSD. BP in the HSD group was similar to that in the SSD group. This is not consistent with the results of the previous chapter, in which BP increased after 3-4 days and remained stably high after 1 week of the HSD. An important difference between these results is the method of BP measurement. The previous chapter collected BP data from conscious, freely moving mice by radiotelemetry, whereas mice were anaesthetised using the barbiturate thiobarbiturate prior to data collection in this chapter's experiments. Barbiturates administrated intravenously have been shown to suppress circulatory haemodynamics through inhibition of the central nervous system (160), thus this could potentially interfere with BP measurements obtained this way.

4.4.3 The acute pressure natriuresis relationship in salt-sensitive C57BL6/JCrl mice

The systemic haemodynamic changes that occur during high dietary salt intake in an individual defined as salt-resistant are as follows; ECFV increases due to a now positive sodium balance, resulting in temporary increases in CO and thus BP. This in-turn triggers the acute PN response, increasing sodium excretion and normalising ECFV and BP. Hence, the changes in BP are short-lived and equilibrium is quickly restored.

In salt-sensitivity, however, these changes are said only to stimulate an increase in sodium excretion at a higher pressure due to renal dysfunction, resulting in sodium retention and sustained increases in BP (57). This is evident within data from rats, for example in kidneys isolated from the Dahl salt-sensitive strain. Girardin *et al*. reported that pre-hypertensive kidneys from this strain displayed a similar relationship to that of kidneys from the equivalent salt-resistant strain (161). However, after increasing dietary salt intake, hypertension was induced and the acute PN response was significantly diminished. This was observed by a decrease in the gradient of the PN curve (161), suggesting that PN shifts to a higher pressure in order to match sodium intake with output. Roman also found that these rats excreted significantly less sodium whilst in a salt-induced hypertensive state compared to salt-resistant Dahl rats, confirming the blunting of the acute PN response with salt-sensitivity (162). Research within human participants has similarly noted this phenomenon (163, 164). Therefore, this shift in the acute PN response, resulting in the maintenance of sodium balance only at higher pressures, is considered a vital determinant of salt-sensitive hypertension in this field.

In my thesis, the acute PN response was augmented after 3 days of high salt intake in C57BL6/JCrl mice. The PN curve was shifted to the left, with a steepening gradient, as compared to their contemporaneous controls on the SSD, displaying that mice excreted increased amounts of sodium at any given BP. This illustrates that the intrinsic ability of the kidneys to expel

sodium and water in an attempt to normalise pressure was not impaired by dietary salt but, in fact, improved.

4.4.4 Renal sodium transporter activity and availability after high salt intake

The mechanisms through which the acute PN response is implemented are complex and yet to be fully defined. Research suggests it is governed by transporter activity, supporting the transepithelial movement of sodium and water between the tubule lumen and the bloodstream (Figure 4.16). If pressure rises, the kidney must respond via natriuresis, during which transporter-mediated sodium reabsorption is inhibited. This occurs throughout the nephron, and potentially originates from an increase in renal interstitial hydrostatic pressure. Regulation of medullary blood flow through the vasa recta is poor, and thus rises with renal perfusion pressure (165). Consequently, the organ-wide pressure elevation triggers the localised production of signalling agents NO and adenosine triphosphate (ATP) which act in a paracrine fashion to inhibit nearby tubular sodium transporters. For example, the literature notes roles for these agents in the modulation of NHE3 activity in the proximal tubule (166) and NKCC2 activity in the loop of Henle (167).

Furthermore, research into diseases characterised by abnormal BP regulation have uncovered the importance of the distal nephron as well. ENaC is the predominant regulator of sodium transport within the distal nephron, and uncontrolled activity from a gain-of-function mutation results in hypertension and ECFV expansion, known as Liddle's syndrome (168), due to depressed natriuresis. Data from salt-sensitive Dahl rats also displays aberrant activation of ENaC compared to their salt-resistant counterparts. Therefore, the inhibition of these transporters may be a pivotal event in the kidney's response to increased pressure.

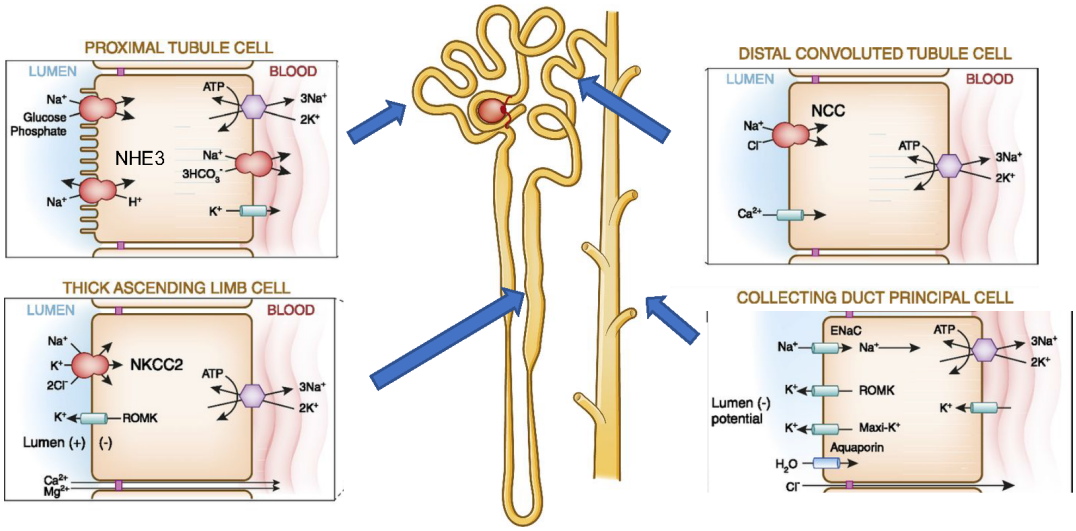

Figure 4.16: Renal sodium transporters along the nephron.
Schematic diagram depicting the location and structure of the key transporters responsible for sodium reabsorption in each segment of the nephron, adapted from Hoenig & Zeidel (169). All transporters are located on the apical membrane of the tubular cells. Sodium-proton exchanger 3 (NHE3) is localised to the cells lining the proximal tubule. The sodium-potassium-chloride cotransporter (NKCC2) residues in thick ascending limb. The sodium-chloride transporter (NCC) is located in the cells of the distal convoluted tubule, and the epithelial sodium channel (ENaC) can be found in the principal cells of the collecting duct.

Thus, I aimed to determine their status in C57BL6/JCrl mice following high dietary salt intake. I approached this using qPCR, as studies in rats have observed decreased expression of NCC from the apical membrane following high dietary salt intake (170), whereas an upregulation in the expression of NCC as well as NKCC2 was seen in salt-sensitive strains (171, 172).

In my experiments in C57BL6/JCrl mice, neither NCC nor NKCC2 expression was up- or downregulated after 3 days, 1 week and 2 weeks of the HSD compared to the SSD. Nevertheless, the transcriptionally active α subunit of ENaC was downregulated after both 3 days and 1 week of the HSD. This expressional change was also accompanied by a downregulation in NHE3 expression after 1 week of the HSD. Sodium reabsorption is distributed throughout the length of the nephron, with the proximal tubule accounting for the highest proportion of net reabsorption and the distal convoluted tubule for the lowest. NHE3 is the main transporter within the proximal tubule (Figure 4.16) and thus, quantitatively, is the most prominent regulator of overall

sodium reabsorption (86). Despite this, disturbances in the distal convoluted tubule, in which ENaC residues and contributes to around 5-10% of net reabsorption (Figure 4.16), appear to have a greater impact on renal sodium handling and BP control than those occurring in the proximal tubule (86). For example, the gain-of-function mutations underlying BP disorders as described above. This indicates that proximal tubule NHE3 and distal ENaC potentially have the most influence over net sodium reabsorption. In the case of C57BL6/JCrl mice, early downregulation of ENaC occurs, closely followed by NHE3, with high salt intake, suggesting an appropriate adaptative response of these major transporters. This makes impaired renal sodium reabsorption an unlikely candidate for the causative mechanism underlying salt-induced hypertension here.

Nonetheless, the regulation of transporter activity mostly occurs downstream of transcription. Following synthesis, transporters reside within intracellular vesicles. They can be trafficked to and from the membrane depending on demand, thus their presence within the apical membrane interfacing with the tubule lumen is an important determinant of their ability to retrieve sodium and chloride. Transporters are also subject to post-translational modifications, for example both NCC and NKCC2 are activated by phosphorylation (173, 174). Therefore, the presence or absence of a change in mRNA expression does not necessarily reflect *in vivo* activity.

4.4.5 Could renal dysfunction contribute to the salt-induced blood pressure increases in C57BL6/JCrl mice?

Table 4.1 provides a summary of the results of this chapter. During the baseline periods, little difference in renal haemodynamics and excretion between the dietary groups was observed in anaesthetised C57BL6/JCrl mice. I explored the relationship between renal perfusion pressure and sodium excretion by acutely measuring the natriuretic response to increasing BP. The response to this manoeuvre was significantly increased sodium excretion in all groups. After both the durations of high dietary salt intake

investigated, transporter-mediated sodium reabsorption decreased, and sodium excretion increased (Table 4.1).

The mechanistic link between renal vascular function and sodium excretion remains, as of yet, unclear. The kidney possesses a strong, unique ability to autoregulate. When challenged with a rise in perfusion pressure, two distinctive mechanisms act hand-in-hand to protect the delicate infrastructure; the myogenic and tubuloglomerular feedback (TGF) responses. Both initially work to buffer the pressure change by adjusting the diameter of the preglomerular arteries. The myogenic response involves the inherent contractile reaction of the VSM to shear stress, whereas the TGF response integrates signals from macula densa cells on the concentration of sodium chloride in the filtrate. The desired end-result is the adaptation and overall maintenance of steady-state RBF, GFR and thus sodium excretion via PN. The current hypothesis, as depicted in Figure 4.17, postulates that a rise in renal perfusion pressure, if not initially safeguarded by autoregulatory vasoconstriction, increases renal interstitial hydrostatic pressure, which in turn inhibits tubular sodium reabsorption and supports excretion (175).

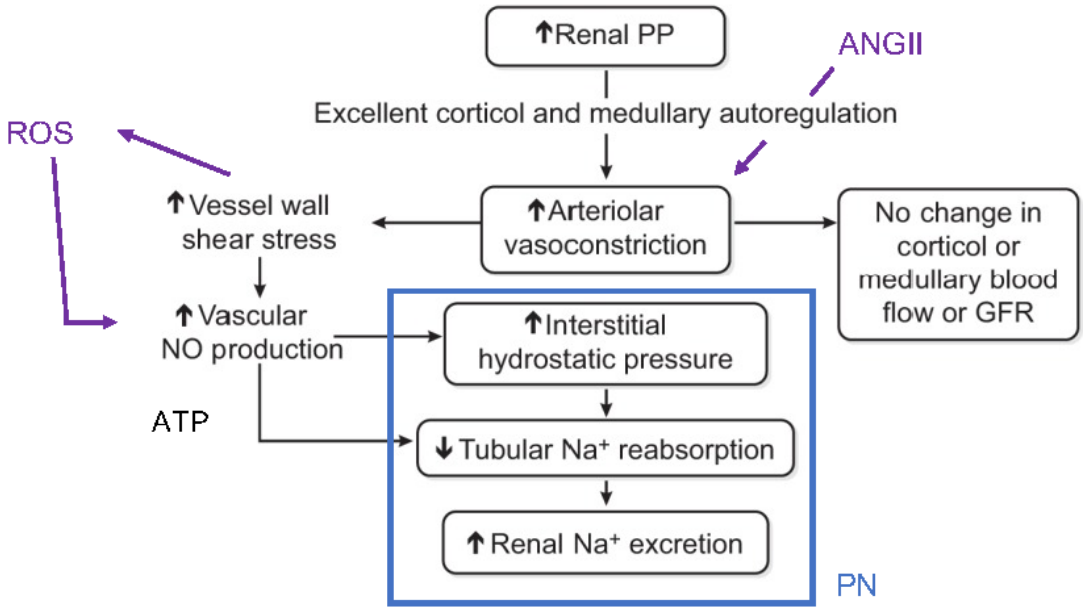

Figure 4.17: Current hypothesis for the mechanism linking renal autoregulation to sodium excretion.
Adapted from Carlström *et al*., (175), this flow-diagram depicts the current hypothesis for the intrarenal mechanism by which an elevation in renal perfusion pressure (PP) stimulates the pressure natriuresis (PN) response. Increased renal PP is initially transduced to the preglomerular vasculature, triggering vasoconstriction. Preglomerular arterioles, such as the afferent arteriole, are subject to this autoregulatory mechanism with the purpose of preventing pressure-induced injury to the glomerulus, damaging its capacity for filtration as well as adversely impacting essential downstream processes such as the reabsorptive and excretory functions of the nephron. A rise in renal PP that is not initially buffered by preglomerular vasoconstriction is said to lead to subsequent rises in renal interstitial hydrostatic pressure, resulting in the inhibition of tubular sodium reabsorption and thus increased expulsion of sodium. A number of signalling pathways can influence this process. Angiotensin-II (ANGII), a potent vasoconstrictor, is known to act upon the preglomerular vasculature. Nitric oxide (NO) production is also stimulated to induce vasodilation and counteract these changes, often governed by the balance of vascular reactive oxygen species (ROS). In addition to their roles as important mediators of vascular tone, NO, ROS and adenosine triphosphate (ATP) have also been implicated as signalling molecules in the regulation of tubular sodium reabsorption stimulated by shear stress. GFR; glomerular filtration rate.

I noted that the natriuretic response to rising BP was different between the high salt groups and the control. After 3 days of high salt intake, RVR was modestly increased and the pressure-induced increase in RBF was blunted compared to the matched controls (Table 4.1). In previous studies of normotensive human subjects, an increase in salt intake induces a rise in RBF, thus increasing GFR and supporting the clearance of salt and water. However, salt-sensitive subjects demonstrate a lower RBF than their normotensive or salt-resistant counterparts upon salt loading. This, accompanied by increases in RVR, led to the conclusion that salt-sensitive

subjects experience elevated renal vasoconstriction (69, 176, 177). My data in the 3-day high salt group are consistent with these previous findings and suggest that, in this early phase, C57BL6/JCrl mice are vasoconstricted. This may be indicative of enhanced myogenic responsiveness, which has been noted in other models of experimental hypertension such as the stroke-prone spontaneously hypertensive rat (178) and in ANGII-induced hypertension (179). Studies have demonstrated a possible link with the RAAS, as mice with a VSMC-specific knockout of the ANGII receptor AT_{1A} display attenuated renal vasoconstriction and a higher RBF, which conferred protection against the development of hypertension (180). Nevertheless, an augmented vasoconstrictor response was associated with sodium retention in these other models, which does not seem likely to apply to C57BL6/JCrl mice here as significantly increased sodium excretion was observed.

After 7 days of high salt intake, RBF and RVR were not significantly different to those measured in the control mice following the SSD (Table 4.1), suggesting comparable autoregulatory mechanisms were in play. Thus, at this timepoint, BP and RBF increased, RVR remained unchanged, transporter-mediated sodium reabsorption decreased, and sodium excretion increased. Yet, some of these responses were equivalent to those measured in the control mice, despite an evident leftward shift in the PN curve. Thus, the adaptation of renal function observed in mice after 3 days of high salt intake also occurred after 7 days, but not to the same extent. The reasons for this are unclear.

Although, the smaller scale of this effect after 7 days could potentially be due to the experimental approach. The second ligation did not raise BP to the same extent as it did during the experiment following 3 days of the HSD. The second ligation induced a ~19 mmHg SBP increase in the mice having received 3 days of the HSD, whereas in the separate experiment following 7 days, SBP increased by only ~9 mmHg. The approach has since been refined, as a more effective and reproducible method of tightening the ligatures is now in practise. Furthermore, it is important to take into

consideration that this was a cross-sectional experimental design, therefore the mice that received 3 days of the HSD or SSD underwent PN surgery in a separate experiment at a different time to the mice that received 7 days of the diets. Due to this, the responses cannot be compared directly.

It is also important to consider the salt-induced events prior to the induction of anaesthesia, which likely impacted BP. In the previous chapter, I demonstrated that BP was increasing on day 3 of high salt intake in C57BL6/JCrl mice, whereas BP was high but had reached a plateau on day 7. It is possible that differing salt-induced mechanisms are contributing to the initiation of salt-induced hypertension, i.e during the initial 3-day period, and the maintenance of it, i.e after 1 week. Here, increased renal vasoconstriction was evident alongside significantly increased urinary excretion after high salt intake, suggesting a vascular, rather than a renal, contribution to the early phase of developing hypertension. It is challenging to draw further conclusions from my experiments and additional investigations are now warranted, directed at resolving the adaptation of renal vascular function and the signalling molecules involved such as components of the RAAS, ROS, NO and ATP (Figure 4.17).

Overall, in this chapter, I have demonstrated that high salt feeding does not impair the acute PN relationship in C57BL6/JCrl mice. After high dietary salt intake, more sodium was excreted at a lower pressure compared to those on the SSD, illustrating adaptation. At similar time-points, the expression of some of the key renal sodium transporters was appropriately downregulated, supporting the view that renal function appears ‘normal’ in these mice despite increases in BP. Therefore, I conclude that increasing dietary salt intake does not adversely alter the intrinsic PN response and is thus unlikely to be a cause of the salt-induced hypertension in C57BL6/JCrl mice observed in the previous chapter.

Table 4.1: Summary of the chapter results.
Comparison of the effects of the pressure ramps and different diets on the parameters measured in this chapter after 3 days or 1 week.

	3 days HSD		**1 week HSD**	
	Pressure ramp	*SSD vs. HSD*	*Pressure ramp*	*SSD vs. HSD*
BP	Increased with each ligation	No differences	Increased with each ligation	No differences
HR	No changes	Slightly lower in the HSD group	No changes	No differences
Haematocrit	No changes	No differences	No changes	No differences
Kidney weight	-	No differences	-	No differences
UFR	Increased with each ligation	Higher in the HSD group	Increased with each ligation	No differences
GFR	Increased with the first ligation, decreased with the second ligation	No differences	Mildly increased with first ligation; decreased with the second ligation	No differences
RBF	Increased with each ligation	Increase significantly blunted in the HSD group	Mildly increased with each ligation	No differences
RVR	No changes	Significantly greater in the HSD group	No changes	No differences
UNa excretion	Increased with each ligation	Significantly greater in the HSD group	Increased with each ligation	No differences
PN curve	Steeper gradient with each ligation	Shifted left in the HSD group	Steeper gradient with each ligation	Mild leftward shift in the HSD group
Sodium transporter expression	-	Downregulated ENaCα expression in the HSD group	-	Downregulated NHE3 and ENaCα expression in the HSD group

HSD; high salt diet, SSD; standard salt diet, BP; blood pressure, HR; heart rate, UFR; urinary flow rate, GFR; glomerular filtration rate, RBF; renal blood flow, RVR; renal vascular resistance, UNa; urinary sodium, PN; pressure natriuresis

4.4.6 Summary of results

1. After 3 days of high dietary salt intake, an increase in urinary sodium excretion was stimulated at a lower SBP compared with the SSD, thus displaying a leftward shift in the PN curve suggestive of an enhancement of the acute PN relationship at this time-point. This effect was observed on a smaller scale after 1 week of high salt intake.
2. RBF remained comparable between the dietary groups until the induction of the pressure ramps, upon which it increased with each ramp. However, this was significantly blunted in mice after 3 days of high salt intake, an effect that was not observed after 1 week of high salt intake.
3. GFR increased with the first pressure ramp, but declined during the second in both dietary groups, illustrating autoregulation.
4. The mRNA abundance of ENaCα decreased in mice after either 3 days, 1 week or 2 weeks of high salt intake. NHE3 abundance was unchanged after 3 days, but declined significantly after 1 week and 2 weeks high salt compared with standard salt intake. Abundance of both NCC and NKCC2 remained comparable, regardless of diet or duration. Thus, the expression of certain key renal sodium transporters was downregulated after high salt.

5 Vascular Effects of High Dietary Salt Intake in C57BL6/JCrl Mice

5.1 Introduction

In chapter 3, I demonstrated that high dietary salt induced a significant increase in BP, and in chapter 4, my experiments showed adaptation of renal function indicating that an impaired PN relationship was not the driving event behind the salt-induced hypertension of C57BL6/JCrl mice. Morris *et al*., (92) has advocated an alternative hypothesis that vasodysfunction underlies sustained salt-induced increases in BP. Specifically they postulate that salt-sensitivity reflects an insufficient decrease in SVR following high salt intake. This is suggestive of impaired vasodilation, thus in this chapter the responses of renal and mesenteries arteries were measured in C57BL6/JCrl mice on the SSD (0.25% Na) or the HSD (3% Na).

5.1.1 Aims

1. To assess the impact of high dietary salt intake on vascular reactivity compared to standard salt intake
2. To begin to explore the molecular mechanisms underlying the vascular response to high salt.

5.1.2 Approach to achieve the chapter aims

- Vascular reactivity was measured using the *ex vivo* wire myograph system. Pharmacological inducers of either vasoconstriction or vasodilation were administered to evaluate the responsiveness of renal and mesenteric arteries after high dietary salt intake compared to that of a control group.

- The underlying processes were interrogated in a separate experiment by measuring the mRNA transcript levels of key vasoactive signalling molecules with qPCR.
- The effect of dietary salt was examined by placing mice on the HSD (3% Na) and comparing the effects with mice on the SSD (0.25% Na). For wire myography, two experiments were performed in which mice in the HSD group received the diet for 3 days or 1 week, compared with contemporaneous controls. For qPCR, a separate experiment was carried out with three groups: SSD, 1 week of the HSD, and 2 weeks of the HSD.

5.2 Methods

The methods used in this chapter are covered in detail in the main Materials and Methods chapter, and below the details and protocols specific to these experiments are outlined.

5.2.1 Diet duration

In the experiments of this chapter, C57BL6/JCrl mice received either the SSD or the HSD in a cross-sectional study design. Separate experiments were performed to evaluate vascular function and mRNA transcript abundance after 3 days, 1 week and 2 weeks of high dietary salt intake. These time-points were assessed as BP initially began to increase after 24 hours, peaked at 3 days and remained high and stable for 1 and 2 weeks of the HSD, as illustrated in chapter 3.

5.2.2 Wire myography

5.2.2.1 Study design

C57BL6/JCrl mice were used in the assessment of artery reactivity *ex vivo* by wire myography after 3 days and after 1 week of the HSD. A separate cohort for each time-point was utilised to investigate the first aim of this chapter, as results produced by this method can vary significantly over time. Contemporaneous control groups were used because, as depicted in Figure 5.1, different contractile responses to phenylephrine (PhE) were obtained

from mice on the SSD around 12 months apart. This reflects variations in the experimental equipment and reagents, for example one possible explanation could be different drug batches, and also the refinement of my ability to perform this challenging technique.

A

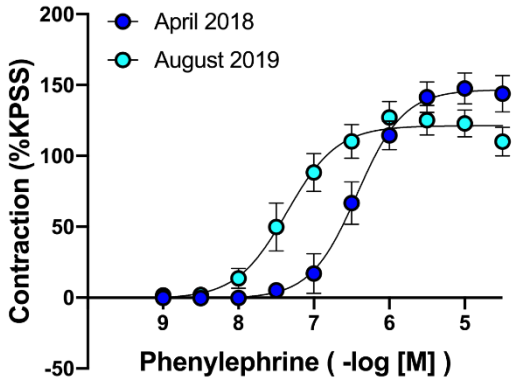

B

	April 2018	*August 2019*	P value
n	4	6	
$logEC_{50}$	6.44 ± 0.13	7.36 ± 0.16	**<0.0001, *******
%Emax	146.3 ± 11.5	121.1 ± 9.7	**0.002, ****

Figure 5.1: Comparison of phenylephrine concentration-response curves between two control groups of mesenteric arteries at different times.
Vascular function was measured via wire myography. Arteries from two control groups of C57BL6/JCrl mice were used and comparisons made within, rather than between, each group due to the variation that can occur over time. Possible explanations include alterations to the equipment or reagents, or as a result of practise and enhancement of the technique. A: phenylephrine concentration-response curves generated one year and 5 months apart using the same equipment and protocol, expressed as a percentage of the maximal contractile force to a high potassium salt solution, KPSS. Contraction was analysed with log(dose) response curves to establish B: the concentration achieving 50% of the maximal response ($logEC_{50}$) and the maximal response (%Emax). Data are presented as mean ± SD. p<0.01 **, p<0.0001 ****.

5.2.2.2 Experimental protocol

After either 3 days or 1 week of the diets, mice were humanely euthanised in the morning and wire myography was performed on the same day. Renal and mesenteric arteries were prepared as described in the Materials and Methods chapter section 2.5. Vessel viability was confirmed with the addition of a high potassium salt solution, referred to as KPSS, three times at the beginning and end of the experiment. Vascular reactivity was explored by generating cumulative concentration-response curves (10^{-9} to 10^{-3} M) to the contractile agent PhE and the vasodilatory agents acetylcholine (ACh) and NO donor sodium nitroprusside (SNP).

5.2.2.3 Data acquisition

Values of force output (mN) were obtained from the data acquisition software Labchart 7 pro version 7.3.2 as depicted within Figure 5.2. Contractile responses were normalised to KPSS-induced depolarisation. This was done by highlighting the area of the trace illustrating the force output produced by each application of KPSS, selecting the maximum value and taking an average (Figure 5.2 A). The same procedure was performed for each dose of vasoconstrictor (Figure 5.2 C) and the resulting values were then expressed as a percentage of the mean KPSS contraction. For vasodilatory responses, data were normalised to the maximum force output produced by PhE-induced pre-constriction. Following this, the minimum value of the selected area for each dose of vasodilator was taken and presented as a percentage of pre-constriction, illustrating the amount of vasoconstriction remaining (Figure 5.2 D).

5.2.2.4 Data analysis

The normalised data were analysed in Graphpad Prism v8.2.0. Nonlinear regression was performed, in which concentration-response curves were generated using the log(dose) vs. response equation. This allowed the calculation of the concentration required to achieve a half-maximal response, referred to as $\log EC_{50}$ for agonists and $\log IC_{50}$ for inhibitors, as well as the maximum point at which the response plateaus, referred to as %Emax for agonists and %Relax for inhibitors. The variable slope model was applied, in which the Hill slope of the data was fitted to the curve rather than assuming and automatically fitting a standard slope of 1. This was beneficial in this case as wire myography generates many data points. The effect of the two factors diet and concentration on vascular reactivity was evaluated using an ordinary two-way ANOVA and multiple comparisons were made with Sidak's test with significance denoted at 0.05.

Figure 5.2: Examples of the acquisition of reactivity data from Labchart.

Arteries from C57BL6/JCrl mice receiving a standard or high salt diet were isolated and reactivity was assessed by wire myography during the daytime. Real-time recordings of force output (mN; y-axis) were acquired using the software Labchart 7 pro version 7.3.2, creating the example traces displayed. Force output is a measure of vessel wall tension, detected by wires within the vessel lumen connected to a force transducer. Changes in vessel wall tension produce the traces displayed for responses to A: KPSS, B: phenylephrine (PhE) followed by acetylcholine (ACh) to test endothelial integrity, D: vasoconstriction such as PhE and E: vasodilation such as by ACh. Grey squares represent the selection boxes drawn to isolate the section of the trace to obtain the maximum/minimum value. The cross, depicted in D, is the cursor and allows the visualisation of the force output at that particular time. CRC; concentration-response curve, M; molar, mN; milliNewtons, KPSS; potassium physiological salt solution.

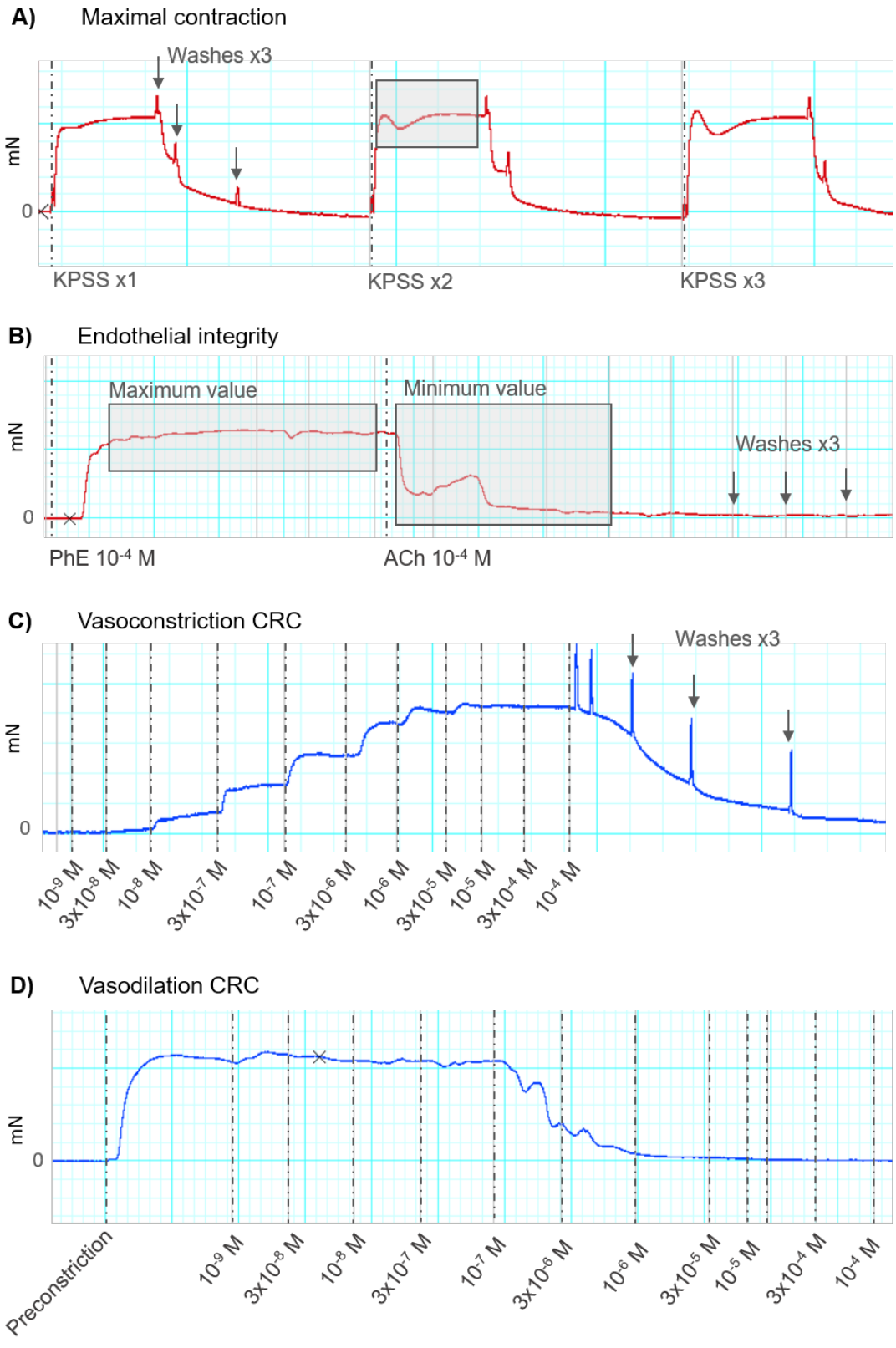
A)
Maximal contraction
Washes x3
mN
0
KPSS x1
KPSS x2
KPSS x3
B)
Endothelial integrity
Maximum value
Minimum value
Washes x3
mN
0
PhE 10-4 M
ACh 10-4 M
C)
Vasoconstriction CRC
Washes x3
mN
0
10-9 M
3x10-8 M
10-8 M
3x10-7 M
10-7 M
3x10-6 M
10-6 M
3x10-5 M
10-5 M
3x10-4 M
10-4 M
D)
Vasodilation CRC
mN
0
Preconstriction
10-9 M
3x10-8 M
10-8 M
3x10-7 M
10-7 M
3x10-6 M
10-6 M
3x10-5 M
10-5 M
3x10-4 M
10-4 M

5.2.3 Determination of vascular mRNA transcript levels

A separate experiment was performed in which three cohorts were investigated receiving either the SSD, 1 week of the HSD or 2 weeks of the HSD. A generalised version of the protocol applicable to all tissue types is detailed in Materials and Methods chapter section 2.4, whereas the specific steps for arteries are described here. Arteries from two mice in the same experimental group were pooled together after dissection during the daytime in order to obtain a sufficient yield of RNA for further analysis.

5.2.3.1 Sample preparation and RNA extraction

Immediately after dissection, samples were stored at 4 ºC in RNA*later* RNA stabilisation reagent (QIAGEN, UK) for 24 hours, and subsequently removed and frozen at -80 ºC for a further 24 hours or until the extraction was carried out. Prior to the extraction, cellular disruption was achieved using pestles (ThermoFisher Scientific, UK). It was essential that the samples did not thaw at any point during disruption and so the pestles were placed on dry ice for ~5 minutes before contact with the samples and the full procedure was executed over dry ice. Once acclimatised, the pestles were used to grind the samples into a fine powder within 2mL Eppendorf tubes. Whilst remaining in the Eppendorf tube, the pestle was covered with 300 µL RLT buffer supplemented with the recommended volume of β-Mercaptoethanol and slowly removed to limit the loss of powdered sample. Pestles were re-sterilised and placed back on dry ice between samples.

Further homogenisation was carried out firstly by stainless steel beads in a TissueLyser II (QIAGEN, UK), followed by incubation in Proteinase K diluted 1:60 with RNase-free water (QIAGEN, UK) at 55 ºC for 10 minutes. Samples were centrifuged at 8,000 xg for 3 minutes and the supernatant was taken forward for RNA isolation using the RNeasy micro kit (QIAGEN, UK) by the manufacturer's instructions. All reagents were freshly prepared on the day of extraction. RNA yield and purity were determined as outlined in Materials and Methods chapter section 2.4.2, and reverse transcription followed by qPCR analysis was carried out as described in sections 2.4.3 and 2.4.4.

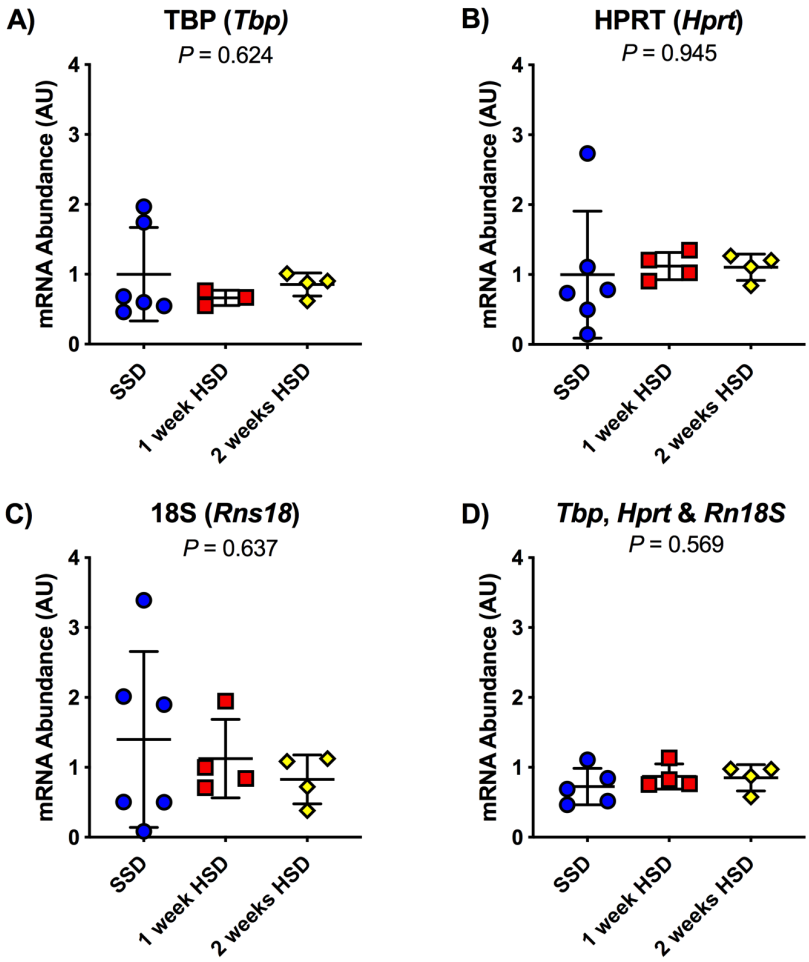

Figure 5.3: Reference gene expression in mesenteric arteries after high dietary salt intake.
After either 1 or 2 weeks of a standard salt (SSD) or a high salt diet (HSD), mesenteric arteries from C57BL6/JCrl mice were isolated during the daytime, cleaned of adherent perivascular fat and pooled together to maximise the yield of RNA extracted (n=4-5 per dietary group). The expression of reference genes A: *Tbp*, B: *Hprt*, and C: *Rn18S* were each adjusted so that the mean concentration of the control group (SSD in these experiments) was equal to 1. The mRNA transcript levels of experimental genes-of-interest were normalised to the mean abundance of these three reference genes displayed in D. Data are presented as mean ± SD and were analysed by ordinary one-way ANOVA with multiple comparisons made by Tukey testing. Significance was denoted as $P<0.05$.

5.2.3.2 Reference genes

The reference genes *Hprt* (HPRT), *Tbp* (TBP) and *Rn18S* (eukaryotic 18S rRNA) were selected as their mRNA abundance was unaffected by increasing dietary salt intake (Figure 5.3 A-C). Therefore, the mRNA abundance of the experimental genes-of-interest in this chapter are presented relative to the averaged abundance of these reference genes (Figure 5.3 D).

5.2.3.3 Data analysis

Analysis of the normalised data was performed in Graphpad Prism v8.2.0. Differences between the three groups were investigated using ordinary one-way ANOVA corrected for multiple comparisons by Tukey testing, with significance denoted at 0.05.

5.3 Results

5.3.1 Mesenteric artery reactivity is unaltered by high salt intake

Mesenteric artery reactivity was determined by wire myography, in which arteries were isolated and their responsiveness to pharmacological stimuli *ex vivo* was examined. The effect of diet upon vascular function was explored by giving C57BL6/JCrl mice access to either the SSD or HSD prior to performing wire myography.

5.3.1.1 Mesenteric artery function after 3 days of high salt

Initially, mice received either diet for a duration of 3 days. Mesenteric arteries from both dietary groups contracted similarly to KPSS administration (SSD 8.68 ± 1.36 mN vs. HSD 9.38 ± 1.61, P=0.361; Figure 5.4 B), illustrating that the ability of the arteries to depolarise was unaffected by high dietary salt intake or the mounting procedure. This depolarisation did not deteriorate throughout the experimental protocol (SSD 96.4 ± 7.3 %KPSS vs. HSD 97.3 ± 5.7 %KPSS, P=0.778) which confirms that vessel integrity was preserved. Concentration-dependent vasoconstriction was induced by PhE after the SSD or HSD (Figure 5.4 A & F). No significant differences were observed in the sensitivity of arteries to PhE represented by $logEC_{50}$ (SSD 7.36 ± 0.16 vs. HSD 7.41 ± 0.35, P=0.763), or the maximum contractile responses to PhE expressed as %Emax (SSD 121.1 ± 9.7 vs. HSD 127.9 ± 5.9, P=0.145; Figure 5.4 A & B).

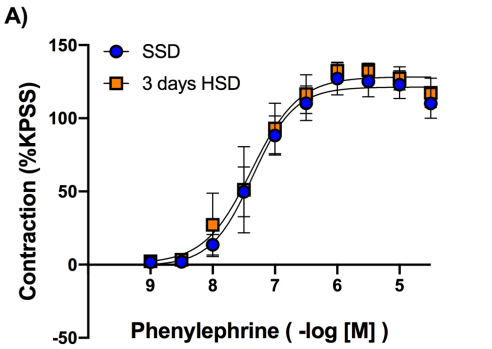

B)

KPSS, PhE	**SSD**	**3 days HSD**	P value
KPSS (mN)	8.68 ± 1.36	9.38 ± 1.61	0.361
%KPSS	96.4 ± 7.3	97.3 ± 5.7	0.778
$logEC_{50}$	7.36 ± 0.16	7.41 ± 0.35	0.763
%Emax	121.1 ± 9.7	127.6 ± 5.9	0.145

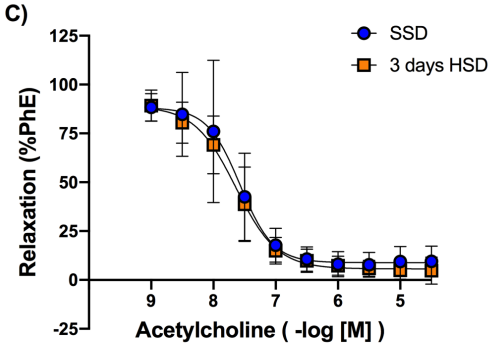

D)

ACh, SNP	**SSD**	**3 days HSD**	*P* value
ACh $logIC_{50}$	7.70 ± 0.28	7.67 ± 0.27	0.818
%Relax	9.0 ± 6.6	6.0 ± 4.9	0.307
SNP $logIC_{50}$	8.09 ± 0.46	7.74 ± 0.56	0.209
%Relax	5.6 ± 3.4	7.0 ± 4.1	0.473

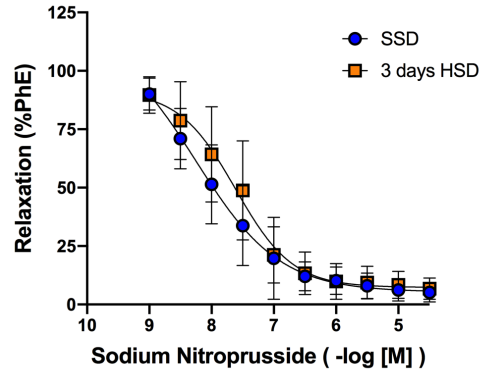

F)

Two-way ANOVA *P* values	*PhE*	*ACh*	*SNP*
Agonist concentration	**<0.0001, ******	**<0.0001, ******	**<0.0001, ******
Diet	**0.018, ***	0.163	**0.030, ***
Interaction	0.971	0.999	0.603

Figure 5.4: Mesenteric artery function after 3 days of a high salt diet.

Wire myography was performed to evaluate the reactivity of mesenteric arteries isolated from C57BL6/JCrl mice (n=8 per dietary group) following 3 days of either a standard salt diet (SSD; 0.25% Na) or a high salt diet (HSD; 3% Na). Concentration-response curves were produced by administering A: phenylephrine (PhE) to induce vasoconstriction, and C: acetylcholine (ACh) and E: sodium nitroprusside (SNP) to induce vasodilation. Contraction is expressed as a percentage of the greatest contractile response to a high potassium physiological salt solution (KPSS). Relaxation is presented as a percentage of residual tension leftover from PhE-induced pre-constriction. Log(dose) response curves were generated to calculate B: $logEC_{50}$ and %Emax for PhE, and D: $logIC_{50}$ and %Relax for ACh and SNP. F: *P* values are presented after determining the effect of dietary group upon mesenteric artery responses using two-way ANOVA with post-hoc Sidak testing for multiple comparisons. Data are mean ± SD. **p*<0.05, *****p*<0.0001.

Mesenteric arteries from both dietary groups exhibited concentration-dependent vasodilation with ACh and SNP administration (Figure 5.4 C-F). There were no significant differences in the sensitivities of the arteries, expressed as $logIC_{50}$, to either ACh (SSD 7.70 ± 0.28 vs HSD 7.67 ± 0.27, *P*=0.818) or SNP (SSD 8.09 ± 0.46 vs HSD 7.74 ± 0.56, *P*=0.209; Figure 5.4 D) between the SSD and HSD groups. Furthermore, no disparities in the maximum dilatory responses, presented as the % of PhE-induced pre-constriction remaining (%Relax), to ACh (SSD 9.0 ± 6.6 vs. HSD 6.0 ± 4.9, *P*=0.307) or SNP (SSD 5.6 ± 3.4 vs. HSD 7.0 ± 4.1, *P*=0.473; Figure 5.4 D) were seen. The two-way ANOVA results display a small but significant effect of diet on SNP-evoked relaxation (Figure 5.4 F); however, this was not reflected in the sensitivity or maximal response. ACh-evoked relaxation is mediated via the endothelial production of NO, whereas SNP is a NO donor and so bypasses the endothelium to evoke vasodilation. The responses to both ACh and SNP were similar which suggests that, together, the production of NO by the endothelium and the responsiveness of the VSM to NO was unaffected after 3 days of high dietary salt intake.

5.3.1.2 Mesenteric artery function after 1 week of high salt

Depolarisation was evaluated by the addition of KPSS and mesenteric arteries from 1 week of the SSD and HSD contracted alike (SSD 5.71 ± 2.90 mN vs HSD 6.77 ± 2.15 mN, *P*=0.354), the intensity of which was maintained until the end of the experimental protocol (SSD 115.8 ± 3.2 %KPSS vs. HSD 107.3 ± 18.6 %KPSS, *P*=0.290; Figure 5.5 B). Mesenteric arteries from both dietary groups exhibited similar PhE-induced contraction, with no significant differences reported in vessel sensitivity ($logEC_{50}$: SSD 6.44 ± 0.13 vs. HSD 6.61 ± 0.33; *P*=0.257) or maximum response (%Emax: SSD 146.3 ± 11.5 vs HSD 139.6 ± 8.4, *P*=0.165; Figure 5.5 A & B). Thus, the contractile responses of mesenteric arteries were unchanged by 1 week of high dietary salt intake.

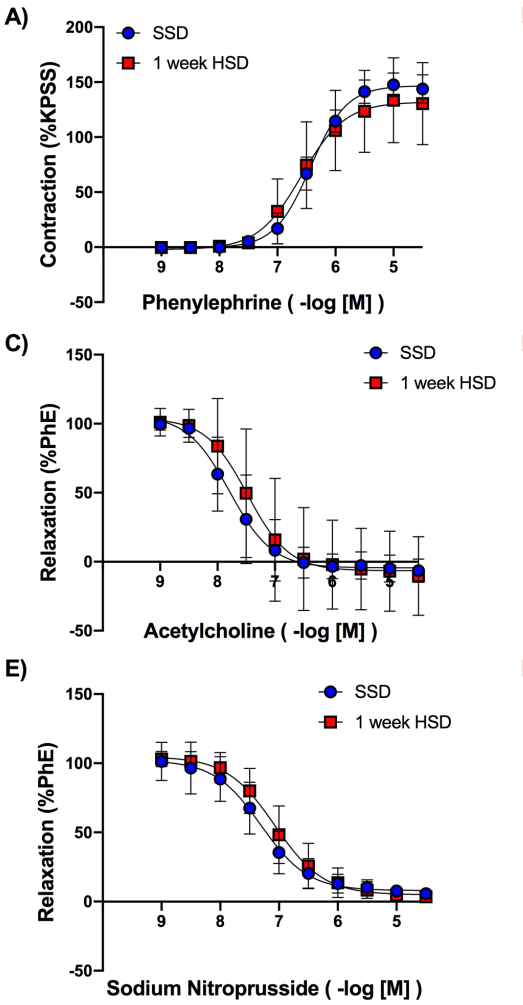

B)

KPSS, PhE	**SSD**	**1 week HSD**	P value
KPSS (mN)	5.71 ± 2.90	6.77 ± 2.15	0.354
%KPSS	115.8 ± 3.2	107.3 ± 18.6	0. 290
$logEC_{50}$	6.44 ± 0.13	6.61 ± 0.33	0.257
%Emax	146.3 ± 11.5	139.6 ± 8.4	0.165

D)

ACh, SNP	**SSD**	**1 week HSD**	*P* value
ACh $logIC_{50}$	7.74 ± 0.41	7.39 ± 0.64	0.232
%Relax	-4.0 ± 9.0	-9.5 ± 28.5	0.659
SNP $logIC_{50}$	7.28 ± 0.22	7.04 ± 0.35	0.154
%Relax	6.8 ± 2.9	4.1 ± 3.8	0.136

F)

Two-way ANOVA P values	*PhE*	*ACh*	*SNP*
Agonist concentration	**<0.0001, ******	**<0.0001, ******	**<0.0001, ******
Diet	0.419	0.309	**0.037, ***
Interaction	0.658	0.951	0.417

Figure 5.5: Mesenteric artery reactivity after 1 week of high salt.

Wire myography was used to evaluate mesenteric artery function from 9-10-week-old male C57BL6/JCrl mice fed either a standard salt diet (SSD, n=4) or a high salt diet (HSD, n=9) for 1 week. Cumulative concentration-response curves were generated with the addition of A: vasoconstrictor phenylephrine (PhE) and C: vasodilators acetylcholine (ACh) and E: sodium nitroprusside (SNP). Contraction is expressed as a percentage of mean high KCl physiological salt solution (KPSS)-induced depolarisation. Relaxation is presented as a percentage of residual tension generated by PhE-induced pre-constriction. The variable-slope log(dose) response model was used to calculate and compare B: $logEC_{50}$ and %Emax for PhE, and D: $logIC_{50}$ and %Relax for ACh and SNP. F: Table displaying *P* values from evaluating the effect of dietary group and drug concentration by ordinary two-way ANOVA corrected for multiple comparisons by Sidak testing. Data are mean ± SD. **p*<0.05, *****p*<0.0001.

As before, endothelium-dependent vasodilatory responses were assessed by ACh and endothelium-independent responses by SNP. All mesenteric arteries relaxed with increasing concentrations of ACh and SNP (Figure 5.5 C & E). The sensitivity of mesenteric arteries, producing a half-maximal inhibition of PhE-induced pre-constriction, to ACh was unaffected after 1 week of the HSD compared to the SSD group ($logIC_{50}$: SSD 7.74 ± 0.41 vs. HSD 7.39 ± 0.64, *P*=0.232), as was the maximum vasodilatory response (%Relax: SSD -4.0 ± 9.0 vs. HSD -9.5 ± 28.5, *P*=0.659; Figure 5.5 D) suggestive of an intact and functioning endothelium. Mesenteric artery sensitivity to SNP was also similar between the dietary groups ($logIC_{50}$: SSD 7.28 ± 0.22 vs. HSD 7.04 ± 0.35, *P*=0.154). The maximal relaxation achieved by SNP in the SSD group was comparable to that achieved by the HSD group (%Relax: SSD 6.8 ± 2.9 vs. HSD 4.1 ± 3.8, *P*=0.136; Figure 5.5 D). The results of the two-way ANOVA demonstrate a modest effect of diet upon relaxation induced by SNP (Figure 5.5 F). This was not observed in the sensitivity or maximal relaxation as stated above. Thus, the capability of arteries to respond to exogenous NO appears to also be mostly unaltered. This illustrates that after 1 week, both the endothelium and the VSM layer were unaltered by high dietary salt intake.

5.3.2 High dietary salt intake increases renal artery sensitivity to phenylephrine

5.3.2.1 Renal artery reactivity after 3 days of high salt

In renal arteries isolated after 3 days of the SSD or HSD, KPSS-induced contraction was not significantly different between groups (SSD 5.91 ± 2.30 mN vs. HSD 7.68 ± 1.63 mN, *P*=0.097). Depolarisation to KPSS was assessed again at the end of the experimental protocol and produced similar results, confirming that the integrity of the arteries had been maintained throughout the procedure (SSD 88.0 ± 5.2 %KPSS vs. HSD 90.3 ± 3.6 %KPSS, *P*=0.304; Figure 5.6 B). Renal arteries from mice on the HSD exhibited similar concentration-dependent contractions to PhE as those from mice on the SSD (Figure 5.6 A), supported by the near-identical values of

sensitivity ($logEC_{50}$: SSD 7.51 ± 0.29 vs. HSD 7.46 ± 0.12, *P*=0.646) and the maximum contractile response (%Emax: SSD 142.6 ± 14.9 vs. HSD 142.1 ± 8.2, *P*=0.932; Figure 5.6 B). Therefore, the ability of renal arteries to contract appears to be unchanged by 3 days of high dietary salt intake, suggesting no salt-induced dysfunction was present.

A)

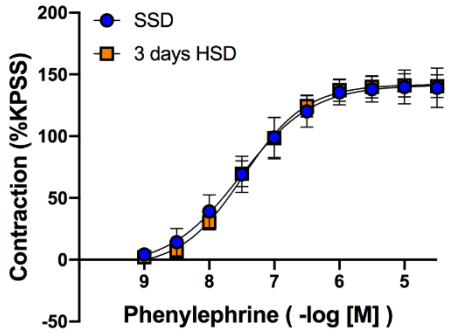

B)

KPSS, PhE	**SSD**	**3 days HSD**	P value
KPSS (mN)	5.91 ± 2.30	7.68 ± 1.63	0.097
%KPSS	88.0 ± 5.2	90.3 ± 3.6	0.304
$logEC_{50}$	7.51 ± 0.29	7.46 ± 0.12	0.646
%Emax	142.6 ± 14.9	142.1 ± 8.2	0.932

C)

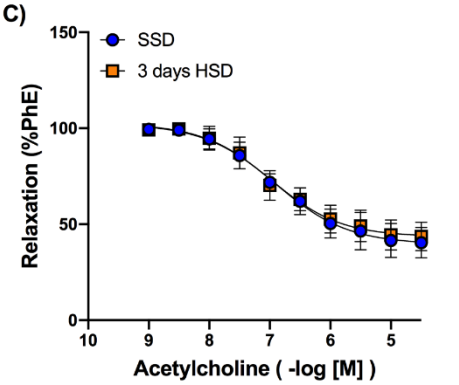

D)

ACh, SNP	**SSD**	**3 days HSD**	P value
ACh $logIC_{50}$	6.96 ± 0.20	7.01 ± 0.23	0.629
%Relax	38.7 ± 9.12	43.2 ± 9.7	0.386
SNP $logIC_{50}$	6.96 ± 0.23	6.70 ± 0.20	0.728
%Relax	39.3 ± 10.4	41.6 ± 8.8	0.647

E)

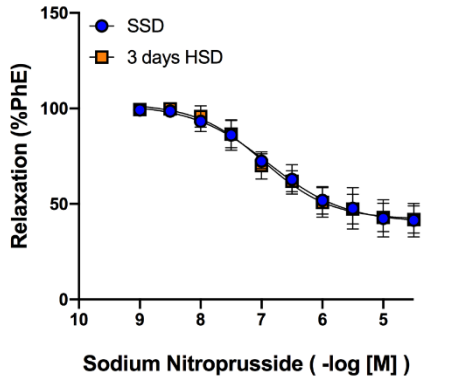

F)

Two-way ANOVA P values	*PhE*	*ACh*	*SNP*
Agonist concentration	**<0.0001,** ****	**<0.0001,** ****	**<0.0001,** ****
Diet	0.654	0.256	0.962
Interaction	0.810	0.995	0.998

Figure 5.6: Renal artery function after 3 days of high dietary salt intake.

Renal artery reactivity was measured using wire myography. C57BL6/JCrl mice (n=8 per dietary group) were humanely culled via carbon dioxide asphyxiation after 3 days of either a standard (SSD; 0.25% Na) or a high salt diet (HSD; 3% Na) and renal arteries were isolated. Cumulative concentrations of A: vasoconstrictor phenylephrine (PhE) were administered and normalised to B: initial mean high potassium physiological salt solution (KPSS)-induced depolarisation. Cumulative concentrations of vasodilators C: acetylcholine (ACh) and E: sodium nitroprusside (SNP) were applied and normalised to PhE-induced pre-constriction. Nonlinear regression model log(dose)-response was used to calculate and compare B: $logEC_{50}$ and %Emax for PhE and C: $logIC_{50}$ and %Relax for vasodilators. F: *P* values generated following analysis of the effect of dietary group by two-way ANOVA corrected for multiple comparisons by Sidak testing. Data are mean ± SD. ****p<0.0001.

As shown in Figure 5.6 C and F, relaxation evoked by the endothelium-dependent vasodilator ACh was similar in renal arteries in the HSD and the SSD groups. Sensitivity to ACh remained equal between the dietary groups ($logIC_{50}$: SSD 6.96 ± 0.20 vs. HSD 7.01 ± 0.23, *P*=0.629), as did the maximum dilatory response (%Relax: SSD 38.7 ± 9.1 vs. HSD 43.2 ± 9.7, *P*=0.386; Figure 5.6 D). There was also no statistically significant difference in SNP-mediated relaxation between renal arteries from the SSD and HSD groups (Figure 5.6 E & F). This was reflected within the sensitivity to SNP ($logIC_{50}$: SSD 6.96 ± 0.23 vs. HSD 6.70 ± 0.20, *P*=0.728) and in the greatest inhibitory effect induced by SNP (%Relax: SSD 39.3 ± 10.4 vs. HSD 41.6 ± 8.8, *P*=0.647; Figure 5.6 D).

5.3.2.2 Renal artery reactivity after 1 week of high salt

Rapid depolarisation of renal arteries by KPSS did not differ between the dietary groups (SSD 3.09 ± 1.27 mN vs. HSD 5.08 ± 3.50 mN, *P*=0.195) and did not deteriorate throughout the experimental protocol (SSD 115.7 ± 25.3 %KPSS vs. HSD 104.1 ± 20.1 %KPSS, *P*=0.287; Figure 5.7 B). The vasoconstrictor PhE induced concentration-dependent contraction in renal arteries from both dietary groups (Figure 5.7 A & F), however renal arteries after 1 week of the HSD reached 50% of their maximum contraction at a significantly lower concentration to those after the SSD ($logEC_{50}$: SSD 6.14 ± 0.03 vs. HSD 6.63 ± 0.41, *P*=0.019; Figure 5.7 B). Thus, renal arteries after high dietary salt intake were more sensitive to PhE. The maximal contractile ability of the renal arteries, presented as %Emax, was comparable between the dietary groups (SSD 138.0 ± 40.3 vs. HSD 135.2 ± 25.5, *P*=0.863; Figure 5.7 B), suggesting that renal arteries contracted to the same extent regardless of diet.

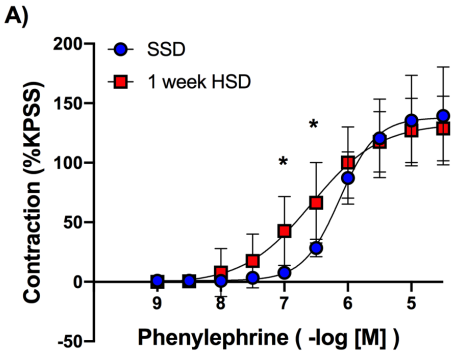

B)

KPSS, PhE	**SSD**	**1 week HSD**	*P* value
KPSS (mN)	3.09 ± 1.27	5.08 ± 3.50	0.195
%KPSS	115.7 ± 25.3	104.1 ± 20.1	0. 287
$logEC_{50}$	6.14 ± 0.03	6.63 ± 0.41	**0.019, ***
%Emax	138.0 ± 40.3	135.2 ± 25.5	0.863

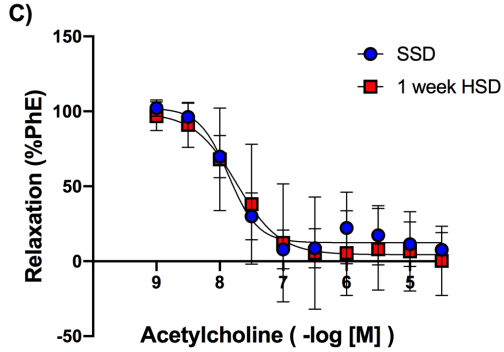

D)

ACh, SNP	**SSD**	**1 week HSD**	P value
ACh $logIC_{50}$	7.84 ± 0.17	7.64 ± 0.58	0.465
%Relax	11.6 ± 14.3	2.7 ± 23.6	0.446
SNP $logIC_{50}$	7.44 ± 1.24	7.18 ± 0.48	0.487
%Relax	21.4 ± 15.5	20.9 ± 10.1	0.923

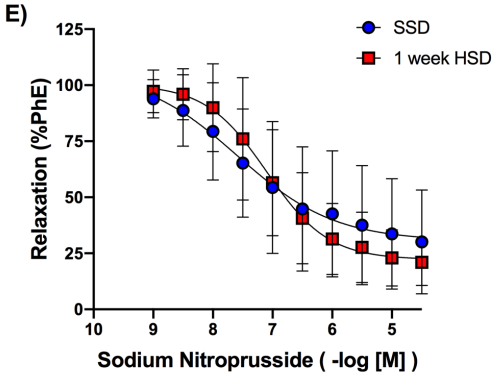

F)

Two-way ANOVA P values	*PhE*	*ACh*	*SNP*
Agonist concentration	**<0.0001, ******	**<0.0001, ******	**<0.0001, ******
Diet	**0.031, ***	0.351	0.709
Interaction	0.056	0.988	0.475

Figure 5.7: Renal artery reactivity following 1 week of high dietary salt intake.

Renal arteries were dissected from C57BL6/JCrl mice after 1 week of either a standard salt diet (SSD, 0.25% Na; n=4) or a high salt diet (HSD, 3% Na; n=9) and function was evaluated using wire myography. Vasoconstriction was induced by A: phenylephrine (PhE) and presented as a percentage of B: mean KPSS-induced depolarisation, a high KCl salt solution. Vasodilation was stimulated by C: acetylcholine (ACh) and E: sodium nitroprusside (SNP), expressed as a percentage of residual tone remaining from pre-constriction. Log(dose) response curves were used to determine and compare B: PhE $logEC_{50}$ and %Emax, and D: ACh and SNP $logIC_{50}$ and %Relax values. F: Two-way ANOVA was utilised to evaluate the link between dietary group and renal artery activity, with multiple comparisons made by Sidak post-hoc testing. Data are mean ± SD. **p*<0.05, *****p*<0.0001.

Vasodilation evoked by both ACh and SNP was concentration-dependent within pre-constricted renal arteries from the SSD and the HSD groups (Figure 5.7 C, E, F). Sensitivity was similar between arteries from the different dietary groups to ACh ($logIC_{50}$: SSD 7.84 ± 0.17 vs. HSD 7.64 ± 0.58, *P*=0.465), as was the maximal dilatory response achieved by ACh (SSD 11.6 ± 14.3 vs. HSD 2.7 ± 23.6, *P*=0.446). This demonstrates that endothelial function was similar between the two groups, thus was unaffected by diet. Furthermore, there was no difference in the sensitivity of arteries to SNP ($logIC_{50}$: SSD 7.44 ± 1.24 vs. HSD 7.18 ± 0.48, *P*=0.487), nor in the maximum relaxation evoked between the dietary groups (SSD 21.4 ± 15.5 vs. HSD 20.9 ± 10.1, *P*=0.923; Figure 5.7 D), suggesting that the VSM response to NO is also intact. Overall, no significant effect of diet was observed upon the responsiveness of renal arteries to vasodilators, suggesting that 1 week of high dietary salt intake does not impact renal artery relaxation.

5.3.3 Effect of high dietary salt intake on mesenteric artery mRNA abundance

qPCR was used to interrogate the effect of high salt intake on the transcriptional profile of genes involved in vasomotor tone. As can be seen in Figure 5.8 A, 1 and 2 weeks of the HSD had no significant effect upon the mesenteric artery mRNA transcript levels of enzyme eNOS (*P*=0.851). The expression of α_1-adrenergic receptors (ARs), which govern the contractile response to PhE, was also unchanged in the HSD groups compared to the SSD group (*Adra1a P*=0.627; *Adra1b P*=0.322; *Adra1d P*=0.257; Figure 5.8 B-D). ANGII is also a potent vasoconstrictor, acting via the AT_{1A} receptor located on the VSM. Overall, the HSD had a significant effect upon mesenteric artery AT_{1A} receptor expression (*P*=0.029), with a reduction in expression observed in the HSD group receiving the diet for 2 weeks (*P*=0.024; Figure 5.8 E). However, expression after 1 week of the HSD was similar to that after the SSD.

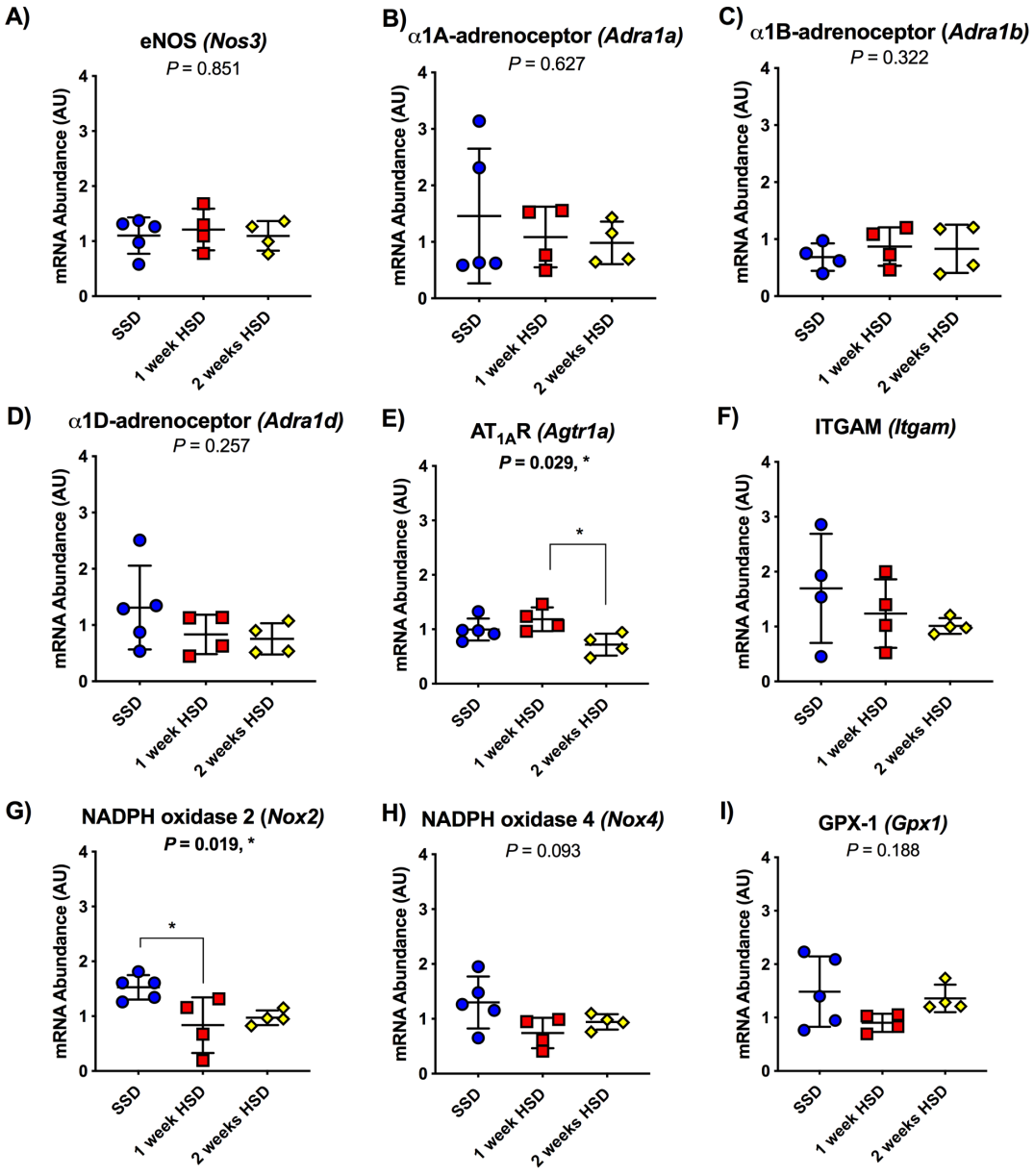

Figure 5.8: Mesenteric artery mRNA transcript abundance after 1-2 weeks of high dietary salt intake.

Mesenteric arteries were dissected from C57BL6/JCrl mice after 1 or 2 weeks of a standard salt diet (SSD; 0.25% Na) or a high salt diet (HSD; 3% Na), pooled together (n=4-5 per dietary group) and mRNA abundance was measured by qPCR. The names of the proteins are presented alongside the names of the genes-of-interest within brackets, and expression was normalised to the average expression of reference genes *Tbp*, *Hprt* and *Rn18S*. Transcript levels involved in vascular function assessed in this chapter (A-D), renin-angiotensin-system signalling (E), inflammatory response (F) and oxidative stress (G-I) were tested. Data are mean ± SD. Ordinary one-way ANOVA was performed followed by post-hoc Tukey testing for multiple comparisons. *p<0.05.

Integrin αM (ITGAM), also known as CD11B, is a glycoprotein responsible for the adhesion of leukocytes to the endothelium during the inflammatory response, and so expression was used as a marker of inflammation potentially induced by dietary salt. However, no differences in ITGAM expression were observed between the standard and high salt dietary groups here (*P*=0.391; Figure 5.8 F).

A major source of vascular reactive oxygen species (ROS) is NADPH oxidase, and so an insight into the oxidative stress status of mesenteric arteries following the HSD was obtained by assessing the mRNA abundance of NADPH oxidase subunits and scavenger glutathione peroxidase-1 (GPX-1; Figure 5.8 G-I). A modest but statistically significant downregulation in the expression of NADPH oxidase subunit 2 was observed after 1 week of the HSD (*P*=0.028). This downregulation was also seen in the group fed 2 weeks of the HSD, although this did not pass the significance threshold (*P*=0.054). In contrast, the expression of NADPH oxidase subunit 4 (*P*=0.093) and GPX1 (*P*=0.188) were not different in the HSD groups as compared to the SSD group.

5.4 Discussion

The vascular impact of dietary salt intake in this chapter was determined by investigating artery reactivity to contractile and dilatory compounds following the SSD or HSD. Excessive salt intake is detrimental to cardiovascular health as it has been linked to an increased risk of stroke and mortality (18, 68). Over the past few decades, much research has gone into elucidating the processes responsible. The literature outlining the injurious impact of dietary salt upon vascular health is vast. In this section, I have therefore limited the discussion to cover representative studies illustrating such effects of salt, both in the presence and absence of salt-induced hypertension.

The vasodysfunction model, detailed by Morris *et al*. (92), supports the role of the vasculature in the induction of salt-induced hypertension within salt-sensitivity. This challenges the predominant, Guytonian model as it draws attention away from impaired renal sodium handling and retention as the critical, initiating event with salt-sensitivity. In salt-resistant individuals, the initial haemodynamic events following increased salt intake include temporary elevations in CO, ECFV, sodium balance and then excretion, which successfully combat any pathologic alterations in BP. Upon occasion, research within humans has not noticed any concerning changes to renal sodium retention with salt-sensitivity compared to salt-resistance, yet increases in MABP were still present after salt loading (73). Alongside this, a decrease in SVR was observed in salt-resistant individuals, which was not observed to the same extent in salt-sensitive individuals, suggesting a compromised vasodilatory response (92, 181). This has led to the generation of the vasodysfunction paradigm, which proposes that an abnormal vascular response to salt-induced haemodynamic changes underlies the provocation and maintenance of an elevated BP in salt-sensitivity (92, 182).

Previously, I have shown that C57BL6/JCrl mice have a BP that increases with dietary salt intake in the absence of prominent changes to renal sodium handling. This led to the hypothesis, derived from the vasodysfunction theory, that impaired vasodilatory responses triggered by high dietary salt intake underly the salt-sensitivity of BP in these mice. In this work, mesenteric arteries were selected to represent resistance arteries, which have an integral influence upon SVR and its contribution to BP as they are able to adjust their internal diameter to regulate blood flow and vascular tone. In this capacity, mesenteric arteries in particular are widely used, possessing a luminal diameter (<500 μm) amendable to analysis by wire myography (183). In addition to this, renal arteries were investigated.

5.4.1 Wire myography in the measurement of vascular function

Wire myography is an *ex vivo* technique, first developed in 1990 (183), that enables researchers to assess the reactivity of isolated artery segments with

a luminal diameter of <500 μm (184). These artery segments are carefully dissected from various parts of the vascular system, mounted within separate organ baths and placed under isometric tension, which circumvents the need for VSM involvement whilst also introducing tension similar to that experienced *in vivo*. Arteries are plied with ionic solutions and pharmacological agents to evaluate vasoconstrictor and vasodilatory responses.

The advantages of the wire myograph system are plentiful. Such a system allows researchers to explore the intrinsic functional properties of arteries without the potentially confounding influence of the environment, such as from blood flow or the peripheral nervous system. The use of multiple channels each containing an organ bath, a feature of the four-channel system used in this thesis, enables different artery segments to be studied individually and concurrently. This is a particularly important feature as the conditions at the time of the experiment can significantly impact the results produced, as depicted in Figure 5.1, thus comparisons can only be made between data sets obtained either simultaneously or within a few days of each other. The multichannel system also supports the measurement of vascular function in a range of species, vascular networks and experimental conditions, such as function with/without the endothelium or pharmacological inhibitors, and so forth (184).

However, there are several limitations. The isolation and mounting procedures are fiddly, error-prone processes and can easily result in damage to artery segments, impacting vessel functionality. Thus, sufficient training is required. Furthermore, other techniques exist with improved sensitivity such as pressure myography (185), which is further discussed below in section 5.4.1.1. Yet, the main disadvantage is that inherent vascular function as measured by wire myography may not be an accurate reflection of function *in vivo*. This could be due to the exclusion of many important stimuli mediating artery reactivity, such as chemicals, the mechanical stress of blood flow or the ‘conduction’ of signals via gap junctions from upstream branches of the

vascular tree (186, 187). For example, the surrounding perivascular adipose tissue (PVAT) is a major source of vasoactive agents and thus plays a critical role in contractility (188). Consequently, vessel integrity and function may not be preserved when transferred to the wire myograph system.

5.4.1.1 Comparison to pressure myography

Pressure myography is an alternative *ex vivo* technique to wire myography in which artery segments are maintained under isobaric conditions. In this case, artery segments are transferred to a perfusion chamber and cannulated using glass micropipettes connected to a pressure regulator. This way, intraluminal pressure can be adjusted whilst the vessel is continuously perfused with salt solution and vessel diameter can be visualised (189). Pressure myography solves most of the drawbacks of wire myography in that it incorporates the additional variable of pressure. This allows for the measurement of pressure-induced changes such as the myogenic response, as well as the influence of vasoactive drugs on arterial diameter (189). As a result, contractile responses to ANGII have been detected in mesenteric arteries using pressure myography, which were not seen using wire myography (190).

The wire myograph system (DMT, Denmark) was used in this thesis as the equipment and expertise were readily available in the Centre, and it appropriately addressed the chapter aims.

5.4.1.2 Renal artery function after 3 days of high salt with wire myography

In this chapter, near-identical vasodilatory responses were observed in renal arteries from mice fed the SSD or the HSD for 3 days. The maximal efficacy, however, expressed as %Relax reached 38.7 ± 9.1 and 43.2 ± 9.7 for ACh, and 39.3 ± 10.4 and 41.6 ± 8.8 for SNP, respectively. This illustrates that a substantial amount of PhE-induced tension remained. Although we are unable to directly compare data sets, %Relax values after 1 week HSD were a lot lower at 11.6 ± 14.3 and 2.7 ± 23.6 for ACh and 21.4 ± 15.5 and 20.9 ± 10.1 for SNP, respectively. Based on prior experience with renal artery read-outs using wire myography on the SSD, %Relax >38 for renal arteries is

abnormal and suggestive of vessel damage. ACh relies upon the endogenous production of endothelial NO, whereas SNP is a NO donor. Neither generated a %Relax <38 after 3 days of either the SSD or the HSD, implying that both the responsiveness of the endothelium and the VSM was affected. Due to this, the effect of dietary salt upon renal artery function cannot be distinguished with confidence at this time-point.

5.4.2 Impaired vasodilatory responses to high dietary salt intake

Vascular dysfunction generally refers to the defective or absent response of arteries to stimuli, usually characterised by reduced NO bioavailability, thus resulting in impaired vasodilation.

5.4.2.1 Endothelium-dependent vasodilation

NO is an important regulator of normal vascular tone and BP. It is synthesised by the endothelium via the conversion of the dietary amino acid L-arginine by the endothelial-specific enzyme isoform eNOS (Figure 5.9). Upon release, NO acts against VSM contraction, causing a decrease in tone and hence vasodilation. Its production is stimulated by chemicals such as hormones, or by shear stress evoking the FMD response (191, 192).

One such chemical utilised to experimentally interrogate endothelium-dependent mechanisms of vasodilation is ACh. It acts via endothelial muscarinic receptors to stimulate the synthesis of NO and override the VSM response, inducing relaxation. Increased dietary salt has been reported to decrease NO production and consequently blunt relaxation originating from the endothelium (193-195). Researchers have noted impairments in ACh-induced vasodilation following short-term high salt diets, which is an abnormal response similar to that evoked by the suppression of NO signalling (196-198). For example, the vasodilatory responses of skeletal muscle arterioles induced by the administration of ACh were diminished following high dietary salt intake (7% NaCl) in C57BL6/J mice (193). In humans, the FMD response can be evaluated in the brachial artery by measuring Doppler shift with an ultrasound transducer and has found to be reduced following salt loading (101).

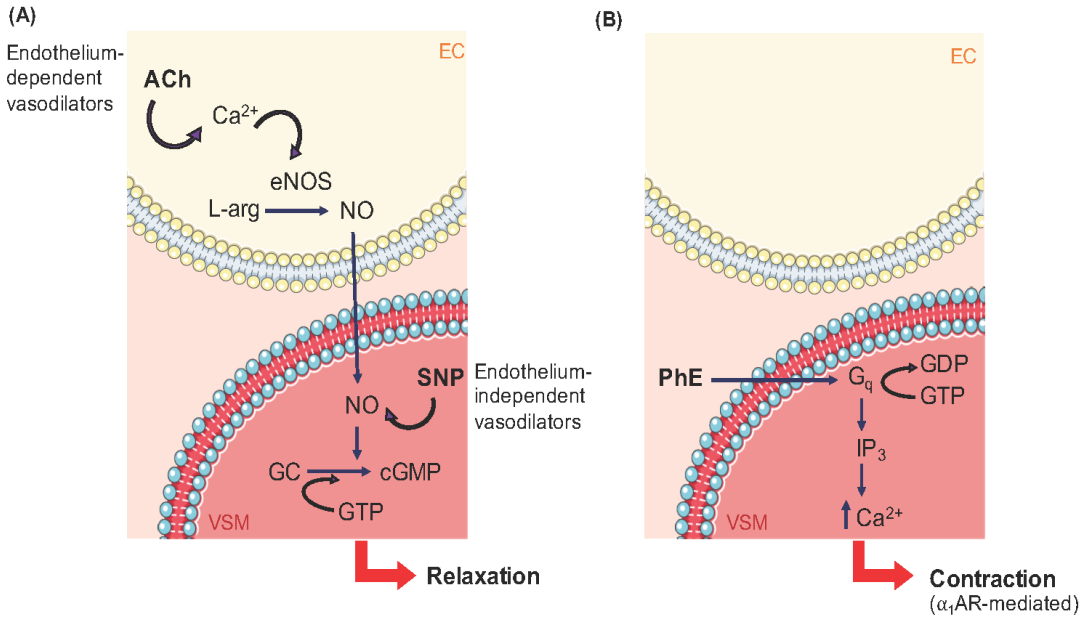

Figure 5.9: Vascular signalling pathways underlying vasoconstriction and dilation.
Schematic diagrams depicting the mechanisms underlying the (A) vasodilatory and (B) contractile responses elicited by the pharmacological agents acetylcholine (ACh), sodium nitroprusside (SNP), and phenylephrine (PhE). Endothelium-dependent vasodilators, such as ACh, stimulate calcium-mediated conversion of L-arginine (L-arg) to nitric oxide (NO) facilitated by the enzyme endothelial nitric oxide synthase (eNOS). NO diffuses from the endothelial cell (EC) to the vascular smooth muscle (VSM) layer, in which it provokes relaxation through activation of guanylyl cyclase (GC). Endothelium-independent vasodilators, such as SNP, are NO donors and so activate GC and thus relaxation without endothelial involvement. PhE elicits vasoconstriction via the α_1-adrenergic receptor, a G_q-coupled receptor. Subsequently, inositol 1,4,5-triphosphate (IP_3) is produced via the hydrolysis of phospholipase C and proceeds to activate downstream calcium signalling, evoking contraction of the VSM layer. cGMP; cyclic guanosine monophosphate, GTP; guanosine triphosphate, GDP; guanosine diphosphate.

Previous studies have noted an influence of salt on NO bioavailability, eNOS uncoupling and the generation of oxidative stress as mechanisms implicated behind these salt-induced vascular effects. We investigated this by interrogating functional responses to endothelium-dependent vasodilation via ACh and the underlying transcriptional profile by qPCR. Mesenteric artery function was unaffected by the group receiving the ten-fold increase in dietary sodium content, as similar vasodilatory responses to ACh were observed between the SSD and HSD arteries. This was reflected in the expression of key components of vascular signalling pathways, such as eNOS. Here, similar eNOS mRNA levels were observed after the SSD and the HSD, suggesting that the expression was not altered by dietary salt in

these mice. Various other mechanisms regulate eNOS activity and the resulting NO production. For example, eNOS is regulated through the phosphorylation of Ser-1179 which governs its functionality and location within the cell, as well as through the phosphorylation of Thr495/Tyr-657 by a shift in the redox status quo, leading to the uncoupling of eNOS mediated by NADPH oxidases (199, 200). A major contributory event is the reduction in tetrahydrobiopterin (BH4), which has been noted within both hypertension and salt-sensitivity (108, 201). Mice lacking the synthesis enzyme GTP-cychohydrolase-1 have negligible amounts of BH4, increased ROS and as a result, endothelium-dependent vasorelaxation is impaired in mesenteric arteries (202).

5.4.2.2 Endothelium-independent vasodilaton

Researchers also assess the responsiveness of the VSM to NO by administering sources of exogenous NO, thus circumventing the input of the endothelium. This stimulates soluble guanylate cyclase and evokes cGMP-dependent vasodilation (Figure 5.9). The NO donors in research and clinical use consist of nitroglycerin, SNP and isosorbide mononitrate (203). Therefore, if impaired vasodilatory responses to ACh are observed, the interrogation of responses using NO donors can determine whether the functional defect is localised to the endothelium or not.

Similar vasodilatory responses to the NO donor SNP were evoked in both mesenteric and renal arteries regardless of dietary group in this experiment. This illustrates that VSM responsiveness to NO is unaltered by dietary salt, an observation that has been made by other researchers in the field. For example, Sylvester *et al*., noted that a high salt diet (4% NaCl) diminished vasodilation in rat cerebral arteries evoked by ACh but not by SNP (194), thus confirming that the salt-induced impairment was originating from the endothelium.

5.4.3 Vasoconstriction in renal arteries following high dietary salt

Aberrantly increased vasoconstriction is a functional change associated with hypertension. Ordinarily, contraction can be induced intrinsically by the autoregulatory myogenic response or through stimulation by extraneous signals such as circulating adrenaline or input from SNS innervation. An abnormal reduction in luminal diameter could be consequence to a number of processes, such as VSM hyper-sensitivity to these extraneous stimuli, impaired endothelial function or heightened myogenic responsiveness, all of which have been noted in experimental hypertension.

In this work, the vasoconstrictor responses of mesenteric arteries from C57BL6/JCrl mice accompanying increasing BP (3 days HSD) and established high BP (1 week HSD) were unaffected by dietary salt. Conversely, renal artery sensitivity to PhE increased after 1 week of high dietary salt intake whilst contractile responses to the high potassium solution, KPSS, were not different. This suggests an impact of high dietary salt upon the intrinsic ion-channel-mediated mechanisms within these renal arteries is unlikely, thus implying that those facilitated by receptor signalling upstream may be affected by dietary salt and so could be accountable for the enhanced sensitivity. A variety of events could possess a consequential role. Since PhE acts through α_1-ARs (Figure 5.9), an increase in α_1-AR density or ligand affinity, or an impairment in the β_2-AR-induced vasodilation which offsets α_1-AR constriction could be occurring. Further investigations would be necessary to pinpoint the causative agent and hence define the nature of these salt-induced effects on renal artery function.

A)

Report Name: RA 7HSD nanodrop Report Full Mode: Ignore

Sample ID	User ID	Date	Time	ng/ul	A260	A280	260/280	260/230	Constant	Cursor Pos.	Cursor abs.	340 raw
210, 211 RA	Default	25/07/2019	22:01	7.35	0.184	0.129	1.43	0.43	40.00	230	0.431	0.103
208, 209 RA	Default	25/07/2019	22:02	6.09	0.152	0.095	1.61	0.47	40.00	230	0.326	-0.008
216, 217 RA	Default	25/07/2019	22:02	7.76	0.194	0.127	1.53	0.73	40.00	230	0.266	0.040
212, 213 RA	Default	25/07/2019	22:03	10.36	0.259	0.163	1.59	0.64	40.00	230	0.404	0.134
204, 205 RA	Default	25/07/2019	22:03	18.95	0.474	0.273	1.74	0.45	40.00	230	1.042	0.338
206, 207 RA	Default	25/07/2019	22:04	36.87	0.922	0.614	1.50	0.66	40.00	230	1.394	1.423
200, 201 RA	Default	25/07/2019	22:05	3.17	0.079	0.052	1.53	0.46	40.00	230	0.173	-0.030
214, 215 RA	Default	25/07/2019	22:05	4.84	0.121	0.090	1.35	0.40	40.00	230	0.300	0.022
202, 203 RA	Default	25/07/2019	22:06	4.89	0.122	0.073	1.66	0.53	40.00	230	0.230	0.045
218, 219 RA	Default	25/07/2019	22:06	6.24	0.156	0.069	2.27	0.58	40.00	230	0.269	0.031

B)

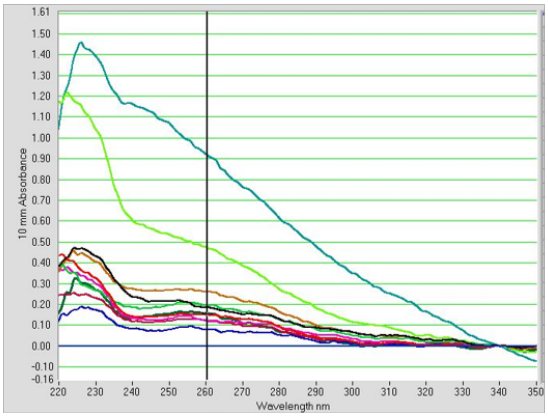

C)

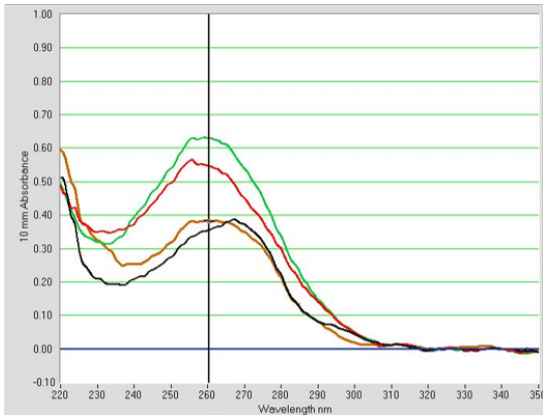

Figure 5.10: Renal artery RNA purity report and plot.

Renal arteries were dissected from C57BL6/JCrl mice (n=10 per dietary group, pooled to n=5) after either 1 week of a high salt or a standard salt diet. RNA was extracted and purity was assessed by the Nanodrop 1000 spectrophotometer (ThermoScientific, UK). A) Numerical report generated after analysis. The red boxes highlight the poor yield (ng/uL) and the sample A260/280 ratio below 1.7. Plots of wavelength vs absorbance are illustrated for the renal arteries (B) and the successful RNA isolation of the mesenteric arteries (C) as a comparison.

5.4.4 Effect of high dietary salt on vascular mRNA expression profile

5.4.4.1 Extracting RNA from small arteries

The isolation of RNA from small blood vessels, such as mesenteric and renal arteries, from mice presented as a significant challenge. Successful isolation of a sufficient quantity and purity of RNA is determined by a sample A260/280 ratio of between 1.7 and 2.2, as assessed by the Nanodrop 1000 spectrophotometer described in Materials & Methods section 2.4.2. In order to maximise RNA yield, arteries from two mice were pooled. This was effective for mesenteric arteries as a satisfactory RNA yield was obtained, and A260/280 ratios ranged 1.7 – 1.9.

Unfortunately, a sufficient yield and quality of RNA could not be successfully isolated from renal arteries using this method. Figure 5.9 displays a report and absorbance plot produced following spectrophotometric analysis of RNA isolated from renal arteries. As can be seen, a poor yield was attained and each sample A260/280 ratio was outside the previously defined range for 'pure' RNA. The peak of each spectrum does not occur at A260nm, but is shifted far to the left instead, further evidence of contaminants or an extremely low concentration of RNA. Due to time and budget constraints, I was unable to carry out further protocol optimisation and apply purification and/or amplification kits to rectify this for my thesis.

5.4.4.2 Statistical analysis

The initial question to ask of a data set is whether it follows the normal distribution or not, as this determines whether parametric or nonparametric testing is required. Normality tests are available to aid this decision. If a data set fails a normality test, it is likely distributed differently or skewed. Since biological samples can follow a lognormal distribution, data can be transformed and normality re-tested. On the other hand, nonparametric testing can be employed in which assumptions are not made about distribution. An advantage of utilising a nonparametric test is that it helps avoid the risk of misconstruing an experimental outcome. However, it has less statistical power compared to parametric testing and an increased likelihood of making a type I error, i.e missing a potentially important observation.

Results generated from qPCR analysis can leave us at a crossroads. Establishing normality can be problematic due to the small number of biological replicates. In this case, n=4-5 and the Shapiro-Wilk normality test was inconclusive, an outcome that was unaffected by log-transforming the data. Thus, the distribution was uncertain. Initially, parametric testing in the form of a one-way ANOVA was executed and group means compared. This generated $P<0.05$ for the effect of diet on the mRNA expression of NADPH oxidase 2 ($P=0.019$; Figure 5.8 G). Upon performing a Kruskal-Wallis

nonparametric test in which the medians of each group were compared, $P<0.05$ was also generated ($P=0.011$). This illustrates that significance is preserved despite the test used and that either is an appropriate measure of central tendency for this data set, whether normal or skewed. Hence, parametric testing was utilised, and further parameters were taken into consideration upon whether biological significance was also apparent, as described below.

5.4.5 Statistical significance vs biological significance

The purpose of statistical testing is to aid scientists in the determination of whether an experimental result or difference is due to a random occurrence or not. The *P* value is the probability of the difference occurring solely by chance in the population the data was sampled from, i.e if the groups compared genuinely are not different. Nowadays, $P<0.05$ is generally considered as interchangeable with the phrase 'statistically significant', however it is not necessarily implying something of biological importance (204, 205).

Occasionally in this chapter, *P* values are reported beyond the statistical threshold of 0.05, for example $P=0.031$ was generated by a two-way ANOVA for the difference between dietary groups in the renal artery response to SNP. This is suggesting that the probability of a difference occurring due to high dietary salt intake is not due to chance, however it does not simply infer biological significance as well. In order to conclude that a biologically significant effect is occurring, additional information must be considered. It is a complex process that is very much reliant upon interpretation as well as the application of the physiological context. In this case, other measures such as $\log IC_{50}$ and %Relax were evaluated, as well as the visual representation of the data sets in a graph along with previous experience of the results generated by this technique and from these arteries. In this case, SNP is a NO donor and so induces vasodilation by circumventing the endothelium and interacting with the VSM. A *P* value of <0.05 is potentially implying that the sensitivity of the VSM to NO is different in the high salt group. If, in fact, a

meaningful, biological effect of high dietary salt upon renal arteries was occurring, the difference would also be reflected within the ACh-induced vasodilatory response as this is also reliant upon VSM sensitivity to NO. In this case, it is not (*P*=0.351, Figure 5.7 F). Due to the reasons outlined above, some of the small but statistically significant differences generated by one or two-way ANOVA in this chapter have been concluded not to represent a biologically important effect.

5.4.6 Does vasodysfunction contribute to the salt-induced increases in BP of C57BL6/JCrl mice?

It is important to consider the role the different artery types play in the regulation of BP. Vasodysfunction contributing to high BP has been noted within both the macro- and microcirculation (206), suggesting a shared, systemic input. However, small resistance arteries possess the ability to adjust their luminal diameter to regulate blood flow and pressure to downstream tissue; they contribute to 45-50% of SVR (183). With such a high proportion of SVR determined by these arteries, any alterations to their structure or function tend to be reflected within SVR and so, as a result, are deemed to have the most influential impact upon BP (207). Previous studies have found resistance artery dysfunction in hypertension, for example elevated vasoconstriction (208).

Despite this, the contribution of larger arteries to BP control must not be overlooked. An essential function of large, conduit arteries is to stifle the pulsatile flow and pressure of the blood before it arrives at the smaller branches of the arterial system, protecting them from barotrauma (207). This is particularly important for the kidneys, which possess an additional level of control. Blood entering the kidneys through the renal arteries is subject to intense autoregulation in order to shield the fragile capillaries of the glomerulus and the renal microcirculation. Elevations in pressure trigger preglomerular arterial vasoconstriction resulting from the innate myogenic response of arteries. This acts in conjunction with the TGF response, which utilises signals regarding the sodium chloride load of the filtrate to refine or

counteract the contraction (175). Increased pressure and activation of this response stimulates PN, leading to diminished tubular sodium reabsorption and increased excretion (165). Thus, the result is autoregulated vascular as well as tubular function. High pressures can induce glomerular injury and adversely affect renal filtration capacity, which support further injurious changes to BP and entry into a detrimental cycle. Therefore, the renal arteries and their capacity to autoregulate in response to pressure and flow is essential.

Morris *et al*.'s model (92) describes abnormally increased SVR in salt-sensitivity upon salt loading. As resistance arteries account for a large proportion of SVR, mesenteric arteries were assessed in this thesis. However, mesenteric artery function was not different after the HSD, as similar vasoconstrictor and vasodilatory responses were observed between arteries after the SSD and the HSD. eNOS expression levels also were unaffected. A modest downregulation was observed in the expression of NADPH oxidase subunit 2 following 1 week of increased salt intake; however, this was not accompanied by abnormal vasodilatory responses to ACh at this time-point. It is unclear as to why the data here differ from that reported within the literature. Evidence of the adverse effects of dietary salt are reported within a range of conditions, in those that are: salt-sensitive and salt-resistant; hypertensive and normotensive; healthy and with chronic disease. It illustrates that dietary salt has a detrimental impact on vascular health regardless of BP, but the underlying processes are complex and yet to be clearly elucidated. Here, I did not find any impact of high dietary salt upon the vasodilatory responses of mesenteric and renal arteries in C57BL6/JCrl mice and thus reject the above hypothesis.

On the other hand, renal arteries were more sensitive to PhE after 1 week of high dietary salt intake, suggesting that, rather than impaired vasodilation, aberrant renal vasoconstriction may contribute to the salt-sensitive BP of C57BL6/JCrl mice. A number of systemic signalling systems, such as the RAAS and the sympathetic nervous system (SNS), partake in the regulation

of renal and vascular function and excessive activity of both have been previously noted in salt-sensitivity (57, 209). Therefore, the contribution of these will be interrogated as possible drivers of vasoconstriction and salt-induced hypertension in these mice.

5.4.7 Summary of results

1. Mesenteric artery reactivity did not differ with high dietary salt intake as compared to standard salt intake. Vasoconstrictor and vasodilatory responses were similar between the dietary groups.
2. Increased sensitivity of renal arteries after 1 week of high dietary salt intake was observed to the vasoconstrictor phenylephrine.
3. No significant differences were observed in the vascular transcriptional profile of C57BL6/JCrl mice after high dietary salt intake, compared with the standard salt intake.

6 Electrolyte Balance and Neurohormonal Regulation of Salt-Induced Hypertension in C57BL6/JCrl Mice

6.1 Introduction

Multiple systems are involved in the regulation of renal and vascular function and overall BP. Initially, increases in dietary salt intake induce a physiological imbalance, which can affect BP. Most of these neurohormonal and endocrine systems are suppressed by increased salt intake in order to combat this imbalance and restore equilibrium. However, abnormally elevated activity of multiple components of these systems has been identified in salt-sensitivity.

One such system is the sympathetic nervous system (SNS), which is a branch of the involuntary autonomic nervous system. Activation results in an extremely rapid and synchronised action referred to as mass sympathetic discharge – more commonly known as the 'fight-or-flight' response, which increases BP. Neuroeffector junctions connect sympathetic nerve terminals to effector tissues. This enable the regulation of tissue function directly via the release of the neurotransmitter noradrenaline, or indirectly via the release of catecholamines from the adrenal medulla into the circulation. These consist of both noradrenaline and adrenaline. Sympathetic nerve activity is transduced by α- and β-ARs localised to the neuroeffector junction or postganglionic nerve terminals. Binding to ARs triggers downstream G-protein-dependent second-messenger systems, for example α_1-AR on the VSM induces vasoconstriction. SNS over-activity been implicated in the salt-induced effects observed in salt-sensitive humans with hypertension (209).

In this chapter, salt and water balance were assessed along with the status of the SNS and the RAAS in response to high salt intake.

6.1.1 Aims

- To measure water and sodium homeostasis in C57BL6/JCrl mice before and after increasing dietary salt intake.
- To decipher the effect of high dietary salt intake on the circulating concentrations of aldosterone, an indicator of RAAS activity.
- To interrogate the status of the SNS after high dietary salt intake and its contribution to the salt-induced BP effects observed in C57BL6/JCrl mice.

6.1.2 Approach to achieve the chapter aims

- Water and sodium intake and excretion were investigated whilst mice were singly housed in metabolic cages. Urine and faeces were collected at 24-hour time-points to observe the day-to-day effects, and 12-hour time-points to observe day-night variation.
- Circulating concentrations of aldosterone were determined in the plasma of mice using an ELISA kit.
- SNS activity was initially evaluated by measuring the urinary excretion of the catecholamines adrenaline and noradrenaline by ELISA. Its contribution to the BP effects observed in chapter 3 was then examined by acutely administering the inhibitor hexamethonium whilst BP was measured by radiotelemetry.
- The effect of dietary salt intake on excretion and BP was investigated by taking measurements before (SSD) and after the HSD for 3 days, 1 week and 2 weeks. The exception was upon measuring plasma aldosterone concentration, for which separate dietary groups were used.

6.2 Methods

The procedures performed to obtain the results in this chapter are described in detail in the main Materials and Methods chapter. Specific experimental details, mouse cohorts and the timelines assessed are presented below.

6.2.1 Metabolic cage experiments

6.2.1.1 24-hour studies

In the first experiment of this chapter, a single cohort of male C57BL6/JCrl mice aged 10 weeks (n=7) were placed individually in specialised cages that enabled the monitoring of fluid and diet intake as well as the collection of urine to measure electrolyte excretion. This cohort was housed continuously in the metabolic cages. The effect of high dietary salt on water and sodium intake and excretion was investigated using a repeated measures study design in which mice were given access to the SSD for 1 week before being transferred to the HSD for a further 1-week period. Measurements were obtained every 24-hours between 7-10AM before and after dietary manipulation. Urinary sodium and water excretion were determined, and balance was calculated.

Since research mice are generally accustomed to living in groups within standard caging, accommodating them in metabolic cages can act as a stressor which can impact cardiovascular function (129). Consequently, mice were placed in the cages five days prior to the beginning of the experiment for them to habituate to the set-up. This acclimatisation process was monitored through body weight (Figure 6.1), in which weight initially dropped within the first 2 days in some of the mice, as indicated by the purple arrow. Following this, body weight normalised after the 5 days and remained relatively stable at the beginning of the experimental period.

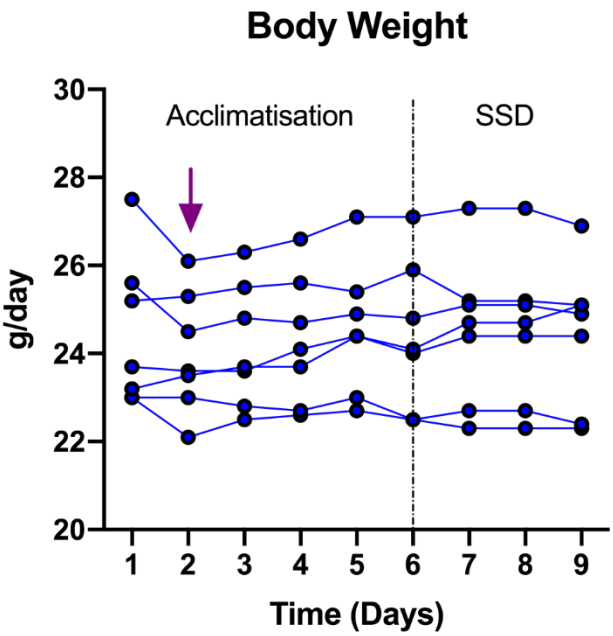

Figure 6.1: Acclimatisation of C57BL6/JCrl mice to metabolic cages via tracking body weight. Body weight was monitored as an indicator of the familiarisation of C57BL6/JCrl mice to being housed in the metabolic cages. This graph depicts body weight (g per day) during a 5-day acclimatisation period followed by the beginning of the experiment in which measurements were taken on the standard salt diet (SSD; days 6-9 on this graph). The arrow indicates an initial dip in body weight which normalised over the following days.

6.2.1.2 12-hour studies

Follow-up experiments were carried out to investigate day-night variability in water and sodium intake and excretion. To achieve this, a separate cohort of 12-week-old male C57BL6/JCrl mice (n=7-9) were placed in metabolic cages for 24-hours at a time at the following time-points: on day 7 of the SSD, on day 3 of the HSD, and then on day 7 of the HSD. This enabled the collection of 12-hour urine samples for the daytime (7AM-7PM) and the night-time (7PM-7AM). The diurnal regulation of urinary sodium and catecholamine excretion was assessed from these samples, with the effect of high salt intake upon this measured via administering the HSD.

6.2.2 Measuring plasma aldosterone concentration

In these experiments, aldosterone concentration was determined via ELISA in plasma samples (Methods 2.7). The chosen kit required 50 µL of plasma, which is a substantial volume from small animals such as mice. To obtain a

sufficient volume of plasma for this, mice were culled by decapitation using a guillotine by the manager of the Centre's *in vivo* Physiology Laboratory Mr Kevin Stewart or Dr Celine Grenier, both of whom were experienced in the procedure. Therefore, a cross-sectional design was used due to the terminal nature of this blood sampling technique.

Three separate time-points were assessed in 10-12-week-old male C57BL6/JCrl mice: 3 days HSD (n=7), 1 week HSD (n=10) and 2 weeks HSD (n=8). These were compared to contemporaneous controls receiving the SSD (n=7-10).

6.2.3 Acute pharmacological blockade of the sympathetic nervous system activity during blood pressure measurement

The ganglionic blocker hexamethonium was administered acutely during radiotelemetry to a third cohort of C57BL6/JCrl mice (n=7) before and after the HSD. This was to explore the role of the SNS in the salt-induced effects on BP observed in chapter 3, by transiently inhibiting it and measuring the BP response.

Following the set-up and implantation of telemeter devices (Methods section 2.2), BP was recorded by radiotelemetry in 9-12-week-old male mice as detailed in Figure 6.2. A dose of 30mg/kg (210) was introduced via intraperitoneal injection (IP) between 8 and 9AM on three occasions: after 1 week of baseline measurements on the SSD, at 1 week of the HSD and lastly at 3 weeks of the HSD (Figure 6.2). Throughout the majority of the experiment, the telemeter devices were set to record BP over one minute every half an hour. On the mornings of the IP, this was adjusted to measure BP continuously to observe the effect of the compound, as it is reported to have a half-life of 20 minutes (210).

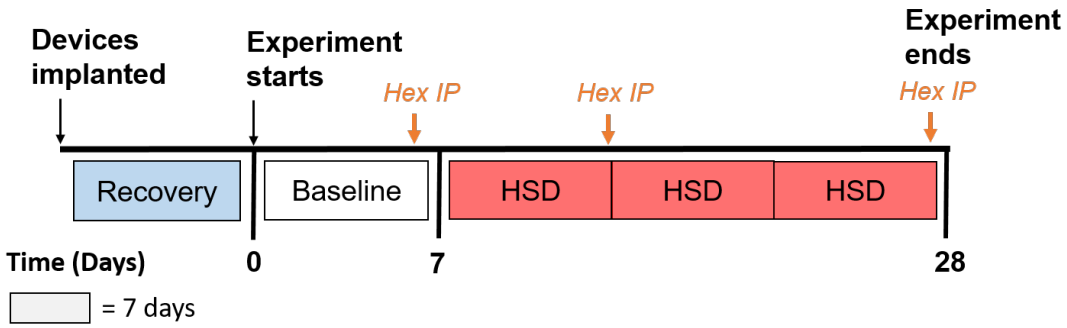

Figure 6.2: Timeline for radiotelemetry experiment with hexamethonium injections.
Radiotelemeter devices were inserted into anaesthetised C57BL6/JCrl mice (n=7; 9-12 weeks old). Following a recovery period of 1 week, baseline measurements of BP were obtained from mice fed a standard salt diet (0.25% Na) for a further week. Mice were then fed a high salt diet (HSD; 3% Na) for the remainder of the experimental period (3 weeks). Intraperitoneal injections (IP) of the ganglionic blocker hexamethonium (hex) were administered on three different occasions: at the 1 week time-point of baseline, at 1 week of the HSD, and finally at 3 weeks of the HSD. The rectangular boxes illustrate 7-day periods. The BP response to this blockade was measured.

6.2.3.1 Data analysis

BP data was plotted minute-by-minute for each mouse over a period of 2 hours and 30 minutes (usually between 8AM and 11AM) to visualise the response to hexamethonium (Figure 6.3). A pre-IP baseline was determined by averaging the BP data collected 1 hour prior to each injection. Since the effect of SNS inhibition is reportedly antihypertensive, the negative peaks were included in the area under the curve (AUC) analysis performed in Graphpad prism v8.2.0. Cessation of the effects of hexamethonium and recovery of BP was concluded upon the return of BP to the pre-IP baseline level.

Four parameters were extracted from the data (Figure 6.3):

1. The peak occurring upon IP (mmHg)
2. The maximum drop in BP (mmHg)
3. The time taken to recover (mins)
4. The area of the negative peak (AUC).

Repeated measures one-way ANOVA was utilised to compare the three time-points, with *P* values corrected for multiple comparisons via Tukey testing.

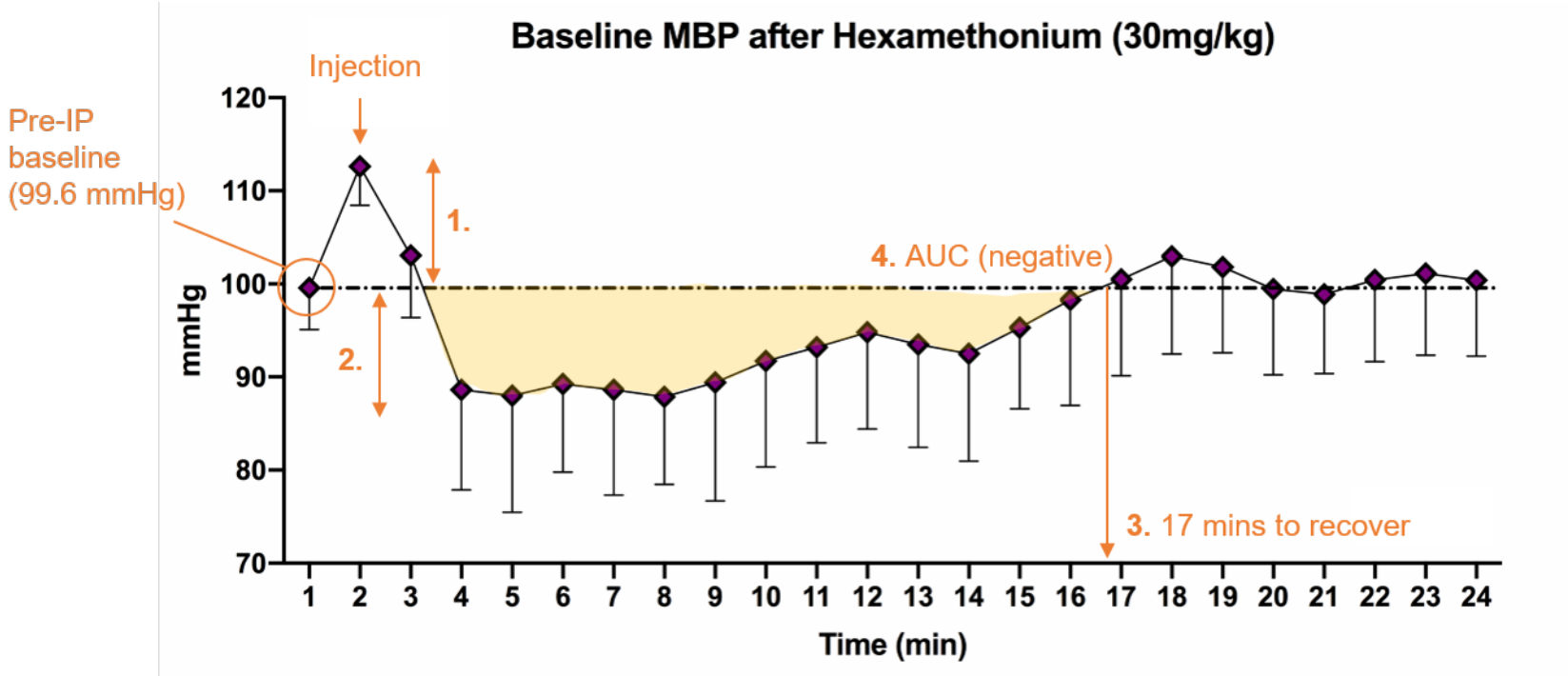

Figure 6.3: Example of analysis of the BP effects of acute sympathetic nervous system blockade.

Mean blood pressure (MBP) was assessed by radiotelemetry in C57BL6/JCrl mice. After 1 week of a standard salt diet, an intraperitoneal injection (IP) of the sympathetic nervous system inhibitor hexamethonium (30mg/kg) was administered. This graph depicts the resulting MBP trace from an individual mouse and illustrates the method used to extract data on the effects of hexamethonium. The horizontal dashed line indicates the pre-IP baseline level. 1: The rapid rise in BP during injection. 2: The degree to which BP is lowered. 3: The time taken for BP to return to pre-IP baseline levels (99.6 mmHg here). 4: Area under the curve (AUC) analysis.

6.3 Results

6.3.1 Body weight and diet intake during high salt intake

Figure 6.4 A & B depict the effects of the HSD on body weight. Mice were maintained at 24.2 ± 0.4 g whilst on the SSD in the metabolic cages and, on average, displayed a 4.4 ± 3.9 % increase in body weight during this week. Whilst receiving the HSD, body weight significantly declined to 22.7 ± 1.7 g after 3 days (P=0.0009 compared to the SSD) and to 22.4 ± 1.4 g at the 1-week time-point (P<0.0001; Figure 6.4 B). Overall, mice illustrated a -3.6 ± 2.1 % change in body weight across the week of receiving the HSD.

On the SSD, mice consumed an average of 4.2 ± 0.4 g per day (g/24-h). On the HSD, consumption was slightly decreased but not significantly different at 3.6 ± 0.9 g/24-h after 3 days (P=0.124) and 3.9 ± 0.5 g/24-h after 1 week (P=0.401) compared to intake of the SSD (Figure 6.4 C & D).

The HSD had a significant effect upon faecal output in these mice. During 1 week of the SSD, 1.6 ± 0.2 g was collected per day. This decreased dramatically during the first 24 hours of the HSD (Figure 6.4 E). After 3 days of the HSD, faecal output was significantly lower at 0.3 ± 0.1 g/24-h (P <0.0001) compared to output during the SSD. This remained constant at 0.3 ± 0.1 g/24-h at the 1 week time-point of the HSD (P <0.0001; Figure 6.4 F). These results show that the HSD reduced faecal output in C57B6/JCrl mice within the first few days, which did not change throughout the rest of the week.

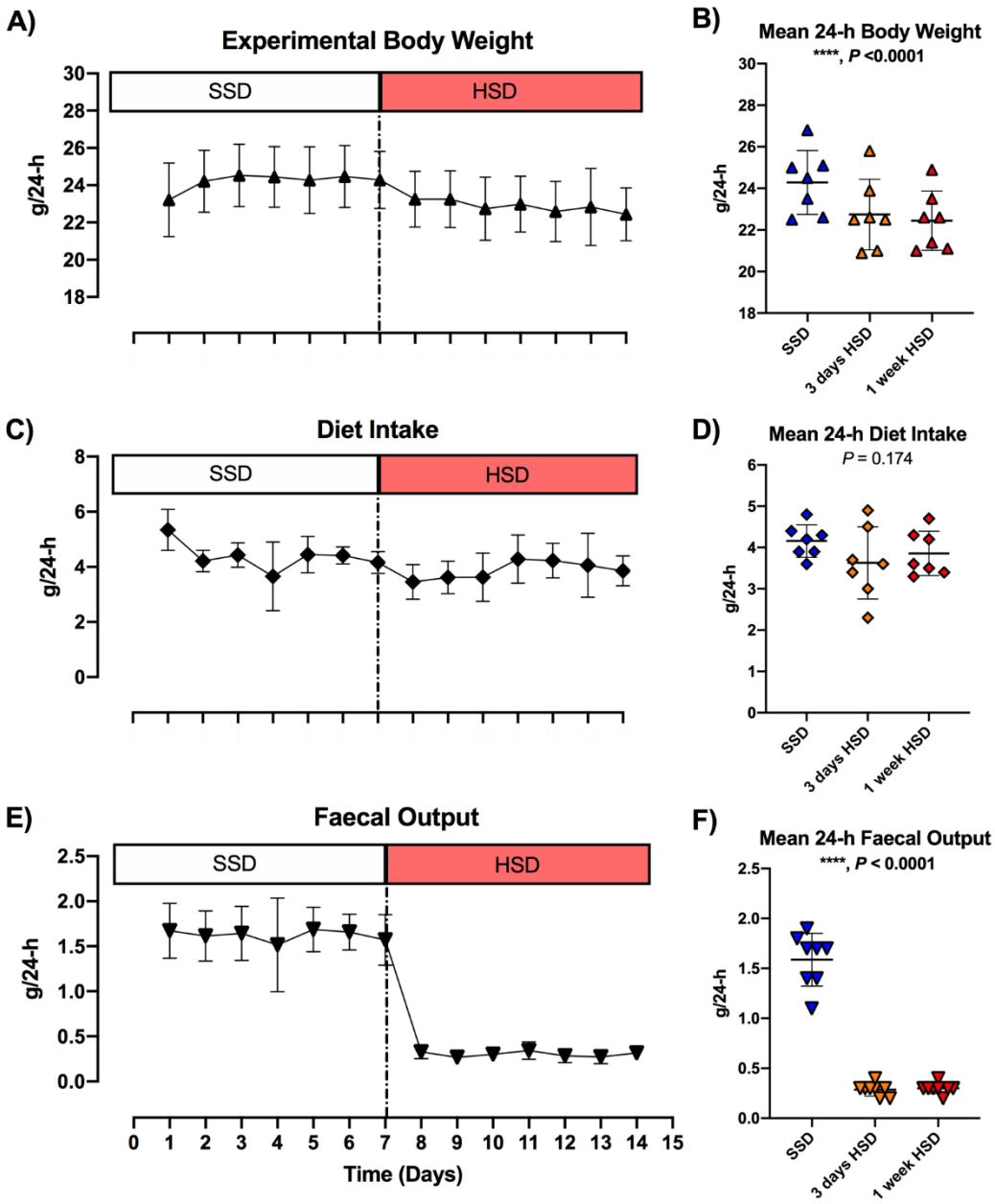

Figure 6.4: Daily (24-hour) body weight, diet intake and faecal output during high salt feeding.
Male C57BL6/JCrl mice (n=7) were maintained on a standard salt diet (SSD; 0.25% Na) for 1 week, before being transferred to a high salt diet (HSD; 3% Na) for a further week whilst housed individually in metabolic cages. An acclimatisation period of 5 days preceded 24-hourly (24-h) experimental measurements of A-B: body weight (g), C-D: diet intake (g) and E-F: faecal output (g) obtained in the morning (7-10AM). Graphs on the left depict day-to-day means over the 2-week experimental period, whereas graphs on the right depict 24-h means for day 7 SSD and days 3 and 7 (1 week) HSD. Data are mean ± SD and were analysed via one-way repeated measures ANOVA, corrected for Tukey's multiple comparisons testing. P<0.05 for significance.

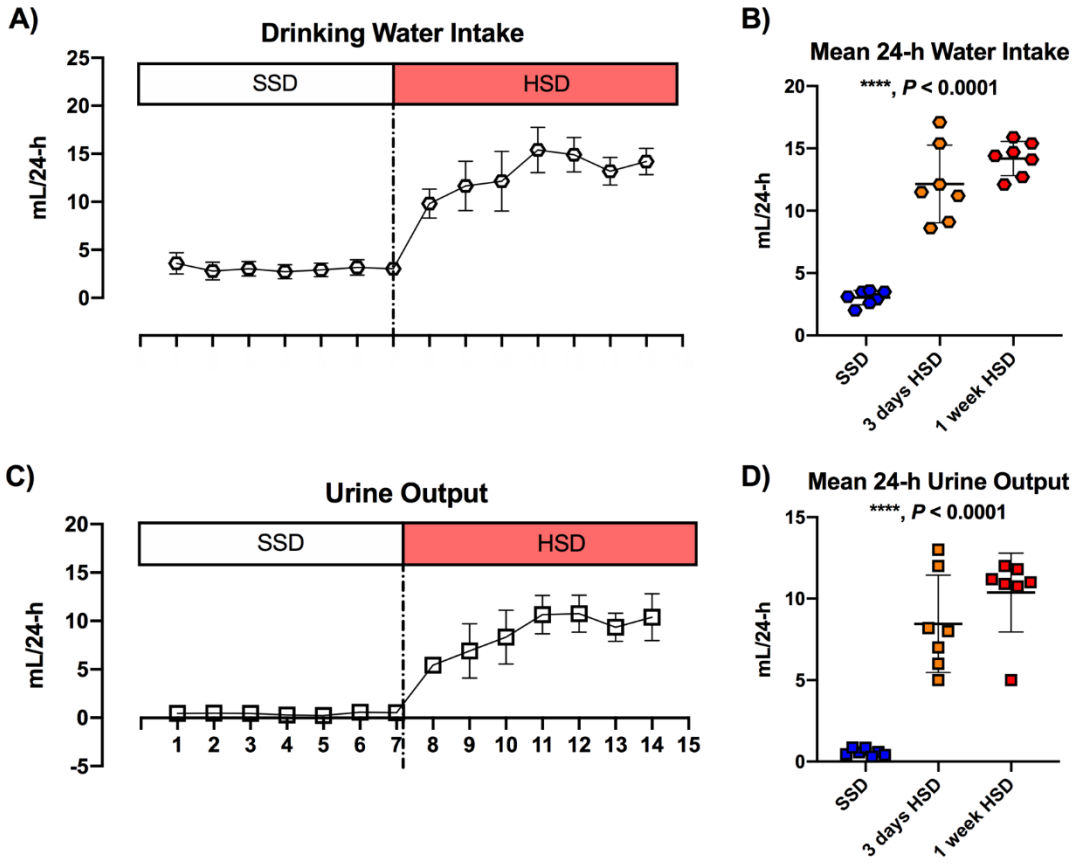

Figure 6.5: Daily (24-hour) water intake and urine output during high dietary salt intake.
Drinking water intake (A-B) and urine output (C-D) were monitored in adult male C57BL6/JCrl mice (n=7) singly housed in metabolic cages. Mice were given access to a standard salt diet (SSD; 0.25% Na) for 1 week, followed by a high salt diet (HSD; 3% Na) for a further week. Measurements were taken every 24 hours (24-h) between 7 and 10AM. Data are daily mean ± SD (A, C) and means from 1 week SSD and 3 days and 1 week HSD (B, D). Data were analysed by one-way repeated measures ANOVA corrected for multiple comparisons via Tukey testing.

6.3.2 Effect of high dietary salt intake on water balance

Mice consumed an average of 3.0 ± 0.6 mL drinking water daily over the course of 1 week of the SSD. Upon increasing the sodium content of this diet, mice consumed significantly more of the drinking water (Figure 6.5 A). After 3 days of the HSD, water intake had increased to 12.1 ± 3.1 mL (P=0.0004 compared to the SSD). At 1 week, water intake was significantly higher than that during the SSD (P<0.0001) at 14.1 ± 1.4 mL (Figure 6.5 B). This illustrates that the daily volume of drinking water increased in these mice whilst consuming high dietary salt.

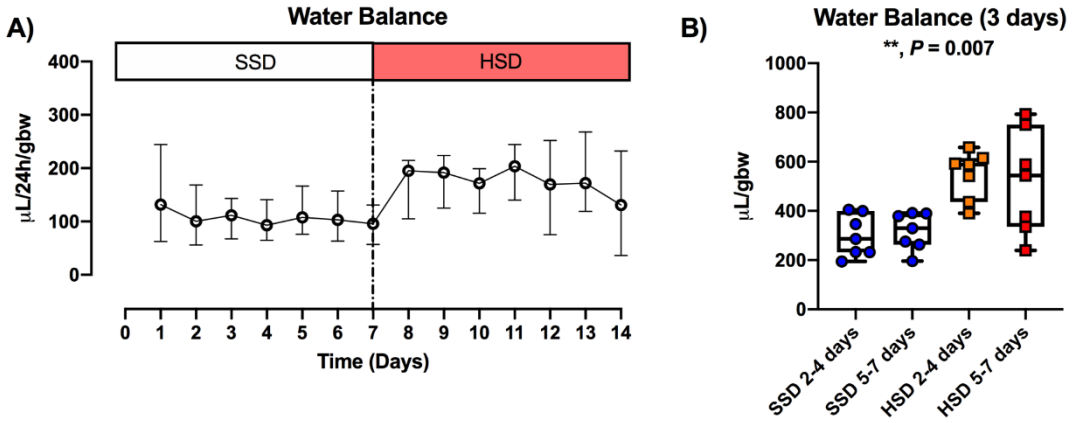

Figure 6.6: Water balance before and after high dietary salt intake.

Adult male C57BL6/JCrl mice (n=7) received a standard salt diet (SSD; 0.25% Na) for 1 week before a high salt diet (HSD; 3% Na) was administered for a further week. Volumes of water intake and urine output were measured whilst housed individually in metabolic cages. Water balance (A) and cumulative water balance over 3-day periods (B) were calculated by subtracting urine volume from the volume of drinking water consumed and expressed as grams of body weight (gbw). Balance data are medians and ranges analysed by Kruskal-Wallis test corrected for multiple comparisons via Dunn's. Significance is denoted as $P<0.05$.

The volume of urine produced, referred to as urine output, also increased on the HSD (Figure 6.5 C). C57BL6/JCrl mice produced a daily average of 0.6 ± 0.2 mL of urine whilst receiving the SSD. This significantly elevated to 8.5 ± 3.0 mL after 3 days of the HSD (P=0.002) and to 10.4 ± 2.4 mL after 1 week (P=0.0002; Figure 6.5 D). Thus, mice produced a higher volume of urine per day whilst consuming increased dietary salt.

Intake and output were used to calculate water balance (Figure 6.6). During the SSD, C57BL6/JCrl mice had a positive water balance, displaying a cumulative median of 287 (Interquartile range; IQR = 232-400) between days 2 and 4 and 330 (IQR = 263-390) between days 5 and 7. This was increased during the HSD, in which cumulative water balance was calculated as 588 (IQR = 436-615) between days 2 and 4, and 544 (IQR = 336-750; Figure 6.6 A & B). Multiple comparisons revealed that water balance after 2-4 days HSD was significantly higher compared to 2-4 days SSD (P=0.023) and 5-7 days SSD (P=0.038). Thus, C57BL6/JCrl mice had a significantly greater water balance within the first few days of receiving the HSD, which remained high in some mice but decreased in others.

Figure 6.7: Daily (24-h) sodium intake, output and balance receiving a high salt diet.

Dietary intake and urinary excretion of sodium (UNa) was monitored in adult male C57BL6/JCrl mice singly housed in metabolic cages receiving a standard salt diet (SSD; 0.25% Na) for 1 week followed by a high salt diet (HSD; 3% Na) for a further week. Measurements were taken every 24 hours (24-h) between 7-10AM. Sodium intake (A-B) was calculated from food intake, and urinary sodium (C-D) via an electrolyte analyser normalised to urine volume. Both measures are expressed as grams per body weight (gbw). Graphs on the left depict day-to-day means, whereas graphs on the right depict 24-h means for SSD, day 3 HSD and 1 week HSD. These are mean ± SD and were analysed via one-way repeated measures ANOVA, corrected for multiple comparisons via Tukey testing. Cumulative sodium balance (E) was calculated from intake and excretion over 3-day periods. Data are median with ranges and analysed via Kruskal-Wallis test with Dunn's multiple comparisons test. $P<0.05$ for significance.

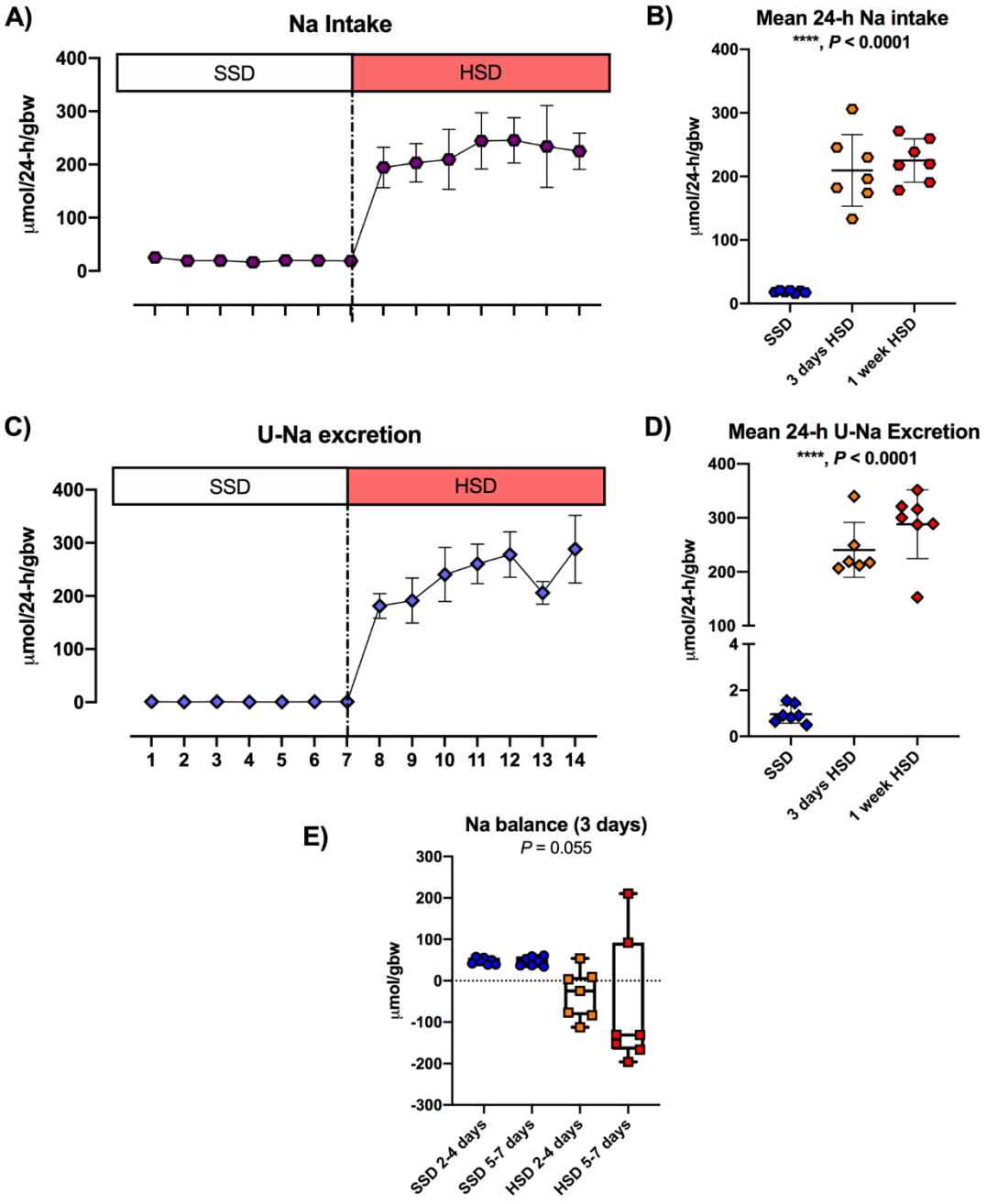
A)
Na Intake
SSD
HSD
µmol/24-h/gbw
400
300
200
100
0
B)
Mean 24-h Na intake
****, P < 0.0001
µmol/24-h/gbw
SSD
3 days HSD
1 week HSD
C)
U-Na excretion
SSD
HSD
µmol/24-h/gbw
1 2 3 4 5 6 7 8 9 10 11 12 13 14
D)
Mean 24-h U-Na Excretion
****, P < 0.0001
µmol/24-h/gbw
SSD
3 days HSD
1 week HSD
E)
Na balance (3 days)
P = 0.055
µmol/gbw
SSD 2-4 days
SSD 5-7 days
HSD 2-4 days
HSD 5-7 days

6.3.3 Sodium handling as dietary salt intake was increased

Figure 6.7 depicts sodium intake, output and balance in C57BL6/JCrl mice during the SSD and the HSD. Throughout 1 week of the SSD, daily average dietary sodium intake was 19.8 ± 1.8 µmol/24h/gbw. This suitably elevated following the administration of the HSD to the same mice (Figure 6.7 A). After 3 days, dietary sodium intake was significantly greater at 209.5 ± 56.3 µmol/24h/gbw (P=0.0002) and remained high after 1 week at 225.0 ± 34.2 µmol/24h/gbw (P<0.0001) compared to intake on the SSD (Figure 6.7 B). This confirms that the mice were ingesting higher amounts of sodium on the HSD.

Sodium output, i.e urinary sodium excretion, was calculated by analysing the sodium concentration in the collected urine. Mice receiving the SSD for 1 week had a daily average sodium excretion of 0.8 ± 0.2 µmol/24h/gbw, which was rapidly increased upon placing them on the HSD. This high level persisted throughout the rest of the high salt experimental period (Figure 6.7 C). During the HSD, sodium excretion increased to 240.6 ± 50.8 µmol/24h/gbw after 3 days (P=0.0002) and 288.2 ± 63.7 µmol/24h/gbw after 1 week (P<0.0001) in contrast to that from these mice during the SSD (Figure 6.7 D). This shows that C57BL6/JCrl mice respond to an elevation in dietary sodium with a rise in urinary sodium expulsion.

Sodium balance, expressed over 3-day periods, is depicted by Figure 6.7 E. Mice have a stably positive sodium balance over the course of the SSD, calculated at 47 (IQR = 39-57) over the days 2-4 and at 47 (IQR = 37-59) over the days 5-7. Upon administration of the HSD for 3 days, sodium balance became highly variable but overall negative, calculated at -25 (IQR = -83-54). This was exacerbated after 1 week, calculated at -131 (IQR = -166-92). The effect of the HSD was not statistically significant, as demonstrated by the Kruskal-Wallis test results (Figure 6.7 E).

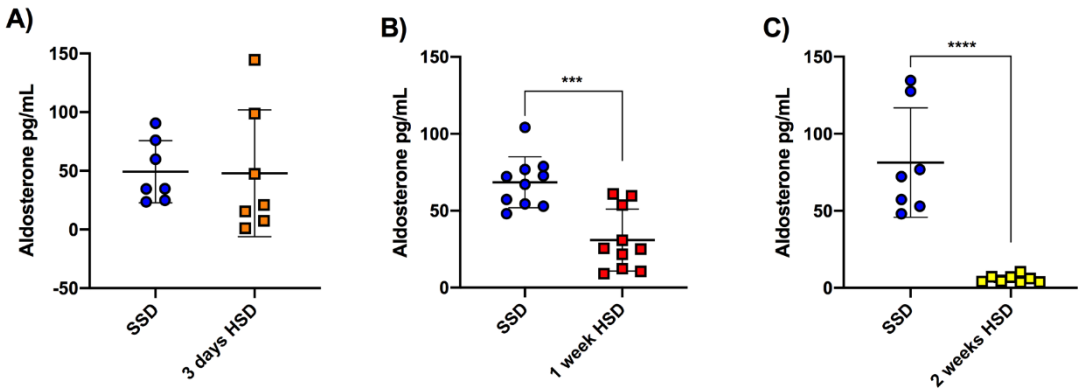

Figure 6.8: Plasma aldosterone concentration after high dietary salt intake.

The effect of dietary salt intake on plasma aldosterone concentration was determined via ELISA. Adult male C57BL6/JCrl mice were placed on either a standard salt diet (SSD; 0.25% Na) or a high salt diet (HSD; 3% Na) for 3 days (A: n=7 per diet), 1 week (B: n=10 per diet) or 2 weeks (C: SSD n=7; HSD n=8). Mice were culled during the daytime by decapitation to obtain a sufficient blood sample volume. Data are presented as mean ± SD and analysed using unpaired *t* test, with significance threshold at $P<0.05$. ***$p<0.001$, ****$p<0.0001$.

6.3.4 Effect of high dietary salt intake on plasma aldosterone concentration

Aldosterone concentration was measured in plasma samples obtained from C57BL6/JCrl mice on three separate occasions: after 3 days, 1 week or 2 weeks of either the SSD or the HSD. The results are presented in Figure 6.8.

High dietary salt intake had no effect upon the plasma concentration of aldosterone after 3 days, as no difference was observed between the SSD group with a concentration of 49.2 ± 26.5 pg/mL and the HSD group with a concentration of 47.9 ± 54.1 pg/mL ($P=0.956$; Figure 6.8 A).

Nevertheless, plasma aldosterone concentration was significantly reduced after a longer duration of the HSD. After 1 week of the HSD, concentration was 30.9 ± 20.1 pg/mL compared to 68.5 ± 16.6 pg/mL measured in mice on the SSD ($P=0.0002$; Figure 6.8 B). Upon extending the HSD to 2 weeks, plasma aldosterone concentration was further reduced, measured at 5.8 ± 2.4 pg/mL as compared to 81.3 ± 35.5 pg/mL in mice receiving the SSD ($P<0.0001$; Figure 6.8 C).

These results demonstrate that the concentration of circulating aldosterone was appropriately suppressed in response to 1 and 2 weeks of high salt intake. The absence of downregulation after 3 days of the HSD suggest that this is not an instantaneous response in C57BL6/JCrl mice.

6.3.5 Effect of high dietary salt intake on the day-night pattern of urinary electrolyte excretion

Mice exhibited minor day-night variability in the volume of drinking water consumed on the SSD. During the daytime, intake was 1.1 ± 0.8 mL, which doubled at night (2.3 ± 1.0 mL; Figure 6.9 A) however this did not cross the threshold for statistical significance (P=0.050). After switching the SSD for the HSD for 3 days, mice drank 3.9 ± 2.6 mL of water in the daytime and 7.0 ± 2.6 mL at night (P=0.530). Neither of these 12-hour time periods were significantly different to that recorded during the SSD. Later on, at the 1-week time-point, daytime consumption had declined slightly to 3.3 ± 2.1 mL and night-time consumption to 4.5 ± 1.8 mL (P=0.868), despite a significant effect as demonstrated by the one-way ANOVA and visualising the graph.

Urine output significantly increased during the night compared to the day on the SSD (Figure 6.9 B). Mice produced 0.4 ± 0.2 mL of urine over the course of the day, which quadrupled at night (1.6 ± 0.3 mL; P=0.0007) illustrating that urine output may be diurnally regulated. After 3 days of the HSD, daytime urine output increased to 2.7 ± 1.5 mL and night-time output to 5.5 ± 1.8 mL, which were both significantly higher than that on the SSD (P=0.041 day; P=0.005 night). However, the administration of the HSD appeared to flatten the day-night variation, as the difference between the 12-hour time periods was no longer significant (P=0.124). Mice remained on the HSD until the end of the week, at which urine output had reduced slightly. At 1 week of the HSD, the mice produced 2.3 ± 1.3 mL of urine during the day and 2.6 ± 1.2 mL during the night (P=0.997; Figure 6.9 B), demonstrating further flattening of the day-night variation. These results show that the day-night rhythm of urine output seen on the SSD was significantly reduced by high dietary salt intake.

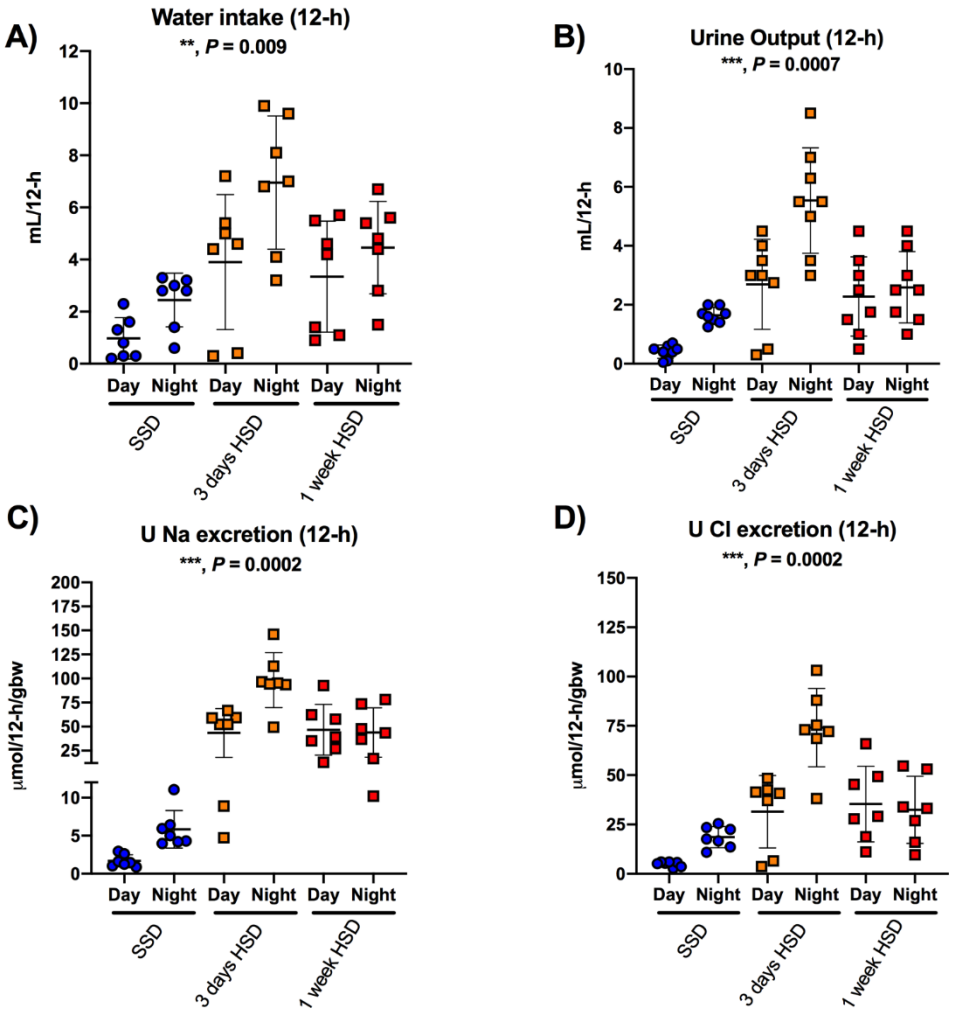

Figure 6.9: Day-night variability in electrolyte excretion before and after high dietary salt intake. Housed singly in metabolic cages,12-hour (12-h) urine collections occurred from male C57BL6/JCrl mice for day (7AM-7PM) and night (7PM-7AM) measurements of A: drinking water intake, B: volume of urine excreted, referred to as urine output, C: urinary sodium (Na) and D: urinary chloride (UCl) excretion. The effect of diet was assessed by placing these mice (n=7; 12-14 weeks old) on a standard salt diet (SSD; 0.25% Na) and then a high salt diet (HSD; 3% Na) each for 1 week. Electrolyte levels were determined via an electrolyte analyser and normalised to urine output and grams per body weight (gbw). Data are presented as mean ± SD and analysed using one-way repeated measures ANOVA, corrected for multiple comparisons via Tukey testing. $P<0.05$ was denoted as statistically significant.

Figure 6.9 C depicts 12-h urinary sodium excretion in these mice. On the SSD, daytime excretion was 1.2 ± 0.8 µmol/12h/gbw. This significantly increased over the course of the night to 5.8 ± 2.5 µmol/12h/gbw (P=0.003) demonstrating a robust day-night pattern. Both daytime and night-time excretion of sodium was amplified after mice were transferred to the HSD. Daytime excretion rose to 43.4 ± 25.5 and night-time to 98.3 ± 26.8

μmol/12h/gbw after 3 days of the HSD, which were significantly greater than that of the SSD (*P*=0.037 day-time comparison; *P*=0.0013 night-time comparison). However, the significance of the day-night variation was lost (*P*=0.128). This was also reflected by urinary sodium excretion at 1 week of the HSD. Daytime excretion was higher than during the SSD at 46.7 ± 28.4 μmol/12h/gbw (*P*=0.028), although night-time excretion had lowered to 43.8 ± 25.8 μmol/24h/gbw (P = 0.064). Urinary sodium excretion during the day and the night were very similar (*P*>0.999), implying that the diurnal regulation previously seen had disappeared altogether by 1 week. This suggests that high salt intake increased urinary sodium excretion but flattened out the diurnal variation in C57BL6/JCrl mice.

Urinary chloride excretion also exhibited day-night variation that was influenced by increasing dietary salt intake (Figure 6.9 D). On the SSD, excretion was calculated at 4.9 ± 1.3 μmol/12h/gbw during the day, which was significantly elevated to 18.6 ± 5.4 μmol/12h/gbw during the night (*P*=0.003), establishing the presence of a day-night pattern. Once this diet was swapped for the HSD, both daytime and night-time urinary chloride excretion increased. After 3 days, daytime excretion had risen to 31.8 ± 18.4 and night-time to 74.1 ± 19.9 μmol/12h/gbw, both of which were greater than that measured on the SSD (*P*=0.0007 day; *P*=0.002 night). However, at this time-point the day-night variation had been lost, as urinary chloride excretion during the day and night were not significantly different (*P*=0.090). After 1 week of the HSD, daytime excretion remained higher than SSD daytime excretion at 35.3 ± 19.1 (*P*=0.035), however night-time excretion had dropped to 32.5 ± 17.0 μmol/24h/gbw (*P*=0.388). No difference was noted between day-time and night-time urinary chloride excretion at 1 week of the HSD (*P*=0.999), demonstrating an attenuation of diurnal variation with high salt intake.

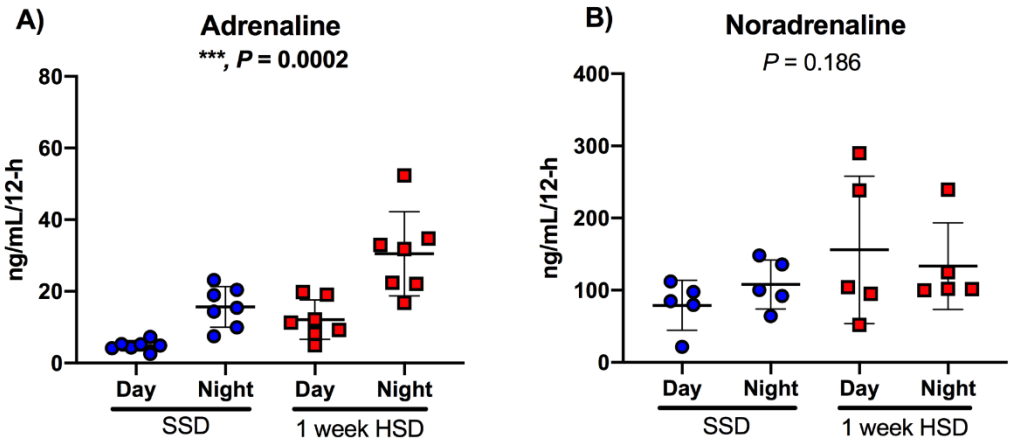

Figure 6.10: Diurnal variation in urinary catecholamine excretion before and after high dietary salt intake.

Urinary excretion of A) adrenaline and B) noradrenaline was determined via ELISA. Adult male C57BL6/JCrl mice (n=9) received a standard salt diet (SSD; 0.25% Na) for 1 week, before being switched to a high salt diet (HSD; 3% Na) for a further week. After 1 week of each diet, mice were individually housed in metabolic cages from which urine samples were collected after 12-hour (12-h) periods. Daytime samples were obtained between 7AM and 7PM, and night-time samples between 7PM and 7AM. Data are mean ± SD and analysed via one-way repeated measures ANOVA, corrected for multiple comparisons made by Tukey. Significance threshold was at $P<0.05$.

6.3.6 High dietary salt intake increases urinary adrenaline excretion during both day and night

In C57BL6/JCrl mice, urinary excretion of adrenaline varied significantly between the day and the night on the SSD (Figure 6.10 A). Mice excreted 4.8 ± 1.4 ng/mL during the day, which increased to 15.7 ± 5.7 ng/mL at night (P=0.007), illustrating a day-night rhythm. This rhythm was maintained on the HSD (P=0.016), but urinary adrenaline excretion was greater over both 12-hour periods compared to the SSD. Daytime excretion reached 12.1 ± 5.5 ng/mL (P=0.038) and night-time excretion 30.5 ± 11.7 ng/mL (P=0.027).

On the SSD, daytime urinary noradrenaline excretion was measured at a concentration of 79.1 ± 34.5 ng/mL and night-time excretion at 108.0 ± 34.0 ng/mL (Figure 6.10 B). This was not a statistically significant difference (P=0.521), suggesting that noradrenaline levels were not under circadian regulation here. The HSD had no impact upon urinary noradrenaline excretion, as after 1 week daytime levels were 155.9 ± 102.4 ng/mL and

night-time levels were 133.5 ± 60.0 ng/mL (*P*=0.850), which were also not different to those on the SSD.

6.3.7 Effect of acute sympathetic nervous system blockade on salt-induced increases in blood pressure

Figure 6.11 depicts the effects of an IP of the sympathetic ganglionic blocker hexamethonium on SBP. Pre-IP SBP was significantly higher after 3 weeks of the HSD at 139.2 ± 6.5 mmHg compared to pre-IP SBP on the SSD at 115.7 ± 6.6 mmHg (*P*=0.004; Figure 6.13 A), confirming a salt-induced increase. Initially, the injection induced a sharp elevation in SBP visualised as a 'peak' on the trace, which did not differ depending on the sodium content of the diet (Figure 6.11 B & F). Shortly following this peak, SNS inhibition induced a drop in SBP (Figure 6.11 C). In mice on the SSD, SBP dropped by -21.6 ± 8.7 mmHg. After 1 week of the HSD, SBP dropped by a similar amount, for example by -23.1 ± 6.2 mmHg (*P*=0.911). After 3 weeks of the HSD, SBP decreased by -37.2 ± 13.6 mmHg which, although it was slightly more variable, was significantly greater than on the SSD (*P*=0.013; Figure 6.11 C & F). The time taken to recover back to pre-IP SBP was 16 ± 7 mins on the SSD (Figure 6.11 D). This was comparable following 1 week of the HSD at 16 ± 8 mins (*P*=0.996). After 3 weeks of the HSD, the recovery time was significantly longer, having increased to 54 ± 22 mins (*P*=0.012; Figure 6.11 D & F). The AUC of the negative peaks was analysed and displayed in Figure 6.13 E & F. The AUC following SNS inhibition on the SSD was -167.6 ± 85.2 AU. Upon transferring mice to the HSD, this decreased very slightly but remained on par at 1 week at -122.3 ± 78.3 AU (*P*=0.689). Although, this became highly variable and increased to -792.3 ± 580.7 AU after 3 weeks of the HSD. In comparison to baseline, this was not statistically significant (*P*=0.065; Figure 6.11 E). However, the significance of the overall effect (Figure 6.11 F), and compared with 1 week of the HSD (*P*=0.047), suggests a possible tend towards a greater response.

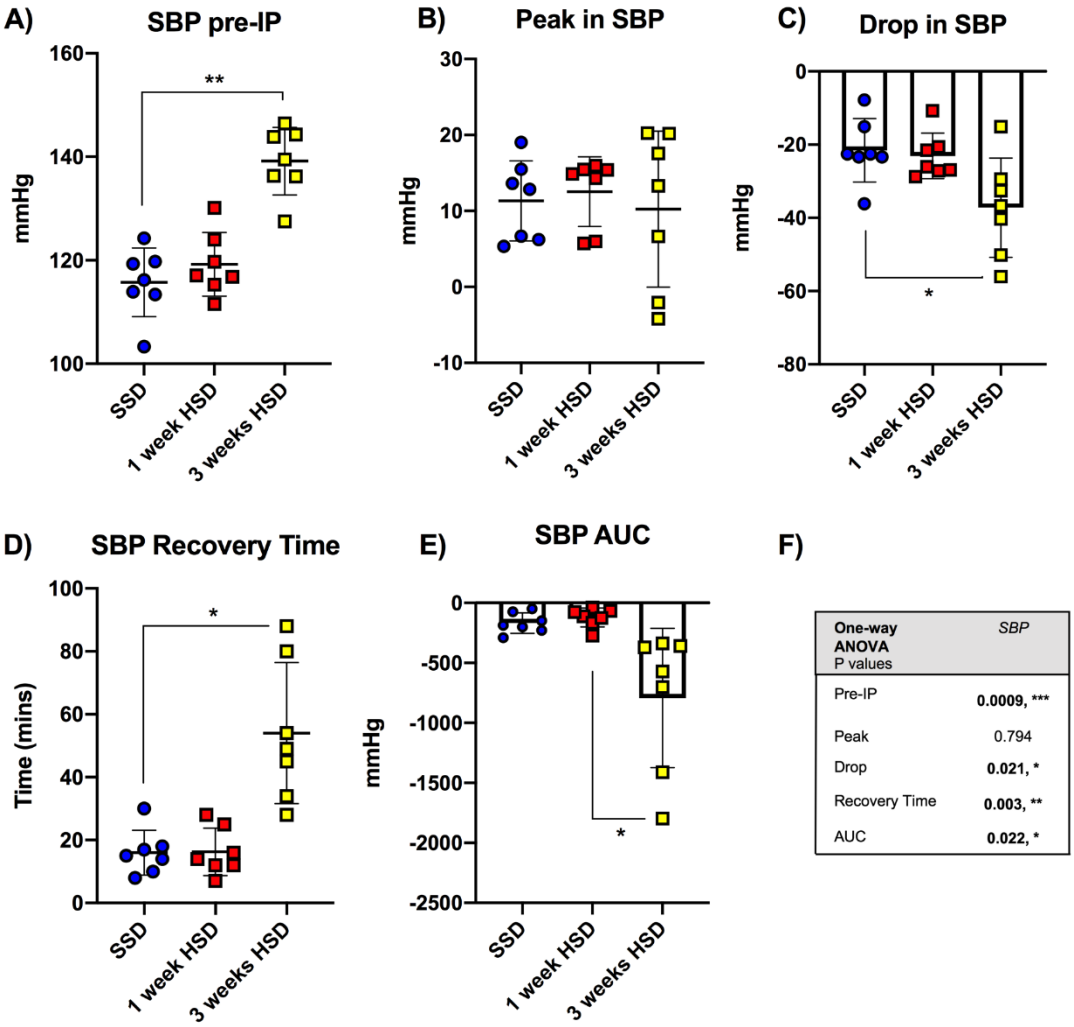

Figure 6.11: Systolic blood pressure following sympathetic nervous system inhibition before and after high dietary salt intake.

Systolic blood pressure (SBP) was measured via radiotelemetry in C57BL6/JCrl mice (n=7) on a standard salt diet (SSD; 0.25% Na) for 1 week before being placed on a high salt diet (HSD; 3% Na) for 3 weeks. Inhibition of the sympathetic nervous system was achieved via an intraperitoneal injection (IP) of hexamethonium (30 mg/kg) on the SSD, which was repeated after 1 week and 3 weeks of the HSD. Pre-IP SBP (A), the initial post-injection peak in SBP (B), the maximal drop in SBP (C), recovery time (D) and the area-under-the-curve (AUC; E) are presented as mean ± SD. F) is a table presenting *P* values from one-way repeated measures ANOVA corrected for multiple comparisons made via Tukey testing. **p*<0.05, ***p*<0.01, ****p*<0.001.

Pre-IP DBP was at 85.2 ± 9.4 mmHg, which became significantly higher at 101.9 ± 6.4 mmHg after 3 weeks of the HSD (*P*=0.020; Figure 6.12 A). At the time of the IP of hexamethonium, DBP transiently increased by 11.7 ± 6.0 mmHg on the SSD, 11.0 ± 5.4 mmHg after 1 week of the HSD and 11.5 ± 8.8 mmHg after 3 weeks of the HSD, depicting that dietary salt intake did not have an influence upon this (Figure 6.12 B & F). Hexamethonium induced a decrease in DBP (Figure 6.12 C). DBP decreased similarly on the SSD as compared with 1 week of the HSD, by -18.0 ± 9.9 mmHg and -16.1 ± 8.0 mmHg respectively (*P*=0.948). After 3 weeks HSD, this decline was slightly greater, as DBP dropped by -26.0 ± 11.3 mmHg, however this did not cross the threshold of statistical significance (*P*=0.146; Figure 6.12 C & F). On the SSD, DBP recovered back to the pre-IP baseline in 10 ± 4 mins, which was similar at 12 ± 7 mins after 1 week of the HSD (*P*=0.843). However, by 3 weeks of the HSD, recovery time had elongated to 38 ± 20 mins (*P*=0.028; Figure 6.12 D & F). AUC analysis demonstrated that hexamethonium induced a reduction in DBP with an AUC of -91.7 ± 81.0 AU on the SSD. Once on the HSD, this increased very slightly to -66.6 ± 72.9 AU after 1 week but remained comparable with that on the SSD (*P*=0.827). After 3 weeks of the HSD, the DBP AUC was variable. Overall, AUC was measured at -365.2 ± 278.9 AU, which was not statistically different from the SSD (*P*=0.140; Figure 6.12 E & F).

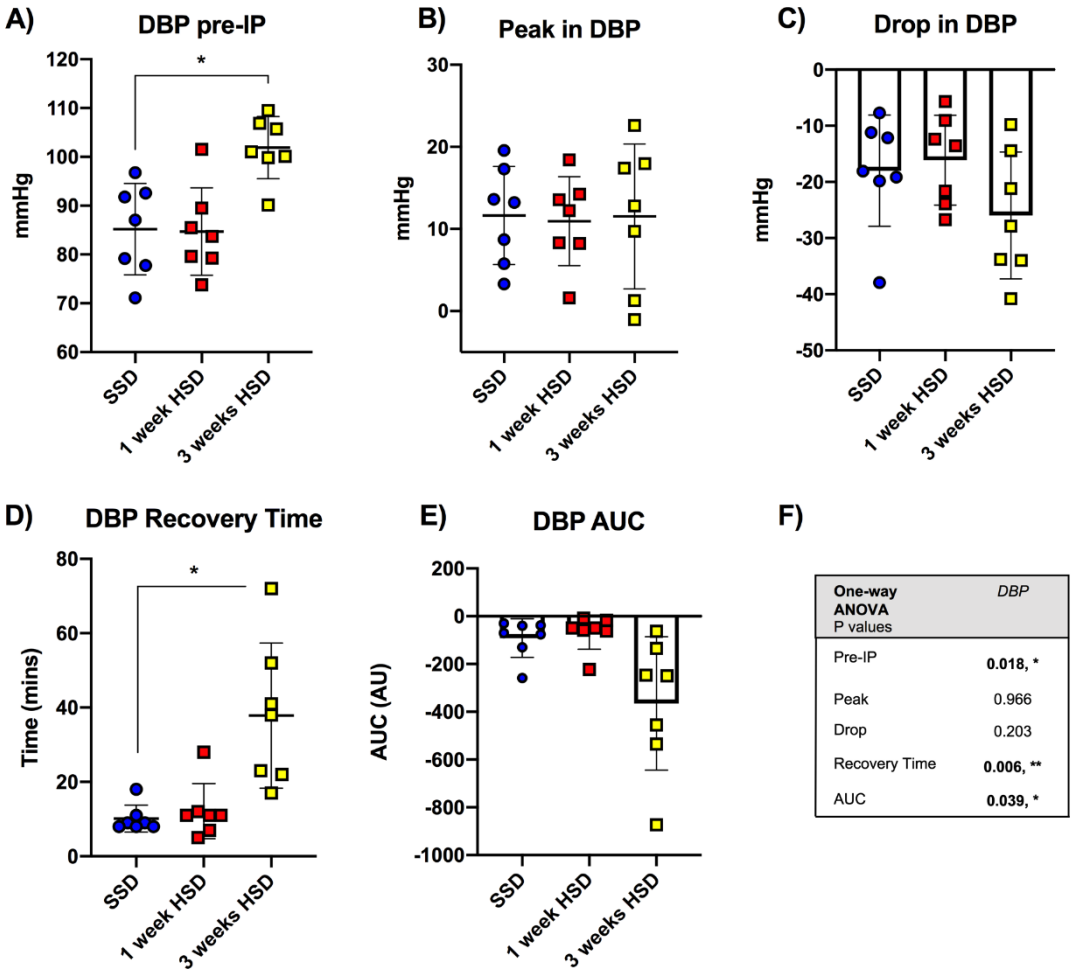

Figure 6.12: Diastolic blood pressure with inhibition of the sympathetic nervous system before and after high dietary salt intake.

Diastolic blood pressure (DBP) was measured by radiotelemetry in adult male C57BL6/JCrl mice (n=7). Mice were placed on a standard salt diet (SSD; 0.25% Na) before being transferred to a high salt diet (HSD; 3% Na) for 3 weeks. Sympathetic nervous system inhibition was achieved through intraperitoneal injection (IP) of hexamethonium (30mg/kg) on the SSD, after 1 week and after 3 weeks of the HSD. Data are mean ± SD as A) pre-IP DBP, B) post-injection peak in DBP, C) maximal drop in DBP, D) time taken for DBP to recover to pre-IP levels, E) area-under-the-curve (AUC) and F) table presenting the *P* values from repeated measures one-way ANOVA corrected for multiple comparisons by Tukey testing. **p*<0.05, ***p*<0.01.

Similar effects of hexamethonium were observed on MBP. After the HSD, pre-IP MBP was significantly greater at 119.1 ± 3.2 mmHg as compared to MBP on the SSD at 99.9 ± 4.5 mmHg (*P*=0.0004; Figure 6.13 A & F). Upon injection, MBP temporarily increased by 15.2 ± 3.4 mmHg on the SSD. This did not differ with dietary salt intake, as MBP increased by 13.0 ± 6.9 mmHg (*P*=0.822) and by 12.4 ± 6.4 mmHg after 1 and 3 weeks of the HSD respectively (*P*=0.519; Figure 6.13 B & F). Figure 6.13 C depicts the hexamethonium-induced drop measured in MBP. On the SSD, MBP declined by 17.0 ± 9.0 mmHg and similarly by 17.7 ± 7.0 mmHg after 1 week of the HSD (*P*=0.978). Following 3 weeks of the HSD, MBP dropped with hexamethnium by 29.6 ± 11.6 mmHg, which was not significantly different to that on the SSD (*P*=0.101; Figure 6.13 C & F). The time taken to recover back to pre-IP baseline levels was 14 ± 9 mins on the SSD, which was slightly shortened to 10 ± 8 mins after 1 week of the HSD (*P*=0.650). After 3 weeks HSD, the recovery time was longer at 46 ± 27 mins. In comparison to the SSD, this was not a statistically significant elongation (*P*=0.077). However, the significance of the overall effect and that compared to 1 week of the HSD (*P*=0.021) suggests a possible trend towards a longer recovery time of MBP after 3 weeks of high salt intake (Figure 6.13 D & F). The AUC of MBP following hexamethonium injection was -126.7 ± 102.5 AU on the SSD. This rose slightly but insignificantly to -74.7 ± 72.0 AU after 1 week of the HSD (*P*=0.528). At 3 weeks of high salt, AUC was -606.3 ± 567.7 AU. This was substantially increased within a few of the mice, but less so in others, and thus the difference was not statistically significant (*P*=0.138; Figure 6.13 E & F).

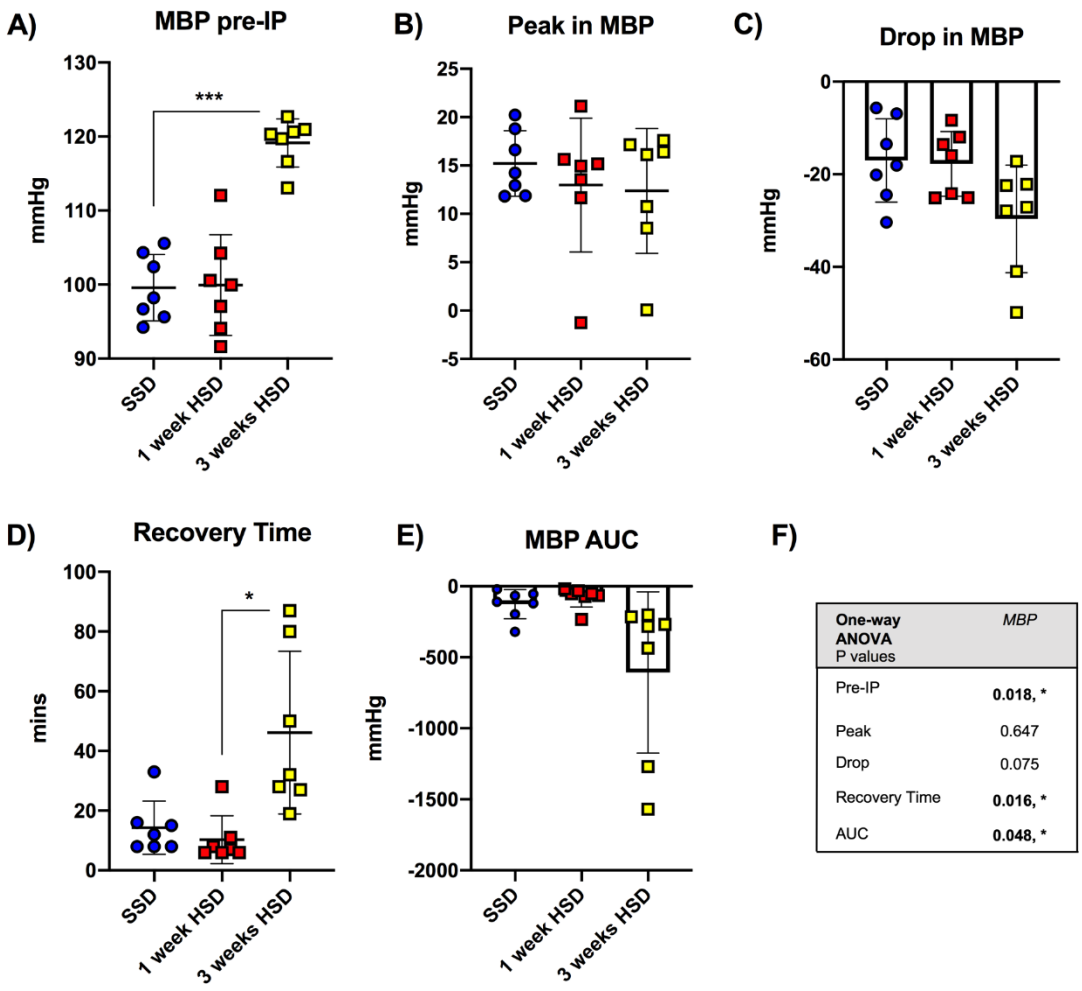

Figure 6.13: Mean blood pressure during sympathetic nervous system inhibition before and after high dietary salt intake.

Radiotelemetry measured mean blood pressure (MBP) in adult male C57BL6/JCrl mice (n=7) placed on a standard salt diet (SSD; 0.25% Na) for 1 week and then swapped to a high salt diet (HSD; 3% Na) for 3 weeks. Intraperitoneal (IP) injection of the ganglionic blocker hexamethonium (30mg/kg) was administered on the SSD, 1 week and 3 weeks after the HSD. Data are mean ± SD presented as A) pre-IP MBP, B) peak in DBP following injection, C) maximal drop in MBP, D) recovery time and E) area-under-the-curve (AUC) and F) table depicting *P* values from repeated measures one-way ANOVA corrected for multiple comparisons by Tukey testing. **p*<0.05, ****p*<0.001.

6.4 Discussion

6.4.1 Impact of high dietary salt intake on water balance

The aim of these experiments was to gain an insight into the changes in water balance in C57BL6/JCrl mice during increased salt intake. Mice displayed polydipsia and polyuria. However, the intake of drinking water significantly outweighed the volume of urine produced and consequently, mice had a positive water balance. This implies that some of the water consumed was being retained during the increase in salt intake. Due to this observation, it was possible that fluid retention occurred in C57BL6/JCrl mice following high dietary salt intake.

On the contrary, haematocrit was assessed in the experiments of chapter 4 in post-operative C57BL6/JCrl mice in a cross-sectional study design. Had fluid retention and ECFV expansion occurred, % haematocrit would likely decrease. No changes of note were revealed, as haematocrit was equal between the dietary groups after 3 days of the HSD. After 1 week of the HSD, a trend was observed towards haematocrit being lower; however, this was not a significant difference. This final observation raises some questions regarding the calculation of water balance in these mice. Firstly, insensible water loss was not included in the balance calculation. From visualisation alone, the decreased weight and dry appearance of the faeces during high salt intake did not indicate a high-water content; however, mice are reported to lose 80% of this water via respiration (211) which was also not included in the calculation here.

Further limitations of this approach must be considered. Haematocrit was measured in a separate cohort of mice having undergone 1-2 hours of a surgical procedure under general anaesthesia, thus is unlikely to be reflective of that within conscious animals. Moreover, haematocrit obtained in this way is a rather rudimentary measure of the cellular content of blood and, by process of elimination, plasma volume.

Other, more sensitive techniques exist in which fluid volumes can be determined. For example, the administration of a known concentration of Evan's blue dye can be used to quantify plasma volume (212). Additionally, ECFV and other fluid volumes can be estimated through bioimpedance spectroscopy, in which the application of a small electrical current over a range of frequencies can determine the resistance and thus the volume contained within the different fluid compartments (213).

6.4.2 Sodium balance and high dietary salt intake

According to Guyton's hypothesis, a positive sodium balance due to a disparity between sodium intake and excretion stimulates downstream changes in BP (77). For this reason, the sodium status of C57BL6/JCrl mice before and during increased salt intake was measured. With standard salt intake, mice displayed a positive sodium balance. With high dietary salt intake, however, sodium balance was extremely variable and even became negative in some mice after 1 week, an effect that was bordering on statistical significance. This suggests sodium wasting was potentially occurring and that, based on Guyton's theory, mice were primed to expel as much sodium as possible to normalise BP.

Although, recent research has uncovered that sodium can be stored in the body, for example in the skin interstitium and muscle (214, 215). Such stores are not permanent – they are dynamic, thus enabling the transfer of sodium into and out of them, as demonstrated by the Mars 500 study (216). With this in mind, the simple 'intake should equal output' approach and thus calculation of balance may be a lot more complex in animals and humans.

Technical notes include that faecal sodium output was not measured in this experiment, and so these values were absent from the balance calculations. The inclusion of sodium excretion values from the gut could, in fact, cross the threshold of statistical significance for this effect of high dietary salt intake on sodium balance.

6.4.3 Body weight and dietary salt intake

An unexpected finding of this experiment was a decreasing body weight with increased salt intake. Body weight has been used as an indicator of fluid and sodium status in a clinical setting. For example, an increase in body weight is suggestive of water and/or sodium retention (217). Conversely, a positive water balance was noted with no alterations to haematocrit with high salt, and so in this case does not account for the decline in weight. Furthermore, food intake was equal before and after the diet switch. However, food intake was measured in grams, rather than in calories. The diets administered to C57BL6/JCrl mice in these experiments were not calorie-matched, and energy expenditure was not monitored. It is uncertain as to where this loss originated. Caloric and energy expenditure analysis, performed in specialised metabolism cages with calorimetry modules, may help elucidate the cause.

Previous literature has reported mixed results regarding the relationship between body weight and dietary salt. In humans, high dietary salt intake has been linked to weight gain and an increased risk of obesity (218, 219), and that weight loss paired with dietary sodium restriction could reduce BP (220). However, these observations may be species-dependent. DeClercg *et al*. (221) found that high salt intake suppressed the weight gain usually induced by a high fat diet in C57BL6/J mice. Additionally, Weidemann *et al*. (222) observed this same effect and that high salt intake decreased digestive efficiency in these mice, which was restored with ANGII infusion. Thus, these findings suggest a potential role for RAAS in the salt-induced effects on weight in mice.

6.4.4 High dietary salt flattens the day-night pattern in urinary sodium excretion: what does this mean for blood pressure?

In my experiment, C57BL6/JCrl mice displayed diurnal variation in urine volume and urinary sodium excretion under normal conditions, i.e on a SSD. Excretion was upregulated during the night, which is the active phase for nocturnal animals such as mice, and decreased significantly in the day during the inactive phase. These findings adhere to previous observations (223,

224) and so provide confidence in the techniques applied here to measure endogenous patterns.

High dietary salt intake attenuated this variation after 1 week. Both urine volume and urinary sodium excretion between day and night became indistinguishable, showing that mice were less able to expel the excess sodium when active at night. Previous literature highlights a strong association between disturbances in the day-night differences of urinary sodium excretion and persistently high BP at rest (71, 225, 226). An impaired ability to excrete a sufficient amount of sodium during active periods results in the need for equal or higher amounts to be excreted during inactive periods (227). My results from this experiment reflect this.

However, I established in chapter 3 of this thesis that C57BL6/JCrl mice exhibited robust day-night rhythmicity of BP, which not only persisted during high salt intake but also increased at night. Thus, these findings illustrate that urinary sodium excretion is unlikely to be involved in the regulation of the salt-induced effects seen in BP in these mice.

6.4.5 Evaluating the role of the sympathetic nervous system in blood pressure control

The SNS is considered an important regulator of BP, with excessive activation linked to salt-sensitivity. Nonetheless, it has proven rather difficult to measure reliably. Researchers have applied the following experimental approaches to investigate its input: the measurement of urinary catecholamine concentrations, pharmacological inhibition and renal denervation.

6.4.5.1 Urinary excretion of catecholamines

Urinary excretion of the neurotransmitter noradrenaline, along with the hormone adrenaline, has been treated as an index of total SNS activity. This can be carried out by collecting urine samples and measuring concentration via ELISA (228), a method that has been used in clinical practice. It is often informally referred to as ‘urinary spill-over’, as it is an indirect measure of the

run-off of neurotransmitter from the neuroeffector junction, which includes secretion from the adrenal medulla as well.

However, there are limitations to this approach. It makes the assumption that all noradrenaline and adrenaline synthesised over a defined experimental period is expelled in urine. Production may not necessarily equal release, and so it does not account for other activities such as breakdown, recycling or reuptake and storage. Furthermore, it cannot distinguish between the origins of the urinary catecholamines, which can also be released from the central nervous system.

6.4.5.2 Pharmacological inhibition

SNS activity can be modulated pharmacologically. Researchers have administered inhibitors to try to elucidate its role in BP control and have noted antihypertensive effects (229-231). Examples of such inhibitors are the ganglionic blockers trimethaphan and hexamethonium. Whilst Santagjuliana *et al*. (210) found that both are equally effective at lowering BP, hexamethonium was chosen for the experiment in this chapter. Its mechanism of action is direct, specific and reversible, as it binds non-competitively to or around the site for ACh on nicotinic receptors located within sympathetic ganglia and interrupts sympathetic nerve transmission alone. Trimethaphan, on the other hand, has been reported to have off-target effects (232, 233); thus, its BP-lowering properties are likely to be nonspecific and multifaceted.

6.4.5.3 Renal denervation (RDN)

RDN is achieved by severing the sympathetic connections to the kidney. This can be approached chemically by applying phenol in ethanol to the major blood vessels supplying the kidney (234, 235), or mechanically by peeling the nerves away from these vessels by hand under a microscope (236). The reported effects are mixed, with some observing decreases in BP and others observing no effect at all.

Sympathetic input on renal function is threefold: it has been shown to contribute to tubular water and sodium reabsorption, renal haemodynamics and renin release (237). All of the above processes have been implicated in salt-sensitive hypertension, thus the rationale behind the removal of SNS input is that it can lead to an amelioration of these effects.

6.4.6 Summary of results

1. High dietary salt intake produced a decrease in body weight after 1 week, which is unlikely to be related to food intake or fluid balance in C57BL6/JCrl mice.
2. Water intake, urine volume, and urinary sodium excretion were substantially greater after 1 week of high salt intake. Water balance was positive after 3 days of high salt intake; however, this did not take into account insensible water loss.
3. The day-night variability of urine output and urinary sodium excretion was significantly attenuated after 1 week of high salt intake.
4. Plasma aldosterone concentration was appropriately downregulated after 1 and 2 weeks of high dietary salt intake.
5. Both daytime and night-time urinary excretion of adrenaline increased with the sodium content of the diet after 1 week. No effects of dietary salt were observed on noradrenaline excretion.
6. Three weeks of high dietary salt intake induced a modest drop in SBP and significantly prolonged the recovery of BP to SNS inhibition via hexamethonium.

7 Discussion

The work in this thesis aimed to address the overarching question of how high dietary salt intake initiates and sustains high BP. The main findings confirm that C57BL6/JCrl mice develop salt-induced hypertension. No effect was found upon intrinsic renal function or systemic vascular function; however, indicators of SNS function show increased activity with high salt, and the effects of acute inhibition on SBP were greater with prolonged intake.

7.1 Renal vs. Vascular Dysfunction

High dietary salt intake is evidently linked to increasing BP and hypertension. However, the mechanisms remain elusive. The two main controversies in the field are that high salt intake induces functional changes to the kidney or the systemic vasculature, which in turn mediates the detrimental effects on BP.

7.1.1 Challenges to the conventional approach

Guyton's hypothesis, which has been the cornerstone of hypertension theory for ~50 years, states that any increase in pressure will be normalised by salt and water excretion unless disturbances in salt consumption and/or the renal PN relationship occur (78). Such disturbances are considered to lead to sodium retention and support long-term increases in BP. The work in this thesis shows that dietary salt consumption was indeed altered in C57BL6/JCrl mice with the administration of the HSD, as demonstrated by the dramatic and significant increases in intake and urinary excretion of sodium in chapter 6. The renal PN relationship shifted to support this, illustrating that mice adapted to excrete more sodium under pressure.

Conflicting ideas over the role of sodium balance in the generation of salt-induced hypertension exist. Hall's approach (57) identifies a positive sodium balance, indicative of sodium retention, as a critical event in the initiation and

maintenance of salt-induced hypertension. Previously, researchers have noted a positive sodium balance in salt-sensitive, hypertensive patients and concluded that sodium retention contributes to the salt-sensitivity of BP (58, 238). However, others have reported no differences compared to normotensive participants, suggesting they experience a similarly high but temporary sodium balance with high salt intake (73). Hall argues that no differences in sodium balance between those with a higher BP and those with a standard BP is abnormal in itself (57). Such higher pressures entering the kidney should induce significant changes in sodium balance, retention and excretion in comparison. Herein, I observed a positive sodium balance in C57BL6/JCrl mice with standard salt intake, which then became negative with high salt. This suggests that mice were expelling as much sodium as possible. The significant downregulation of some of the key tubular sodium transporters after 1 and 2 weeks of high salt further supports this finding.

A continued argument within the field is that hypertension cannot be maintained without contributory renal dysfunction. In this case, C57BL6/JCrl mice exhibited salt-induced increases in BP over 3 days of HSD, which stabilised after 1 week and remained high for a total of 3 weeks. Here, I report no intrinsic impairment of the acute PN relationship after 3 days or 1 week of the HSD, despite my previous experiments illustrating high BP at these time-points. Research by Girardin *et al*. measured the PN relationship in isolated kidneys from salt-sensitive Dahl rats after 3 and 7 weeks of HSD, and observed that kidneys only displayed a PN impairment after 7 weeks of the HSD (161), suggesting that the salt-induced hypertension was the cause, rather than the consequence. It is possible that in C57BL6/JCrl mice, renal dysfunction is not an initiator of salt-induced hypertension but rather it develops consequentially and contributes to the maintenance of hypertension at a later stage. Therefore, future work could involve assessing the acute PN relationship at a later time-point, for example after 3 weeks of high salt intake.

Adaptation of intrinsic renal function, consisting of an enhanced PN relationship accompanied by a negative sodium balance and decreased expression of some key sodium transporters, suggests that dysregulated function of the kidney was unlikely to be the source of the salt-induced increases in BP seen in C57BL6/JCrl mice. Thus, the focus moved to the vasculature.

7.1.2 Vasodysfunction

The vasodysfunction theory makes a case for an inappropriate decrease in SVR in response to high salt intake as the cause of salt-induced hypertension (92). This is suggestive of an impaired vasodilatory reaction in those with a salt-sensitive BP, and so I hypothesised that the inherent ability of the arteries of C57BL6/JCrl mice to vasodilate was compromised following high salt intake. For this reason, arteries were isolated and their intrinsic function interrogated via pharmacological induction of endothelium-dependent and -independent vasodilation in my thesis.

The experiments in chapter 5 display no significant alterations in the vasodilatory responses of arteries following high salt intake, as compared to standard salt intake, in C57BL6/JCrl mice. In mesenteric arteries, which were assessed as representatives of systemic resistance arteries, vasoconstrictor responses and eNOS expression were similarly unchanged between the diets. Alternatively, renal vascular dysfunction was observed. Whilst intrinsic renal artery reactivity was somewhat inconclusive after 3 days of high salt intake, an increased sensitivity to phenylephrine was evident after 1 week. Previous research has elucidated a role for enhanced renal vasoconstriction in hypertension. A study in humans with normal to moderately high BPs revealed that salt loading induced renal haemodynamic changes in those with a salt-sensitive BP suggestive of renal vasoconstriction compared to those with a salt-resistant BP. RBF decreased and RVR increased, whilst GFR remained unchanged. These alterations were initially associated with the salt-induced changes in MABP, but remained after the pressor effect of salt was inhibited, suggesting that this haemodynamic response was in

reaction to salt loading and not just the changes in MABP (239). These findings imply that salt-induced renal vasoconstriction could be the initiating event of BP increases with high salt intake. However others oppose this, as vascular abnormalities seem to resolve upon the treatment of hypertension via targeting renal function, thus implying they were secondary events (57).

In this case, my data show increased renal artery sensitivity to vasoconstriction after high salt. After 3 days of high salt intake, RVR was greater and RBF was lower compared with the standard salt controls, which is in-line with the observations described above. Together, this suggests mice experience renal vasoconstriction with high salt intake. However, no functional and expressional changes in mesenteric arteries were observed overall and no haemodynamic changes are reported after 1 week. The heterogeneity of these responses following high salt intake are challenging to interpret. Firstly, the experimental approaches must be evaluated. Isolated artery function measured *in vitro* does not necessarily apply to vascular function *in vivo*, as many external and mechanical stimuli also regulate reactivity. For this reason, the absence of evidence in the systemic resistance vasculature may not be evidence of absence, and thus warrants further investigation. To address this, resistance artery function can be measured via pressure myography in which changes in arterial diameter can be observed and interrogated. Furthermore, the *in vivo* SVR response to high salt was not measured in this thesis. Lastly, renal haemodynamics after salt intake were examined by experimentally induced pressure increases upon the kidney and under general anaesthesia, which also eliminates some extrarenal input.

7.2 Increased Sympathetic Activity in Salt-Induced Hypertension

Fujita *et al.* (209) noted that salt-induced effects on vascular resistance, haemodynamics and vasoconstriction varied region-by-region in salt-sensitivity. This was attributed to SNS activity. An association was made between the mass sympathetic discharge that occurs upon activation of the system, i.e the fight-or-flight response, and these salt-induced effects (209).

This led me to hypothesise that SNS activity was playing a key role in the regulation of renal vascular function in the salt-induced hypertension seen in C57BL6/JCrl mice.

In this thesis, urinary catecholamine excretion was utilised as an indicator of SNS activity in C57BL6/JCrl mice. It is an indirect measure of the overflow of noradrenaline and adrenaline from neuroeffector junctions, including the adrenal medulla, expelled in the urine. The adaptation of catecholamine production to changes in salt intake in healthy, normotensive humans has been previously characterised. In a study by Romoff *et al.* (240), subjects received 10, 100 and 200 mEq/day sodium each for one week after which plasma catecholamine levels were measured. Results illustrated that plasma levels of both adrenaline and noradrenaline were highest after the low sodium diet and greatly reduced after the high (240). This inverse relationship has also been demonstrated in urinary samples by Luft *et al*. (241) who observed diminished urinary noradrenaline excretion with high salt intake. Hence, catecholamine production is suppressed by high salt intake in healthy humans, and therefore implies suppression of total SNS activity as well. Campese *et al*. reports that plasma noradrenaline was appropriately suppressed with high salt in both normotensive and salt-resistant hypertensive humans but remained high in those who were salt-sensitive (217), thus this salt-induced effect appears to be abolished in hypertensive salt-sensitive humans.

In the experiments of chapter 6, I observed increased urinary adrenaline excretion and a trend towards an increase in urinary noradrenaline excretion after 1 week of high salt intake. Data regarding murine catecholamine levels, let alone those of C57BL6/J mice specifically, and the effect of salt appears to be scarce in the literature. With the data previously outlined in humans in mind, this suggests that the appropriate salt-induced suppression of urinary catecholamine excretion is not present in these mice. In fact, adrenaline levels seem to display a positive relationship with salt. No distinctive, overall effect was observed on urinary noradrenaline levels. Despite previously

reported increases in noradrenaline levels with high salt, the fact that levels did not decrease with high salt as they did in normal, healthy humans is an abnormal response in itself. Furthermore, Fujita *et al*., (238) noted temporal variation in plasma noradrenaline levels with high salt intake in salt-sensitive subjects; noradrenaline was suppressed after 3 days, however this reversed and levels rapidly increased after 4 days.

BP in C57BL6/JCrl mice exhibited a robust day-night rhythm, which became more conspicuous during high salt intake. In healthy humans, adrenaline levels also follow a diurnal pattern, with plasma levels rising during awakening and decreasing during sleep (242). As increased excretion of adrenaline was observed in C57BL6/JCrl mice, the effect on diurnal variation was also investigated. Adrenaline excretion presented a similar pattern to BP with high salt intake; urinary levels increased during both the day and the night, maintaining the day-night rhythm. However, diurnal variation in urinary norepinephrine excretion was not evident here. Changes in plasma noradrenaline levels were only noted in humans upon changing position, i.e from lying supine to standing up straight, rather than from awakening (242). Thus, the similarity of the changes to the day-night pattern of both BP and adrenaline excretion with salt led me to hypothesise a central role for the SNS and investigate via application of an SNS inhibitor.

SNS inhibition with the ganglionic blocker hexamethonium elicited a modestly increased reduction in SBP with an extended recovery time after 3 weeks of high salt intake, evidencing potentially increased SNS involvement with continuing salt intake. Similar trends were noted in DBP and MBP that did not reach statistical significance. A lack of power is suspected, as the BP response to hexamethonium in mice was highly variable, thus a certain degree of caution is applied upon interpretation. For further experiments, the study sample size would be determined via performing a power calculation. The minimum biologically relevant difference and variance in SNS inhibition before and after high salt intake can be estimated from this data. For example, SBP dropped by 21.6 ± 8.7 mmHg with hexamethonium IP during

standard salt intake which increased to 37.2 ± 13.6 mmHg after 3 weeks of high salt intake, a change that passed the significance threshold. Thus, for SBP, the minimum significant difference is 15.6 mmHg. Using the standard equation for continuous data depicted below, n = 10.9 and, therefore, 11 mice would be used.

$$n = f(\alpha, \beta) \cdot \frac{2s^2}{\delta^2}$$

α = 0.05 significance level

β = 0.2, ensuring 80% power

s = standard deviation

δ = minimal significant difference.

Research has shown that the sodium concentration of cerebrospinal fluid (CSF) varies with dietary salt intake; it increases with high intake, and decreases with low intake in hypertensive humans depending on their salt-BP status (243, 244). These variations in CSF sodium alter SNS outflow (245), thus providing a possible mechanism through which high dietary salt intake contributes to SNS activity and BP.

7.2.1 Proposed role for the sympathetic nervous system in salt-induced hypertension in C57BL6/JCrl mice

Hyper-activity of the SNS has been implicated in the development and maintenance of hypertension. The initial aim of my thesis was to characterise the BP response to high salt intake in C57BL6/JCrl mice. High salt led to an increase in BP over 1 week, which then remained elevated for a further 2 weeks, confirming the establishment of salt-induced hypertension in these mice. Following this, the aims I wished to address involved attempting to gain mechanistic insights into the generation of this salt-sensitive BP response. The potential role for the SNS in C57BL6/JCrl mice is depicted in Figure 7.1. Acute SNS blockade evoked a decrease in BP, from which mice took longer to recover from, after 3 weeks of high salt intake. This suggests that

increased systemic SNS activity potentially plays a part in maintaining salt-induced hypertension in these mice, and so poses the question of what is occurring during the initiation.

Innervation by efferent sympathetic nerve fibres regulates both tubular and vascular function within the kidney. Increased sympathetic outflow reduces RBF, elevates RVR and enhances vasoconstriction, which are reversed by severing these nerves in renal denervation studies (237). Increased sensitivity of renal arteries to the vasoconstrictor phenylephrine, along with elevated excretion of adrenaline after 1 week of high salt intake were observed. Phenylephrine and the mediators of the SNS induce vasoconstriction via very similar receptor-mediated pathways: both bind and activate α-ARs. Noradrenaline and adrenaline, whether circulating in the bloodstream or released at neuroeffector junctions, are able to elicit vasoconstrictor responses via the binding of ARs on the VSM layer. Increased adrenaline has been noted to provoke vasoconstriction through α-ARs, which was amplified in hypertensive patients (246). Thus, high circulating levels of catecholamines may be associated with the increased sensitivity to α-AR vasoconstriction after 1 week of high salt intake.

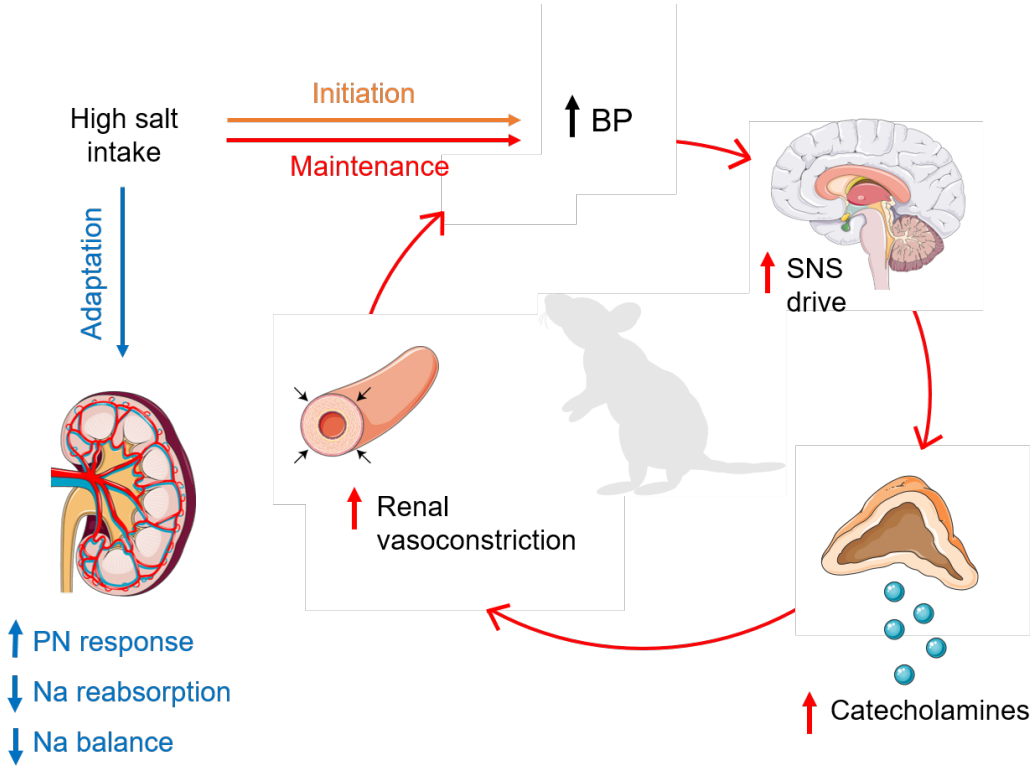

Figure 7.1: Proposition for the adaptive and maladaptive responses of C57BL6/JCrl mice to high salt intake, resulting in high blood pressure.

Schematic summarising the physiological response of C57BL6/JCrl mice to high salt intake and the potential mechanisms underlying the maintenance of salt-induced hypertension. High salt intake led to a sustained increase in blood pressure (BP). At the time of this increase and the establishment of high BP, renal function adapted appropriately as the pressure natriuresis (PN) relationship shifted to expel as much sodium (Na) as possible, reabsorption is downregulated and overall balance does not increase. Possible hyperactivity of the sympathetic nervous system (SNS) was noted with extended salt intake, as blockade decreased BP. Preceding this, high salt did not suppress excretion of catecholamines, suggesting high circulating levels. Increased intrinsic sensitivity of renal arteries to vasoconstrictors was observed, concluding that increased sympathetic drive may be contributing to the maintenance of salt-induced hypertension in C57BL6/JCrl mice via renal α-AR-mediated vasoconstriction. Initiation remains unclear.

Additionally, noradrenaline has been shown to blunt the PN relationship, causing a rightward shift in the curve and inducing sodium retention (84). Thus, increased SNS outflow via high concentrations of catecholamines and/or renal sympathetic nerve activity disrupts the renal physiological response to high salt intake. My experiments show that increased adrenaline excretion is present and noradrenaline excretion was not suppressed by high salt, indicative of abnormal circulating levels; however, an adversely shifted PN relationship, suggesting impairment, was not observed in these mice at this time-point. Renal function appears suitably adapted to increased salt

intake. Studies have noted that increased catecholamine concentration can, in fact, enhance the ability of the kidney to respond to increased pressure via increased sodium excretion, demonstrating that these mediators have both natriuretic as well as antinatriuretic effects (84, 157). Perhaps this is the case here in C57BL6/JCrl mice. Alternatively, the PN relationship was interrogated in these mice whilst unconscious. A barbiturate anaesthetic was utilised, which has been shown to diminish sympathetic nerve activity in humans (247). Information has not been obtained on the activity of renal sympathetic nerve fibres; however, depression of both skin (247) and muscle (248) sympathetic nerve activity via barbiturates implies that systemic SNS inhibition is highly likely. In this case, the administration of thiopentalbarbitol may have depressed the input of the SNS on the PN relationship measured in C57BL6/JCrl mice.

Therefore, I propose that increased SNS outflow contributes to the maintenance of salt-induced hypertension via renal α-AR-mediated vasoconstriction, possibly due to increased vascular sensitivity to catecholamines. Initiation of salt-induced hypertension remains undetermined in these mice.

7.2.2 Limitations of this model

The approaches I have used to measure SNS activity in this thesis indicate SNS involvement in salt-induced high BP; however, they only offer a limited insight into its contribution. Due to the complexity of the SNS, non-invasive measurement of urinary catecholamine excretion is used as a surrogate for activity, although it may not be wholly representative of systemic SNS activity. The composition of urinary catecholamines is heavily influenced by the kidney; renal production accounts for 70% of noradrenaline expelled in the urine, leaving only 30% filtered from systemic circulation (237). This excretion of noradrenaline is strongly associated with renal efferent sympathetic nerve activity (249) which is increased in hypertension (250), further supporting that this measure may be more reflective of renal rather than total SNS activity in high BP.

In addition, catecholamine levels are subject to multiple regulatory steps that are not taken into account using this approach, such as synthesis, enzymatic conversion of noradrenaline to adrenaline, recycling, and enzymatic breakdown by catechol-O-methyltransferase and monoamine oxidase.

A further concern is the stability of urinary catecholamines during collection. Due to the presence of a benzene ring within the chemical structure, catecholamines are photosensitive and susceptible to oxidation (251). Experimentally, this means that the initial steps taken to process and store urine samples are crucial for the correct quantification of the catecholamines they contain. Two controllable environmental factors that have a significant impact on the analytical outcome are pH and temperature. Previous research has noted that unless urine samples are acidified to a pH below 3.5, 15-50% displayed catecholamine degradation (252, 253). Similarly, immediate storage within a stabilising reagent, such as an acid, and at a temperature below -20 ºC has been suggested to preserve catecholamine integrity (251, 254). In this thesis, urinary samples were collected, centrifuged, acidified by the addition of hydrochloric acid (pH ~2.0) and stored at -80 ºC. It is possible that an unknown degree of degradation had occurred between the removal of the sample from the metabolic cage to the addition of hydrochloric acid. A potential additive to this approach would be to analyse the concentration of urinary catecholamine metabolites, such as the methyl derivatives metadrenaline and normetadrenaline, as well. These metabolites have been reported to have a much more stable profile in urine, for example studies have revealed that integrity was conserved even after spending a week at room temperature in the absence of a stabilising reagent (253). Thus, the measurement of both urinary catecholamines and their methyl derivatives would not only shed light on the stability of the results obtained from free catecholamine quantification, but also provide information on the status of the metabolism of circulating catecholamines.

Further to this, SNS outflow varies region-by-region – the SNS innervates multiple effector tissues in the body involved in cardiovascular function, each

of which receive individualised input. Hexamethonium acts upon nicotinic receptors, preventing the binding of acetylcholine released from preganglionic neurons and thus the transmission of signals along sympathetic postganglionic neurons to effector tissues. The intermediate steps between this blockade and the modest reduction in BP seen with longer term high salt intake, i.e the mechanisms at the level of the effector tissues, are currently unknown. Regional-specific investigation of SNS activity with high salt intake may shed light on these. Additionally, the application of a different mode of SNS inhibition, for example an alternative pharmacological or mechanical approach that reduces SNS activity, could confirm and further strengthen the role of the SNS in the maintenance of salt-induced hypertension.

Finally, in this thesis, intrinsic renal and vascular function were evaluated. Thus, any external humoral and/or neurogenic regulation of function and so the ability to detect any effects of high salt intake on these may not have been possible. As discussed above, the SNS innervates both the kidneys and the vasculature and exerts a certain level of control over their function. Another system is the RAAS. The extent of its contribution to the salt-induced hypertension observed in C57BL6/JCrl mice has not been evaluated in this thesis. The suppression of plasma aldosterone following 1 and 2 weeks of high salt intake suggested appropriate modulation of this system, however suppression was not observed initially after 3 days high salt intake. Additionally, RAAS is also regulated locally and measurements of local aldosterone and ANGII could more accurately reflect function or even dysfunction with high salt and high BP (255, 256).

7.3 Dietary Salt, Blood Pressure and Cardiovascular Risk

Dietary salt classically refers to sodium chloride, from which we obtain most of our dietary sodium (130). Initially, the sodium ion alone was thought to be responsible for the exaggerated BP response to dietary salt. However, evidence from both experimental models of salt-sensitive hypertension and human disease illuminates the pivotal role of the combination of sodium and

its anion. Other sodium-containing compounds, such as sodium bicarbonate, exist as a source of dietary sodium, however the most substantial effects observed upon BP result from the pairing of sodium with chloride. In a variety of animal models, including the Dahl salt-sensitive rat (257) and the stroke-prone spontaneously hypertensive rat (258), SBP rose significantly on a high sodium chloride diet, whereas SBP on a high sodium bicarbonate diet remained comparable to measurements on a standard diet. When rodents were administered a diet high in each ion individually, minimal BP effects were observed (259, 260). Thus, the development of hypertension was dependent upon the excessive consumption of both ions combined. Similar effects have been recorded within hypertensive humans, for example diets high in sodium paired with the anions bicarbonate (73, 261), phosphate (262) and citrate (263) did not increase BP to the same extent as a diet high in sodium chloride. Therefore, it is essential to consider the collective contribution of sodium and chloride to the initiation and sustainment of salt-induced hypertension, which was done so in this thesis.

In the experiments of Chapter 3, BP rose with increased dietary salt whilst maintaining normal day-night rhythmicity. Encouragingly, and despite enormous heterogeneity, similar BP responses have been noted within humans (60). These, together with numerous animal studies, strengthen the relationship salt has with BP. Hypertension is among the most prominent yet modifiable risk factors of disease worldwide, responsible for over 33% deaths in 2010 (264). There is a strong association with high habitual salt intake and adverse cardiovascular outcomes, such as left-ventricular hypertrophy, stroke and death (68). A meta-analysis performed by Strazzullo *et al*. (18) reported a substantially increased risk of total cardiovascular disease associated with high salt intake; a convincing link which has also been reported across the globe, for example in Japan (265) and throughout Europe (266, 267). This global burden is particularly concerning as there appears to be a direct link between increasing BP and cardiovascular risk

(133). Consequently, every mmHg increase in BP is important and can be detrimental.

The World Health Organisation is currently promoting an ongoing strategy known as SHAKE to reduce worldwide habitual salt intake (268). Evidence has shown that restricting salt intake by ~3g per day reduced BP by an average of 5 mmHg and improved overall cardiovascular risk, for example a 22% reduction in the number of stroke cases is predicted (131, 269, 270). In this work, high dietary salt intake induced an increase in BP, which persisted throughout the experimental period. Following this, the HSD was replaced with the standard salt (0.25% Na) diet received during baseline measurements to investigate the hypothesis that decreasing dietary salt content would also decrease any salt-induced BP changes. BP remained significantly higher than it was at baseline despite 10 days of dietary salt reduction. This unanticipated outcome could be due to the 6-day disruption in the light-day cycle acting as a stressor and so masking or preventing any diet effects. Additionally, many of the studies investigating the impact of dietary sodium restriction upon BP utilise a low salt diet, equivalent to 0.01-0.03% sodium, which is lower by at least 10-fold than the standard salt diet used here. Thus, the drop in the sodium content of the diet administered in this experiment may not have been sufficient to observe any improvement in BP over this time course. Therefore, due to the small number of days that accurate measurements were taken from and the failure of the light-dark cycle, the impact of dietary salt reduction on these salt-induced BP changes could not be determined in this thesis.

Dietary salt is a major modifiable risk factor for the world's most prominent and life-threatening diseases (271). A singular, beneficial effect is a reduction in salt intake. Striving to reduce population salt intake and thus relieve some of this burden, including that upon health systems worldwide, is a priority. However, this poses more of a challenge than anticipated. Studies have illustrated an increased, unconscious drive in heart failure patients to consume salt, thus adherence to a sodium-restricted diet was poor and

uncontrolled (272). Furthermore, hidden salt in supermarket-bought foods is a major source of the dietary intake of salt nowadays. Efforts to reveal and reduce the salt content of manufactured foods are underway; however, in the interim, there is a requirement for other means of intervention.

7.4 Sympathetic Nervous System Inhibition in the Treatment of Hypertension

A recent study has reported that the most effective intervention for salt-sensitive hypertension was a calcium channel antagonist (CCA) paired with the diuretic hydrochlorothiazide in combination with reduced salt intake (273). Although both CCA and diuretics have indirect actions upon the SNS, for example long-term use of the CCA verapamil was found to decrease plasma noradrenaline and heart rate (274), this meta-analysis did not include antihypertensive medication that directly blocks the contribution of the SNS in their action to reduce BP. This could be due to the discontinued use of some central sympatholytic mediators, such as clonidine, as they bring on undesirable side-effects through their action on α_2-ARs, such as nausea, drowsiness and rebound hypertension (275).

However, second-generation sympatholytic agents have been tested and found to reduce BP effectively without affecting quality of life. One such agent is moxonidine, a centrally acting agonist that strongly binds central nonadrenergic imidazoline (I_1)-receptors over α_2-ARs. A double-blind placebo-controlled trial observed beneficial effects in both normotensive and hypertensive humans, as moxonidine reduced muscle sympathetic nerve activity and plasma noradrenaline concentration compared to the placebo. BP reduction was also seen in both groups and was attributed to the inhibition of central sympathetic nerve outflow (276). Other studies have noted this effect to correlate significantly with I_1-receptor occupation (277). Moxonidine has been well-received thus far with few reports of unfavourable side-effects, potentially due to its stronger affinity for I_1-receptors rather than α_2-ARs. Despite its clearance by the kidneys, dosages in accordance with estimated GFR have been proven safe in the treatment of hypertension

accompanied by renal injury (278). Controlled trials exist in which moxonidine has been compared with other popular first-line antihypertensives, for example hydrochlorothiazide (279) and the CCA nifedipine (280). In both these studies, moxonidine demonstrated comparable hypotensive effects with equal or even improved tolerability. Thus, these findings show that moxonidine can successfully reduce BP, either alone or in combination with other first-line medications in the treatment of hypertension.

In addition to BP reduction, SNS inhibition has also been shown to improve other conditions and pathologies associated with high salt and an increased risk for CVD. In hypertensive obese rats, moxondine administration normalised BP exacerbated by high salt intake, whilst also improving glucose tolerance, dyslipidaemia and hyperinsulinemia (281). Further, treatment even partially reversed renal injury accelerated by high salt (281), illustrating that SNS inhibition may counteract the adverse effects of salt which contribute to an individual's disease risk and/or progression. This highlights the potential benefit of clinical intervention.

7.4.1 Renal denervation and resistant hypertension

In cases whereby antihypertensive medication does little to curb or maintain control of hypertension, referred to as resistant hypertension, additional intervention is necessary. RDN is a possible option; however, mixed results regarding its effectiveness have been reported over the last decade (282-284).

The relationship between salt-sensitivity, hypertension and the potential benefits of RDN has been investigated in both animals and humans. In the Dahl salt-sensitive rat strain, RDN did not curtail the initiation of salt-induced hypertension, as increases in BP were seen just 24 hours after high salt feeding in rats with intact and removed renal nerves (285). However, when these rats were underwent RDN after 3 weeks of high salt intake, a substantial decrease in MABP was observed, illustrating RDN potentially has a role in the amelioration of sustained salt-induced hypertension (286).

In humans, studies have noted both the presence and absence of increased sympathetic nerve activity accompanying resistant hypertension, which could potentially explain why the benefits of RDN are not experienced universally. The implications here are that those with hypertension characterised by increased SNS activity may benefit from RDN. Thus, the ability to detect increased activity is key in the recommendation of this intervention. Recently, de Beus *et al*. (287) measured the effects of RDN on urinary sodium excretion and BP in patients with resistant hypertension. They report that, 6 months after RDN, BP had indeed decreased, however this was unrelated to urinary sodium excretion or salt-sensitive status (287). Thus, urinary sodium excretion, as a measure of dietary salt intake, could not be used in this study to infer whether a patient would benefit from RDN or not.

7.5 Conclusion

The work in this thesis evidences a possible role for increased SNS drive in the maintenance of salt-induced hypertension, potentially via increased α_1-AR vasoconstriction, in C57BL6/JCrl mice. Initiation of hypertension in response to high salt intake remains unclear in this mouse, as we have demonstrated that renal function adapts appropriately to the increase in salt and pressure. Advancing our knowledge of the salt-induced mechanisms driving the initiation and sustainment of salt-induced hypertension could lead to the development of targeted, individualised interventions in a salt-saturated society.

References

1. Rodriguez-Iturbe B, Romero F, Johnson RJ. Pathophysiological mechanisms of salt-dependent hypertension. *Am J Kidney Dis*. 2007;**50**(4):655-72.

2. Stanaway JD, Afshin A, Gakidou E, Lim SS, Abate D, Abate KH, et al. Global, regional, and national comparative risk assessment of 84 behavioural, environmental and occupational, and metabolic risks or clusters of risks for 195 countries and territories, 1990–2017: a systematic analysis for the Global Burden of Disease Study 2017. *The Lancet*. 2018;**392**(10159):1923-94.

3. WHO. Guideline: sodium intake for adults and children [Online report]. Geneva: World Health Organisation (WHO); 2012 [cited 2020 16/02]. Available from: https://www.who.int/nutrition/publications/guidelines/sodium_intake_printversion.pdf.

4. WHO. A comprehensive global monitoring framework including indicators and a set of voluntary global targets for the prevention and control of noncommunicable diseases. Revised WHO discussion paper Geneva, Switzerland: World Health Organisation (WHO); 2012 [updated 25/07/2012; cited 2020 16/02]. Available from: https://www.who.int/nmh/events/2012/discussion_paper2_20120322.pdf.

5. Brown IJ, Tzoulaki I, Candeias V, Elliott P. Salt intakes around the world: implications for public health. *Int J Epidemiol*. 2009;**38**(3):791-813.

6. Powles J, Fahimi S, Micha R, Khatibzadeh S, Shi P, Ezzati M, et al. Global, regional and national sodium intakes in 1990 and 2010: a systematic analysis of 24 h urinary sodium excretion and dietary surveys worldwide. *BMJ Open*. 2013;**3**(12):e003733.

7. Thout SR, Santos JA, McKenzie B, Trieu K, Johnson C, McLean R, et al. The Science of Salt: Updating the evidence on global estimates of salt intake. *J Clin Hypertens (Greenwich)*. 2019;**21**(6):710-21.

8. He FJ, MacGregor GA. Reducing population salt intake worldwide: from evidence to implementation. *Prog Cardiovasc Dis*. 2010;**52**(5):363-82.

9. Henderson L, Irving K, Gregory J, Bates CJ, Prentice A, Perks J, et al. National Diet & Nutrition Survey: Adults Aged 19 to 64. London, England: Elseiver Science; 2003 [cited 2020 16/02]. Available from: https://sp.ukdataservice.ac.uk/doc/5140/mrdoc/pdf/5140userguide.pdf.

10. Anderson CA, Appel LJ, Okuda N, Brown IJ, Chan Q, Zhao L, et al. Dietary sources of sodium in China, Japan, the United Kingdom, and the

United States, women and men aged 40 to 59 years: the INTERMAP study. *J Am Diet Assoc*. 2010;**110**(5):736-45.

11. Laatikainen T, Pietinen P, Valsta L, Sundvall J, Reinivuo H, Tuomilehto J. Sodium in the Finnish diet: 20-year trends in urinary sodium excretion among the adult population. Eur J Clin Nutr. 2006;**60**(8):965-70.

12. Pietinen P, Valsta LM, Hirvonen T, Sinkko H. Labelling the salt content in foods: a useful tool in reducing sodium intake in Finland. *Public Health Nutr*. 2008;**11**(4):335-40.

13. Webster JL, Dunford EK, Hawkes C, Neal BC. Salt reduction initiatives around the world. *J Hypertens*. 2011;**29**(6):1043-50.

14. Sadler K, Nicholson S, Steer T, Valdeep G, Bates B, Tipping S, et al. National Diet and Nutrition Survey - Assessment of dietary sodium in adults (aged 19 to 64 years) in England, 2011: Department of Health; 2012 [Available from: https://assets.publishing.service.gov.uk/government/uploads/system/uploads/attachment_data/file/213420/Sodium-Survey-England-2011_Text_to-DH_FINAL1.pdf.

15. He FJ, Brinsden HC, MacGregor GA. Salt reduction in the United Kingdom: a successful experiment in public health. *J Hum Hypertens*. 2014;**28**(6):345-52.

16. FSA. Guide to creating a front of pack (FoP) nutrition label for pre-packed products sold through retail outlets Department of Health: Food Standards Agency; 2016 [cited 2020 08/02]. Available from: https://www.food.gov.uk/sites/default/files/media/document/fop-guidance_0.pdf.

17. Bibbins-Domingo K, Chertow GM, Coxson PG, Moran A, Lightwood JM, Pletcher MJ, et al. Projected effect of dietary salt reductions on future cardiovascular disease. *N Engl J Med*. 2010;**362**(7):590-9.

18. Strazzullo P, D'Elia L, Kandala NB, Cappuccio FP. Salt intake, stroke, and cardiovascular disease: meta-analysis of prospective studies. *BMJ*. 2009;**339**:b4567.

19. Xie JX, Sasaki S, Joossens JV, Kesteloot H. The relationship between urinary cations obtained from the intersalt study and cerebrovascular mortality. *J Hum Hypertens*. 1992;**6**(1):17-21.

20. Kupari M, Koskinen P, Virolainen J. Correlates of left ventricular mass in a population sample aged 36 to 37 years. Focus on lifestyle and salt intake. *Circulation*. 1994;**89**(3):1041-50.

21. Cook NR, Cutler JA, Obarzanek E, Buring JE, Rexrode KM, Kumanyika SK, et al. Long term effects of dietary sodium reduction on cardiovascular disease outcomes: observational follow-up of the trials of hypertension prevention (TOHP). *BMJ*. 2007;**334**(7599):885-8.

22. He FJ, MacGregor GA. Salt reduction lowers cardiovascular risk: meta-analysis of outcome trials. *Lancet*. 2011;**378**(9789):380-2.

23. Puska P, Vartiainen E, Tuomilehto J, Salomaa V, Nissinen A. Changes in premature deaths in Finland: successful long-term prevention of cardiovascular diseases. *Bull World Health Organ*. 1998;**76**(4):419-25.

24. Mente A, O'Donnell M, Rangarajan S, McQueen M, Dagenais G, Wielgosz A, et al. Urinary sodium excretion, blood pressure, cardiovascular disease, and mortality: a community-level prospective epidemiological cohort study. *Lancet*. 2018;**392**(10146):496-506.

25. Arnlöv J, Evans JC, Meigs JB, Wang TJ, Fox CS, Levy D, et al. Low-grade albuminuria and incidence of cardiovascular disease events in nonhypertensive and nondiabetic individuals - The Framingham heart study. *Circulation*. 2005;**112**(7):969-75.

26. Verhave JC, Hillege HL, Burgerhof JGM, Janssen WMT, Gansevoort RT, Navis GJ, et al. Sodium intake affects urinary albumin excretion especially in overweight subjects. *J Intern Med*. 2004;**256**(4):324-30.

27. He FJ, Marciniak M, Visagie E, Markandu ND, Anand V, Dalton RN, et al. Effect of modest salt reduction on blood pressure, urinary albumin, and pulse wave velocity in white, black, and Asian mild hypertensives. *Hypertension*. 2009;**54**(3):482-8.

28. Slagman MC, Waanders F, Hemmelder MH, Woittiez AJ, Janssen WM, Lambers Heerspink HJ, et al. Moderate dietary sodium restriction added to angiotensin converting enzyme inhibition compared with dual blockade in lowering proteinuria and blood pressure: randomised controlled trial. *BMJ*. 2011;**343**:d4366.

29. He FJ, Markandu ND, Sagnella GA, MacGregor GA. Effect of salt intake on renal excretion of water in humans. *Hypertension*. 2001;**38**(3):317-20.

30. He FJ, Marrero NM, MacGregor GA. Salt intake is related to soft drink consumption in children and adolescents: a link to obesity? *Hypertension*. 2008;**51**(3):629-34.

31. Vartanian LR, Schwartz MB, Brownell KD. Effects of soft drink consumption on nutrition and health: a systematic review and meta-analysis. *Am J Public Health*. 2007;**97**(4):667-75.

32. D'Elia L, Rossi G, Ippolito R, Cappuccio FP, Strazzullo P. Habitual salt intake and risk of gastric cancer: a meta-analysis of prospective studies. *Clin Nutr*. 2012;**31**(4):489-98.

33. Kleinewielfeld M. Sodium chloride drives autoimmune disease by the induction of pathogenic TH17 cells. *Nature*. 2013;**496**(7446):518-22.

34. Scrivo R, Massaro L, Barbati C, Vomero M, Ceccarelli F, Spinelli FR, et al. The role of dietary sodium intake on the modulation of T helper 17 cells and regulatory T cells in patients with rheumatoid arthritis and systemic lupus erythematosus. *PLoS One*. 2017;**12**(9):e0184449.

35. Farez MF, Fiol MP, Gaitan MI, Quintana FJ, Correale J. Sodium intake is associated with increased disease activity in multiple sclerosis. *J Neurol Neurosurg Psychiatry*. 2015;**86**(1):26-31.

36. Thomas MC, Moran J, Forsblom C, Harjutsalo V, Thorn L, Ahola A, et al. The association between dietary sodium intake, ESRD, and all-cause mortality in patients with type 1 diabetes. *Diabetes Care*. 2011;**34**(4):861-6.

37. Ekinci EI, Clarke S, Thomas MC, Moran JL, Cheong K, MacIsaac RJ, et al. Dietary salt intake and mortality in patients with type 2 diabetes. *Diabetes Care*. 2011;**34**(3):703-9.

38. Dahl LK. Possible role of chronic excess salt consumption in the pathogenesis of essential hypertension. *Am J Cardiol*. 1961;**8**(4):571-5.

39. Dahl LK. Salt and hypertension. *Am J Clin Nutr*. 1972;**25**(2):231-44.

40. Froment A, Milon H, Gravier C. Relationship of sodium intake and arterial hypertension. Contribution of geographical epidemiology. *Rev Epidemiol Sante Publique*. 1979;**27**:437-54.

41. Oliver WJ, Cohen EJ, Neel JV. Blood pressure, sodium intake, and sodium related hormones in the Yanomamo Indians, a "no-salt" culture. *Circulation*. 1975;**52**:146-51.

42. Intersalt. Intersalt: an international study of electrolyte excretion and blood pressure. Results for 24 hour urinary sodium and potassium excretion. Intersalt Cooperative Research Group. *BMJ*. 1988;**297**(6644):319-28.

43. Elliott P, Stamler J, Nichols R, Dyer A, Stamler R, Kesteloot H, et al. Intersalt revisited: further analyses of 24 hour sodium excretion and blood pressure within and across populations. Intersalt Cooperative Research Group. *BMJ*. 1996;**312**(7041):1249-53.

44. Hanneman RL. Intersalt: hypertension rise with age revisited. *BMJ*. 1996;**312**(7041):1283-4.

45. Midgley JP, Matthew AG, Greenwood CM, Logan AG. Effect of reduced dietary sodium on blood pressure: a meta-analysis of randomized controlled trials. *JAMA*. 1996;**275**(20):1590-7.

46. He FJ, MacGregor GA. Effect of modest salt reduction on blood pressure: a meta-analysis of randomized trials. Implications for public health. *J Hum Hypertens*. 2002;**16**(11):761-70.

47. Graudal NA, Galløe AM, Garred P. Effects of sodium restriction on blood pressure, renin, aldosterone, catecholamines, cholesterols, and triglyceride. A meta-analysis. *JAMA*. 1998;**279**:1383-91.

48. Hooper L, Bartlett C, Davey Smith G, Ebrahim S. Systematic review of long term effects of advice to reduce dietary salt in adults. *BMJ*. 2002;**325**(7365):628.

49. Obarzanek E, Proschan MA, Vollmer WM, Moore TJ, Sacks FM, Appel LJ, et al. Individual blood pressure responses to changes in salt intake: results from the DASH-Sodium trial. *Hypertension*. 2003;**42**(4):459-67.

50. Miller JZ, Daugherty SA, Weinberger MH, Grim CE, Christian JC, Lang CL. Blood pressure response to dietary sodium restriction in normotensive adults. *Hypertension*. 1983;**5**(5):790-5.

51. Dahl LK, Love RA. Evidence of relationship between sodium (chloride) intake and human essential hypertension. *Arch Intern Med*. 1954;**94**:525.

52. Dahl LK. Effects of chronic excess salt feeding. Induction of self-sustaining hypertension in rats. *J Exp Med*. 1961;**114**:231-6.

53. Dahl LK, Heine M, Tassinari L. Effects of chronic salt ingestion: evidence that genetic factors play an important role in susceptibility to experimental hypertension. *J Exp Med*. 1962;**115**:1173-90.

54. Dahl LK, Heine M, Tassinari L. Role of genetic factors in susceptibility to experimental hypertension due to chronic excess salt ingestion. *Nature*. 1962;**194**:480-2.

55. Rapp JP, Dene H. Development and characteristics of inbred strains of Dahl salt-sensitive and salt-resistant rats. *Hypertension*. 1985;**7**:340-9.

56. Lerman LO, Kurtz TW, Touyz RM, Ellison DH, Chade AR, Crowley SD, et al. Animal models of hypertension: a scientific statement from the American Heart Association. *Hypertension*. 2019;**73**(6):e87-e120.

57. Hall JE. Renal dysfunction, rather than nonrenal vascular dysfunction, mediates salt-induced hypertension. *Circulation*. 2016;**133**(9):894-906.

58. Kawasaki T, Delea CS, Bartter FC, Smith H. The effect of high-sodium and low-sodium intakes on blood pressure and other related variables in human subjects with idiopathic hypertension. *Am J Med*. 1978;**64**(2):193-8.

59. Weinberger MH, Fineberg NS, Fineberg SE, Weinberger M. Salt sensitivity, pulse pressure, and death in normal and hypertensive humans. *Hypertension*. 2001;**37**(2 Pt 2):429-32.

60. Weinberger MH. Salt sensitivity of blood pressure in humans. *Hypertension*. 1996;**27**(3 Pt 2):481-90.

61. Weinberger MH, Fineberg NS. Sodium and volume sensitivity of blood pressure. Age and pressure change over time. *Hypertension*. 1991;**18**(1):67-71.

62. Weinberger MH, Miller J, Luft F, Grim C, Fineberg N. Definitions and characteristics of sodium sensitivity and blood pressure resistance. *Hypertension*. 1986;**8**(6):127-34.

63. Miller JZ, Weinberger MH, Christian JC, Daugherty SA. Familial resemblance in the blood pressure response to sodium restriction. *Am J Epidemiol*. 1987;**126**(5):822-30.

64. Svetkey LP, McKeown SP, Wilson AF. Heritability of salt sensitivity in black Americans. *Hypertension*. 1996;**28**(5):854-8.

65. Carey RM, Schoeffel CD, Gildea JJ, Jones JE, McGrath HE, Gordon LN, et al. Salt sensitivity of blood pressure is associated with polymorphisms in the sodium-bicarbonate cotransporter. *Hypertension*. 2012;**60**(5):1359-66.

66. Beeks E, Kessels AG, Kroon AA, van der Klauw MM, de Leeuw PW. Genetic predisposition to salt-sensitivity: a systematic review. *J Hypertens*. 2004;**22**(7):1243-9.

67. Felder RA, White MJ, Williams SM, Jose PA. Diagnostic tools for hypertension and salt sensitivity testing. *Curr Opin Nephrol Hypertens*. 2013;**22**(1):65-76.

68. Morimoto A, Uzu T, Fujii T, Nishimura M, Kuroda S, Nakamura S, et al. Sodium sensitivity and cardiovascular events in patients with essential hypertension. *Lancet*. 1997;**350**(9093):1734-7.

69. Bigazzi R, Bianchi S, Baldari D, Sgherri G, Baldari G, Campese VM. Microalbuminuria in salt-sensitive patients. A marker for renal and cardiovascular risk factors. *Hypertension*. 1994;**23**(2):195-9.

70. Uzu T, Kazembe FS, Ishikawa K, Nakamura S, Inenaga T, Kimura G. High sodium sensitivity implicates nocturnal hypertension in essential hypertension. *Hypertension*. 1996;**28**(1):139-42.

71. Uzu T, Ishikawa K, Fujii T, Nakamura S, Inenaga T, Kimura G. Sodium restriction shifts circadian rhythm of blood pressure from nondipper to dipper in essential hypertension. *Circulation*. 1997;**96**(6):1859-62.

72. Luft FC, Rankin LI, Bloch R, Weyman AE, Willis LR, Murray RH, et al. Cardiovascular and humoral responses to extremes of sodium intake in normal black and white men. *Circulation*. 1979;**60**(3):697-706.

73. Schmidlin O, Sebastian A, Morris RC, Jr. What initiates the pressor effect of salt in salt-sensitive humans? Observations in normotensive blacks. *Hypertension*. 2007;**49**(5):1032-9.

74. Kato N, Kanda T, Sagara M, Bos A, Moriguchi EH, Moriguchi Y, et al. Proposition of a feasible protocol to evaluate salt sensitivity in a population-based setting. *Hypertens Res*. 2002;**25**(6):801-9.

75. Esteva-Font C, Wang X, Ars E, Guillen-Gomez E, Sans L, Gonzalez Saavedra I, et al. Are sodium transporters in urinary exosomes reliable markers of tubular sodium reabsorption in hypertensive patients? *Nephron Physiol*. 2010;**114**(3):p25-34.

76. Coffman TM. Under pressure: the search for the essential mechanisms of hypertension. *Nat Med*. 2011;**17**(11):1402-9.

77. Guyton AC, Coleman TG, Granger HJ. Circulation: overall regulation. *Ann Rev Physiol*. 1972;**34**:13-46.

78. Guyton AC. The surprising kidney-fluid mechanism for pressure control – its infinite gain! *Hypertension*. 1990;**16**:725-30.

79. Mullins LJ, Bailey MA, Mullins JJ. Hypertension, kidney, and transgenics: a fresh perspective. *Physiol Rev*. 2006;**86**(2):709-46.

80. Koomans HA, Roos JC, Boer P, Geyskes GG, Mees EJ. Salt sensitivity of blood pressure in chronic renal failure. Evidence for renal control of body fluid distribution in man. *Hypertension*. 1982;**4**(2):190-7.

81. Konishi Y, Okada N, Okamura M, Morikawa T, Okumura M, Yoshioka K, et al. Sodium sensitivity of blood pressure appearing before hypertension and related to histological damage in immunoglobulin A nephropathy. *Hypertension*. 2001;**38**(1):81-5.

82. Hall JE, Guyton AC, Brands MW. Pressure-volume regulation in hypertension. *Kidney Int Suppl*. 1996;**55**:S35-41.

83. Curtis JJ, Luke RG, Dustan HP, Kashgarian M, Whelchel JD, Jones P, et al. Remission of essential hypertension after renal transplantation. *N Engl J Med*. 1983;**309**(17):1009-15.

84. Hall JE, Mizelle HL, Woods LL, Montani JP. Pressure natriuresis and control of arterial pressure during chronic norepinephrine infusion. *J Hypertens*. 1988;**6**(9):723-31.

85. Hall JE. The kidney, hypertension, and obesity. *Hypertension*. 2003;**41**(3):625-33.

86. Palmer LG, Schnermann J. Integrated control of Na transport along the nephron. *Clin J Am Soc Nephrol*. 2015;**10**(4):676-87.

87. Zhao Q, Gu D, Hixson JE, Liu DP, Rao DC, Jaquish CE, et al. Common variants in epithelial sodium channel genes contribute to salt sensitivity of blood pressure: The GenSalt study. *Circ Cardiovasc Genet*. 2011;**4**(4):375-80.

88. Trudu M, Janas S, Lanzani C, Debaix H, Schaeffer C, Ikehata M, et al. Common noncoding UMOD gene variants induce salt-sensitive hypertension and kidney damage by increasing uromodulin expression. *Nat Med*. 2013;**19**(12):1655-60.

89. Hall JE, Guyton AC, Smith MJ, Jr., Coleman TG. Blood pressure and renal function during chronic changes in sodium intake: role of angiotensin. *Am J Physiol Ren Physiol*. 1980;**239**(3):F271-80.

90. Funder JW, Carey RM, Fardella C, Gomez-Sanchez CE, Mantero F, Stowasser M, et al. Case detection, diagnosis, and treatment of patients with primary aldosteronism: An endocrine society clinical practice guideline. *J Clin Endocrinol Metab*. 2008;**93**(9):3266-81.

91. Brilla CG, Weber KT. Mineralocorticoid excess, dietary sodium, and myocardial fibrosis. *J Lab Clin Med*. 1992;**120**(6):893-901.

92. Morris RC, Jr, Schmidlin O, Sebastian A, Tanaka M, Kurtz TW. Vasodyfunction that involves renal vasodysfunction, not abnormally increased renal retention of sodium, accounts for the initiation of salt-induced hypertension. *Circulation*. 2016;**133**(9):881-93.

93. Mark AL, Lawton WJ, Abboud FM, Fitz AE, Connor WE, Heistad DD. Effects of high and low sodium intake on arterial pressure and forearm vascular resistance in borderline hypertension. A preliminary report. *Circ Res*. 1975;**36**(6 Suppl 1):194-8.

94. Touyz RM, Alves-Lopes R, Rios FJ, Camargo LL, Anagnostopoulou A, Arner A, et al. Vascular smooth muscle contraction in hypertension. *Cardiovasc Res*. 2018;**114**(4):529-39.

95. Furchgott RF, Zawadzki JV. The obligatory role of endothelial cells in the relaxation of arterial smooth muscle by acetylcholine. *Nature*. 1980;**288**(5789):373-6.

96. Deanfield JE, Halcox JP, Rabelink TJ. Endothelial function and dsyfunction. *Circulation*. 2007;**115**:1285-95.

97. Corson MA, James NL, Latta SE, Nerem RM, Berk BC, Harrison DG. Phosphorylation of endothelial nitric oxide synthase in response to fluid shear stress. *Circ Res*. 1996;**79**(5):984-91.

98. Miyoshi A, Suzuki H, Fujiwara M, Masai M, Iwasaki T. Impairment of endothelial function in salt-sensitive hypertension in humans. *Am J Hypertens*. 1997;**10**(10 Pt 1):1083-90.

99. Tzemos N, Lim PO, Wong S, Struthers AD, MacDonald TM. Adverse cardiovascular effects of acute salt loading in young normotensive individuals. *Hypertension*. 2008;**51**(6):1525-30.

100. Jablonski KL, Racine ML, Geolfos CJ, Gates PE, Chonchol M, McQueen MB, et al. Dietary sodium restriction reverses vascular endothelial dysfunction in middle-aged/older adults with moderately elevated systolic blood pressure. *J Am Coll Cardiol*. 2013;**61**(3):335-43.

101. DuPont JJ, Greaney JL, Wenner MM, Lennon-Edwards SL, Sanders PW, Farquhar WB, et al. High dietary sodium intake impairs endothelium-dependent dilation in healthy salt-resistant humans. *J Hypertens*. 2013;**31**(3):530-6.

102. Barić L, Drenjancevic I, Matic A, Stupin M, Kolar L, Mihaljevic Z, et al. Seven-day salt loading impairs microvascular endothelium-dependent vasodilation without changes in blood pressure, body composition and fluid status in healthy young humans. *Kidney Blood Press Res*. 2019;**44**(4):835-47.

103. Yeboah J, Folsom AR, Burke GL, Johnson C, Polak JF, Post W, et al. Predictive value of brachial flow-mediated dilation for incident cardiovascular events in a population-based study: the multi-ethnic study of atherosclerosis. *Circulation*. 2009;**120**(6):502-9.

104. Chen PY, Gladish RD, Sanders PW. Vascular smooth muscle nitric oxide synthase anomalies in Dahl/Rapp salt-sensitive rats. *Hypertension*. 1998;**31**(4):918-24.

105. Tolins JP, Shultz PJ. Endogenous nitric oxide synthesis determines sensitivity to the pressor effect of salt. *Kidney Int*. 1994;**46**(1):230-6.

106. Chen PY, Sander PW. L-arginine abrogates salt-sensitive hypertension in Dahl/Rapp rats. *J Clin Invest*. 1991;**88**(5):1559-67.

107. Nurkiewicz TR, Wu G, Li P, Boegehold MA. Decreased arteriolar tetrahydrobiopterin is linked to superoxide generation from nitric oxide synthase in mice fed high salt. *Microcirculation*. 2010;**17**(2):147-57.

108. Landmesser U, Dikalov S, Price SR, McCann L, Fukai T, Holland SM, et al. Oxidation of tetrahydrobiopterin leads to uncoupling of endothelial cell nitric oxide synthase in hypertension. *J Clin Invest*. 2003;**111**(8):1201-9.

109. Machnik A, Neuhofer W, Jantsch J, Dahlmann A, Tammela T, Machura K, et al. Macrophages regulate salt-dependent volume and blood pressure by a vascular endothelial growth factor-C-dependent buffering mechanism. *Nat Med*. 2009;**15**(5):545-52.

110. Lu X, Crowley SD. Inflammation in salt-sensitive hypertension and renal damage. *Curr Hypertens Rep*. 2018;**20**(12):103.

111. Evans LC, Ivy JR, Wyrwoll C, McNairn JA, Menzies RI, Christensen TH, et al. Conditional deletion of Hsd11b2 in the brain causes salt appetite and hypertension. *Circulation*. 2016;**133**(14):1360-70.

112. Carlson SH, Wyss JM. Long-term telemetric recording of arterial pressure and heart rate in mice fed basal and high NaCl diets. *Hypertension*. 2000;**35**(2):E1-5.

113. Sanders PW. Salt-sensitive hypertension: lessons from animal models. *Am J Kidney Dis*. 1996;**28**:775-82.

114. Elijovich F, Weinberger MH, Anderson CA, Appel LJ, Bursztyn M, Cook NR, et al. Salt sensitivity of blood pressure: a scientific statement from the American Heart Association. *Hypertension*. 2016;**68**(3):e7-e46.

115. Bailey MA, Craigie E, Livingstone DEW, Kotelevtsev YV, Al-Dujaili EAS, Kenyon CJ, et al. Hsd11b2 haploinsufficiency in mice causes salt sensitivity of blood pressure. *Hypertension*. 2011;**57**(3):515-20.

116. Bertorello AM, Pires N, Igreja B, Pinho MJ, Vorkapic E, Wågsäter D, et al. Increased arterial blood pressure and vascular remodelling in mice lacking salt-inducible kinase 1 (SIK1). *Circ Res*. 2015;**116**:642-52.

117. Hartner A, Cordasic N, Klanke B, Veelken R, Hilgers KF. Strain differences in the development of hypertension and glomerular lesions

induced by deoxycorticosterone acetate salt in mice. *Nephrol Dial Transplant*. 2003;**18**(10):1999-2004.

118. Jönsson S, Becirovic-Agic M, Isackson H, Tveitaras MK, Skogstrand T, Narfstrom F, et al. Angiotensin II and salt-induced decompensation in Balb/CJ mice is aggravated by fluid retention related to low oxidative stress. *Am J Physiol Renal Physiol*. 2019;**316**(5):F914-F33.

119. Mangrum AJ, Gomez RA, Norwood VF. Effects of AT(1A) receptor deletion on blood pressure and sodium excretion during altered dietary salt intake. *Am J Physiol Renal Physiol*. 2002;**283**(3):F447-F53.

120. Kopkan L, Hess A, Huskova Z, Cervenka L, Navar LG, Majid DS. High-salt intake enhances superoxide activity in eNOS knockout mice leading to the development of salt sensitivity. *Am J Physiol Renal Physiol*. 2010;**299**(3):F656-63.

121. Oliverio MI, Best CF, Smithies O, Coffman TM. Regulation of sodium balance and blood pressure by the AT(1A) receptor for angiotensin II. *Hypertension*. 2000;**35**(2):550-4.

122. Combe R, Mudgett J, El Fertak L, Champy M, Ayme-Dietrich E, Petit-Demouliere B, et al. How does circadian rhythm impact salt sensitivity of blood pressure in mice? A study in two close C57Bl/6 substrains. *PLoS One*. 2016;**11**(4):e153472.

123. Helkamaa T, Mannisto PT, Rauhala P, Cheng ZJ, Finckenberg P, Huotari M, et al. Resistance to salt-induced hypertension in catechol-O-methyltransferase-gene-disrupted mice. *J Hypertens*. 2003;**21**(12):2365-74.

124. Qi Z, Whitt I, Mehta A, Jin J, Zhao M, Harris RC, et al. Serial determination of glomerular filtration rate in conscious mice using FITC-inulin clearance. *Am J Physiol Renal Physiol*. 2004;**286**(3):F590-6.

125. Cicinnati VR, Shen Q, Sotiropoulos GC, Radtke A, Gerken G, Beckebaum S. Validation of putative reference genes for gene expression studies in human hepatocellular carcinoma using real-time quantitative RT-PCR. *BMC Cancer*. 2008;**8**:350.

126. Majewski J, Ott J. Distribution and characterization of regulatory elements in the human genome. *Genome Res*. 2002;**12**:1827-36.

127. Ayakannu T, Taylor AH, Willets JM, Brown L, Lambert DG, McDonald J, et al. Validation of endogenous control reference genes for normalizing gene expression studies in endometrial carcinoma. *Mol Hum Reprod*. 2015;**21**(9):723-35.

128. Prince R. Wire myograph: Pharmacology Teaching Material [Figure]. United Kingdom2015 [cited 2019 21/10]. Available from: https://personalpages.manchester.ac.uk/staff/richard.prince/.

129. Hoppe CC, Mortiz KM, Fitzgerald SM, Bertram JF, Evans RG. Transient hypertension and sustained tachycardia in mice housed individually in metabolism cages. *Physiol Res*. 2009;**58**:69-75.

130. Kotchen TA, Cowley AW, Frohlich ED. Salt in health and disease — a delicate balance. *N Engl J Med*. 2013;**368**:1229-37.

131. Asaria P, Chrisholm D, Mathers C, Ezzati M, Beaglehole R. Chronic disease prevention: health effects and financial costs of strategies to reduce salt intake and control tobacco use. *Lancet*. 2007;**370**(9604):2044-53.

132. Mozaffarian D, Fahimi S, Singh GM, Micha R, Khatibzadeh S. Global sodium consumption and death from cariovascular causes. *N Engl J Med*. 2014;**371**(7):624-34.

133. Lewington S, Clarke R, Qizilbash N, Peto R, Collins R, Prospective Studies C. Age-specific relevance of usual blood pressure to vascular mortality: a meta-analysis of individual data for one million adults in 61 prospective studies. *Lancet*. 2002;**360**(9349):1903-13.

134. Van Huysse JW, Amin MS, Yang B, Leenen FHH. Salt-induced hypertension in a mouse model of Liddle's syndrome is mediated by epithelial sodium channels in the brain. *Hypertension*. 2012;**60**(3):691-6.

135. Van Vliet BN, Chafet LL, Montani JP. Characteristics of 24 h telemetered blood pressure in eNOS-knockout and C57Bl/6J control mice. *J Physiol*. 2003;**15**(549):313-25.

136. Leelahavanichkul A, Yan Q, Hu X, Eisner C, Huang Y, Chen R, et al. Rapid CKD progression in a new mouse kidney remnant model: strain-dependent resistance is overcome by angiontensin II. *Kidney Int*. 2010;**78**(11):1136-53.

137. Feng M, Whitesall S, Zhang Y, Beibel M, D'Alecy L, DiPetrillo K. Validation of volume-pressure recording tail-cuff blood pressure measurements. *Am J Hypertens*. 2008;**21**(12):1288-91.

138. Krege JH, Hodgin JB, Hagaman JR, Smithies O. A noninvasive computerized tail-cuff system for measuring blood pressure in mice. *Hypertension*. 1995;**25**(5):1111-5.

139. Hem NA, Phie J, Chilton L, Kinobe R. A volume-pressure tail cuff method for hemodynamic parameters: Comparison of restraint and light

isoflurane anesthesia in normotensive male Lewis rats. *J Pharmacol Toxicol Methods*. 2019;**100**:106601.

140. Gross V. Exercising restraint in measuring blood pressure in conscious mice. *Hypertension*. 2003;**41**(4):879-81.

141. Kramer K, Remie R. Hypertension: Methods and Protocols. 108 ed. New Jersey: Humana Press Inc.; 2005.

142. Mattson DL. Long-term measurement of arterial blood pressure in conscious mice. *Am J Physiol*. 1998;**274**(2):R564-70.

143. Kurtz TW, Griffin KA, Bidani AK, Davisson RL, Hall JE. Recommendations for blood pressure measurement in humans and experimental animals. *Arterioscler Thromb Vasc Biol*. 2005;**25**(3):22-33.

144. Mills PA, Huetteman DA, Brockway BP, Zwiers LM, Gelsema AJ, Schwartz RS, et al. A new method for measurement of blood pressure, heart rate, and activity in the mouse by radiotelemetry. *J Appl Physiol (1985)*. 2000;**88**(5):1537-44.

145. McGuire JJ, Van Vliet BN, Halfyard SJ. Blood pressures, heart rate and locomotor activity during salt loading and angiotensin II infusion in protease-activated receptor 2 (PAR2) knockout mice. *BMC Physiol*. 2008;**8**:20.

146. Sheward WJ, Naylor E, Knowles-Barley S, Armstrong JD, Brooker GA. Circadian control of mouse heart rate and blood pressure by the suprachiasmatic nuclei: behavioral effects are more significant than direct outputs. *PLoS One*. 2010;**22**(5):e9783.

147. Douma LG, Gumz ML. Circadian clock-mediated regulation of blood pressure. *Free Radic Biol Med*. 2018;**119**:108-14.

148. Elliott WJ. Circadian variation in the timing of stroke onset: a meta-analysis. *Stroke*. 1998;**29**(5):992-6.

149. De la Sierra A, Gorostidi M, Banegas JR, Segura J, de la Cruz JJ, Ruilope LM. Nocturnal hypertension or nondipping: which is better associated with the cardiovascular risk profile? *Am J Hypertens*. 2014;**27**(5):680-7.

150. Friedman O, Logan AG. Can nocturnal hypertension predict cardiovascular risk? *Integr Blood Press Control*. 2009;**2**:25-37.

151. Todd WD, Gall AJ, Weiner JA, Blumberg MS. Distinct retinohypothalamic innervation patterns predict the developmental emergence of species-typical circadian phase preference in nocturnal norway rats and diurnal nile grass rats. J *Comp Neurol*. 2012;**520**(14):3277-92.

152. Sanmarco ME, Philips CM, Marquez LA, Hall C, Davila JC. Measurement of cardiac output by thermal dilution. *Am J Cardiol*. 1979;**28**:54-8.

153. Vogel J. Measurement of cardiac output in small laboratory animals using recordings of blood conductivity. *Am J Physiol Hear Circ Physiol*. 1997;**273**:H2520-H7.

154. Montani J-P, Van Vliet BN. Understanding the contribution of Guyton's large circulatory model to long-term control of arterial pressure. *Exp Physiol*. 2009;**94**(4):382-8.

155. Dresser T, Lynch R, EG S, Knox F. Effect of increases in blood pressure on pressure and reabsorption in the proximal tubule. *Am J Physiol*. 1971;**220**(2):444-7.

156. Roman RJ, Cowley AW, Jr. Characterization of a new model for the study of pressure-natriuresis in the rat. *Am J Physiol*. 1985;**248**(2 Pt 2):F190-8.

157. Kuanu RT, Lameire NH. The effect of an acute increase in renal perfusion pressure on sodium transport in the rat kidney. *Circ Res*. 1976;**39**(5):689-95.

158. Hall JE, Granger JP, Smith MJ, Jr., Premen AJ. Role of renal hemodynamics and arterial pressure in aldosterone "escape". *Hypertension*. 1984;**6**(2 Pt 2):I183-92.

159. Hall JE, Montani J-P, Woods LL, Mizelle HL. Renal escape from vasopressin: role of pressure diuresis. *Am J Physiol*. 1986;**250**(5 Pt 2):F907-F16.

160. Peiss CN, Manning JW. Effects of sodium pentobarbital on electrical and reflex activation of the cardiovascular system. *Circ Res*. 1964;**14**:228-35.

161. Girardin E, Caverzasio J, Iwai J, Bonjour JP, Muller AF, Grandcamp A. Pressure natriuresis in isolated kidneys from hypertension-prone and hypertension-resistant rats (Dahl rats). *Kidney Int*. 1980;**18**(1):10-9.

162. Roman RJ. Abnormal renal hemodynamics and pressure-natiuresis relationship in Dahl salt-sensitive rats. *Am J Physiol*. 1986;**251**(1 Pt 2):F57-65.

163. Hall JE, Brands MW, Shek EW. Central role of the kidney and abnormal fluid volume control in hypertension. *J Hum Hypertens*. 1996;**10**(10):633-9.

164. Kimura G, Brenner BM. A method for distinguishing salt-sensitive from non-salt-sensitive forms of human and experimental hypertension. *Curr Opin Nephrol Hypertens*. 1993;**2**(3):341-9.

165. Roman RJ, Cowley AW, Jr., Garcia-Estan J, Lombard JH. Pressure-diuresis in volume-expanded rats. Cortical and medullary hemodynamics. *Hypertension*. 1988;**12**(2):168-76.

166. Bailey MA. Inhibition of bicarbonate reabsorption in the rat proximal tubule by activation of luminal P2Y1 receptors. *Am J Physiol: Ren Physiol*

. 2004;**287**(5):F789-F96.

167. Ortiz PA, Hong NJ, Garvin JL. NO decreases thick ascending limb chloride absorption by reducing Na(+)-K(+)-2Cl(-) cotransporter activity. *Am J Physiol Ren Physiol*. 2001;**281**(5):5.

168. Snyder PM, Price MP, McDonald FJ, Adams CM, Volk KA. Mechanism by which Liddle's syndrome mutations increase activity of a human epithelial Na+ channel. *Cell*. 1995;**83**(6):969-78.

169. Hoenig MP, Zeidel ML. Homeostasis, the Milieu Intérieur, and the Wisdom of the Nephron. *Clin J Am Soc Nephrol*. 2014;**15**.

170. Sandberg MB, Maunsbach AB, McDonough AA. Redistribution of distal tubule Na+-Cl- cotransporter (NCC) in response to a high-salt diet. *Am J Physiol Renal Physiol*. 2006;**291**(2):F503-8.

171. Capasso G, Rizzo M, Garavaglia ML, Trepiccione F, Zacchia M, Mugione A, et al. Upregulation of apical sodium-chloride cotransporter and basolateral chloride channels is responsible for the maintenance of salt-sensitive hypertension. *Am J Physiol Renal Physiol*. 2008;**295**(2):F556-F67.

172. Haque MZ, Ares GR, Caceres PS, Ortiz PA. High salt differentially regulates surface NKCC2 expression in thick ascending limbs of Dahl salt-sensitive and salt-resistant rats. *Am J Physiol Renal Physiol*. 2011;**300**(5):F1096-104.

173. Gimenez I, Forbush B. Short-term stimulation of the renal Na-K-Cl cotransporter (NKCC2) by vasopressin involves phosphorylation and membrane translocation of the protein. *J Biol Chem*. 2003;**278**(29):26946-51.

174. Mutig K, Saritas T, Uchida S, Kahl T, Borowski T, Paliege A, et al. Short-term stimulation of the thiazide-sensitive Na+-Cl- cotransporter by vasopressin involves phosphorylation and membrane translocation. *Am J Physiol Renal Physiol*. 2010;**298**(3):F502-9.

175. Carlstörm M, Wilcox CS, Arendshorst WJ. Renal autoregulation in health and disease. *Am J Physiol*. 2015;**95**:405-511.

176. Campese VM, Parise M, Karubian F, Bigazzi R. Abnormal renal hemodynamics in black salt-sensitive patients with hypertension. *Hypertension*. 1991;**18**:805-12.

177. Arendshorst WJ, Beierwaltes WH. Renal and nephron hemodynamics in spontaneously hypertensive rats. *Am J Physiol*. 1979;**236**:F246-F51.

178. Griffin KA, Churchill PC, Picken M, Webb RC, Kurtz TW, Bidani AK. Differential salt-sensitivity in the pathogenesis of renal damage in SHR and stroke prone SHR. *Am J Hypertens*. 2001;**14**:311-20.

179. Polichnowski AJ, Griffin KA, Long J, Williamson GA, Bidani AK. Blood pressure-renal blood flow relationships in conscious angiotensin II- and phenylephrine-infused rats. *Am J Physiol Renal Physiol*. 2013;**305**:F1074-84.

180. Sparks MA, Stegbauer J, Chen DD, Gomez JA, Griffiths RC, Azad HA, et al. Vascular Type 1A Angiotensin II Receptors Control BP by Regulating Renal Blood Flow and Urinary Sodium Excretion. *J Am Soc Nephrol*. 2015;**26**:2953-62.

181. Schmidlin O, Forman A, Leone A, Sebastian A, Morris RC. Salt sensitivity in blacks: evidence that the initial pressor effect of NaCl Involves inhibition of vasodilatation by asymmetrical dimethylarginine. *Hypertension*. 2011;**58**(3):380-U93.

182. Feng W, Dell'Italia LJ, Sanders PW. Novel Paradigms of Salt and Hypertension. *J Am Soc Nephrol*. 2017;**28**(5):1362-9.

183. Mulvany M, Aalkjaer C. Structure and function of small arteries. *Physiol Rev*. 1990;**70**(4):921-61.

184. Spiers A, Padmanabhan N. A Guide to Wire Myography. 108 ed. New Jersey: Humana Press Inc; 2005.

185. Dunn WR, Wellman GC, Bevan JA. Enhanced resistance artery sensitivity to agonists under isobaric compared with isometric conditions. *Am J Physiol*. 1994;**266**(1 Pt 2):H147-55.

186. Bagher P, Segal SS. Regulation of blood flow in the microcirculation: role of conducted vasodilation. *Acta Physiol (Oxf)*. 2011;**202**(3):271-84.

187. Nyberg M, Gliemann L, Hellsten Y. Vascular function in health, hypertension, and diabetes: effect of physical activity on skeletal muscle microcirculation. *Scand J Med Sci Sports*. 2015;**25** ((Suppl 4)):60-73.

188. Villacorta L, Chang L. The role of perivascular adipose tissue in vasoconstriction, arterial stiffness, and aneurysm. *Horm Mol Biol Clin Investig*. 2015;**21**(2):137-47.

189. Jadeja RN, Rachakonda V, Bagi Z, Khurana S. Assessing myogenic response and vasoactivity in resistance mesenteric arteries using pressure myography. *J Vis Exp*. 2015;**101**:e50997.

190. Falloon BJ, Stephens N, Tulip JR, Heagerty AM. Comparison of small artery sensitivity and morphology in pressurized and wire-mounted preparations. *Am J Physiol Hear Circ Physiol*. 1995;**268**(2 Pt 2):H670-8.

191. Raitakari OT, Celermajer DS. Flow-mediated dilatation. *Br J Clin Pharmacol*. 2000;**50**(5):397-404.

192. Zhao Y, Vanhoutte PM, Leung SW. Vascular nitric oxide: Beyond eNOS. *J Pharmacol Sci*. 2015;**129**(2):83-94.

193. Nurkiewicz TR, Boegehold MA. High salt intake reduces endothelium-dependent dilation of mouse arterioles via superoxide anion generated from nitric oxide synthase. *Am J Physiol Regul Integr Comp Physiol*. 2007;**292**(4):R1550-6.

194. Sylvester FA, Stepp DW, Frisbee JC, Lombard JH. High-salt diet depresses acetylcholine reactivity proximal to NOS activation in cerebral arteries. *Am J Physiol Heart Circ Physiol*. 2002;**283**(1):H353-63.

195. Liu Y, Rusch NJ, Lombard JH. Loss of endothelium and receptor-mediated dilation in pial arterioles of rats fed a short-term high salt diet. *Hypertension*. 1999;**33**(2):686-8.

196. Lenda DM, Sauls BA, Boegehold MA. Reactive oxygen species may contribute to reduced endothelium-dependent dilation in rats fed high salt. *Am J Physiol Hear Circ Physiol*. 2000;**279**(1):H7-H14.

197. Zhu JX, Mori T, Huang T, Lombard JH. Effect of high-salt diet on NO release and superoxide production in rat aorta. *Am J Physiol Hear Circ Physiol*. 2004;**286**(2):H575-H83.

198. Boegehold MA. Effect of dietary salt on arteriolar nitric oxide in striated muscle of normotensive rats. *Am J Physiol*. 1993;**264**(6 Pt 2):H1810-6.

199. Daiber A, Di Lisa F, Oelze M, Kroller-Schon S, Steven S, Schulz E, et al. Crosstalk of mitochondria with NADPH oxidase via reactive oxygen and nitrogen species signalling and its role for vascular function. *Br J Pharmacol*. 2017;**174**(12):1670-89.

200. Münzel T, Daiber A, Ullrich V, Mulsch A. Vascular consequences of endothelial nitric oxide synthase uncoupling for the activity and expression of the soluble guanylyl cyclase and the cGMP-dependent protein kinase. *Arterioscler Thromb Vasc Biol*. 2005;**25**(8):1551-7.

201. Xie HH, Zhou S, Chen DD, Channon KM, Su DF, Chen AF. GTP cyclohydrolase I/BH4 pathway protects EPCs via suppressing oxidative stress and thrombospondin-1 in salt-sensitive hypertension. *Hypertension*. 2010;**56**(6):1137-44.

202. Chuaiphichai S, Crabtree MJ, McNeill E, Hale AB, Trelfa L, Channon KM, et al. A key role for tetrahydrobiopterin-dependent endothelial NOS regulation in resistance arteries: studies in endothelial cell tetrahydrobiopterin-deficient mice. *Br J Pharmacol*. 2017;**174**(8):657-71.

203. Miller MR, Megson IL. Recent developments in nitric oxide donor drugs. *Br J Pharmacol*. 2007;**151**(3):305-21.

204. Lovell DP. Biological importance and statistical sigificance. *J Agric Food Chem*. 2013;**61**(35):8340-8.

205. Ioannidis JPA. Why most published research findings are false. *Plos Medicine*. 2005;**2**(8):696-701.

206. Flammer AJ, Anderson T, Celermajer DS, Creager MA, Deanfield JE, Ganz P, et al. The assessment of endothelial function: from research into clinical practice. *Circulation*. 2012;**126**:753-67.

207. Laurent S, Boutouyrie P. The structural factor of hypertension: large and small artery alterations. *Circ Res*. 2015;**116**:1007-21.

208. Folkow B. Hypertensive structural changes in systemic precapillary resistance vessels: how important are they for in vivo haemodynamics? *J Hypertens*. 1995;**13**:1546-59.

209. Fujita T, Ando K, Ogata E. Systemic and regional hemodynamics in patients with salt-sensitive hypertension. *Hypertension*. 1990;**16**(3):235-44.

210. Santajuilana D. Use of ganglionic blockers to assess neurogenic pressor activity in conscious rats. *J Pharmacol Toxicol Methods*. 1996;**35**:45-54.

211. Nicolaus ML, Bergdall VK, Davis IC, Hickman-Davis JM. Effect of ventilated caging on water intake and loss in 4 strains of laboratory mice. *J Am Assoc Lab Anim Sci*. 2016;**55**(5):525-33.

212. Wang HL, Lai TW. Optimization of Evans blue quantitation in limited rat tissue samples. *Sci Rep*. 2014;**4**:6588.

213. Chapman ME, Hu L, Plato CF, Kohan DE. Bioimpedance spectroscopy for the estimation of body fluid volumes in mice. *Am J Physiol Renal Physiol*. 2010;**299**(1):F280-3.

214. Titze J, Lang R, Ilies C, Schwind KH, Kirsch KA, Dietsch P, et al. Osmotically inactive skin Na+ storage in rats. *Am J Physiol Renal Physiol*. 2003;**285**(6):F1108-17.

215. Kopp C, Linz P, Wachsmuth L, Dahlmann A, Horbach T, Schofl C, et al. (23)Na magnetic resonance imaging of tissue sodium. *Hypertension*. 2012;**59**(1):167-72.

216. Rakova N, Juttner K. Long-term space flight stimulation reveals infradian rhythmycity in human Na+ balance. *Cell Metab*. 2013;**17**:125-31.

217. Campese VM, Romoff MS, Levitan D, Saglikes Y, Friedler RM, Massry SG. Abnormal relationship between sodium intake and sympathetic nervous system activity in salt-sensitive patients with essential hypertension. *Kidney Int*. 1982;**21**(2):371-8.

218. Hoffman IS, Cubeddu LX. Salt and the metabolic syndrome. *Nutri Metab Cardiovasc Dis*. 2009;**19**(2):123-8.

219. Oh SW, Han KH, Han SY, Koo HS, Kim S, Chin HJ. Association of sodium excretion with metabolic syndrome, insulin resistance, and body fat. *Medicine (Baltimore)*. 2015;**94**(39):e1650.

220. Whelton PK, Appel L, Charleston J, Dalcin A, Haythornthwaite J, Rosofsky W, et al. Effects of weight loss and sodium reduction intervention on blood pressure and hypertension incidence in overweight people with high-normal blood pressure - The trials of hypertension prevention, phase II. *Arch Intern Med*. 1997;**157**(6):657-67.

221. DeClercg V, Goldsby JS, McMurray DN, Chapkin RS. Distinct adipose depots from mice differentially respond to a high-fat, high-salt diet. *J Nutri*. 2016;**146**(6):1189-96.

222. Weidermann BJ, Voong S, Morales-Santiago FI, Kahn MZ, Ni J, Littlejohn NK, et al. Dietary sodium suppresses digestive efficiency via the renin-angiotensin system. *Sci Rep*. 2015;**5**:1123.

223. Manchester RC. The diurnal rhythm in water and mineral exchange. *J Clin Invest*. 1933;**12**(6):995-1008.

224. Boemke W, Palm U, Corea M, Seeliger E, Reinhardt HW. Endogenous variations and sodium intake-dependent components of diurnal sodium excretion patterns in dogs. *J Physiol*. 1994;**476**(3):547-52.

225. Fukuda M, Goto N, Kimura G. Hypothesis on renal mechanism of non-dipper pattern of circadian blood pressure rhythm. *Med Hypotheses*. 2006;**67**(4):802-6.

226. Dyer AR, Stamler R, Grimm R, Stamler J, Berman R. Do hypertensive patients have a different diurnal pattern of electrolyte excretion? *Hypertension*. 1987;**10**:417-24.

227. Bankir L, Bochud M, Maillard M, Bovet P, Gabriel A, Burnier M. Nighttime blood pressure and nocturnal dipping are associated with daytime urinary sodium excretion in African subjects. *Hypertension*. 2008;**51**(4):891-8.

228. Saxena AR, Chamarthi B, Williams GH, Hopkins PN, Seely EW. Predictors of plasma and urinary catecholamine levels in normotensive and hypertensive men and women. *J Hum Hypertens*. 2014;**28**(5):292-7.

229. Nunes FC, Braga VA. Chronic angiotensin II infusion modulates angiotensin II type I receptor expression in the subfornical organ and the rostral ventrolateral medulla in hypertensive rats. *J Renin Angiotensin Aldosterone Syst*. 2011;**12**(4):440-5.

230. Harington M, Rosenheim ML. Hexamethonium in the treatment of hypertension. *Lancet*. 1954;**266**(6801):7-13.

231. Li P, Gong JX, Sun W, Zhou B, Kong XQ. Hexamethonium attenuates sympathetic activity and blood pressure in spontaneously hypertensive rats. *Mol Med Rep*. 2015;**12**(5):7116-22.

232. Fahmy NR, Soter NA. Effects of trimethaphan on arterial blood histamine and systemic hemodynamics in humans. *Anesthesiology*. 1985;**62**(5):562-6.

233. Harioka T, Hatano Y, Mori K, Toda N. Trimethaphan is a direct arterial vasodilator and an alpha-adrenoceptor antagonist. *Anesth Analg*. 1984;**63**(3):290-6.

234. Jacob F, Clark LA, Guzman PA, Osborn JW. Role of renal nerves in development of hypertension in DOCA-salt model in rats: a telemetric approach. *Am J Physiol Heart Circ Physiol*. 2005;**289**(4):H1519-29.

235. O'Hagan KP, Thomas GD, Zambraski EJ. Renal denervation decreases blood pressure in DOCA-treated minature swine with established hypertension. *Am J Hypertens*. 1990;**3**(1):62-4.

236. Dias LD, Casali KR, Leguisamo NM, Azambuja F, Souza MS, Okamoto M, et al. Renal denervation in an animal model of diabetes and hypertension: impact on the autonomic nervous system and nephropathy. *Cardiovasc Diabetol*. 2011;**10**:33.

237. DiBona GF, Kopp UC. Neural control of renal function. *Physiol Rev*. 1997;**77**(1):75-197.

238. Fujita T, Henry WL, Bartter FC, Lake CR, Delea CS. Factors influencing blood pressure in salt-sensitive patients with hypertension. *Am J Med*. 1980;**69**(3):334-44.

239. Schmidlin O, Forman A, Tanaka M, Sebastian A, Morris RC, Jr. NaCl-induced renal vasoconstriction in salt-sensitive African Americans: antipressor and hemodynamic effects of potassium bicarbonate. *Hypertension*. 1999;**33**(2):633-9.

240. Romoff MS, Keusch G, Campese VM, Wang MS, Friedler RM, Weidmann P, et al. Effect of sodium intake on plasma catecholamines in normal subjects. *J Clin Endocrinol Metab*. 1979;**48**(1):26-31.

241. Luft FC, Rankin LI, Henry DP, Bloch R, Grim CE, Weyman AE, et al. Plasma and urinary norepinephrine values at extremes of sodium-Intake in normal man. *Hypertension*. 1979;**1**(3):261-6.

242. Dodt C, Breckling U, Derad I, Fehm HL, Born J. Plasma epinephrine and norepinephrine concentrations of healthy humans associated with nighttime sleep and morning arousal. *Hypertension*. 1997;**30**(1 Pt 1):71-6.

243. Kawano Y, Yoshida K, Kawamura M, Yoshimi H, Ashida T, Abe H, et al. Sodium and noradrenaline in cerebrospinal fluid and blood in salt-sensitive and non-salt-sensitive essential hypertension. *Clin Exp Pharmacol Physiol*. 1992;**19**(4):235-41.

244. Gotoh E. Relation of sodium concentration in cerebrospinal fluid to systemic blood pressure levels in salt-sensitive and nonsalt-sensitive, essential hypertension patients. *Jap Circ J*. 1981;**45**:998.

245. Stocker SD, Lang SM, Simmonds SS, Wenner MM, Farquhar WB. CSF hypernatremia elevates sympathetic nerve activity and blood pressure via the rostral ventrolateral medulla. *Hypertension*. 2015;**66**(6):1184-90.

246. Bolli P, Erne P, Ji BH, Block LH, Kiowski W, Buhler FR. Adrenaline induces vasoconstriction through post-junctional alpha 2 adrenoceptors and this response is enhanced in patients with essential hypertension *J Hypertens Suppl*. 1984;**2**(3):S115-8.

247. Wallin BG, König U. Changes of skin nerve sympathetic activity during induction of general anaesthesia with thiopentone in man. *Brain Res*. 1976;**103**(1):157-60.

248. Sellgren J, Ponten J, Wallin BG. Characteristics of muscle nerve sympathetic activity during general anaesthesia in humans. *Acta Anaesthesiol Scand*. 1992;**36**(4):336-45.

249. Deka-Starosta A, Garty M, Zukowska-Grojec Z, Keiser HR, Kopin IJ, Goldstein DS. Renal sympathetic nerve activity and norepinephrine release in rats. *Am J Physiol Regul Integr Comp Physiol*. 1989;**257**(1 Pt 2):R229-36.

250. Esler M, Jennings G, Korner P, Willett I, Dudley F, Hasking G, et al. Assessment of human sympathetic nervous system activity from measurements of norepinephrine turnover. *Hypertension*. 1988;**11**(1):3-20.

251. Peaston RT, Weinkove C. Measurement of catecholamines and their metabolites. *Ann Clin Biochem*. 2004;41:17-38.

252. Roberts NB, Higgins G, Sargazi M. A study on the stability of urinary free catecholamines and free methyl-derivatives at different pH, temperature and time of storage. *Clin Chem Lab Med*. 2010;**48**:81-7.

253. Willemsen JJ, Ross HA, Lenders JWM, Sweep FCGJ. Stability of urinary fractionated metanephrines and catecholamines during collection, shipment, and storage of samples. *Clin Chem*. 2007;**53**(2):268-72.

254. Miki K, Sudo A. Effect of storage, time and temperature on stability of catecholamines, cortisol and creatinine. *Clin Chem*. 1998;44:1759-61.

255. Bayorh MA, Ganafa AA, Emmett N, Socci RR, Eatman D, Fridie IL. Alterations in aldosterone and angiotensin II levels in salt-induced hypertension. *Clin Exp Hypertens*. 2005;**27**(4):355-67.

256. Drenjančević-Perić I, Jelakovic B, Lombard JH, Kunert MP, Kibel A, Gros M. High-salt diet and hypertension: focus on the renin-angiotensin system. *Kidney Blood Press Res*. 2011;**34**(1):1-11.

257. Kotchen TA, Luke RG, Ott CE, Galla JH, Whitescarver S. Effect of chloride on renin and blood pressure responses to sodium chloride. *Ann Intern Med*. 1983;**98**:817-22.

258. Luft FC, Steinberg H, Ganten U, Meyer D, Gless KH, Lang RE, et al. Effect of sodium chloride and sodium bicarbonate on blood pressure in stroke-prone spontaneously hypertension rats. *Clin Sci (Lond)*. 1988;**74**:577-85.

259. Whitescarver SA, Ott CE, Jackson BA, Guthrie Jr GP, Kotchen TA. Salt-sensitive hypertension: contribution of chloride. *Science*. 1984;**223**:1430-2.

260. Wyss JM, Liumsiricharoen M, Sripairojthikoon W, Brown D, Gist R, Oparil S. Exacerbation of hypertension by high chloride, moderate sodium diet in the salt-sensitive spontaneously hypertensive rat. *Hypertension*. 1987;**9**:171-5.

261. Morgan TO. Effect of potassium and bicarbonate ions on the rise in blood pressure caused by sodium chloride. *Clin Sci (Lond)*. 1982;**63**:S407-9.

262. Shore AC, Markandu ND, MacGregor GA. A randomized crossover study to compare the blood pressure response to sodium loading with and without chloride in patients with essential hypertension. *J Hypertens*. 1988;**6**:613-7.

263. Kurtz TW, Al-Bander HA, Morris RC. "Salt-sensitive" essential hypertension in men. Is the sodium ion alone important? *N Engl J Med*. 1987;**317**:1043-8.

264. Lim SS, Vos T, Flaxman AD, Danaei G, Shibuya K, Adair-Rohani H, et al. A comparative risk assessment of burden of disease and injury attributable to 67 risk factors and risk factor clusters in 21 regions, 1990–2010: a systematic analysis for the Global Burden of Disease Study 2010. *Lancet*. 2012;**380**(9859):2224-60.

265. Nagata C, Takatsuka N, Shimizu N, Shimizu H. Sodium intake and risk of death from stroke in Japanese men and women. *Stroke*. 2004;**35**(7):1543-7.

266. Perry IJ, Beevers DG. Salt intake and stroke: a possible direct effect. *J Hum Hypertens*. 1992;**6**(1):23-5.

267. Tuomilehto J, Jousilahti P, Rastenyte D, Moltchanov V, Tanskanen A, Pietinen P, et al. Urinary sodium excretion and cardiovascular mortality in Finland: a prospective study. *Lancet*. 2001;**357**(9259):848-51.

268. WHO. Shake the Salt Habit: The SHAKE Technical Package for Salt Reduction [Online report] Geneva, Switzerland2016 [Available from: https://apps.who.int/iris/bitstream/handle/10665/250135/9789241511346-eng.pdf;jsessionid=2DAEB373E6034055064D9835071018BD?sequence=1.

269. Law MR, Frost CD. By how much does dietary salt reduction lower blood pressure? III--Analysis of data from trials of salt reduction. *BMJ*. 1991;**302**(6780):819-24.

270. Sacks FM, Svetkey LP, Vollmer WM, Appel LJ, Bray GA, Harsha D, et al. Effects on blood pressure of reduced dietary sodium and the Dietary Approaches to Stop Hypertension (DASH) diet. DASH-Sodium Collaborative Research Group. *N Engl J Med*. 2001;**344**(1):3-10.

271. Yusuf S, Joseph P, Rangarajan S, Islam S, Mente A, Hystad P, et al. Modifiable risk factors, cardiovascular disease, and mortality in 155 722 individuals from 21 high-income, middle-income, and low-income countries (PURE): a prospective cohort study: *Lancet*; 2019 [updated Sep 3. Available from: https://www.ncbi.nlm.nih.gov/pubmed/31492503.

272. de Souza JT, Matsubara LS, Menani JV, Matsubara BB, Johnson AK, De Gobbi JI. Higher salt preference in heart failure patients. *Appetite*. 2012;**58**(1):418-23.

273. Qi H, Liu Z, Cao H, Sun WP, Peng WJ, Liu B, et al. Comparative efficacy of antihypertensive agents in salt-sensitive hypertensive patients: a network meta-analysis. *Am J Hypertens*. 2018;**31**(7):835-46.

274. Kailasam MT, Parmer RJ, Cervenka JH, Wu RA, Ziegler MG. Divergent effects of dihydropyridine and phenyalkylamine calcium channel antagonist classes on autonomic function in human hypertension. *Hypertension*. 1995;**26**:143-9.

275. Rupp H, Maisch B, Brilla CG. Drug withdrawal and rebound hypertension: differential action of the central antihypertensive drugs moxonidine and clonidine. *Cardiovasc Drugs Ther*. 1996;**10** (Suppl 1):251-62.

276. Wenzel RR, Spieker L, Qui S, Shaw S, Luscher TF, Noll G. I1-imidazoline agonist moxonidine decreases sympathetic nerve activity and blood pressure in hypertensives. *Hypertension*. 1998;**32**(6):1022-7.

277. Chrisp P, Faulds D. Moxonidine - a review of its pharmacology, and therapeutic use in essential hypertension. *Drugs*. 1992;**44**(6):993-1012.

278. Kirch W, Hutt HJ, Planitz V. The influence of renal function on clinical pharmacokinetics of moxonidine. *Clin Pharmacokinet*. 1988;**15**(4):245-53.

279. Frei M. Moxonidine and hydrochlorothiazide in combination: a syngeristic antihypertensive effect. *J Cardiovasc Pharma*. 1994;**24**((suppl 1)):S25-8.

280. Wolf R. The treatment of hypertensive patients with a calcium-antagonist or moxonidine - a comparison. *J Cardiovasc Pharma*. 1992;**20**:S42-S4.

281. Ernsberger P, Koletsky RJ, Collins LA, Bedol D. Sympathetic nervous system in salt-sensitive and obese hypertension: amelioration of multiple abnormalities by a central sympatholytic agent. *Cardiovasc Drugs Ther*. 1996;**10** (Suppl 1):275-82.

282. Bhatt DL, Kandzari DE, O'Neill WW, D'Agostino R, Flack JM, Katzen BT, et al. A controlled trial of renal denervation for resistant hypertension. *N Engl J Med*. 2014;**370**(15):1393-401.

283. Pancholy SB, Shantha GP, Patel TM, Sobotka PA, Kandzari DE. Meta-analysis of the effect of renal denervation on blood pressure and pulse pressure in patients with resistant systemic hypertension. *Am J Cardiol*. 2014;**114**(6):856-61.

284. Krum H, Schlaich M, Whitbourn R, Sobotka PA, Sadowski J, Bartus K, et al. Catheter-based renal sympathetic denervation for resistant hypertension: a multicentre safety and proof-of-principle cohort study. *Lancet*. 2009;**373**(9671):1275-81.

285. Osborn JL, Roman RJ, Ewens JD. Renal nerves and the development of Dahl salt-sensitive hypertension. *Hypertension*. 1988;**11**(6 Pt 1):523-8.

286. Foss JD, Fink GD, Osborn JW. Differential role of afferent and efferent renal nerves in the maintenance of early- and late-phase Dahl S hypertension. *Am J Physiol Regul Integr Comp Physiol*. 2016;**310**(3):R262-7.

287. de Beus E, de Jager RL, Beeftink MM, Sanders MF, Spiering W, Vonken EJ, et al. Salt intake and blood pressure response to percutaneous renal denervation in resistant hypertension. *J Clin Hypertens (Greenwich)*. 2017;**19**(11):1125-33.